Synthesis, bioanalysis and pharmacology of nucleoside and nucleotide analogs

ISBN/EAN: 978-94-901-2252-2

© 2009, Robert Jansen, Amsterdam

Omslag ontwerp: Robert Jan van Oosten, Wageningen
Druk: Gildeprint drukkerijen, Enschede

Synthesis, bioanalysis and pharmacology of nucleoside and nucleotide analogs

Synthese, bioanalyse en farmacologie
van nucleoside en nucleotide analogen

(met een samenvatting in het Nederlands)

PROEFSCHRIFT

ter verkrijging van de graad van doctor aan de Universiteit Utrecht
op gezag van de rector magnificus, prof. dr. J.C. Stoof.,
ingevolge het besluit van het college voor promoties
in het openbaar te verdedigen
op woensdag 2 september 2009 des middags te 2.30 uur

door

Robert Sander Jansen

geboren op 16 mei 1980 te Voorburg

Promotoren:
Prof. dr. J.H. Beijnen
Prof. dr. J.H.M. Schellens

Co-promotor:
Dr. H. Rosing

The research described in this thesis was performed at the Department of Pharmacy & Pharmacology of the Netherlands Cancer Institute / Slotervaart Hospital, Amsterdam, The Netherlands

Publication of this thesis was financially supported by:

Eli Lilly Nederland BV, Houten, The Netherlands
Gilead Sciences Netherlands BV, Amsterdam, The Netherlands
GlaxoSmithKline, Zeist, The Netherlands
Janssen-Cilag B.V., Tilburg, The Netherlands
J.E. Jurriaanse Stichting, Rotterdam, The Netherlands
Pfizer bv, Capelle aan den IJssel, The Netherlands
Shimadzu Benelux, 's Hertogenbosch, The Netherlands
The Netherlands Laboratory for Anticancer Drug Formulation, Amsterdam, The Netherlands

De eekhoorn vroeg zich af hoe het zou zijn als je je nooit meer verbaasde.
Heel vreemd, dacht hij, heel vreemd.

Toon tellegen

Voor mijn ouders

Preface

Cancer and HIV/AIDS are among the top 10 causes of death worldwide. Together they account for over ten million deaths per year [1]. Besides their lethality, they also share their way to proliferate. Both diseases require replication of their genetic material (DNA and RNA) to thrive. By mimicking nucleosides, the natural building blocks of DNA and RNA, nucleoside analogs interfere with the replication of genetic material and thus with virus and tumor cell proliferation.

Nucleoside analogs, and variants thereof, were among the first drugs used against cancer. 6-Mercaptopurine (6-MP), a base analog, was already approved by the American Food and Drug Administration (FDA) for the treatment of leukemias in 1953 [2]. The first anticancer nucleoside analog, cytarabine (ara-C), followed in 1969. Almost 20 years later (1987) zidovudine (AZT), a nucleoside analog initially developed for the treatment of cancer, was the first drug ever to be approved for the treatment of HIV/AIDS [3]. In 2009, decades after their introduction, all three analogs are still widely used in antiviral and anticancer therapy and many more have been, and are still being, developed.

Although much is known about the pharmacology of nucleoside analogs, the introduction of new analogs, and the application of older analogs in different dosing schemes and routes of administration, keeps raising new questions. Nucleoside analogs are prodrugs that require activation to their mono-, di and triphosphorylated form, also called nucleotides. This activation only occurs inside cells. To fully understand the pharmacology of the drugs it is, therefore, essential to measure these nucleotide analogs inside cells. Liquid chromatography coupled with tandem mass spectrometry (LC-MS/MS) is a technique that is widely used for the sensitive quantification of drugs in biological matrices. The ionic nature of the nucleotide analogs, however, poses multiple technical challenges to LC-MS/MS analysis.

The aim of this thesis project was to develop sensitive LC-MS/MS assays to quantitate nucleoside and nucleotide analogs in cells, and to apply these assays to preclinical and clinical studies in order to increase the knowledge of nucleoside analog pharmacology.

In *chapter 1* the chemical phosphorylation of small quantities of nucleoside analogs to their nucleotides is described (*chapter 1.1*). The methodology made it possible to synthesize desired reference materials and internal standards that were not commercially available.

Chapter 2 focuses on the analysis of intracellular nucleoside and nucleotide analogs. First, an overview of the literature on the analysis of intracellular nucleotide analogs with LC-MS/MS is provided (*chapter 2.1*). Then, two chapters describe the development and validation of LC-MS/MS assays based on weak anion-exchange liquid chromatography. Cladribine mono-, di- and triphosphate are quantitated in a cell line and culture medium in *chapter 2.2*, whereas emtricitabine mono-, di- and triphosphate and tenofovir, tenofovir mono- and diphosphate are simultaneously determined in human white blood cells (*chapter 2.3*).
The development of a novel chromatographic system for the separation of nucleosides and nucleotides using porous graphitic carbon is outlined in *chapter 2.4*. In *chapter 2.5*, this separation technique is developed further to the validated quantification of gemcitabine, its metabolite dFdU and their mono-, di- and triphosphate in human white blood cells. The section ends with the comparison of protein and DNA determinations to count the number of cells isolated from blood (*chapter 2.6*).

Chapter 3 covers pharmacological aspects and (pre)clinical applications of nucleotide analog analysis. The role of the drug-efflux pump BCRP in resistance against nucleoside analogs is investigated in the preclinical study presented in *chapter 3.1*. A clinical and pharmacological study on the oral administration of gemcitabine is described in *chapter 3.2*. In *chapter 3.3*, the formation and possible pharmacological activity of deoxuridine analogs in deoxycytidine therapy is discussed.
Finally, a method is described for the LC-MS/MS analysis of intracellular decitabine nucleotides. The method is applied to determine decitabine triphosphate levels in white blood cells from patients during prolonged low-dose decitabine administration and may serve further optimization of decitabine dosing (*chapter 3.4*).

References

[1] The world health report 2008: Primary health care, now more than ever; World Health Organization
[2] Listing of approved oncology drugs with approved indications; US Food and Drug administration (http://www.accessdata.fda.gov/scripts/cder/onctools/druglist.cfm)
[3] Drugs used in the treatment of HIV infection; US Food and Drug administration (http://www.fda.gov/oashi/aids/virals.html

Contents

Chapter 1

Synthesis
of nucleotide analogs

Chapter 1.1

Facile small scale synthesis of nucleoside 5'-phosphate mixtures

Robert S Jansen, Hilde Rosing, Jan HM Schellens and Jos H Beijnen

Submitted for publication

Abstract

We present a facile method to phosphorylate small amounts of nucleosides (0.05 µmoles) into mixtures of their 5'-mono-, di-, and triphosphates in a one-pot reaction. The nucleosides were first converted into their dichlorophosphates using a large excess (15-18 equivalents) of phosphorous oxychloride in trimethylphosphate. The large excess resulted in good dichlorophosphate yields (46-76%) for the four nucleosides tested. Upon the addition of tributylammonium-phosphate with additional tributylamine (20 equivalents both), the dichlorophosphate was converted into a mixture containing equal amounts of the mono-, di- and triphosphate. The presented method was successfully applied to synthesize mixtures of stable isotope labelled nucleotides, which can be used as internal standards in quantitative mass spectrometric assays.

Introduction

Nucleoside analogs are used in anti-cancer, anti-(retro)viral and immunosuppressive therapies. The analogs are phosphorylated to nucleoside mono-, di- and triphosphates intracellularly. The triphosphate form inhibits human and viral polymerases and reverse transcriptases and is incorporated into nucleic acids. Although the mono- and diphosphates are not the main active metabolites, they possess pharmacological activity as well.

Monitoring of the intracellular concentration of these metabolites is pivotal in understanding the pharmacology and toxicology of nucleoside analogs. In the past decade, liquid chromatography coupled to tandem mass spectrometry (LC-MS/MS) has become the method of choice to analyze nucleotide analogs in cells. For optimal performance of LC-MS/MS assays an internal standard should be used to correct for interferences caused by other sample constituents. Stable isotope labelled analytes are the ideal internal standards because they have identical physico-chemical properties, but their mass difference can be distinguished in the mass spectrometer.

The availability of stable isotope labelled nucleotide analogs is, however, limited. Many of their non-phosphorylated, stable isotope labelled nucleosides, on the other hand, are commercially available. We therefore explored the possibility to phosphorylate small quantities of nucleosides to a mixture of their mono-, di- and triphosphate to serve as internal standards for LC-MS/MS analysis.

Many methods to synthesize nucleoside triphosphates have been developed, as reviewed by Burgess and Cook [1]. Most of these methods first convert the nucleoside into an activated monophosphate, such as a dichlorophosphate or phosphoramidate.

A commonly used phosphytilating agent is phosphorous oxychloride ($POCl_3$). When $POCl_3$ is used in a trialkylphosphate solution it results in selective phosphorylation of the 5′-hydroxyl group of the nucleoside [2;3].

Addition of tributylammonium(TBA)-pyrophosphate to the thus formed nucleoside dichlorophosphate results in the formation of the nucleoside 5′-triphosphate [4]. Reaction with water, on the other hand, deactivates the dichlorophosphate intermediate resulting in the formation of a nucleoside 5′-monophosphate.

In attempt to synthesize the 5′-diphosphate, Mishra and Broom added TBA-phosphate to the nucleoside dichlorophosphate [5]. To their surprise the 5′-triphosphate was formed instead of the 5′-diphosphate. Similarly, Hoffmann et al. added crystalline phosphoric acid in combination with different organic bases [6]. Depending on the organic base added, they obtained mixtures of 5′-mono-, di- and triphosphates in different ratios.

In this paper we describe the optimization of nucleoside phosphorylation with $POCl_3$, and the pitfalls that we encountered. Moreover, the subsequent conversion of the nucleoside dichlorophosphate into mixtures of mono-, di- and triphosphates is presented (scheme 1). We applied these reactions to obtain stable isotope labelled nucleotides. These mixtures were successfully applied in quantitative LC-MS/MS analyses.

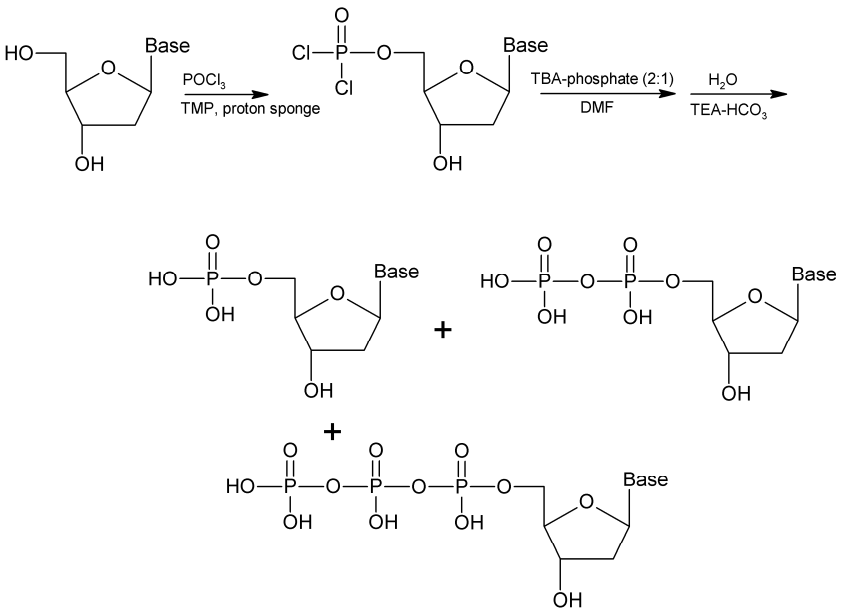

Scheme 1. Reagents and conditions: $POCl_3$ (15-18 equivalents), trimethylphosphate (TMP), tributylammonium(TBA)-phosphate (2:1, mole/mole, 20 equivalents), *N,N*-dimethylformamide (DMF), 1 M triethylammonium-bicarbonate (TEA-HCO_3).

Materials and Methods

Chemicals

2-Chloro-2′-deoxyadenosine (cladribine, 2CdA) was obtained from Sequoia Research Products (Pangbourne, UK), 2′, 2′ -difluoro 2′-deoxycytidine (gemcitabine, dFdC)·HCl and 2′, 2′ -difluoro 2′-deoxyuridine (dFdU) were kindly provided by Eli lilly and company (Indianapolis, IN, USA), whereas 5-aza-2′-deoxycytidine (decitabine, aza-dC) was purchased from Sigma. ^{13}C, $^{15}N_2$-labeled dFdC (*dFdC) and dFdU (*dFdU) were obtained from Toronto Research Chemicals (North York, ON, Canada). The structural formulas of the starting nucleosides are presented in figure 1.

Trimethylphosphate and *N,N*-dimethylformamide (DMF) were from Aldrich (St. Louis, MO, USA), whereas 1 M triethylammonium bicarbonate pH 8.5 and 3 Å molecular sieves were from Fluka (St. Louis, MO, USA). 1,8-Bis(dimethylamino)naphthalene (Proton sponge), phosphoric acid crystals and tributylammonium(TBA)-pyrophosphate (1.5 moles TBA per mole pyrophosphate, (1.5:1, mole/mole)) were bought from Sigma. Phosphorous oxychloride ($POCl_3$) and tributylamine (TBA) were obtained from Fluka and Sigma Aldrich, respectively. All solvents used in the synthesis were purchased as anhydrous and required no further drying.

Tetrabutylammonium dihydrogenphosphate, potassium dihydrogen phosphate, 25% ammonia and 2-propanol were all from Merck (Darmstadt, Germany) and methanol from Biosolve Ltd (Amsterdam, The Netherlands).

TBA-phosphate (1:1. mole/mole) in DMF (250 µM) was prepared by mixing 600 µL TBA with 245 mg phosphoric acid crystals and adding DMF to 10 mL. TBA-phosphate (2:1, mole/mole) was prepared in the same way, but by adding 1200 µL TBA. Water attracted during preparation was removed by overnight storage over 3 Å molecular sieves.

TBA-pyrophosphate (2.4:1, mole/mole) in DMF (250 µM) was prepared by dissolving 0.163 mmol TBA-pyrophosphate (1.5:1, mole/mole) in 620 µL DMF and adding 33 µL TBA.

Monitoring of reactions

The reactions were monitored using ion-pairing high performance liquid chromatography with ultraviolet detection (HPLC-UV). In-process samples of 10 µL were hydrolyzed in 90 µL 1 M triethylammonium-bicarbonate on ice. The nucleoside dichlorophosphate intermediates were thus converted into nucleoside monophosphates.

HPLC-UV experiments were executed on an Agilent 1100 series liquid chromatograph system (Agilent technologies, Palo Alto, CA, USA) consisting of a binary pump, an in-line degasser, autosampler and UV

detector. Data were acquired using Chromeleon 6.50 software (Dionex corp., Sunnyvale, CA, USA).
The mobile phase consisted of 10 mM tetrabutylammonium dihydrogenphosphate with 70 mM potassium dihydrogen phosphate in methanol-water (16:84, v/v) and was delivered isocratically to a Synergi hydro-RP column (150 x 2.0 mm ID, 4 µm particles; Phenomenex, Torrance, CA, USA) with a flow of 0.25 mL/min. Injections of 1 µL were carried out with the autosampler thermostated at 4 °C. Absorption was measured at 268 nm (dFdC), 264 nm (2CdA), 258 nm (dFdU) and 243 nm (aza-dC).
Alternatively, reactions could be monitored semi-quantitatively using thin layer chromatography. Using a capillary, 1 µL of the hydrolyzed in-process samples was spotted onto a HPTLC silica gel F_{254} plate (Merck, Darmstadt, Germany). The reaction products were separated using 2-propanol, 25% ammonia and water (55:35:10, v/v/v). Formation of the nucleoside dichlorophosphate was observed under UV light (254 nm) as the appearance of a spot with an R_f lower (~0.7) than that of the starting nucleoside (R_f ~ 0.9).

Optimization of the phosphorylation of nucleoside dichlorophosphates

A quantity of 0.05 mmole dFdC·HCl was treated with $POCl_3$ as described under "Final phosphorylation procedure". After 150 minutes, 150 µL aliquots of the reaction mixture were transferred to 1.5 mL tubes on ice with 240 µL DMF containing TBA-pyrophosphate (2.4:1, mole/mole), TBA-phosphate (1:1, mole/mole), TBA-phosphate (2:1, mole/mole) or no reagent. The reagents were tested in an excess of 5, 10, 15 and 20 equivalents. In-process samples were taken after 1 and 5 minutes, and the reaction was quenched after 10 minutes by the addition of 880 µL 1 M triethylammonium-bicarbonate.

Final phosphorylation procedure

The glassware and, if the melting point allowed it, nucleosides were dried overnight at 85°C. In a 10 mL round flask, 0.05 mmole nucleoside (1 equivalent) was dissolved in 2.5 mL trimethylphosphate together with 0.1 mmol (2 equivalents) Proton sponge. dFdC·HCl and aza-dC required gentle heating over a flame to dissolve. $POCl_3$ (0.8 mmol, 16 equivalents) was added dropwise to the stirred solution on ice in about 10 minutes. After addition of all the $POCl_3$, the reaction was continued at room temperature until maximal nucleoside dichlorophosphate was formed (2.5-6.5 hours). Then, the reaction mixture was again cooled on ice, and 4 mL cold 250 µM TBA-phosphate (2:1, mole/mole) in DMF was added under vigorous stirring. After 10 minutes, the reaction mixture was quenched by pouring it into 20 mL 1 M triethylammonium-bicarbonate buffer. Finally, the reaction

product was lyophilized overnight to remove the volatile reactants, resulting in a solid white residue.

Purification

Although not required for their use as internal standards, further purification could be performed after reconstitution of the crude lyophilized reaction mixture in water. Volumes of 100 µL product (reconstituted in 500 µL water) were injected onto a Biosep DEAE-PEI column (75 x 7.8 mm ID, 7µm particles; Phenomenex) and separated using an ammonium-bicarbonate gradient (0-900 mM) at 0.5 mL/min. The UV-absorption of the eluate was monitored and the fractions containing the products were lyophilized twice to remove all mobile phase components.

Identification

Identity of the synthesized nucleotides was assessed using weak anion exchange chromatography (2CdA) and porous graphitic carbon chromatography (dFdC, dFdU, aza-dC) coupled with tandem mass spectrometric detection (HPLC-MS/MS) [7;8]. The identity was confirmed based on retention time and specific mass transitions

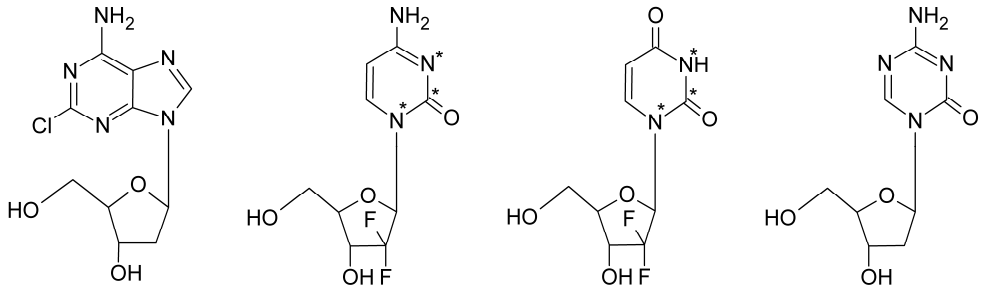

Figure 1. Structural formulas of the nucleosides described in the experiments. The asterisks indicate the position of ^{13}C- and ^{15}N-atoms in the stable isotope labelled compounds.

Results and discussion

Hydrolyzation buffer

In our initial experiments with 2CdA we used 2 equivalents of $POCl_3$, and 2 mL 0.2 M triethylammonium-bicarbonate buffer (4 equivalents) to hydrolyze the nucleoside dichlorophosphate to the nucleoside monophosphate. The desired product 2CdA monophosphate (2CdAMP) was, however, not observed in the final reaction mixture. We did, on the other hand, mainly observe a peak that we identified as 2-chloro-adenine, the base of 2CdA. This base is formed after cleavage of the acid-labile N-glycosidic bond between the sugar and the base of 2CdA. Although the final pH was around 8.5 we hypothesized that HCl, formed in the reaction between $POCl_3$ and water, caused local acidity resulting in the cleavage of this glycosidic bond. Indeed, 2-chloro-adenine was no longer found in reaction products that were hydrolyzed with 10 mL 1 M triethylammonium-bicarbonate (200 equivalents). A buffer with a sufficient capacity thus prevented acid hydrolysis of the reaction products.

Drying of nucleosides

Still, the obtained 2CdAMP yields (~4%) were far below the yields commonly reported for other nucleosides (60-90%) [9]. HPLC-UV analysis of the final reaction product showed that it consisted mainly of unreacted nucleoside. Any water present in the nucleoside starting material will react with $POCl_3$ to form HCl and phosphate, thereby inactivating the phosphytilating agent. We argued that traces of water present in the starting material reacted with the $POCl_3$ instead of the nucleosides. We therefore 1) dried 2CdA before use (85 °C, overnight) and 2) added extra $POCl_3$. Both approaches resulted in a marked increase in nucleoside dichlorophosphate formation, as shown in figure 2. Using the dried 2CdA starting material, 2CdAMP was already observed after the addition of 1 $POCl_3$ equivalent. In contrast, similar 2CdAMP formation was only observed after the addition of 3 $POCl_3$ equivalents to the non-dried material. Drying of the nucleoside starting material thus improves the phosphorylation reaction. Considerable yields could, however, still be obtained with the non-dried material if sufficient amounts of $POCl_3$ were added.

Excess of phosphorous oxychloride

Drying of the nucleosides at elevated temperatures was, however, not feasible for compounds with a low melting point such as dFdU (51-53 °C) and nucleosides might still contain water after drying overnight. Moreover, water can originate from solvents, glassware and the air. Others have dried nucleosides in vacuum, used distilled $POCl_3$ and carried out reactions

under nitrogen to perform the reaction under anhydrous conditions [10;11]. We hypothesized that further increasing the $POCl_3$ excess was another, easier approach.

Throughout the literature $POCl_3$ is used in small excesses (1.5-3 equivalents) [5;12-14] . Risbood et al. , on the other hand, recently used a very large excess (43 equivalents) [15].

We have increased the excess of $POCl_3$ up to 43 equivalents and found that increasing the amount of $POCl_3$ resulted in improved nucleoside dichlorophosphate formation. To decrease the risk of interference from unreacted $POCl_3$ in the subsequent reaction step, we used 15-18 $POCl_3$ equivalents in further experiments. The reaction with this excess of $POCl_3$ was monitored for all experiments. The results are shown in figure 3. The phosphorylation of the same dFdU starting material was repeated and was found to be reproducible (49.7 and 57.3% after 4 hours). The reaction was, on the other hand, dependent on the type of nucleoside and their origin, as illustrated by the difference between dFdC-dFdU and between dFdU-*dFdU phosphorylation. Still, acceptable nucleoside dichlorophosphate yields (46-76%) were obtained if the reaction time was adjusted for each nucleoside. Monitoring of the reaction is, however, indispensable to obtain optimal yields.

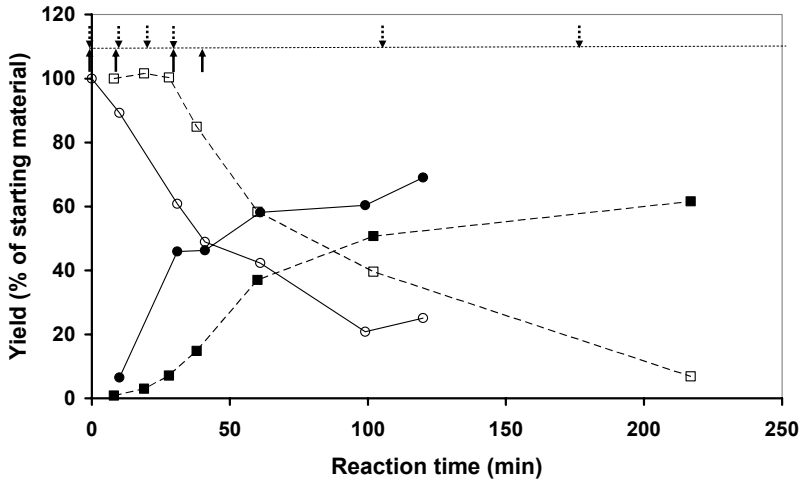

Figure 2. Formation of 2CdA dichlorophosphate and the decrease of 2CdA using dried (● and ○, respectively) and non-dried (■ and □, respectively) 2CdA starting material. The arrows represent the addition of $POCl_3$ equivalents to dried (solid arrow) and non-dried (dotted arrow) 2CdA.

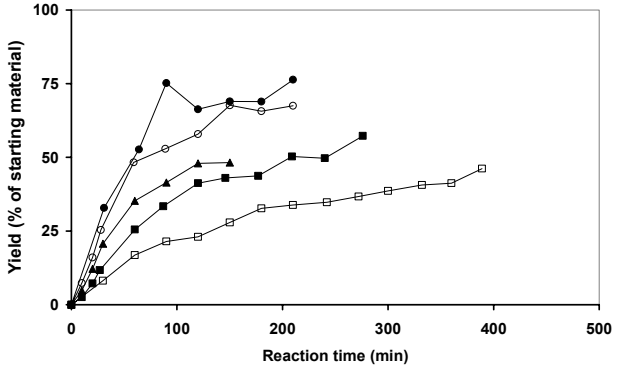

Figure 3. Formation of nucleoside dichlorophosphates of dFdC (●) , *dFdC(○), dFdU (■), *dFdU (□) and aza-dC (▲) with 15-18 equivalents $POCl_3$ added.

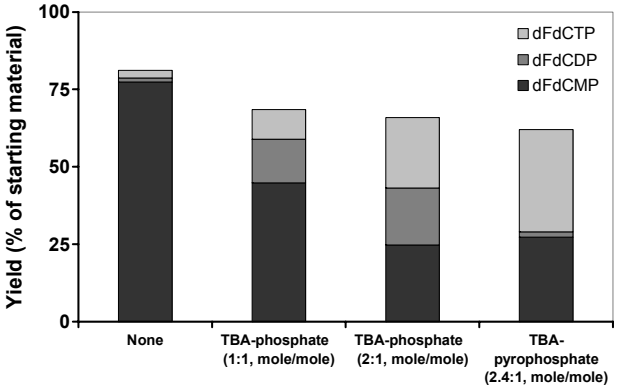

Figure 4. Effect of the reagent on the formation of dFdC nucleotides (20 equivalents, 10 minute reaction).

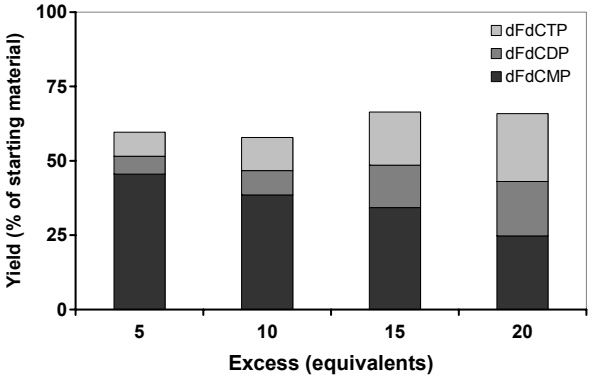

Figure 5. Effect of the excess of TBA-phosphate (2:1, mole/mole) on the formation of dFdC nucleotides (10 minute reaction).

Conversion of nucleoside dichlorophosphate to nucleotide mixture

Hoffmann et al. showed that the addition of phosphoric acid to a nucleoside dichlorophosphate, in the presence of an organic base, resulted in the formation of nucleoside mono-, di- and triphosphates in different ratios [6]. Of the organic bases tested, TBA resulted in the most balanced nucleotide formation. We therefore used TBA as organic base in our experiments.

We performed the reaction with several equivalents of TBA-phosphate (1:1, mole/mole) and (2:1, mole/mole) and TBA-pyrophosphate (2.4:1, mole/mole). We added extra TBA because Ludwig et al. reported that this increased the yield in a similar triphosphate synthesis [4].

The reaction mixtures were assayed after 1, 5 and 10 minutes. The reaction time of the second reaction step was, however, of minor importance as the reaction was already complete after 1 minute (data not shown).

The type of reagent and the excess in which it was used were, on the other hand, pivotal to obtain equimolar nucleotide mixtures. The effect of the type of reagent is shown in figure 4. When no reagent was added the overall yield was the highest, but the product mainly consisted of nucleoside monophosphate. The amount of di- and triphosphate was higher when TBA-phosphate (1:1, mole/mole) was added and increased even further with extra TBA (2:1, mole/mole). TBA most likely increases the activation for the nucleophilic phosphate attack [6]. With TBA-pyrophosphate (2.4:1, mole/mole), the main product formed was the triphosphate, but the monophosphate was only slightly less abundant.

All reagents showed an increased formation of higher phosphates when applied in a larger excess. The effect of the excess of TBA-phosphate (2:1, mole/mole) on the formation of the dFdC nucleotides is depicted in figure 5.

Based on these results we concluded that 20 equivalents of TBA-phosphate (2:1, mole/mole) were optimal to obtain an equimolar mixture of nucleoside mono- di- and triphosphates.

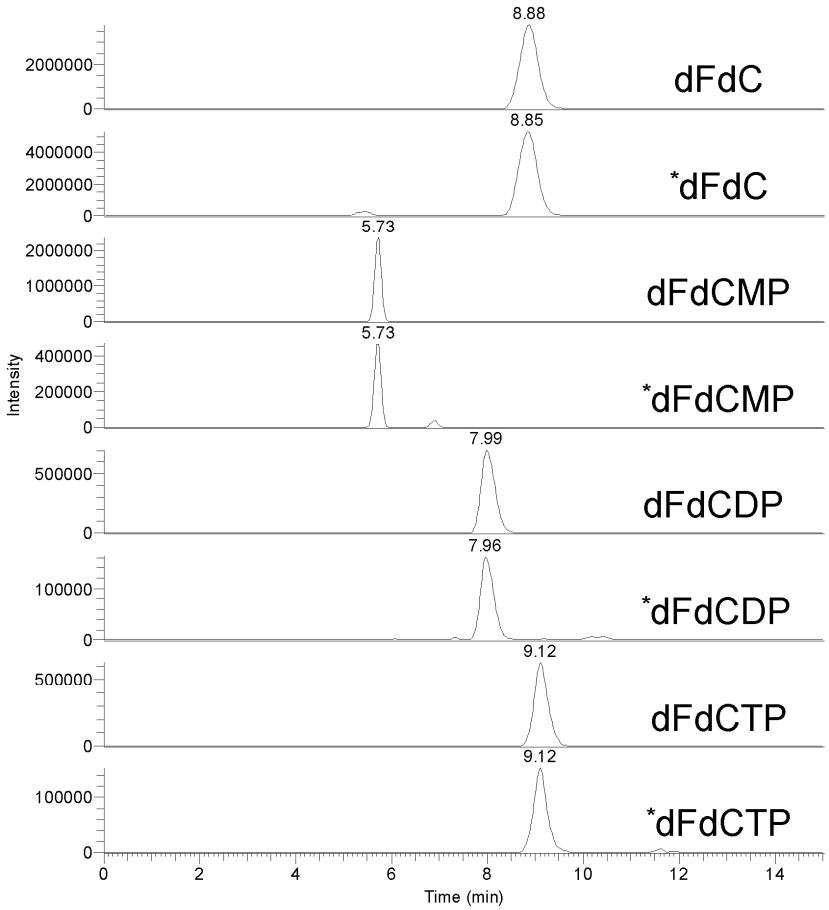

Figure 6. HPLC-MS/MS chromatograms of a mixture of dFdC, dFdCMP, dFdCDP and dFdCTP and their stable isotope labelled internal standards. Conditions were as previously described [7], with the following mass transitions: 264→112 and 267→115 for dFdC and *dFdC, 344→246 and 347→249 for dFdCMP and *dFdCMP, 424→326 and 427→329 for dFdCDP and *dFdCDP and 504→326 and 507→329 for dFdCTP and *dFdCTP

Application to an LC-MS/MS assay

The final method was successfully used to synthesize mixtures of *dFdC- and *dFdU nucleotides. The reaction mixtures could be used as internal standards for an LC-MS/MS assay without further purification. Figure 6 shows a typical chromatogram of dFdC and *dFdC and their mono-, di- and triphosphate using porous graphitic carbon chromatography, under previously described conditions [7]. Because the synthesized *dFdC internal standards elute at the same time as their unlabelled variants, compounds that interfere with the signal intensity will affect the signal of the dFdC analytes as much as that of the *dFdC analytes. The ratio of the two signals will therefore remain constant under the variable conditions in biological matrices, resulting in improved accuracy and precision of the quantitative method.

We have experienced several problems in the general phosphorylation methods described by others. Likewise, Risbood et al. were not able to synthesize dFdCTP using these methods. They, therefore, first synthesized, isolated and purified dFdCMP, and then used a second reaction to phosphorylate dFdCMP to dFdCTP. We found that an $POCl_3$ excess of 15-18 equivalents resulted in increased nucleoside phosphorylation, and that the formed nucleoside dichlorophosphate intermediate could readily be converted into a well balanced mixture of mono-, di- and triphosphates.

Conclusion

We identified residual water in nucleoside starting material and cleavage of the N-glycosylic bond as pitfalls in the reaction of nucleosides with $POCl_3$. These problems could be avoided by using a large excess of $POCl_3$ and a hydrolyzation buffer with sufficient capacity. By adding TBA-phosphate (2:1, mole/mole) the formed nucleoside dichlorophosphate can subsequently be converted into a well-balanced mixture of the mono-, di- and triphosphate. This mixture can readily be used as internal standard for quantitative tandem mass spectrometric assays.
The described reaction can easily be executed in laboratories with limited experience in organic chemistry, without extensive drying procedures.

References

[1] K. Burgess, D. Cook, Chem. Rev. 100 (2000) 2047.

[2] M. Yoshikawa, T. Kato, T. Takenishi, Tetrahedron Lett. 8 (1967) 5065.

[3] M. Yoshikawa, T. Kato, T. Takenishi, Bull. Chem. Soc. Jpn. 42 (1969) 3505.

[4] J. Ludwig, Acta Biochim. et biophys. Acad. Sci. Hung. 16 (1981) 131.

[5] N. C. Mishra, A. D. Broom, J. Chem. Soc. , Chem. Commun. (1991) 1276.

[6] C. Hoffmann, H.-G. Genieser, M. Veron, B. Jastorff, Bioorg. Med. Chem. Lett. 6 (1996) 2571.

[7] R. S. Jansen, H. Rosing, J. H. Schellens, J. H. Beijnen, J. Chromatogr. A 1216 (2009) 3168.

[8] R. S. Jansen, H. Rosing, C. J. de Wolf, J. H. Beijnen, Rapid Commun. Mass Spectrom. 21 (2007) 4049.

[9] J. L. Ruth, Y. C. Cheng, Mol. Pharmacol. 20 (1981) 415.

[10] B. Fischer, J. L. Boyer, C. H. Hoyle, A. U. Ziganshin, A. L. Brizzolara, G. E. Knight, J. Zimmet, G. Burnstock, T. K. Harden, K. A. Jacobson, J. Med. Chem. 36 (1993) 3937.

[11] B. H. A. Knoblauch, C. E. Muller, L. Jarlebark, G. Lawoko, T. Kottke, M. A. Wikstrom, E. Heilbronn, Eur. J. Med. Chem. 34 (1999) 809.

[12] E. L. White, W. B. Parker, L. J. Macy, S. C. Shaddix, G. McCaleb, J. A. Secrist, III, R. Vince, W. M. Shannon, Biochem. Biophys. Res. Commun. 161 (1989) 393.

[13] I. Shoshani, V. Boudou, C. Pierra, G. Gosselin, R. A. Johnson, J. Biol. Chem. 274 (1999) 34735.

[14] F. Seela, H. Muth, A. Roling, Helv. Chim. Acta 74 (1991) 554.

[15] P. A. Risbood, C. T. Kane, Jr., M. T. Hossain, S. Vadapalli, S. K. Chadda, Bioorg. Med. Chem. Lett. 18 (2008) 2957.

Chapter 2

Bioanalysis

of intracellular nucleoside and nucleotide analogs

Chapter 2.1

Mass spectrometry in the quantitative analysis of intracellular nucleotide analogs

Robert S Jansen, Hilde Rosing, Jan HM Schellens and Jos H Beijnen

Submitted for publication

Abstract

Nucleoside analogs are widely used in anti-cancer, anti-(retro)viral and immunosuppressive therapy. Nucleosides are prodrugs that require intracellular activation to mono-, di- and finally triphosphates. Monitoring of these intracellular nucleotides is important to understand their pharmacology.
The relatively involatile salts and ion-pairing agents traditionally used for the separation of these ionic analytes, limit the applicability of mass spectrometry (MS) for detection. Both indirect and direct methods have been developed to circumvent this apparent incompatibility. Indirect methods consist of dephosphorylation of the nucleotides into nucleosides before the actual analysis. Various direct approaches have been developed, ranging from the use of relatively volatile or very low levels of regular ion-pairing agents, hydrophilic interaction chromatography (HILIC), weak anion-exchange or porous graphitic carbon columns to capillary electrophoresis and MALDI-TOF-MS.
In this review we present an overview of the publications describing the quantitative analysis of therapeutic intracellular nucleotide analogs using MS. The focus is on the different approaches for their direct analysis. We conclude that despite the technical hurdles, several useful MS-compatible chromatographic approaches have been developed, enabling the use of the excellent selectivity and sensitivity of MS for the quantitative analysis of intracellular nucleotides.

Introduction

Nucleoside analogs form a class of drugs that is widely used in anti-cancer, anti-(retro)viral and immunosuppressive therapy. Their structural formulas are composed of a sugar and a base moiety (figure 1). The base moiety can consist of a pyrimidine base (cytosine (C), thymine (T), uracil (U)) or a purine base (adenine (A), guanine (G)), whereas the sugar moiety consists of ribose or deoxyribose. Nucleoside analogs can be modified at the base moiety as well as at the sugar moiety (figure 2 and 3). Nucleoside analogs are anti-metabolites that are metabolized through the same pathways as their natural counterparts. Through these pathways they are consecutively converted into their monophosphate (MP), diphosphate (DP) and finally triphosphate (TP) in cells. The phosphorylation of nucleoside analogs is depicted in figure 4, with zidovudine (AZT) as example. Other analogs are administered as nucleoside analog prodrug (abacavir (ABC)), base (6-mercaptopurine (6-MP)) or non-hydrolysable monophosphate (tenofovir (PMPA), adefovir (PMEA)) and undergo slightly different activation pathways.

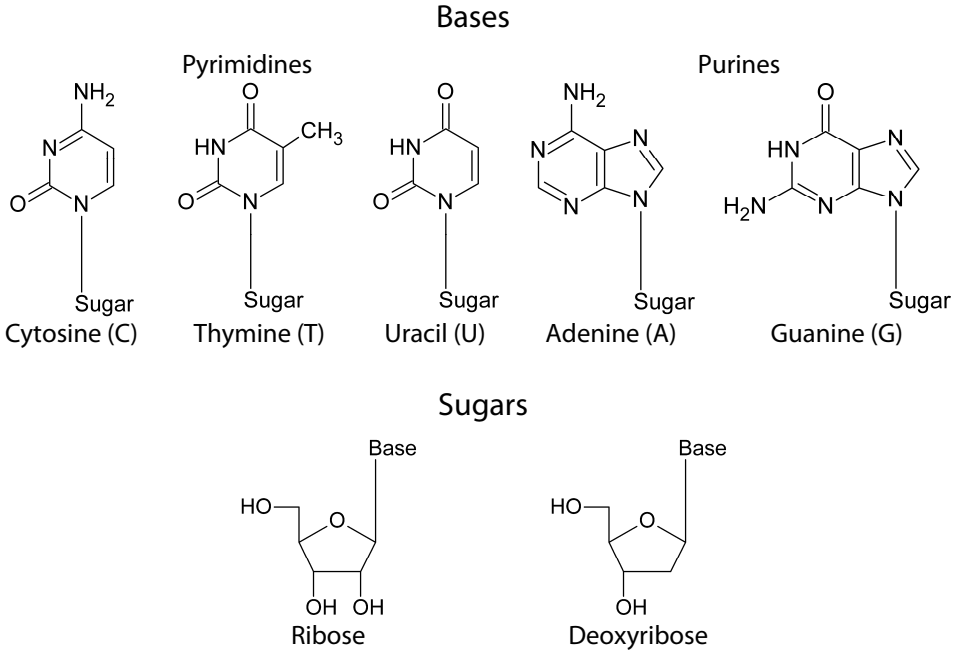

Figure 1. Structural elements of nucleosides

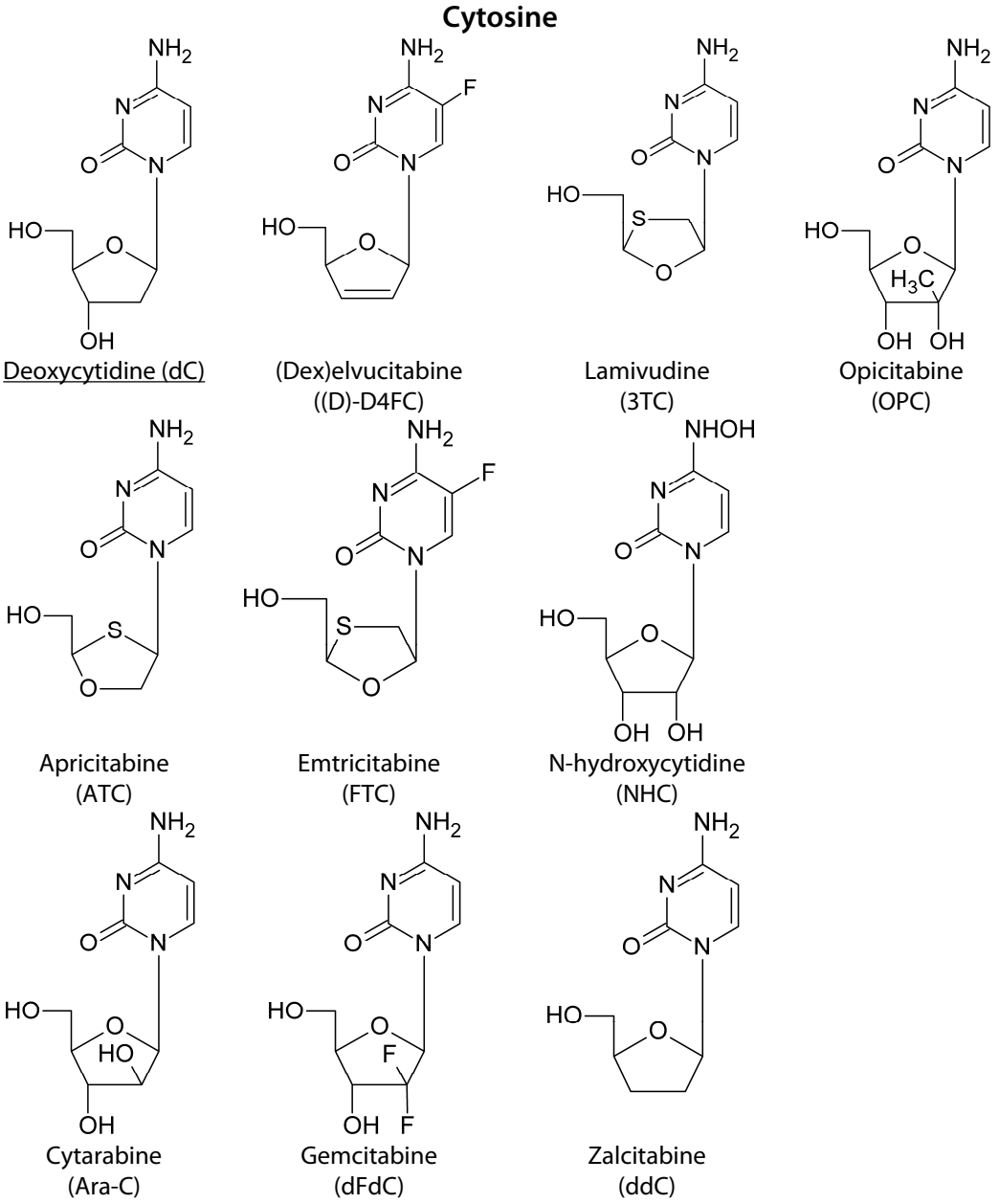

Figure 2. Chemical structures of pyrimidine analogs and their natural counterparts

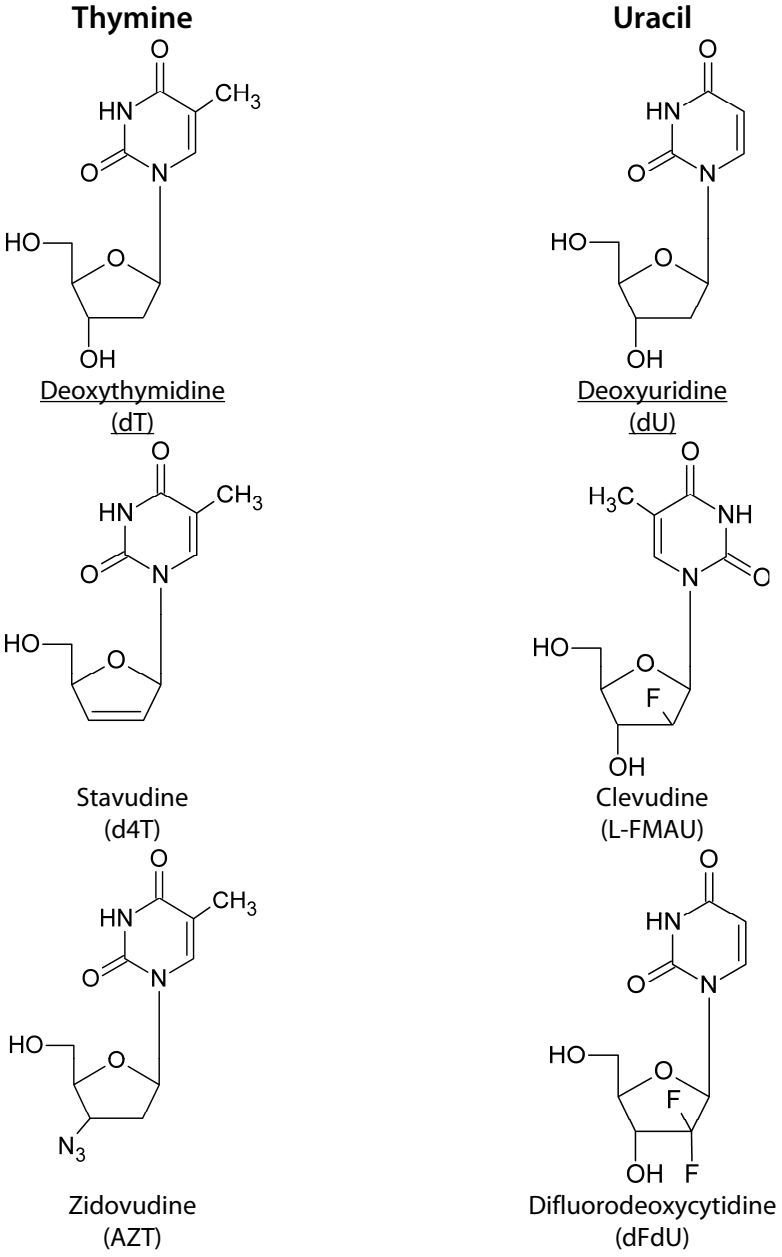

Figure 2. Chemical structures of pyrimidine analogs and their natural counterparts (continued)

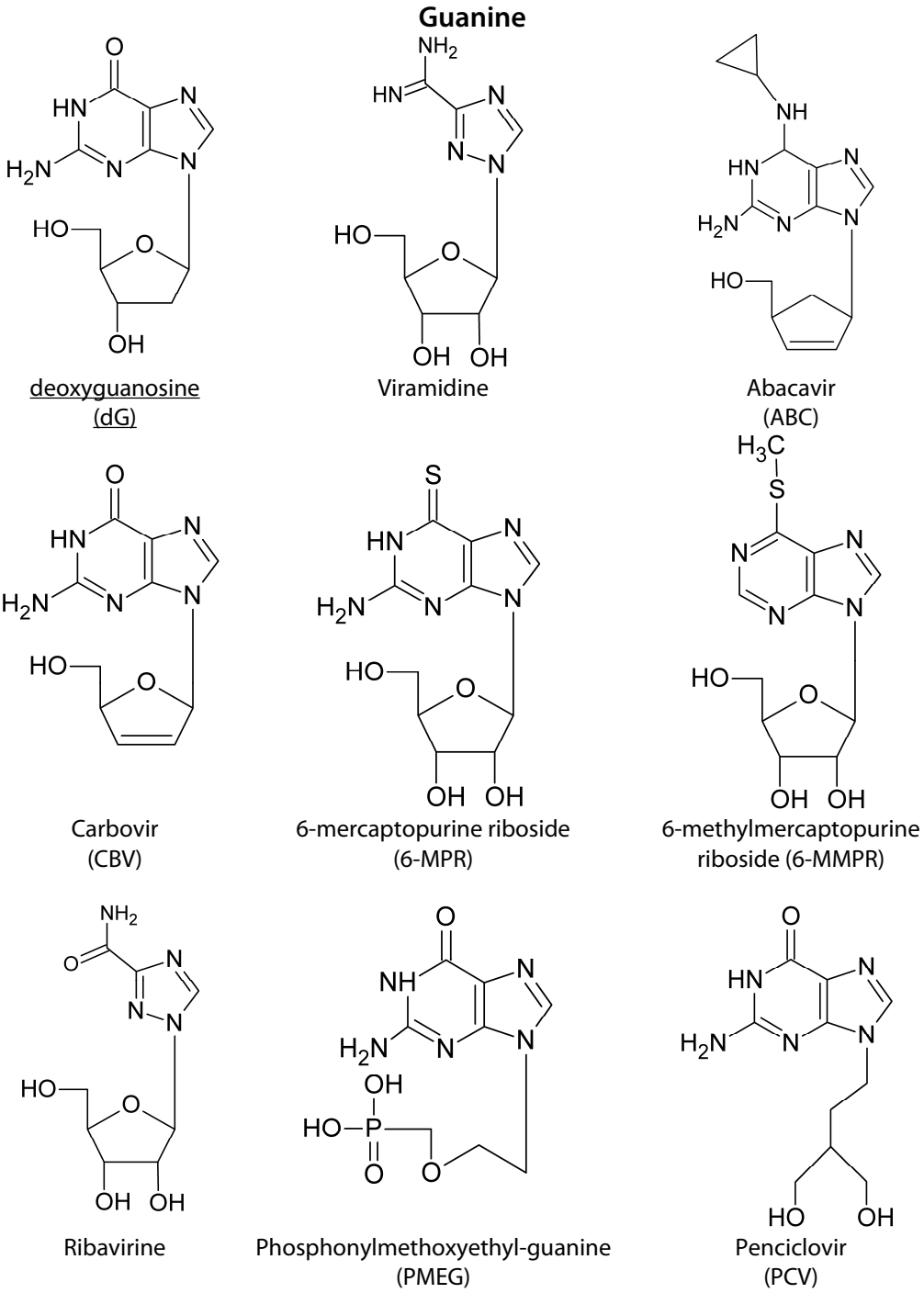

Figure 3. Chemical structures of purine analogs and their natural counterparts

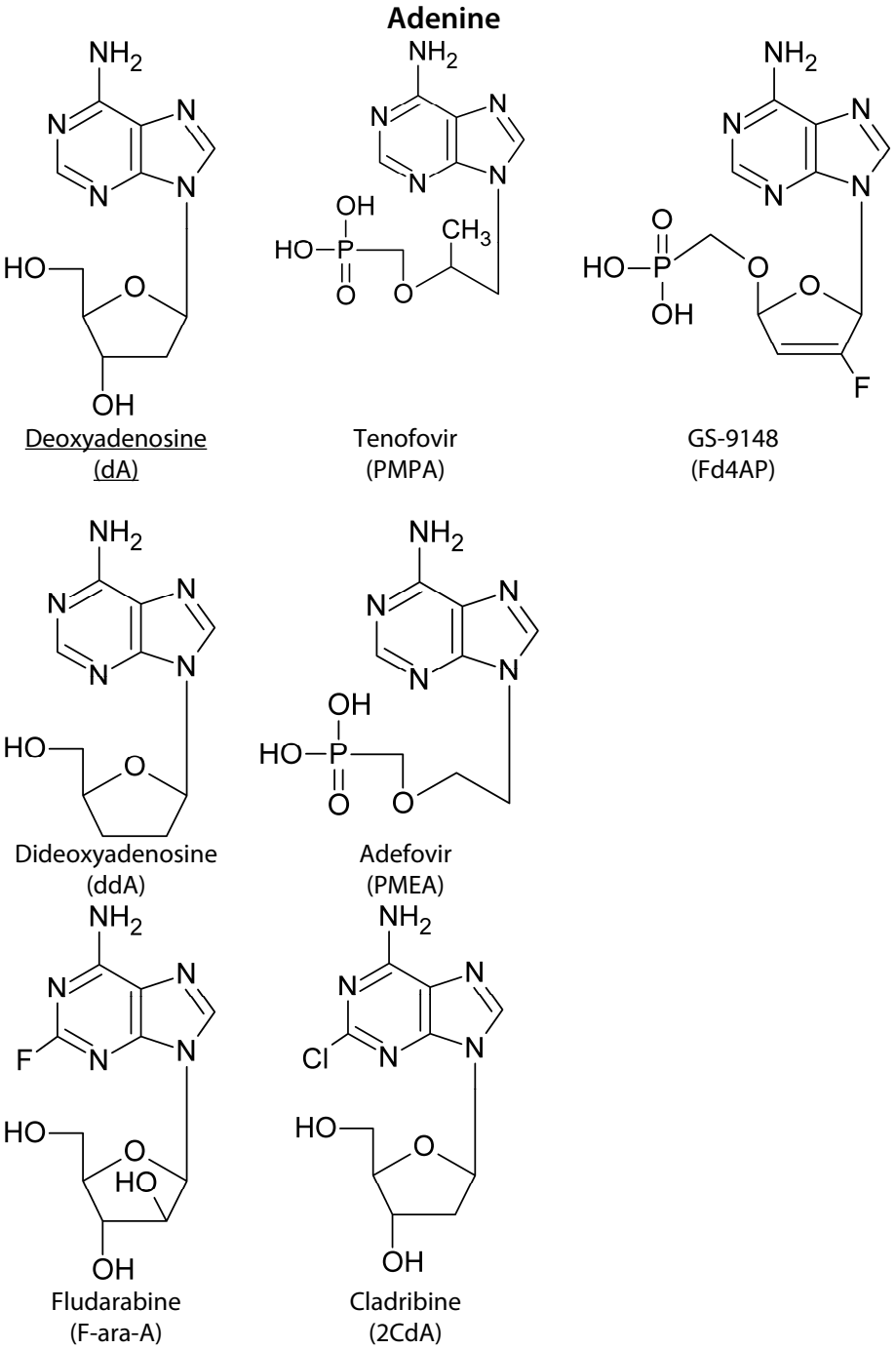

Figure 3. Chemical structures of purine analogs and their natural counterparts (continued)

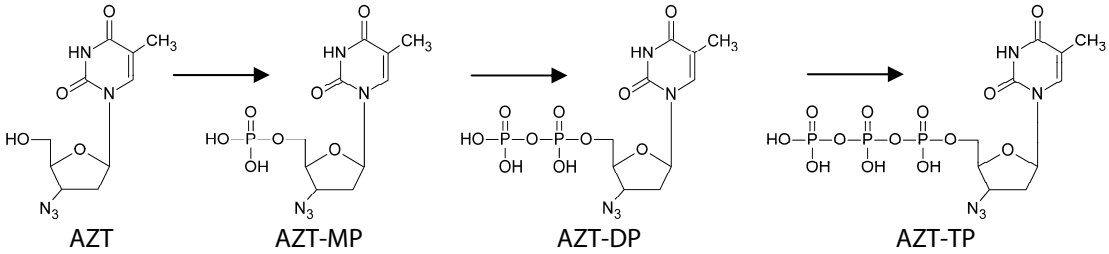

Figure 4. Phosphorylation route of zidovudine (AZT)

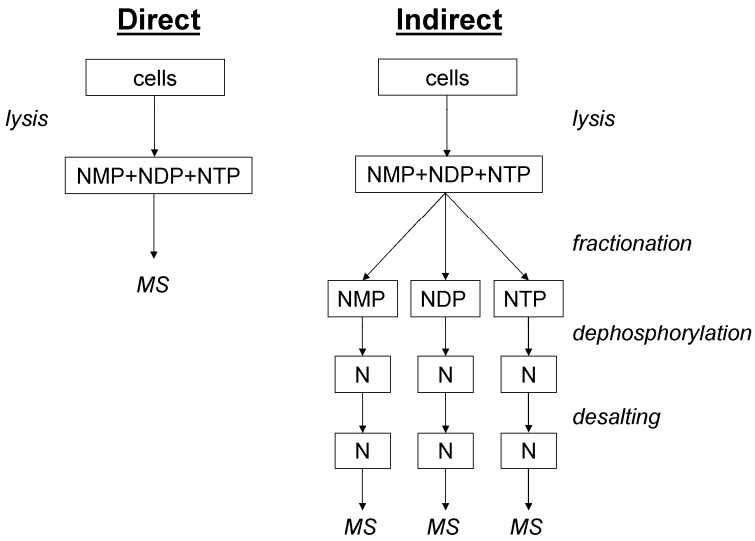

Figure 5. Schematic representation of direct and indirect methods for the analysis of nucleotides (N = nucleoside; NMP, NDP and NDP = nucleoside mono-, di- and triphosphate)

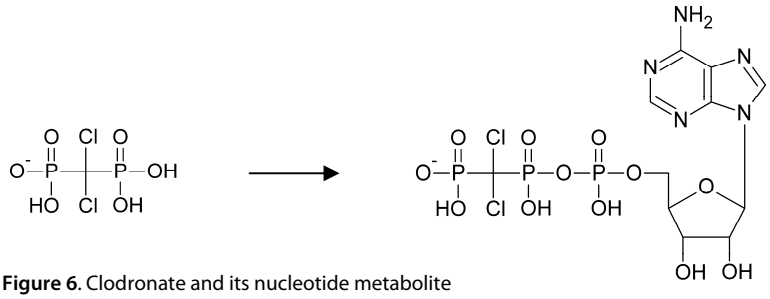

Figure 6. Clodronate and its nucleotide metabolite

The TP form inhibits human and viral DNA and RNA polymerases and is incorporated into nucleic acids, slowing down cell proliferation or viral replication. Therefore, the TP form is considered to be the main active metabolite. The MP and DP, however, can be pharmacologically active as well. Monitoring of these intracellular nucleotide analogs is imperative to understand their pharmacology [1] and can be used for therapeutic drug monitoring [2].

It is therefore not surprising that a myriad of analytical methods has been developed for the quantitative determination of nucleotide analogs in cells. A review on the analysis of nucleoside reverse transcriptase inhibitors (NRTIs) and their phosphorylated metabolites in human immunodeficiency virus (HIV)-infected matrices has recently been published by Lai et al. [3]. The analytical methods can be divided into direct and indirect methods.

Indirect methods consist of a dephosphorylation step, in which the nucleotides are reconverted into nucleosides, followed by quantification (figure 5). The dephosphorylation can be performed with or without prior fractionation of the nucleotides on an anion exchange column, resulting in separate results for the MP, DP and TP or in a total nucleotide amount. The subsequent quantification has been performed using radioimmunoassays [4;5] and high performance liquid chromatography (HPLC) with ultraviolet [6] or fluorescence detection [7]. More recently, mass spectrometric (MS) detection was introduced for subsequent quantification.

Direct methods do not use a dephosphorylation step, and analyze the nucleotides as such (figure 5). Immunoassays have been used without any sample separation [8;9], but most methods require chromatographic separation before detection.

Traditionally, strong anion exchange (SAX) and ion-pairing liquid chromatography (IP-LC) have been used to separate these ionic analytes, which were then quantified using an enzymatic assay or radioactivity [10], ultraviolet [11] or fluorescence [12;13] detection. The use of relatively involatile salts and IP-agents, however, hamper the applicability of MS for detection. Nevertheless, various MS methods have now been developed for the direct analysis of nucleotides ranging from the use of relatively volatile or very low levels of regular IP-agents, weak anion-exchange (WAX) or porous graphitic carbon (PGC) columns to capillary electrophoresis (CE) and matrix assisted light desorption-time of flight (MALDI-TOF)-MS.

In this review we present an overview of the publications describing the quantitative analysis of intracellular nucleotide analogs of therapeutic nucleosides using MS, with the focus being on approaches for their direct analysis.

Sample collection

Matrix

Monitoring intracellular nucleotide analogs is more informative than monitoring nucleoside analogs because the active metabolites are determined, rather than their prodrug. Moreover, these active metabolites are determined at the target site. For this reason, nucleotide analogs active against hepatitis, acquired immunodeficiency syndrome (AIDS) and leukaemia have been measured (both *in-vitro* and *in-vivo*) in hepatocytes, peripheral blood mononuclear cells (PBMCs) and leukaemic blasts respectively [14-16]. Matrices associated with toxicity have also been analyzed, such as erythrocytes in ribavirin therapy [17]. Target tissue can, however, be difficult to obtain *in-vivo*. Therefore, surrogate matrices such as erythrocytes and PBMC's have been analyzed often to monitor therapy against inflammatory bowel disease and solid tumours [18;19]. Nucleotide levels may, however, differ between cell types [20;21], and even cell subtypes, as was shown for zidovudine (AZT) and lamivudine (3TC) nucleotides in PBMCs [22]. Therefore, careful selection and isolation of the matrix is pivotal for obtaining relevant results.

Cell isolation

Most methods use PBMCs as matrix. PBMCs can be isolated from relatively large volumes (5-25 mL) of whole blood by density gradient centrifugation. Whole blood is layered over a density gradient such as Ficoll-paque or directly drawn into commercially available cell preparation tubes containing a density gradient. Although rich in PBMCs, other cell types can be present as well. Special attention should be given to erythrocyte contamination. Samples with a pink or red color, an indication of erythrocyte contamination, showed a larger and more variable matrix effect [23]. Endogenous nucleotides originating from the red blood cells most likely caused ionization suppression observed as the changed matrix effect. More importantly, some analogs are phosphorylated in erythrocytes. Erythrocyte contamination can thus severely alter the amount of analyte present in a sample. Indeed, deliberately increasing the number of erythrocytes in a sample increased the amount of PMPA-DP. Clinical samples contained up to 7-fold more PMPA-DP with erythrocyte contamination compared to the same sample without erythrocyte contamination [21]. To prevent contamination an extra erythrocyte lysis step can be executed [21;24].

Because cells are still intact during isolation, ongoing analyte metabolism *ex-vivo* must be prevented. Isolation should therefore be performed as quickly as possible, and preferably on ice [25]. Finally, to express the

determined concentration per cell, the number of cells isolated should be quantitated. The most straightforward approach is to count the number of cells using a haemocytometer, microscope or flow cytometry, but protein [26] and DNA [27] determinations have also proven to be useful. Concluding, the cell isolation should remove interfering cells, after which the cells of interest can be processed further.

Extraction of nucleotides from cells

The nucleotide extraction step should be performed with a solution that completely extracts nucleotides, precipitates and inactivates proteins and in which the analytes are stable [28]. Moreover, the solution should not interfere with subsequent chromatography or MS detection.

Traditionally, extraction of nucleotides from cells has been executed with strong acids like perchloric acid. Although extraction yields with perchloric acid are good, analytes can be unstable at low pH and the perchloric acid and pH can influence the HPLC and pollute the MS. Although some MS methods still use perchloric acid, the vast majority of the described methods use MS-friendly 60-80% methanol (MeOH) or acetonitrile (ACN) with or without buffers and metal chelators. Mixtures of organic solvents and water are hypotonic and disrupt cell membranes, thus effectively extracting nucleotides [29;30]. Furthermore, the analytes are stable in MeOH lysate during lysis [31], and when stored at -70^{o}C [32]. Finally, organic solvent lysates can easily be concentrated by evaporation. Solutions containing 60-80% MeOH or ACN thus fulfill all requirements of an MS-compatible extraction solvent.

Bioanalytical methods

Indirect methods

Sample pretreatment

Indirect methods have been applied to determine the total as well as speciated nucleotide concentrations. Fractionation required for the speciation has been performed on WAX- (NH_2) and SAX- (QMA) solid phase extraction (SPE) columns, using high salt concentrations for elution. Proper separation of the nucleotides is pivotal for their correct quantification, but cannot be confirmed for each sample. As a consequence, the fractionation must be reproducible and well characterized to prevent co-elution of the nucleotides [33;34].

Dephosphorylation has mainly been performed using acid or alkaline phosphatase. Methods for the quantification of phosphorylated 6-mercaptopurine riboside (6-MPR) and 6-methylmercaptopurine riboside (6-MMPR) have, however, used hydrolysis (100 °C, 60 min), degrading the nucleotide analogs to their base and a derivative thereof [35]. Finally, an SPE purification step is performed to remove salts and enzymes from the crude dephosphorylated samples. Although the fractionation and dephosphorylation are critical in the analytical process, most methods do not use an internal standard during these steps. Moreover, systematic differences have been observed between hydrolysis techniques [36], and between indirect and direct methods [37].

It is evident that indirect methods are labour intensive because samples have to be fractionated, dephosphorylated and purified before the actual analysis. Also, each fraction has to be analyzed separately, requiring extra instrument time. Moreover, the extensive and relatively uncontrolled sample pretreatment is a potential source of errors. The final analysis is, however, relatively simple, fast and selective.

Concluding, dephosphorylation simplifies the final analysis, but increases analysis time and introduces potential pitfalls in sample pretreatment.

Separation and detection

LC-MS

After dephosphorylation the nucleosides have been separated on normal and polar-modified C_{18} columns using isocratic elution or straightforward gradients of ACN or MeOH in formate or acetate buffers. All methods applied the positive ion mode for detection, except one method for AZT [38]. The developed methods have been used to support large clinical studies [39;40]. The indirect methods for the quantification of intracellular nucleotide analogs are summarized in table 1.

Accelerator mass spectrometry

Accelerator mass spectrometry (AMS) is an ultra sensitive technique to specifically measure isotopes such as ^{14}C, a carbon isotope with a very low natural abundance [41]. The method can therefore be used to specifically detect ^{14}C-containing drugs and their metabolites at very low concentrations.

All structural information is, however, lost because samples need to be graphitized before analysis. The method has been used to measure ^{14}C-labeled AZT in PBMCs [42], but because no separation was performed, the found concentrations were the sum of all AZT metabolites in the PBMCs, including those incorporated in nucleic acids. After isolation and dephosphorylation of AZT-TP the methodology could, however, be used for the specific quantification of ^{14}C-labeled AZT-TP in PBMCs [43]. The results obtained with this AMS method were in very good agreement with a conventional indirect LC-MS/MS [44], but the AMS method about 30,000-fold more sensitive, enabling ^{14}C detection in the atto- to zeptogram range (10^{-18}–10^{-21} g). Therefore, AMS can be used to reduce sample size or to answer specific research questions requiring extreme sensitivity.

Direct methods

In this section methods for the direct determination of nucleotide analogs in cells are described. The validation parameters that should be assessed for these methods have been described in detail by Becher et al. [28].

Sample pre-treatment

After PBMC isolation, further sample pretreatment of direct methods generally consists of sample pre-concentration by evaporation of the organic phase or neutralization of the lysis solution. Other sample pretreatment has, however, also been performed. For example, IP-SPE [14], WAX-SPE [45;46] and regular SPE [47] have been applied for the analysis of emtricitabine (FTC)-TP, ara-CTP and PMPA-DP. Using immobilized metal affinity chromatography (IMAC), Tuytten et al. were able to trap nucleotides on a column [48]. The electron-donating phosphate groups of the nucleotides complexated with immobilized Fe^{3+}-ions on the column and could subsequently be eluted using a basic phosphate buffer. In this pilot study the methodology was used for on-line sample pre treatment in

Table 1. Indirect methods for the quantification of intracellular nucleotide analogs

Matrix	Analyte	Extraction	Further sample pretreatment	Column	Mobile phase	MS (polarity)	LLQ	Val.	Ref.
PBMCs CEM_{ss} cells	AZT-TP	70% MeOH	F: Sep-Pak QMA, DP: ACP, DS: XAD resin	Hypersil C_{18} (100X2.1 mm ID)	H-Ac:ACN:MeOH:W (0.25:10:30:59.75, v/v)	QqQ (+)	4.0 fmol/10^6 cells (LOD)	No	[112]
PBMCs	3TC-TP AZT-TP d4T-TP	60% MeOH	F: Sep-Pak QMA, DP: ACP, DS: Sep-Pak C_{18}	Columbus C_{18} (100X1 mm)	10 mM A-Ac:ACN (86:14, (v/v)	QqQ (+)	0.2 pmol/sample[a] 0.2 pmol/sample[a] 0.2 pmol/sample[a]	Yes	[109]
PBMCs	3TC-TP AZT-TP	70% MeOH	F: Sep-Pak QMA, DP: ACP, DS: XAD resin	Hypersil C_{18} (100X2.1 mm)	H-Ac:ACN:MeOH:W (0.25:10:30:59.75, v/v)	QqQ (+)	0.4 pmol/sample[b] 0.1 pmol/sample[b]	No	[119]
CEM-T4 cells	ddA-TP	70% MeOH, pH 7.4	F: Sep-Pak QMA, DP: ACP, DS: Sep-Pak C_{18}	Purospher RP-18e (30X2.1 mm)	1% H-Fo in: MeOH:W (25:75, v/v)	QqQ (+)	0.02 ng/mL[c]	Partial	[114]
Spleen tissue	3TC-MP AZT-MP	Homogenization	F: Isolute NH_2, DP: ACP, DS: Isolute ENV+	Polaris C_{18} (150X2.0 mm)	**A**: 0.1% H-Fo **B**: ACN	Q (+/-)	< 10 ng/g < 10 ng/g	Partial	[38]
PBMCs	3TC-TP	60% MeOH	F: Waters QMA Accell, DP: ALP, DS: Isolute C_{18}	Columbus C_{18} (100X1 mm)	10 mM A-Ac:ACN (86:14, (v/v)	NS (+)	Not specified	No	[110]
Erythrocytes	6-MPR (total) 6-MMPR (total)	70% PCA, dithiothreitol	DP: Hydrolysis (100°C, 60 min)	Atlantis dC_{18} (150X2.1 mm)	**A**: 0.1% H-Fo in 2.5 mM A-Ac,; **B**: 0.1% H-Fo in ACN	QqQ (+)	110 pmol/8X10^8 cells[d] 18 pmol/8X10^8 cells[d]	Yes	[18]
Liver tissue (human monkey)	Ribavirin (total)	5.0% PCA	Neutralization, DP: ACP, DS: Supelco NH_2	Zorbax SB C_{18} (150X4.6 mm)	**A**: 0.1% H-Ac; **B**: 0.1% H-Ac in MeOH	QqQ (+)	1.0 µg/g	Yes	[113]
PBMCs	AZT-TP	70% MeOH	F: Waters QMA Accell plus, DP: ACP, DS: Oasis HLB	Xterra rp18 (150X2.1 mm)	**A**: 0.1% H-Ac; **B**: ACN:W (10:90, v,v)	QqQ (+)	5.0 fmol/10^6 cells[e]	Yes	[44]
PBMCs	PMPA-DP	70% MeOH	F: Waters QMA Accell plus, DP: ACP, DS: Oasis HLB	Synergi polar, 80A (150X2.0 mm)	H-Ac:ACN:W (1:3:96, v/v)	QqQ (+)	10 fmol/10^6 cells[f]	Yes	[115]
PBMCs, CEM_{ss} cells	AZT-TP d4T-TP	70% MeOH, TRIS	F: Sep-Pak QMA, DP: ACP, DS: XAD resin	Luna (100X2.1 mm)	H-Ac:ACN:MeOH:W (0.25:10:30:59.75, v/v)	QqQ (+)	40 fmol/sample[g] 54 fmol/sample[g]	No	[83]
Erythrocytes (monkey)	Ribavirin (total) Viramidin (total)	8 8 % PCA	Neutralization, DP: ACP, DS: Supelco NH_2	Zorbax SB C_{18} (150X4.6 mm)	**A**: 0.1% H-Ac; **B**: 0.1% H-Ac in MeOH	QqQ (+)	0.412 µM[h] 0.412 µM[h]	Yes	[17]
PBMCs	3TC-TP AZT-TP CBV-TP	70% MeOH	F: Sep-Pak QMA, DP: ACP, DS: Oasis HLB	Aquasil C_{18} (50X2.1 mm)	**A**: 0.1% H-Ac; **B**: 0.1% H-Ac in MeOH	QqQ (+)	100 fmol/10^6 cells[i] 2 fmol/10^6 cells[i] 3.75 fmol/10^6 cells[i]	Partial	[33]
PBMCs	3TC-TP APC-TP	70% MeOH, TRIS-HCl	F: Waters QMA Accell, DP: ALP, DS: Varian C_{18}	YMC ODS AQ C_{18} (100X2.0 mm)	**A**: 0.2% H-Fo in ACN; **B**: 0.2 % H-Fo in MeOH:W (50:50, v/v)	QqQ (+)	59.2 fmol/10^6 cells[j] 59.2 fmol/10^6 cells[j]	No	[108]
PBMCs	CBV-TP	70% MeOH	F: Waters QMA Accell, DP: ALP, DS: Varian C_{18}	YMC ODS AQ C_{18} (50X2.0 mm)	Not specified	QqQ (+)	0.05 ng/mL[k]	Yes	[125]

Table 1. Indirect methods for the quantification of intracellular nucleotide analog (continued)

Matrix	Analyte	Extraction	Further sample pretreatment	Column	Mobile phase	MS (polarity)	LLQ	Val.	Ref.
PBMCs	AZT-TP	70% MeOH	F: ND, DP: ND, DS: HLB, Graphitized	Not applicable	Not applicable	AMS	About 30,000-fold more sensitive than LC-MS/MS	No	[43]

[a] mean of $28X10^6$ cells/sample
[b] usually $16X10^6$ cells/sample
[c] $10X10^6$ cells/400 mL
[d] about $1.1X10^9$ cells/sample (100 µL erythrocytes)
[e] $10X10^6$ cells/sample
[f] $5X10^6$ cells/sample
[g] mean of $30X10^6$ cells/sample
[h] 100 µL erythrocytes.sample
[I] $10X10^6$ cells/sample
[j] mininum yield of $36X10^6$ cells/sample
[k] using 500 µL PBMC extract from about 8 mL whole blood

a column switching set-up. A 1 µL loop filled with the eluted nucleotides was injected onto an analytical reversed phase column and separated using the IP-agent dimethylhexylamine (DMHA).
Others successfully used an on-line WAX trap-column followed by IP-chromatography for the quantification of several nucleotide analogs in PBMCs [49]. The nucleotides were loaded and trapped on the WAX column using a neutral ammonium acetate solution. The analytes were then eluted onto an analytical column with a phosphate buffer of pH 10, followed by their separation using DMHA. The approach resulted in peaks that had an area approximately 20 times as high as the same technique without the WAX pre-column.
Special sample pretreatments have also been performed for the challenging analysis of AZT nucleotides, which is discussed in detail in section IV C.

Separation and detection

Reversed phase chromatography

Although nucleoside DPs and TPs require IP-agents for retention on C_{18} columns, nucleoside MPs often show sufficient retention for bioanalysis. Like for their analysis in plasma (see for example PMPA in [50], simple gradients starting with a low percentage of MeOH or ACN in ammonium acetate or formate buffers have been applied [51-54]. Although these methods are relatively uncomplicated, the lack of retention for DPs and TPs restricts their applicability. The methods using reversed phase chromatography are summarized in table 2.

Ion-pairing chromatography

Both low amounts of involatile tetraalkylammonium salts and relatively volatile alkylamines have been used as IP-agents to separate nucleotide analogs. Here we describe the methods using these IP-agents

Tetrabutylammonium salts

Witters et al. were the first to explore the use of tetrabutylammonium (TBA) in combination with MS. Despite the relative involatility of TBA they were able to separate and detect endogenous cyclic nucleotides without a loss in sensitivity over the tested period of several days [55].
The first method using TBA for the analysis of therapeutic nucleotide analogs, was used for the quantification of FTC-TP [14]. TBA was selected because it was effective in relatively low concentrations. By using 1.0 mm internal diameter columns with a flow of 50 µL/min and by using a divert valve, the amount of involatile mobile phase constituents (2 mM TBA and 10 mM ammonium phosphate) delivered to the MS was kept to a minimum. Furthermore, a flow of 20% MeOH was continuously pumped

through the source of the MS at a flow of 10 µL/min to prevent clogging of the electrospray ionization (ESI) capillary. No residue was detected on the ESI capillary, but despite the precautions a brownish-red viscous liquid was observed on the sample cone. The same method was used later for the simultaneous quantification of lamivudine (3TC)-TP, carbovir (CBV)-TP and PMPA-DP [56]. Because the MS signal was strongly related to the amount of salts in the mobile phase, lower amounts have also been tested [57]. The amount of TBA could be decreased by increasing the amount of TBA in the injection solvent up to 200 mM. Later, the method was made suitable for the separation of MPs, DPs and TPs by introducing an ACN gradient, as shown for PMEA and its phosphorylated anabolites [16]. Similar methods were applied for several other nucleotide analogs [24;58-61].
Despite all improvements, the use of TBA in the injection solvent still caused significant ion suppression during the first 9-10 minutes of the analysis. Moreover, phosphate clusters and their ammoniated adducts were identified as a potential cause of interference [62].
Concluding, the use of TBA in combination with phosphates has some important drawbacks such as pollution of the MS source and ion suppression. Notwithstanding these drawbacks, many applications have been developed. Only one of these methods was extensively validated. All methods using TBA are summarized in table 3.

Alkylamines

Trialkylamines are generally more volatile than tetraalkylammonium salts, which makes them more suitable for a combination with MS detection. Therefore IP-agents such as tripropylamine [63;64] and triethylamine [65] have been used to analyze nucleotides in combination with MS detection. However, all but a few methods described in this section use N,N- or 1,5-dimethylhexylamine (DMHA) as IP-agent. The first reported use of DMHA for the LC-MS analysis of nucleotide analogs dates back to 1996, when Smyrnis et al applied it to penciclovir (PCV) and its nucleotides [66]. Little was, however, reported on the tested matrix or sensitivity.
Later DMHA was employed for the identification and quantification of bisphosphonate nucleotides [67;68]. Bisphosphonates are synthetic pyrophosphate analogs that are used in the treatment of metabolic bone disorders. The nucleotide metabolites of these drugs are the result of the addition of a nucleoside to the bisphosphonate, rather than the addition of a phosphate to a nucleoside (figure 6). Tuytten et al. systematically assessed the effect of N,N-DMHA on the separation and MS detection of 12 endogenous nucleosides and nucleotides [69]. Fung et al. were the first to fully describe a method for determination of a nucleoside analog and its nucleotides [63]. They separated ABC and four of its nucleotides using 20 mM DMHA in an acetate buffer. The same method was later used for the quantification of a prodrug of PMPA and its metabolites [52].

A similar method, using 1,5-DMHA with a formate buffer (pH 10.5), was developed for the anabolites of stavudine (d4T) [25]. The method, however, suffered from a long cycle time (26 minutes) and poor robustness; the column had to be replaced every 2 weeks because of the high pH. The robustness was later improved by using a more pH stable column. The improved method was adapted for the quantification of several other TPs [70;71;71] and was successfully used to support clinical studies [72;73]. By increasing the amount of ACN in the mobile phase Lee et al. were able to quantitate clevudine (L-FMAU)-TP [74]. Interfering peaks, however, prevented its application to AZT-TP(see section IV C). AZT-TP could, on the other hand, be analyzed with the same method after an immunoaffinity extraction [75], or by selecting a less abundant, but specific transition for AZT-TP [76]. The resultant loss in sensitivity was unconventionally corrected for by spiking all samples with a small amount of analyte. Moreover, the run time could be reduced to 9.5 minutes by using a shorter column (150 vs 50 mm) with a faster gradient. A slightly adjusted version of this method was used to determine AZT metabolite levels in newborns [77]. Using the faster gradient, the method was again validated for AZT-MP, AZT-TP, 3TC-TP, PMPA-DP and CBV-TP. [21;78].

The concentration of the IP-agents were constant in most methods, except for the method described by Hernandez-Santiago et al. who used a gradient with a decreasing DMHA concentration for the quantification of N-hydroxycytidine (NHC)-TP [79]. Others used a decreasing hexylamine concentration and pH in combination with increasing MeOH [80;81;81].

Although DMHA is more volatile than TBA and phosphate, the presented methods still require flushing of the ESI source to prevent clogging and a loss of signal [78]. Pollution could be repressed by reducing the column diameter and flow. Compared to the methods using TBA, relatively large column diameters are used (2.0-2.1 mm). The use of microbore columns was investigated by Becher et al., but no improvement was achieved [70]. Cai et al, on the other hand, could reduce the DMHA concentration to 10 mM and 5 mM by changing the column diameter to 1.0 and 0.5 mm respectively. Concomitantly, the MS signal increased 5-10 fold [82]. In contrast to previous reports [3], a clear relation between column diameter and DMHA concentration can not be inferred from the methods described in this review.

Even though DMHA has successfully been used by some groups, others were less successful due to ion suppression, source pollution, strong binding of the IP-agent to the analytical system, carryover and reproducibility problems [44;46;83].

Despite the fact that DMHA is more volatile than TBA, and phosphate is not used, the IP-agent has still been associated with source pollution and ion suppression. Nevertheless, the method has proven its value in many applications, making it one of the methods of choice. The methods using

alkylamines as IP-agents for the separation of nucleotide analogs are summarized in table 4.
Concluding, by reducing the amount of IP-agents and salts delivered to the MS, source pollution and ion suppression have been reduced to an acceptable level. Several IP-pairing methods have been developed for the quantification of nucleotide analogs, and their use has been shown in numerous applications. Still, pollution of the source remains a major point of care.

Anion-exchange chromatography

Although anion-exchange has traditionally been the method of choice to analyze nucleotides, the use of involatile competing ions for elution hampered hyphenation with MS. Shi et al., however, used an alternative elution mechanism [23]. By applying a pH gradient (pH 6-10.5) to a WAX-column they changed the charge of the basic functional groups (pKa ~ 8) of the column. As a consequence the capacity of the column decreased at a higher pH, thereby eluting the anionic nucleotides. Therefore, as opposed to classical anion-exchange methods, this method did not require high concentrations of involatile competing ions for elution, making it directly applicable to MS detection. Separation between MPs, DPs and TPs was achieved within only 2 minutes by simultaneously applying an inverse ammonium acetate gradient (10-1 mM). The method was fully validated for the quantification of dexelvucitabine (D-D4FC)-TP in PBMCs. A similar method was later applied to its enantiomer elvucitabine (D4FC)-TP [84].
A less steep, 13-minute gradient was used for the quantification of dFdC-TP in canine melanoma cells [85]. Another gradient, separating dFdC MP, DP and TP in 10 minutes, was used for the validated quantification of dFdC-TP in PBMCs [19], and was later used for the quantification of its deaminated metabolite difluoro-deoxyuridine (dFdU)-TP as well [86]. Simultaneous quantification of MPs, DPs and TPs was also feasible with this gradient, as shown for cladribine (2CdA)-MP, -DP and -TP in cells and culture medium [87]. These WAX methods are robust, very sensitive and MS-friendly, but the lack of retention of nucleosides can be regarded as a drawback. The described WAX methods are summarized in table 5.

Porous graphitic carbon chromatography

Although PGC only consists of carbon sheets, polar and ionic compounds are retained on its surface [88]. Polar or polarizable analytes cause a charge induced dipole at the graphite surface resulting in retention of negatively charged analytes like nucleotides. Charged analytes can be retained on PGC without the need of IP-agents and can subsequently be eluted from

the column without the need of high salt concentrations. PGC is thus very suitable for the analysis of nucleotides with MS detection.
Moreover, it has shown a remarkable selectivity for structurally similar compounds, which is most likely caused by differences in analyte contact area with the planar carbon sheets [89]. PGC has therefore been used to separate cytarabine (ara-C) and its MP from their endogenous stereo-isomers cytidine and its MP [90]. Moreover, Xing et al. have explored the use of PGC for the simultaneous analysis of several endogenous nucleosides and their mono-, di- and triphosphates [91]. Various buffers were tested for their ability to separate the analytes and for their effect on MS signal. Addition of diethylamine (DEA) was required to reduce peak tailing. Finally, separation of 16 nucleosides and nucleotides was achieved in just 15 minutes using a gradient of ACN in water with 50 mM ammonium acetate and 0.1% DEA. More recently, PGC was used in combination with the IP-agent hexylamine to separate ara-CMP, -DP and -TP from their endogenous stereo-isomers cytidine-MP, -DP and -TP [45]. Again, however, as much as 0.4% DEA was required to reduce peak tailing.
Using an ammonium bicarbonate gradient (0-25 mM) in 15 % ACN, Jansen et al. were able to separate dFdC, dFdU and their MP, DP and TP, without the need of DEA addition, in 15 minutes. Strict control of pH and redox state of the column were required to maintain this separation during multiple runs [92]. The developed method was later validated for quantification in PBMCs [93].
Concluding, exceptional separations have been achieved using PGC. Because of its unconventional selectivity, PGC is especially suitable for the separation of isomers or isobaric nucleotides. The methods using PGC for the quantitative determination of nucleotide analogs are presented in table 6.

Capillary electrophoresis

Capillary electrophoresis can be used to separate ionic analytes with a high resolution, which makes it very suitable for the analysis of nucleotides [94-96]. A combination with MS makes the technique even more powerful. Hyphenation of CE with MS has, however, initially posed instrumental problems mainly caused by the separated electrical circuits required for both techniques [97]. Moreover, the electrophoresis run buffer should be compatible with MS detection. Volatile buffers such as ammonium bicarbonate and acetate, however, resulted in good CE separation and MS signal in the analysis of endogenous nucleotides [98-100]. Cai et al. used CE-MS for the simultaneous quantification of intracellular ABC, CBV-MP, CBV-DP and CBV-TP [101]. The nucleotides could be separated using an ammonium acetate buffer on bare fused silica. Similar methods were used to study the metabolism of 3TC in HepG2 cells [102] and d4T- and

didanosine (ddA)-MP and –TP in PBMCs [103]. Bezy et al., however, applied a coaxial sheath liquid composed of decafluoroheptanoic acid in 2,2,2,-trifluoroethanol to improve sensitivity and spray stability.
The high resolution of CE makes CE-MS a good alternative to conventional LC-MS. Table 7 summarizes the methods using CE-MS for nucleotide analog quantification.

MALDI-TOF

Only one article describes the use of MALDI-TOF MS for the quantification of nucleotide analogs [104]. Using anthranilic acid mixed with nicotinic acid as matrix, the investigators were able to detect AZT-TP, as well as several endogenous TPs, in amounts as low as 0.5 fmol per sample. Endogenous nucleotides (adenosine TP (ATP) and deoxyguanosine TP (dGTP)) having the same mass as AZT-TP could, however, only be distinguished using post source decay, which resulted in less sensitivity (see section IV C). Since no validation of the method was performed, the article should be regarded as explorative. The MALDI-TOF method used for the quantification of AZT-TP is summarized in table 8.

Hydrophilic interaction chromatography

In hydrophilic interaction chromatography (HILIC) polar columns are used in combination with mobile phases rich in organic solvents. Polar analytes are eluted from the column by increasing the water content of the mobile phase. Because the applied mobile phases are highly volatile, hyphenation with MS is favourable [105].
HILIC-MS detection was applied to endogenous nucleotides by Bajad et al. [106]. Similarly, silica hydride was used in the normal phase mode [107]. Currently, only one HILIC-MS method for the determination of a nucleotide analog has been described [46]. The method, using an aminopropyl column, was preferred over several other HILIC, PGC and IP-methods because of its sensitivity and selectivity. Still, a 30 minute run time was required. The method is summarized in table 9. The value of HILIC for the analysis of nucleotide analogs should be confirmed in future applications.

Table 2. Direct methods for the quantification of intracellular nucleotide analogs using reversed phase chromatography

Matrix	Analyte	Extraction	Further sample pretreatment	Column	Mobile phase	MS (polarity)	LLQ	Val.	Ref.
PBMCs (dog)	PMPA	70% MeOH	-	Inertsil ODS (150X4.6 mm)	**A,B**: A-Ac with an ACN gradient (0-60%)	IT (+)	Not specified	No	[52]
PBMCs, CCRF-CEM cells	AZT-MP	60% MeOH, 15 mM A-Ac	Lyophilized	Zorbax XDB-C_{18} (150X0.5 mm)	**A**: 15 mm A-Ac (pH 6.65); **B**: MeOH	IT (-)	2 pmol	No	[51;54]
PBMCs	PMPA	70% MeOH, TRIS-HCl	Solvent evaporated	Synergi polar-RP (50X2 mm)	**A,B**: 0.5% H-Fo and a MeOH gradient	QqQ (+)	Not specified	No	[53]

Table 3. Direct methods for the quantification of intracellular nucleotide analogs using tetrabutylammonium salts as ion-pairing agent

Matrix	Analyte	Extraction	Further sample pretreatment	Column	Mobile phase	MS (polarity)	LLQ	Val.	Ref.
PBMCs	FTC-TP	70% MeOH, 10 mM A-Ph	Ion-pairing SPE (Bond Elut C_{18})	Xterra rp18 (100X1.0 mm)	10 mM A-Ph, 2 mM TBA-OH in ACN:W (15:85, v/v)	QqQ (+)	83 fmol/10^6 cells[a]	Partial	[14]
PBMCs	FTC-TP	70% MeOH, TRIS-HCl	Ion-pairing SPE (Bond Elut C_{18})	Xterra MS (100X1.0 mm)	0.5 mM A-Ph, 0.125 mM TBA-OH in ACN:W (15:85, v/v)	QqQ (+)	40 fmol/10^6 cells[b]	No	[57]
HepG2, hepatocytes	PMEA PMEA-MP PMEA-DP	70% MeOH	Solvent evaporated	Xterra MS (100X1.0 mm)	**A**: 0.25 mM TBA-OH, 4 mM A-Ph, in ACN:W (6:94, v/v); **B: A** in ACN:W (20:80, v/v)	QqQ (+)	200-600 fmol/10^6 cells[c]	No	[16]
PBMCs	3TC-TP CBV-TP PMPA-DP	70% MeOH	Ion-pairing SPE	Xterra MS (100X1.0 mm)	10 mM A-Ph, 2 mM TBA-OH in ACN:W (15:85, v/v)	QqQ (+)	24 fmol on column 76 fmol on column 15 fmol on column	No	[56]
PBMCs, CCRF-CEM cells	CBV-TP PMPA PMPA-MP PMPA-DP	70% MeOH	Solvent evaporated	Xterra MS (100X1.0 mm)	**A**: 0.25 mM TBA-OH, 4 mM A-Ph, in ACN:W (6:94, v/v); **B: A** in ACN:W (20:80, v/v)	QqQ (+)	10-40 fmol/10^6 cells[d]	No	[24]
HepG2 cells	PMPA PMPA-MP PMPA-DP	70% MeOH	Solvent evaporated	Xterra MS (100X1.0 mm)	**A**: 0.25 mM TBA-OH, 4 mM A-Ph, in ACN:W (6:94, v/v); **B: A** in ACN:W (20:80, v/v)	QqQ (+)	Not specified	No	[59]
PBMCs CCRF-CEM cells	FTC-TP PMPA PMPA-MP PMPA-DP	70% MeOH	Solvent evaporated	Xterra MS (100X1.0 mm)	**A**: 0.25 mM TBA-OH, 4 mM A-Ph, in ACN:W (6:94, v/v); **B: A** in ACN:W (20:80, v/v)	QqQ (+)	10-40 fmol/10^6 cells[d]	No	[58]
HepG2 cells	PMEA PMEA-MP PMEA-DP	70% MeOH	Solvent evaporated	Luna C_{18} (100X1.0 mm)	**A**: 0.2 mM TBA-Ac, 2 mM A-Ph in ACN:W (5:95, v/v); **B:** 2 mM A-Ph in ACN:W (50:50, v/v)	QqQ (+)	25 fmol on column[e] 50 fmol on column[e] 25 fmol on column[e]	Partial	[62]

Table 3. Direct methods for the quantification of intracellular nucleotide analogs using tetrabutylammonium salts as ion-pairing agent (continued)

Matrix	Analyte	Extraction	Further sample pretreatment	Column	Mobile phase	MS (polarity)	LLQ	Val.	Ref.
PBMCs	PMPA-DP	SPE, elution with MeOH:100 mM A-Ph (99:1, v/v), solvent evaporated		Xterra MS (100X1 mm)	**A**: 2 mM TBA-OH, 5 mM A-Ph (pH 6.0):ACN (95:5, v/v); **B**: 1 mM TBA-OH, 5 mM A-Ph (pH 7.4):ACN (80:20, v/v)	QqQ (+)	20 fmol	Yes	[47]
PBMCs, CCRF-CEM cells	Fd4AP Fd4AP-MP Fd4AP-DP	70% MeOH	Solvent evaporated	Luna C_{18} (100X1.0 mm)	**A**: 0.2 mM TBA-Ac, 2 mM A-Ph in ACN:W (5:95, v/v); **B**: 2 mM A-Ph in ACN:W (50:50, v/v)	QqQ (+)	50-100 fmol/10^6 cells[f]	No	[60]
PBMCs	PMEG-DP	70% MeOH	Solvent evaporated	Luna C_{18} (100X1.0 mm)	**A**: 0.2 mM TBA-Ac, 2 mM A-Ph in ACN:W (5:95, v/v); **B**: 2 mM A-Ph in ACN:W (50:50, v/v)	QqQ (+)	Not specified	No	[61]

[a] approximately 10X10^6 cells/sample
[b] approximately 2-9X10^6 cells/sample
[c] 0.1X10^6 cells/sample
[d] 1-5X10^6 cells/sample
[e] 10 µL injection containing 0.1X10^6 cells
[f] 2-3X10^6 cells/sample

Table 4. Direct methods for the quantification of intracellular nucleotide analogs using alkylamines as ion-pairing agent

Matrix	Analyte	Extraction	Further sample pretreatment	Column	Mobile phase	MS (polarity)	LLQ	Val.	Ref.
Not specified	PCV-MP PCV-DP PCV-TP	Not specified	Not specified	Prodigy C_8 (150X2 mm)	**A**: 5 mM A-Fo, 1 mM DMHA; **B**:20 mM A-Fo, 1 mM DMHA in MeOH:W (70:30, v/v)	QqQ (-)	Not specified	No	[66]
RAW 264 macrophage cells	Clodronate metabolite	60% ACN	Solvent evaporated	Genesis C_{18} (50X2 mm)	**A**: 20 mM DMHA-Fo (pH7); **B**: 2 mM DMHA-Fo (pH7) in MeOH:W (50:50, v/v)	QqQ (-)	0.5 µM[a]	Partial	[68]
PBMCs, HepG2 cells	ABC-MP CBV-MP CBV-DP CBV-TP	60% MeOH	Centrifugation	Luna C_8(2) (50X2.0 mm)	**A**: 20 mM N,N-DMHA (pH 7) **B**: MeOH:W (80:20, v/v)	IT (+)	10 nM[b] 25 nM[b] 25 nM[b] 25 nM[b]	Partial	[63]
MT-2 cells	PMPA PMPA-DP	67% MeOH	Centrifugation	Luna C_8(2) (50X2.0 mm)	**A,B**: 20 mM N,N-DMHA (pH 7) with a MeOH gradient (15-80%)	IT (+)	100 nM[c] 20 nM[c]	No	[52]
PBMCs	d4T-MP d4T-DP d4T-TP	70% MeOH, TRIS-HCl	Solvent evaporated	SMT C_{18} (150X2.1 mm)	**A**: 10 mM 1,5-DMHA, 3 mM A-Fo (pH 10.5); **B: A** in ACN:W (50:50, v/v)	QqQ (-)	21 fmol/10^6 cells[d] 17 fmol/10^6 cells[d] 9.8 fmol/10^6 cells[d]	Yes	[25]
PBMCs	3TC-TP d4T-TP ddA-TP	70% MeOH, TRIS-HCl	Solvent evaporated	Supelcogel ODP-50 (150X2.1 mm)	**A**: 10 mM 1,5-DMHA, 3 mM A-Fo (pH 10.5); **B: A** in ACN:W (50:50, v/v)	QqQ (-)	188 fmol/sample[e] 61.4 fmol/sample[e] 53.4 fmol/sample[e]	No	[70]
PBMCs	AZT-TP	70% MeOH, TRIS-HCl	Immuno affinity extraction	Supelcogel ODP-50 150X2.1 mm)	**A**: 10 mM 1,5-DMHA, 3 mM A-Fo (pH 10.5); **B: A** in ACN:W (50:50, v/v)	QqQ (-)	9.3 fmol/10^6 cells[f]	Yes	[75]
HepG2 and Huh-7 cells	NHC-TP	60% MeOH	Solvent evaporated	Hypersyl BDS C_8 (150X4.6 mm)	**A**: 25 mM N,N-DMHA (pH 7); **B**: 5 mM N,N-DMHA (pH 7) in ACN:W (80:20, v/v)	QqQ (-)	Not specified	No	[79]
Jurkat leukaemia cells	F-ara-ATP	1 M PCA	PCA precipitation/ Neutralization with K-BCa	Prodigy C_8 (100X2.0 mm)	**A**: 0.025% DMHA, 20 mM HAc (pH 7.5); **B**: MeOH	Q (-)	50 fmol on column[g]	Yes	[15]
PBMCs	ddA-TP PMPA-DP	70% MeOH, TRIS-HCl	Solvent evaporated	Supelcogel ODP-50 (150X2.1 mm)	**A**: 10 mM 1,5-DMHA, 3 mM A-Fo (pH 10.5); **B: A** in ACN:W (50:50, v/v)	QqQ (-)	25 fmol/sample[e] 106 fmol/sample[e]	Yes	[71]
PBMCs	L-FMAU-TP	70% MeOH, TRIS-HCl	Solvent evaporated	Hydrosphere C_{18} (50X2.0 mm)	**A**: 10 mM N,N-DMHA, 3 mM A-Fo; **B: A** in ACN:W (90:10, v/v)	QqQ (-)	1.6 pmol/10^6 cells[h]	Yes	[74]
PBMCs	D4FC-TP	70% MeOH, TRIS	Not specified	Luna C_{18}(2) (50X2.0 mm)	**A**: 10 mM N,N-DMHA, 3 mM A-Fo (pH 10); **B: A** in ACN:W (50:50, v/v)	IT (-)	250 fmol/10^6 cells	No	[84]
PBMCs	AZT-MP AZT-TP d4T-TP	70% MeOH, TRIS-HCl	Solvent evaporated	Supelcogel ODP-50 (50X2.1 mm)	**A**: 10 mM 1,5-DMHA, 3 mM A-Fo (pH 10.5); **B: A** in ACN:W (50:50, v/v)	QqQ (-)	300 fmol/sample[f] 150 fmol/sample[f] 63.4 fmol/sample[f]	Yes	[76]

Table 4. Direct methods for the quantification of intracellular nucleotide analogs using alkylamines as ion-pairing agent (continued)

Matrix	Analyte	Extraction	Further sample pretreatment	Column	Mobile phase	MS (polarity)	LLQ	Val.	Ref.
PBMCs, erythrocytes	3TC-TP AZT-MP AZT-TP PMPA-DP	70% MeOH, TRIS-HCl	Solvent evaporated	Supelcogel ODP-50 (50X2.1 mm)	**A**: 10 mM 1,5-DMHA, 3 mM A-Fo (pH 10.5); **B: A** in ACN:W (50:50, v/v)	QqQ (+/-)	1 pmol/10^6 cells[f] 180 fmol/10^6 cells[f] 150 fmol/10^6 cells[f] 95 fmol/10^6 cells[f]	Partial	[21]
PBMCs	3TC-TP CBV-TP PMPA-DP	70% MeOH, TRIS-HCl	Solvent evaporated	Supelcogel ODP-50 (50X2.1 mm)	**A**: 10 mM 1,5-DMHA, 3 mM A-Fo (pH 10.5); **B: A** in ACN:W (50:50, v/v)	QqQ (+)	1000 fmol/sample[f] 200 fmol/sample[f] 100 fmol/sample[f]	Yes	[78]
PBMCs	3TC-MP 3TC-DP 3TC-TP AZT-MP AZT-DP AZT-TP d4T-MP d4T-DP d4T-TP	70% MeOH	Centrifugation	Inertsil ODS (100X3 mm)	**A**: 5 mM HA (pH 6.3) **B**: 10 mM A-Ac (pH 8.5) in MeOH:W (90:10, v/v)	QqQ/ LIT(-)	50 fmol on column[i] 250 fmol on column[i] 25 fmol on column[i] 50 fmol on column[i] 250 fmol on column[i] 25 fmol on column[i] 50 fmol on column[i] 250 fmol on column[i] 25 fmol on column[i]	Partial	[81]
PBMCs (macaque)	3TC-TP FTC-TP PMPA-DP	80% MeOH	Solvent evaporated, on-line WAX-SPE	Not specified	0.5 mM DMHA, 0.5 mM Ph-buffer (pH 6.5) in ACN:W (30:70, v/v)	QqLIT (-)	25 pg/sample 30 pg/sample 17 pg/sample	Partial	[49]

[a] $10X10^6$ cells/mL
[b] $50X10^6$ cells/mL
[c] determined in water
[d] around $14X10^6$ cells/sample
[e] about $7\text{-}10X10^6$ cells/sample
[f] about $10X10^6$ cells/sample
[g] 10 µL injection of about 100 µL containing $2X10^6$ cells
[h] $25X10^6$ cells/sample
[i] LOD; 25 µL injection of 100 µL lysate containing $1X10^6$

Table 5. Direct methods for the quantification of intracellular nucleotide analogs using weak anion exchange chromatography

Matrix	Analyte	Extraction	Further sample pretreatment	Column	Mobile phase	MS (polarity)	LLQ	Val.	Ref.
PBMCs	D-D4FC-TP	60% MeOH	Centrifugation and filtration	Biobasic (20X1.0 mm)	**A**: 10 mM A-Ac in ACN:W (70:30, v/v) (pH 6); **B**: 1 mM A-Ac in ACN:W (70:30, v/v) (pH 10.5)	QqQ (+)	5 fmol/10^6 cells[a]	Yes	[23]
Canine melanoma cells	dFdC-TP	71% ACN	Solvent evaporated	Biobasic AX (50X2.1 mm)	**A**: 10 mM A-Ac in ACN:W (70:30, v/v) (pH 6); **B**: 1 mM A-Ac in ACN:W (70:30, v/v) (pH 10)	Q (-)	1 µg/mL[b]	No	[85]
PBMCs	D4FC-TP	70% MeOH, TRIS	Not specified	Biobasic AX (50X1 mm)	**A**: 10 mM A-Ac (pH 6): ACN(30:70, v/v); **B**: 1 mM A-Ac:ACN (30:70, v/v) (pH 10.5)	QqQ (+)	10 fmol/10^6 cells	Yes	[84]
PBMCs	FTC-TP PMPA-DP	60% MeOH	Solvent evaporated	Thermo AX (100X2.0 mm)	**A**: 40 mM A-Ac (pH 7); **B**: A-OH in W (pH 10.6) **C**: ACN	QqQ (+)	225 fmol on column 22.5 fmol on column	Yes	[111]
PBMCs	dFdC-TP	0.8 M PCA	Neutralization	Biobasic AX (50X2.1 mm)	**A**: 10 mM A-Ac in ACN:W (70:30, v/v) (pH 6); **B**: 1 mM A-Ac in ACN:W (70:30, v/v) (pH 10.5)	QqQ (-)	94 fmol/10^6 cells[c]	Yes	[19]
MDCKII-cells	2CdA-MP 2CdA-DP 2CdA-TP	70% MeOH	Centrifugation	Biobasic AX (50X2.1 mm)	**A**: 10 mM A-Ac in ACN:W (70:30, v/v) (pH 6); **B**: 1 mM A-Ac in ACN:W (70:30, v/v) (pH 10.5)	QqQ (+)	1.11 nM in lysate[d] 0.55 nM in lysate[d] 1.31 nM in lysate[d]	Yes	[87]

[a] 3X10^6 cells/sample
[b] about 0.66X10^6 cells/mL
[c] 3.8X10^6 cells/sample
[d] about 0.6X10^6 cells/mL

Table 6. Direct methods for the quantification of intracellular nucleotide analogs using porous graphitic carbon chromatography

Matrix	Analyte	Extraction	Further sample retreatment	Column	Mobile phase	MS (polarity)	LLQ	Val.	Ref.
CEM-SS cells	Ara-CMP	60% PCA	Neutralization	Hypercarb (10X 4 mm) +(50X2.1 mm)	**A**: 0.1 % H-Fo in W; **B:** 0.1 % H-Fo in ACN:W (80:20, v/v)	Q (+)	10 µM	Yes	[90]
RL-7 and RL-G cells	Ara-CTP	60% MeOH	WAX-SPE	Hypercarb (50X2.1 mm)	**A**: 5 mM HA + 0.4% DEA in W (pH 10); **B**: ACN:W (50:50, v/v	QqQ (-)	100 ng/mL	Yes	[45]
PBMCs	dFdC-MP dFdC-DP dFdC-TP dFdU-MP dFdU-DP dFdU-TP	70% MeOH	Centrifugation	Hypercarb (100X2.1 mm)	**A**: 1 mM A-Ac in ACN:W (15:85, v/v) (pH 5); **B**: 25 mM A-BCa in ACN:W (15:85, v/v)	QqQ (+)	1.41 pmol/10^6 cells[a] 1.52 pmol/10^6 cells[a] 1.79 pmol/10^6 cells[a] 1.23 pmol/10^6 cells[a] 2.10 pmol/10^6 cells[a] 2.56 pmol/10^6 cells[a]	Yes	[93]

[a] Assuming 4X10^6 cells/sample

Table 7. Direct methods for the quantification of intracellular nucleotide analogs using capillary electrophoresis

Matrix	Analyte	Extraction	Further sample pretreatment	Capillary	Mobile phase	MS (polarity)	LLQ	Val.	Ref.
PBMCs	CBV-MP CBV-DP CBV-TP	60% MeOH	-	Bare fused silica (73 cm, 360 µm OD, 50 µm ID)	40 µM A-Ac (pH 9.2)	IT (-)	1 µM[a] 1 µM[a] 1 µM[a]	No	[101]
HepG2 cells	3TC-MP 3TC-DP 3TC-TP	60% MeOH	Solvent evaporated	Bare fused silica (60 cm, 150 µm OD, 50 µm ID)	25 mM A-Ac (pH 10)	Q (-)	100-200 nM[b]	No	[102]
PBMCs	d4T-MP d4T-TP ddA-MP ddA-TP	70% MeOH, TRIS-HCl	-	Bare fused silica (80 cm, 192 µm OD, 50 µm ID)	40 mM A-Ac (pH 10)	QqQ (+)	Not specified 110 ng/mL Not specified 50 ng/mL	Yes	[103]

[a] 50X10^6 cells/mL
[b] 2.05X10^6 cells/mL
[c] 20X10^6 cells/mL

Table 8. Direct methods for the quantification of intracellular nucleotide analogs using MALDI-TOF

Matrix	Analyte	Extraction	Further sample pretreatment	Dopant	Mobile phase	MS (polarity)	LLQ	Val.	Ref.
PBMCs	AZT-TP	60% MeOH	Lyophilization	Anthranilic acid/ nicotinic acid	Not applicable	MALDI-TOF (-)	0.5 fmol/sample[a]	No	[104]

[a] 0.85X10^6 cells/sample

Table 9. Direct methods for the quantification of intracellular nucleotide analogs using hydrophilic interaction chromatography

Matrix	Analyte	Extraction	Further sample pretreatment	Column	Mobile phase	MS (polarity)	LLQ	Val.	Ref.
Liver tissue (rat)	OPC-TP	70% MeOH, 20 mM EDTA/EGTA	WAX-SPE (Strata-X-AW)	Aminopropyl (100X2.0 mm)	**A**: 20 mM A-Ac in ACN:W (5:95, v/v) (pH 9.45); **B**: ACN	QqQ (-)	50 nM	Yes	[46]

Abbreviations

A: Ammonium
A: Mobile phase A
Ac: Acetate
ACN: Acetonitrile
ACP: Acid phosphatase
ALP: Alkaline phosphatase
AMS: Accelerator mass spectrometry
B: Mobile phase B
BCa: Bicarbonate
DMHA: Dimethylhexylamine
DP: Dephosphorylation
DS: Desalting
EDTA: Ethylenediamine tetraacetic acid
EGTA: ethyleneglycol tetraacetic acid
F: Fractionation
Fo: Formate
H-Ac: Acetic acid
H-Fo: Formic acid
IT: Ion trap
LIT Linear ion trap
LLQ: Lower limit of quantification
LOD: Limit of detection
MALDI-TOF Matrix assisted light desorption – time of flight
MeOH: Methanol
NS: Not specified
OH: Hydroxide
PBMC: Peripheral blood mononuclear cell
PCA: Perchloric acid
Q: Single quadrupole
QqQ: Triple quadrupole
SPE: Solid phase extraction
TBA: Tetrabutylammonium
TRIS: Tris(hydroxymethyl)aminomethane
W: Water
WAX: Weak anion exchange

Table 10. Mass transitions used for quantification of the nucleoside and nucleotide analogs

		Ionization mode				
		Positive		Negative		
Compound	Form	Parent	Product	Parent	Product	Ref
Ara-C	TP			482	159	[45]
ddC	TP	452	112 (B)	450	159	[14;74]
ATC	N	230	112 (B)			[108]
3TC	N	230	112 (B)			[33;38;108-110]
	MP			308	79	[81]
	DP			388	79	[81]
	TP	470	112 (B)	468	370, 159	[21;49;70;78;81;111]
dFdC	N	264	112 (B)			[92]
	MP	344	246	342	231	[19;92]
	DP	424	326	422	159	[19;92]
	TP	504	326	502	159	[19;85;92]
D-D4FC/	MP	308	130 (B)			[23]
D4FC	DP	388	130 (B)			[23]
	TP	468	130 (B)	466	159	[23;84]
FTC	TP	488	130 (B), 135	486	388, 159	[14;49;58;111]
NHC	TP			498	159, 400	[79]
OPC	TP			496	159	[46]
d4T	N	225	127 (B)			[83;109]
	MP	305	81	303	125 (B), 177	[25;81;103]
	DP			383	159, 257	[25;81]
	TP	465	81	463	159	[25;70;72;76;81;103]
AZT	N	268	127 (B)	266	233	[33;38;44;83;109;112]
	MP			346	79, 125 (B),177, 303, 346	[21;51;54;76;81]
	DP			426	159	[81]
	TP			506	159, 380	[21;72;76;81;104]
L-FMAU	TP			499	159	[74]
dFdU	N			263	111 (B)	[92]
	MP	345	247			[92]
	DP	425	327			[92]
	TP	505	247	503	159	[86;92]
CBV	N	248	152 (B)			[33]
	MP	328	152 (B)			[63]
	DP	408	152 (B)			[63]
	TP	488	152 (B), 135	486	159	[24;63;78]
ABC	N	287	191 (B)			[63]
	MP	367	191 (B)			[63]
Viramidine	N	244	112 (B)			[17]
Ribavirin	N	245	113 (B)			[17;113]
6-TG	B	168	151			[18]
6-MMP	Deriv	158	110			[18]
PCV	MP			492	158	[66]
	DP			411	158	[66]
	TP			331	78	[66]
ddA	N	236	136 (B)			[114]
	MP	316	136 (B)			[103]
	TP	476	136 (B)	474	159	[70;71;103]
PMEA	Nt	274	162			[16;62]
	MP	354	162			[16;62]
	DP	434	162			[16;24;47;62]
PMPA	Nt	288	270, 206, 176			[52;115]
	DP	448	350, 270, 176, 136	446	348, 177. 159	[16;21;24;47;49;52;58;62;71;78;111]
2CdA	MP	366	170 (B)			[87]
	DP	446	170 (B)			[87]
	TP	526	170 (B)			[87]
Fd4AP	Nt	332	220			[60]
	MP	412	220			[60]
	DP	492	220			[60]
"Clodronate"	TP			572	225	[68]

(B): base ion, N: Nucleoside, Nt: Nucleotide, Deriv.:Derivative

Mass spectrometry

Ionization

Intuitively the anionic nucleotides should be detected in the negative ion mode. Early LC-MS methods for the quantification of nucleotides therefore started method development with the negative ion mode, but surprisingly finally used the positive ion mode [14;63]. Fung et al. argued that N,N-DMHA could mask the negative charges on the phosphate moiety, but Shi et al also used the positive mode, without any IP-agents [23;63]. Table 10 shows that most nucleotide analogs can be detected in the positive as well as in the negative ion mode, even at a high pH (10.5). No increase in signal intensity was observed upon lowering the pH of the mobile phase [62], whereas Shi et al. even noticed an increase in analyte signal in mobile phase B (pH 10.5) over mobile phase A (pH 6.0). Some used post-column addition of formic or acetic acid [84], but for others it did not change [87], or even decreased sensitivity [14;23]. It is unexpected that analytes with such acidic groups show more sensitivity in basic environments using the positive ion mode. Finally, dFdU was not detectable in the positive ion mode whereas its nucleotides, bearing anionic phosphate groups, showed a reasonable response [92].

Interestingly, calculations of the gas-phase proton affinities showed that the most likely site of protonation of some uridine and thymidine MPs is the phosphate group [116]. Others calculated that the addition of a negatively charged phosphate group increases the proton affinity of the nearby base [117].

Still, nucleotides containing a base with an external amino function (A, G and C) are protonated more effectively than those that do not possess this function (T and U) [78;103]. These results are in good agreement with the determined and calculated gas-phase proton affinities of (deoxy)nucleoside MPs (A>G>C>>T/U) [116]. Thymine and uracil containing nucleosides and nucleotides can, however, be detected in the negative ion mode, with the deprotonated base as a common fragment (table 10).

Thus, most nucleotides are efficiently ionized in a wide pH range using both the negative and the positive ionization mode.

Ionization suppression

IP-agents not only pollute the MS, but are also a notorious cause of ion suppression. Ion suppression has clearly been observed with both TBA and DMHA [14;55;69]. Both agents, however, showed an increase in signal intensity at low concentrations. This initial increase is most likely caused by lowering of the surface tension, thereby facilitating the spray process. The concentration at which ion suppression starts is differently reported in

publications and experiments, ranging from 1 mM DMHA-formate [68] to 5 mM (using LC system) and >20 mM (flow injections) DMHA [69] and 0.05 µM TBA-Bromide [55]. Fung et al. still detected a higher $[ATP+H]^+$ signal with 10 mM DMHA compared to no DMHA [63]. It is therefore unclear whether the IP-agents actually cause ion suppression at the concentrations used in the described methods. Most likely the ion-suppressing effect of IP-agents is influenced by other factors, like pH and analyte concentration.
DMHA has also caused the formation of adducts [69]. These adducts have been used as quantifying ions by some [82;118], whereas others found that the product ions were not sufficiently specific [78].
Besides mobile phase components, components originating from the samples can also have an important contribution to the ion suppression. A principal factor in this matrix effect is the number of cells present in a sample. Because the number of cells can vary between samples, the number of cells should either be kept constant [33;74] or a range should be validated [19;28].
In short, IP-agents can cause ion suppression but also ion enhancement, mainly depending on their concentration. The number of cells in a sample has a profound impact on the ionization of the analytes and should be validated thoroughly.

Selectivity

Endogenous nucleosides and their analogs are all based on the same molecular structures (figure 1). As a result their molecular weights and fragmentation patterns are alike. Because of these similarities interfering peaks are often observed. The various interferences will be discussed below, followed by approaches to improve the selectivity.

Endogenous compounds

Many, often high abundant, endogenous nucleotides that can potentially interfere with MS detection are present in cells. Unidentified peaks were observed in the analysis of dFdC-TP [19], OPC-TP [46] and PMPA-DP and CBV-TP [78]. Some interfering compounds were identified, such as deoxycytidine TP (dCTP) in the analysis of dD4FC-TP [23], ATP and dGTP (MW 507.2 for both) in the analysis of AZT-TP [44;70;104] and the Na-adduct of 3TC-TP in the analysis of deoxyadenosine TP (dATP) [78]. Cytosine and its nucleotides were observed in the analysis of their isomers ara-C and its nucleotides [45;90], and cytidine and uridine in the mass transitions of viramidine and ribavirine, respectively [17;113].

Other nucleoside analogs

Besides endogenous nucleosides and nucleotides, other nucleoside and nucleotide analogs, can also interfere with MS detection. For example, apricitabine (ATC) and 3TC are isomers and share the same fragment [108]. Moreover, dFdC (263 Da) and its deaminated metabolite dFdU (264 Da) differ only one Da in molecular weight. A dFdC molecule containing a naturally occurring ^{13}C- or ^{15}N-isotope (about 11%) will therefore have the same mass as dFdU, resulting in a signal in the dFdU mass transition window. Correspondingly dFdC-MP, -DP and -TP will give signals in the transition windows of dFdU-MP, -DP and -TP [92]. Likewise ara-C (243 Da) and ara-uridine (ara-U)(244 Da) and their nucleotides differ only 1 Da in molecular weight. Furthermore, ara-C and ara-U are also stereo-isomers of cytosine and uridine [45;90]. The same is true for ribavirin (244 Da) and its isobaric prodrug viramidine (243 Da), which also share their mass transitions with cytosine and uridine [17].

Another problem occurring during the simultaneous analysis of nucleotides is the up-front fragmentation of higher phosphates into lower phosphates, which for example results in a MS signal in the DP mass transition at the retention time of the TP.

The described forms of interference can be summarized in the following example: when directly analyzing ara-UMP the MS can detect UMP (endogenous isomer), ara-UTP and ara-UDP (up-front fragmentation to ara-UMP), $^{13}C/^{15}N$-ara-CMP and $^{13}C/^{15}N$-CMP (isotope signals), despite the selection of a parent and product ion. These interferences make selective sample pretreatment or chromatographic separation of the analytes indispensable for accurate quantification.

Tools to improve the selectivity

As discussed in section IV A, nucleotides can be ionized in the positive as well as in the negative ion mode. Common fragments in the negative ion mode are the MP (m/z 79) and DP (m/z 159) ion, whereas the protonated base is frequently observed in the positive ion mode (table 10). Although abundant, the DP fragment is formed from every nucleoside DP or TP, thus relying solely on the parent mass for MS selectivity. Though still the same for many nucleosides, the base fragment obtained in the positive ion mode offers much more selectivity [78]. Switching from the negative to the positive ion mode has therefore solved many of the problems related to endogenous peaks [14;23;78].

Switching of polarity is, however, not feasible for all analytes. For example, AZT nucleotides show a lack of signal in the positive ion mode [76]. Several sample pretreatments have been investigated in an attempt to solve this problem.

The separation of nucleosides is easier than the separation of their corresponding nucleotides. Therefore, AZT nucleotides were successfully

quantitated after dephosphorylation [38;44;109;112;119]. Others experimented with direct approaches.

A selective periodate-methylamine reduction of ribonucleotides was used to deplete the interfering ATP [75;76;120], but the remaining dGTP still prevented quantification. Both ATP and dGTP were effectively removed using an immunoaffinity extraction [75], but the need to raise specific antibodies, lack of robustness and low throughput hampered routine use. The best solution for the direct determination of AZT-TP to date is the selection of a low-abundant, but selective, fragment (m/z 380) [76;104]. Others, however, were less successful in using a selective fragment [44].

For the simultaneous quantification of cytidine and uridine analogs, the best approach is to use a selective chromatographic system as recently described [92].

The risk of interferences in mass transitions of internal standards has been limited by using Br- and Cl-subsitued bases, which have a transition for each isotope, or by using thiophosphates that do not result in a normal DP (m/z 159) fragment [70]. Both these effects are seen for the clodronate metabolite.

Despite the use of tandem MS, interfering peaks have often been observed. MS selectivity can be improved by using the positive ionization mode. Otherwise, specific sample preparation or selective chromatographic systems are required.

Absorption to metal

Throughout the literature on the analysis of nucleotides with MS peak tailing is reported. Some groups found that ammonium phosphate improved peak shape [14] and MS signal [69], whereas others observed that peak tailing was reduced by using a shorter stainless steel capillary in the ESI source [23]. Moreover, variation in the MS signal and peak tailing was decreased by replacing the stainless steel capillary by a fused silica capillary [23;87].

Two groups extensively reported on the effect and concluded that it could, at least in part, be due to absorption of phosphate groups to metal surfaces [121;122].

Wakamatsu et al. noticed extensive peak tailing when analyzing adenosine MP (AMP) [122]. The same effect was seen for guanosine MP (GMP) and uridine MP (UMP), but not for adenosine, guanosine or uridine. When phosphate ions were added to the mobile phase, the peak shapes improved considerably. After pre-treatment of the stainless steel capillary with phosphoric acid, peak shapes improved and remained acceptable for several hours.

Tuytten et al. systematically examined the effect and concluded that phosphate-containing analytes, including nucleotides, can be trapped on any steel part of the analytical system (in the following order: MP<DP<TP)

[121]. Besides identifying the injector needle, loop and valve as culprits, they also noticed an extensive loss of analytes on the inner wall of the capillary. Corrosion by prolonged used of the needle made the effect even more pronounced. The nucleotides could only be eluted from the metal surfaces under very basic conditions.
An alternative approach to prevent peak tailing was provided by Asakawa et al., who found that (bi)carbonate was as effective as phosphate in reducing peak tailing [123]. The MS-compatibility of (bi)carbonate offers a great advantage over phosphate.
As opposed to undesired peak tailing, Tuytten et al. have used the effect to their advantage by performing sample clean up and concentration using an IMAC column [48].
Since the nucleotide analysis has traditionally been performed with mobile phases containing phosphate buffers, the adsorption to metal is a problem that specifically emerged in the LC-MS analysis of nucleotides. Several solutions have, however, been provided. Concluding, phosphate ions (introduced before or during analysis), or replacement of the stainless steel capillary by fused silica are effective in reducing peak tailing, but the most promising approach seems to be the addition (bi)carbonate ions to the mobile phase.

Conclusion and perspectives

Both indirect and direct methods have been developed to overcome the apparent incompatibility of nucleotide analysis and MS detection.

Indirect and direct methods for the analysis of drug-related nucleotides show a comparable sensitivity and have successfully been validated and applied to biological samples. The methods, however, differ in their strengths and weaknesses.

Indirect methods are labour intensive because samples have to be fractionated, dephosphorylated and purified before the actual analysis. Indirect methods are also instrument time intensive because each fraction has to be analyzed separately. Moreover, the extensive sample pretreatment is a potential source of errors. The final analysis is, however, relatively simple, fast and selective and can readily be used with MS detection.

Direct methods require little to no sample pretreatment, but sometimes lack selectivity because chromatographic separation is mainly based on the number of phosphate groups. Long run times were initially required, but those of recent methods compete with run times of indirect analyses.

The advantages and drawbacks of both methods are illustrated by a recent discussion between two groups with long experience in the analysis of intracellular nucleotide analogs, using an indirect and a direct method [72;83;124].

Taking everything into account, direct methods seem preferable over indirect methods. The use of IP-agents is well established. Through the reduction of IP-agents and salts delivered to the source, the method has become relatively MS-friendly. Many, however, still report problems with the approach. More recently it was shown that WAX, using a pH gradient instead of salts for elution, is a good and relatively simple alternative. PGC has shown unsurpassed selectivity, which makes it especially attractive for the separation of closely related nucleotides that cannot be fully distinguished with conventional mass spectrometers. CE-MS has also proven its applicability to the analysis of intracellular nucleotides. Though sensitive, the lack of experience and low reproducibility make MALDI-TOF not the method of choice. More applications using HILIC are required to determine its value for the analysis of intracellular nucleotides. Due to its limited accessibility, the use of AMS is most likely only favored for specific research question requiring its ultra-sensitivity.

Despite the initial difficulties, MS has become the method of choice for the quantitative determination of intracellular nucleotide analogs because of its sensitivity and selectivity. With these advantages over other methods, nucleotide analogs can selectively be detected in ever smaller concentrations and sample volumes, enabling further elucidation of the pharmacology of this important class of drugs.

References

[1] J. F. Rodriguez Orengo, J. Santana, I. Febo, C. Diaz, J. L. Rodriguez, R. Garcia, E. Font, O. Rosario, P. R. Health Sci. J. 19 (2000) 19.
[2] M. T. Osterman, R. Kundu, G. R. Lichtenstein, J. D. Lewis, Gastroenterology 130 (2006) 1047.
[3] J. Lai, J. Wang, Z. Cai, J. Chromatogr. B 868 (2008) 1.
[4] H. Kuster, M. Vogt, B. Joos, V. Nadai, R. Luthy, J. Infect. Dis. 164 (1991) 773.
[5] J. T. Slusher, S. K. Kuwahara, F. M. Hamzeh, L. D. Lewis, D. M. Kornhauser, P. S. Lietman, Antimicrob. Agents Chemother. 36 (1992) 2473.
[6] C. Solas, Y. F. Li, M. Y. Xie, J. P. Sommadossi, X. J. Zhou, Antimicrob. Agents Chemother. 42 (1998) 2989.
[7] M. G. Pike, C. L. Franklin, D. C. Mays, J. J. Lipsky, P. W. Lowry, W. J. Sandborn, J. Chromatogr. B Biomed. Sci. Appl. 757 (2001) 1.
[8] L. Goujon, T. Brossette, N. Dereudre-Bosquet, C. Creminon, P. Clayette, D. Dormont, C. Mioskowski, L. Lebeau, J. Grassi, J. Immunol. Methods 218 (1998) 19.
[9] C. Le Saint, R. Terreux, D. Duval, J. Durant, H. Ettesse, P. Dellamonica, R. Guedj, J. P. Vincent, A. Cupo, Antimicrob. Agents Chemother. 48 (2004) 589.
[10] B. L. Robbins, J. Rodman, C. McDonald, R. V. Srinivas, P. M. Flynn, A. Fridland, Antimicrob. Agents Chemother. 38 (1994) 115.
[11] V. Reichelova, F. Albertioni, J. Liliemark, J. Chromatogr. B Biomed. Appl. 682 (1996) 115.
[12] F. Dai, J. A. Kelley, H. Zhang, N. Malinowski, M. F. Kavlick, J. Lietzau, L. Welles, R. Yarchoan, H. Ford, Jr., Anal. Biochem. 288 (2001) 52.
[13] D. M. Tidd, S. Dedhar, J. Chromatogr. 145 (1978) 237.
[14] R. L. Claire, III, Rapid Commun. Mass Spectrom. 14 (2000) 1625.
[15] T. F. Kalhorn, A. G. Ren, J. T. Slattery, J. S. McCune, J. Wang, J. Chromatogr. B 820 (2005) 243.
[16] A. S. Ray, J. E. Vela, L. Olson, A. Fridland, Biochem. Pharmacol. 68 (2004) 1825.
[17] L. T. Yeh, M. Nguyen, S. Dadgostari, W. Bu, C. C. Lin, J. Pharm. Biomed. Anal. 43 (2007) 1057.
[18] T. Dervieux, G. Meyer, R. Barham, M. Matsutani, M. Barry, R. Boulieu, B. Neri, E. Seidman, Clin. Chem. 51 (2005) 2074.
[19] S. A. Veltkamp, M. J. Hillebrand, H. Rosing, R. S. Jansen, E. R. Wickremsinhe, E. J. Perkins, J. H. Schellens, J. H. Beijnen, J. Mass Spectrom. 41 (2006) 1633.
[20] S. Bergan, O. Bentdal, G. Sodal, A. Brun, H. E. Rugstad, O. Stokke, Ther. Drug Monit. 19 (1997) 502.
[21] L. Durand-Gasselin, D. Da Silva, H. Benech, A. Pruvost, J. Grassi, Antimicrob. Agents Chemother. 51 (2007) 2105.
[22] P. L. Anderson, J. H. Zheng, T. King, L. R. Bushman, J. Predhomme, A. Meditz, J. Gerber, C. V. Fletcher, AIDS 21 (2007) 1849.
[23] G. Shi, J. T. Wu, Y. Li, R. Geleziunas, K. Gallagher, T. Emm, T. Olah, S. Unger, Rapid Commun. Mass Spectrom. 16 (2002) 1092.
[24] A. S. Ray, F. Myrick, J. E. Vela, L. Y. Olson, E. J. Eisenberg, K. Borroto-Esodo, M. D. Miller, A. Fridland, Antivir. Ther. 10 (2005) 451.
[25] A. Pruvost, F. Becher, P. Bardouille, C. Guerrero, C. Creminon, J. F. Delfraissy, C. Goujard, J. Grassi, H. Benech, Rapid Commun. Mass Spectrom. 15 (2001) 1401.
[26] M. M. Bradford, Anal. Biochem. 72 (1976) 248.
[27] H. Benech, F. Theodoro, A. Herbet, N. Page, D. Schlemmer, A. Pruvost, J. Grassi, J. R. Deverre, Anal. Biochem. 330 (2004) 172.
[28] F. Becher, A. Pruvost, J. Gale, P. Couerbe, C. Goujard, V. Boutet, E. Ezan, J. Grassi, H. Benech, J. Mass Spectrom. 38 (2003) 879.
[29] M. K. Grob, K. O'Brien, J. J. Chu, D. D. Chen, J. Chromatogr. B 788 (2003) 103.
[30] S. Palmer, S. Cox, J. Chromatogr. A 667 (1994) 316.

[31] E. Kimball, J. D. Rabinowitz, Anal. Biochem. 358 (2006) 273.
[32] L. N. Thevanayagam, A. L. Jayewardene, J. G. Gambertoglio, J. Pharm. Biomed. Anal. 22 (2000) 597.
[33] B. L. Robbins, P. A. Poston, E. F. Neal, C. Slaughter, J. H. Rodman, J. Chromatogr. B 850 (2007) 310.
[34] B. L. Robbins, B. H. Waibel, A. Fridland, Antimicrob. Agents Chemother. 40 (1996) 2651.
[35] T. Dervieux, R. Boulieu, Clin. Chem. 44 (1998) 2511.
[36] M. Shipkova, V. W. Armstrong, E. Wieland, M. Oellerich, Clin. Chem. 49 (2003) 260.
[37] S. Vikingsson, B. Carlsson, S. H. Almer, C. Peterson, Ther. Drug Monit. (2009).
[38] L. D. Williams, L. S. Von Tungeln, F. A. Beland, D. R. Doerge, J. Chromatogr. B Analyt. Technol. Biomed. Life Sci. 798 (2003) 55.
[39] P. L. Anderson, T. N. Kakuda, S. Kawle, C. V. Fletcher, AIDS 17 (2003) 2159.
[40] J. D. Moore, E. P. Acosta, V. A. Johnson, R. Bassett, J. J. Eron, M. A. Fischl, M. C. Long, D. R. Kuritzkes, J. P. Sommadossi, Antivir. Ther. 12 (2007) 981.
[41] R. Hellborg, G. Skog, Mass Spectrom. Rev. 27 (2008) 398.
[42] l. T. Vuong, J. L. Ruckle, A. B. Blood, M. J. Reid, R. D. Wasnich, H. A. Synal, S. R. Dueker, J. Pharm. Sci. 97 (2008) 2833.
[43] Chen, J, Seymour, M, Lee, L, Fuchs, E, Hubbard, W, Parsons, T, Pakes, G, Fletcher, C, Garner, C, and Flexner, C, 16th conference on retroviruses and oppertunistic infections (2009).
[44] T. King, L. Bushman, P. L. Anderson, T. Delahunty, M. Ray, C. V. Fletcher, J. Chromatogr. B 831 (2006) 248.
[45] C. Crauste, I. Lefebvre, M. Hovaneissian, J. Y. Puy, B. Roy, S. Peyrottes, S. Cohen, J. Guitton, C. Dumontet, C. Perigaud, J. Chromatogr. B Analyt. Technol. Biomed. Life Sci. (2009).
[46] V. Pucci, C. Giuliano, R. Zhang, K. A. Koeplinger, J. F. Leone, E. Monteagudo, F. Bonelli, J. Sep. Sci. (2009).
[47] Bartley, S, Begley, JA., and Clark, TN., Proceedings of the 55th ASMS conference on mass spectrometry and allied topics (2007).
[48] R. Tuytten, F. Lemiere, W. Van Dongen, H. Slegers, R. P. Newton, E. L. Esmans, J. Chromatogr. B 809 (2004) 189.
[49] Kuklenyik, Z, Martin, A, Pau, C, Garcia-Lerma, G, Heneine, W, Pirkle, J, and Barr, J, Proceedings of the 56th ASMS conference on mass spectrometry and allied topics (2008).
[50] R. Nirogi, G. Bhyrapuneni, V. Kandikere, K. Mudigonda, P. Komarneni, R. Aleti, K. Mukkanti, Biomed. Chromatogr. (2008).
[51] J. Kim, T. F. Chou, G. W. Griesgraber, C. R. Wagner, Mol. Pharm. 1 (2004) 102.
[52] T. Lynch, G. Eisenberg, M. Kernan, Nucleosides Nucleotides Nucleic Acids 20 (2001) 1415.
[53] L. Bousquet, A. Pruvost, A. C. Guyot, R. Farinotti, A. Mabondzo, Antimicrob. Agents Chemother. 53 (2009) 896.
[54] J. Kim, S. Park, N. Y. Tretyakova, C. R. Wagner, Mol. Pharm. 2 (2005) 233.
[55] E. Witters, W. Van Dongen, E. L. Esmans, H. A. Van Onckelen, J. Chromatogr. B Biomed. Sci. Appl. 694 (1997) 55.
[56] T. Hawkins, W. Veikley, R. L. Claire, III, B. Guyer, N. Clark, B. P. Kearney, J. Acquir. Immune. Defic. Syndr. 39 (2005) 406.
[57] L. H. Wang, J. Begley, C. R. St, III, J. Harris, C. Wakeford, F. S. Rousseau, AIDS Res. Hum. Retroviruses 20 (2004) 1173.
[58] K. Borroto-Esoda, J. E. Vela, F. Myrick, A. S. Ray, M. D. Miller, Antivir. Ther. 11 (2006) 377.
[59] W. E. Delaney, A. S. Ray, H. Yang, X. Qi, S. Xiong, Y. Zhu, M. D. Miller, Antimicrob. Agents Chemother. 50 (2006) 2471.

[60] A. S. Ray, J. E. Vela, C. G. Boojamra, L. Zhang, H. Hui, C. Callebaut, K. Stray, K. Y. Lin, Y. Gao, R. L. Mackman, T. Cihlar, Antimicrob. Agents Chemother. 52 (2008) 648.
[61] H. Reiser, J. Wang, L. Chong, W. J. Watkins, A. S. Ray, R. Shibata, G. Birkus, T. Cihlar, S. Wu, B. Li, X. Liu, I. N. Henne, G. H. Wolfgang, M. Desai, G. R. Rhodes, A. Fridland, W. A. Lee, W. Plunkett, D. Vail, D. H. Thamm, R. Jeraj, D. B. Tumas, Clin. Cancer Res. 14 (2008) 2824.
[62] J. E. Vela, L. Y. Olson, A. Huang, A. Fridland, A. S. Ray, J. Chromatogr. B 848 (2007) 335.
[63] E. N. Fung, Z. Cai, T. C. Burnette, A. K. Sinhababu, J. Chromatogr. B 754 (2001) 285.
[64] H. J. Gaus, S. R. Owens, M. Winniman, S. Cooper, L. L. Cummins, Anal. Chem. 69 (1997) 313.
[65] A. Apffel, J. A. Chakel, S. Fischer, K. Lichtenwalter, W. S. Hancock, J. Chromatogr. A 777 (1997) 3.
[66] Smyrnis, E, Sacks, S, Burton, R, Wall, R, and Abbott, F, Proceedings of the 44th ASMS conference on mass spectrometry and allied topics (1996) 189.
[67] S. Auriola, J. Frith, M. J. Rogers, A. Koivuniemi, J. Monkkonen, J. Chromatogr. B Biomed. Sci. Appl. 704 (1997) 187.
[68] H. Monkkonen, P. Moilanen, J. Monkkonen, J. C. Frith, M. J. Rogers, S. Auriola, J. Chromatogr. B Biomed. Sci. Appl. 738 (2000) 395.
[69] R. Tuytten, F. Lemiere, W. V. Dongen, E. L. Esmans, H. Slegers, Rapid Commun. Mass Spectrom. 16 (2002) 1205.
[70] F. Becher, A. Pruvost, C. Goujard, C. Guerreiro, J. F. Delfraissy, J. Grassi, H. Benech, Rapid Commun. Mass Spectrom. 16 (2002) 555.
[71] A. Pruvost, E. Negredo, H. Benech, F. Theodoro, J. Puig, E. Grau, E. Garcia, J. Molto, J. Grassi, B. Clotet, Antimicrob. Agents Chemother. 49 (2005) 1907.
[72] F. Becher, A. G. Pruvost, D. D. Schlemmer, C. A. Creminon, C. M. Goujard, J. F. Delfraissy, H. C. Benech, J. J. Grassi, AIDS 17 (2003) 555.
[73] F. Becher, R. Landman, S. Mboup, C. N. Kane, A. Canestri, F. Liegeois, M. Vray, M. H. Prevot, G. Leleu, H. Benech, AIDS 18 (2004) 181.
[74] J. Lee, B. C. Yoo, H. S. Lee, H. W. Yoo, H. H. Yoo, M. J. Kang, D. H. Kim, Ther. Drug Monit. 28 (2006) 131.
[75] F. Becher, D. Schlemmer, A. Pruvost, M. C. Nevers, C. Goujard, S. Jorajuria, C. Guerreiro, T. Brossette, L. Lebeau, C. Creminon, J. Grassi, H. Benech, Anal. Chem. 74 (2002) 4220.
[76] S. Compain, L. Durand-Gasselin, J. Grassi, H. Benech, J. Mass Spectrom. 42 (2007) 389.
[77] L. Durand-Gasselin, A. Pruvost, A. Dehee, G. Vaudre, M. D. Tabone, J. Grassi, G. Leverger, A. Garbarg-Chenon, H. Benech, C. Dollfus, Antimicrob. Agents Chemother. 52 (2008) 2555.
[78] A. Pruvost, F. Theodoro, L. Agrofoglio, E. Negredo, H. Benech, J. Mass Spectrom. 43 (2008) 224.
[79] B. I. Hernandez-Santiago, T. Beltran, L. Stuyver, C. K. Chu, R. F. Schinazi, Antimicrob. Agents Chemother. 48 (2004) 4636.
[80] L. Coulier, R. Bas, S. Jespersen, E. Verheij, M. J. van der Werf, T. Hankemeier, Anal. Chem. 78 (2006) 6573.
[81] L. Coulier, J. J. van Kampen, R. de Groot, Gerritsen H.W., R. C. Bas, W. D. van Dongen, L. P. Brull, T. M. Luider, Proteomics -Clinical applications 2 (2008) 1557.
[82] Z. Cai, F. Song, M. S. Yang, J. Chromatogr. A 976 (2002) 135.
[83] M. Melendez, R. Blanco, W. Delgado, R. Garcia, J. Santana, H. Garcia, O. Rosario, J. F. Rodriguez, Antimicrob. Agents Chemother. 50 (2006) 835.
[84] Nguyen, T, Zhang, X, Amin, J, Marlor, C, Mushtaq, G, and Buechter, D, Proceedings of the 54th conference on mass spectrometry and allied topics (2006).
[85] K. J. Freise, T. Martin-Jimenez, J. Vet. Pharmacol. Ther. 29 (2006) 137.

[86] S. A. Veltkamp, R. S. Jansen, S. Callies, D. Pluim, C. M. Visseren-Grul, H. Rosing, S. Kloeker-Rhoades, V. A. Andre, J. H. Beijnen, C. A. Slapak, J. H. Schellens, Clin. Cancer Res. 14 (2008) 3477.
[87] R. S. Jansen, H. Rosing, C. J. de Wolf, J. H. Beijnen, Rapid Commun. Mass Spectrom. 21 (2007) 4049.
[88] G. H. Gu, C. K. Lim, J. Chromatogr. 515 (1990) 183.
[89] Y. Q. Xia, M. Jemal, N. Zheng, X. Shen, Rapid Commun. Mass Spectrom. 20 (2006) 1831.
[90] M. Gouy, H. Fabre, M. Blanchin, S. Peyrottes, C. Périgaud, I. Lefebvre, Anal. Chim. Acta 566 (2006) 178.
[91] J. Xing, A. Apedo, A. Tymiak, N. Zhao, Rapid Commun. Mass Spectrom. 18 (2004) 1599.
[92] R. S. Jansen, H. Rosing, J. H. Schellens, J. H. Beijnen, J. Chromatogr. A 1216 (2009) 3168.
[93] Jansen, R. S., Rosing, H., Schellens, J. H., and Beijnen, J. H., Simultaneous quantification of 2'-2'-difluoro-deoxycytidine and 2'-2'-difluoro-deoxyuridine nucleosides and nucleotides in white blood cells using porous graphitic carbon chromatography coupled with tandem mass spectrometry, Submitted for publication
[94] A. Zinellu, S. Sotgia, V. Pasciu, M. Madeddu, G. G. Leoni, S. Naitana, L. Deiana, C. Carru, Electrophoresis 29 (2008) 3069.
[95] M. Uhrova, Z. Deyl, M. Suchanek, J. Chromatogr. B Biomed. Appl. 681 (1996) 99.
[96] A. P. McKeown, P. N. Shaw, D. A. Barrett, Electrophoresis 22 (2001) 1119.
[97] J. F. Banks, Electrophoresis 18 (1997) 2255.
[98] Y. L. Feng, J. Zhu, Anal. Chem. 78 (2006) 6608.
[99] D. Friedecky, P. Bednar, M. Prochazka, T. Adam, Nucleosides Nucleotides Nucleic Acids 25 (2006) 1233.
[100] T. Soga, T. Ishikawa, S. Igarashi, K. Sugawara, Y. Kakazu, M. Tomita, J. Chromatogr. A 1159 (2007) 125.
[101] Z. Cai, E. N. Fung, A. K. Sinhababu, Electrophoresis 24 (2003) 3160.
[102] C. C. Liu, J. S. Huang, D. L. Tyrrell, N. J. Dovichi, Electrophoresis 26 (2005) 1424.
[103] V. Bezy, P. Chaimbault, P. Morin, S. E. Unger, M. C. Bernard, L. A. Agrofoglio, Electrophoresis 27 (2006) 2464.
[104] J. J. van Kampen, P. L. Fraaij, V. Hira, A. M. van Rossum, N. G. Hartwig, R. de Groot, T. M. Luider, Biochem. Biophys. Res. Commun. 315 (2004) 151.
[105] Y. Hsieh, J. Sep. Sci. 31 (2008) 1481.
[106] S. U. Bajad, W. Lu, E. H. Kimball, J. Yuan, C. Peterson, J. D. Rabinowitz, J. Chromatogr. A 1125 (2006) 76.
[107] J. J. Pesek, M. T. Matyska, M. T. Hearn, R. I. Boysen, J. Chromatogr. A 1216 (2009) 1140.
[108] T. Holdich, L. A. Shiveley, J. Sawyer, Antimicrob. Agents Chemother. 51 (2007) 2943.
[109] J. D. Moore, G. Valette, A. Darque, X. J. Zhou, J. P. Sommadossi, J. Am. Soc. Mass Spectrom. 11 (2000) 1134.
[110] G. J. Yuen, Y. Lou, N. F. Bumgarner, J. P. Bishop, G. A. Smith, V. R. Otto, D. D. Hoelscher, Antimicrob. Agents Chemother. 48 (2004) 176.
[111] Delinsky, DC, Hernandez-Santiago, B., and Schinazi, RF, Proceedings of the 54th ASMS conference on mass spectrometry and allied topics (2006).
[112] E. Font, O. Rosario, J. Santana, H. Garcia, J. P. Sommadossi, J. F. Rodriguez, Antimicrob. Agents Chemother. 43 (1999) 2964.
[113] L. T. Yeh, M. Nguyen, D. Lourenco, C. C. Lin, J. Pharm. Biomed. Anal. 38 (2005) 34.
[114] X. Cahours, T. T. Tran, N. Mesplet, C. Kieda, P. Morin, L. A. Agrofoglio, J. Pharm. Biomed. Anal. 26 (2001) 819.
[115] T. King, L. Bushman, J. Kiser, P. L. Anderson, M. Ray, T. Delahunty, C. V. Fletcher, J. Chromatogr. B 843 (2006) 147.
[116] K. B. Green-Church, P. A. Limbach, J. Am. Soc. Mass Spectrom. 11 (2000) 24.

[117] S. Pan, K. Verhoeven, J. K. Lee, J. Am. Soc. Mass Spectrom. 16 (2005) 1853.
[118] T. Qian, Z. Cai, M. S. Yang, Anal. Biochem. 325 (2004) 77.
[119] J. F. Rodriguez, J. L. Rodriguez, J. Santana, H. Garcia, O. Rosario, Antimicrob. Agents Chemother. 44 (2000) 3097.
[120] G. Hennere, F. Becher, A. Pruvost, C. Goujard, J. Grassi, H. Benech, J. Chromatogr. B 789 (2003) 273.
[121] R. Tuytten, F. Lemiere, E. Witters, W. Van Dongen, H. Slegers, R. P. Newton, H. Van Onckelen, E. L. Esmans, J. Chromatogr. A 1104 (2006) 209.
[122] A. Wakamatsu, K. Morimoto, M. Shimizu, S. Kudoh, J. Sep. Sci. 28 (2005) 1823.
[123] Y. Asakawa, N. Tokida, C. Ozawa, M. Ishiba, O. Tagaya, N. Asakawa, J. Chromatogr. A 1198-1199 (2008) 80.
[124] H. Benech, F. Becher, A. Pruvost, J. J. Grassi, Antimicrob. Agents Chemother. 50 (2006) 2899.
[125] G. Moyle, M. Boffito, C. Fletcher, C. Higgs, P. E. Hay, I. H. Song, Y. Lou, G. J. Yuen, S. S. Min, E. M. Guerini, Antimicrob. Agents Chemother. (2009).

Chapter 2.2

Development and validation of an assay for the quantitative determination of cladribine nucleotides in MDCKII cells and culture medium using weak anion exchange liquid chromatography coupled with tandem mass spectrometry

Robert S Jansen, Hilde Rosing, Cocky JF de Wolf and Jos H Beijnen

Rapid Communications in Mass Spectrometry
Volume 21, Issue 24, Pages 4049-59
2007

Abstract

The development and validation of an assay for the quantitative analysis of cladribine mono-, di- and triphosphate (2-chloro, 2'-deoxyadenosine 5'-mono-, di- and triphosphate or 2CdAMP, 2CdADP and 2CdATP) in culture medium (Optimem) and cell lysate is described. Cladribine mono- and diphosphate reference compounds were obtained by thermal degradation of cladribine triphosphate. The reference compounds were characterized using ion-pairing reversed-phase high-performance liquid chromatography with ultraviolet detection. The bioanalytical assay for 2CdAMP, 2CdADP and 2CdATP is based on weak anion-exchange liquid chromatography coupled with tandem mass spectrometry in the positive ion mode (WAXLC/MS/MS). A fused-silica electrospray capillary was used instead of a stainless steel electrospray capillary to minimize adsorption of analytes and thus decrease variation in the analyte signals. Dynamic ranges of 1.11-27.7, 0.550-55.0 and 1.31-52.3 nM for 2CdAMP, 2CdADP and 2CdATP, respectively, were validated in culture medium and cell lysate. Optimem samples required stabilization with 30% methanol to prevent conversion of 2CdATP into 2CdAMP and 2CdADP. All intra- and interday accuracies and precisions were within ±20%. The stability of the compounds was assessed under various analytically relevant conditions. The method was successfully used to investigate cladribine nucleotide transport *in vitro* in Madin-Darby canine kidney II (MDCKII) cells.

Introduction

2-Chloro-2′-deoxyadenosine (2CdA, cladribine, Leustatin®)(Figure 1) is a nucleoside analog used in anticancer therapy with high activity against hairy cell and chronic lymphocytic leukemias. Like other nucleoside analogs used in anti-HIV (nucleoside reverse transcriptase inhibitors (NRTI´s)) anti-inflammatory and anticancer therapies cladribine requires intracellular metabolic activation. Cladribine is taken up into cells by concentrative (CNT) and equilibrative (ENT) nucleoside transporters [1]. After uptake cladribine is phoshorylated to its 5´-monophosphate (2CdAMP) by deoxycytidine kinase (dCK) and deoxyguanosine kinase (dGK). 2CdAMP is subsequently phosphorylated to cladribine diphosphate (2CdADP) and the active nucleotide cladribine triphosphate (2CdATP) [2]. High levels of 2CdAMP and 2CdATP accumulate in lymphocytes after administration of cladribine [3]. 2CdATP is incorporated into DNA leading to inhibition of nucleic acid synthesis, DNA strand breaks and finally apoptosis [4;5]. Moreover 2CdATP inhibits ribonucleotide reductase (RNR) disturbing endogenous nucleotide concentrations.
The levels of 2CdAMP and 2CdATP are highly variable between patients [6]. Cellular mechanisms related to nucleoside transporter activity, phosphorylation and dephosphorylation can cause resistance to nucleoside analogs [7]. It has been reported that nucleoside monophosphates are substrates for the efflux pumps multidrug resistance protein 4 and 5 (MRP4 and MRP5) [8;9]. These and other drug efflux pumps may be important factors in cladribine therapy outcome. Transwell experiments are very suitable to assess the role of transporters in cellular pharmacokinetics [10]. A transwell assay allows the determination of analytes in medium at the basolateral and apical side of cells and inside cells. A schematic representation of the transwell setup is depicted in Figure 2.

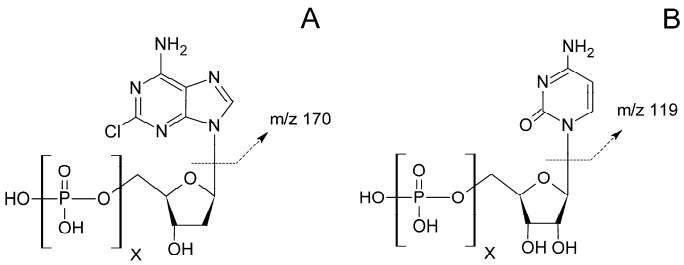

Figure 1. Structure and proposed fragmentation of (a) 2CdA(X=0), 2CdAMP(X=1), 2CdADP(X=2) and 2CdATP(X=3) and of the internal standards (b)*CMP(X=1), *CDP(X=2) and *CTP(X=3)

The first method to determine cladribine nucleotides in leukemic cells determined the total cellular cladribine nucleotide content [11]. A specific ion-pair high performance liquid chromatography (HPLC) method with ultraviolet (UV) detection for 2CdAMP, 2CdADP and 2CdATP was developed later [12].
Anion exchange methods and methods using ion-pair reagents are very suitable to separate the polar nucleotides. The use of high salt concentrations and involatile ion-pair reagents in these methods, however, precludes the use of mass spectrometry (MS) for detection. UV detection usually results in relatively poor sensitivity and selectivity. Both direct and indirect approaches for nucleotide analysis have been applied to circumvent the incompatibility with MS. Indirect methods consist of a separation of the nucleotides on an ion-exchange cartridge or using HPLC. The fractions containing the nucleotides are subsequently dephosphorylated using alkaline or acidic phosphatase. After dephosphorylation the remaining nucleoside can be quantified using a radioimmunoassay (RIA) [13;14], UV [15;16]or MS [17;18] detection. The main drawback of the indirect methods is the extra step in sample pretreatment which is labor intensive and a possible source of errors.
Several direct methods with MS detection have been described. Claire et al. have used eluents with low concentrations of the involatile ion pair reagent tetrabutylammonium in combination with phosphate on a microbore column [19]. Other direct methods have been developed using the volatile ion-pair reagent dimethylhexylamine (DMHA) [20;21]. Recently separation of nucleosides and nucleotides using a porous graphitic carbon column has also been described [22]. Weak anion exchange liquid chromatography is another approach for the separation and direct determination of nucleotides with MS detection [23]. This method uses a pH gradient instead of a salt gradient to separate and elute the nucleotides from a weak anion exchange (WAX) column. This approach has been used earlier with success by us for the quantification of gemcitabine triphosphate [24].
This paper describes the development and validation of a weak anion exchange liquid chromatography method coupled with tandem mass spectrometry (WAXLC-MS/MS) for the simultaneous quantification of the 2CdA nucleotides 2CdAMP, 2CdADP and 2CdATP in both Optimem culture medium and cells.

Experimental

Reagents

Cladribine was obtained from Sigma (Zwijndrecht, The Netherlands). Cladribine triphosphate (lithium salt) originated from Calbiochem (Darmstadt, Germany). 13C9,15N3-Cytidine triphosphate (13C9,15N3CTP, *CTP, internal standard (IS); Figure 1) was purchased from Buchem BV(Apeldoorn, The Netherlands). Ammonium acetate (NH4Ac), aqueous ammonia 25% (NH4OH), glacial acetic acid (HAc), ethylenediaminetetraacetic acid (EDTA), 85% phosphoric acid and triethylamine (TEA) (all analytical grade) were from Merck (Darmstadt, Germany). Methanol (MeOH) and acetonitrile (ACN) were obtained from Biosolve Ltd. (Amsterdam, The Netherlands). Distilled water (H2O) was obtained from B. Braun (Melsungen, Germany). Gibco® Optimem originated from Invitrogen (Carlsbad, CA, USA). Phosphatase inhibitor cocktail set II was obtained from Calbiochem.

Instrumentation

HPLC-UV experiments were performed on an Agilent 1100 series liquid chromatograph system (Agilent technologies, Palo Alto, CA, USA) consisting of a binary pump, an inline degasser, autosampler, column oven and UV detector. Mobile phase A was prepared by mixing 0.1 M TEA solution in water with 0.09 M phosphoric acid solution in water to pH 6.75. Mobile phase B consisted of methanol. Mobile phase A and B (90:10, v/v) were isocratically pumped through a Gemini C18 110A column (150 X 2.0 mm ID, 5 µm, Phenomenex, Torrance, CA, USA) at a flowrate of 0.2 mL/min. The column compartment was thermostated at 45 oC. 10 µL injections were carried out using the autosampler thermostated at 4 oC. UV detection was performed at 265 nm with a total runtime of 30 min. Data was processed with Chromeleon 6.50 software (Dionex corporation, Sunnyvale, CA, USA).

MS experiments were performed using a Thermo Fischer TSQ Quantum Ultra mass spectrometer (Thermo Fisher Scientific Inc, Waltham, MA, USA). The Shimadzu LC system (Shimadzu, Kyoto, Japan) used for the WAXLC-MS/MS experiments consisted of a SIL-HTc autosampler with SCL-10A^{vp} systemcontroller, two LC20-AD Prominence pumps, a FCV-11AL valve unit, a DGU-20A5 inline degasser unit and a CTO-20AC column oven.

A stepwise gradient (Table 1) consisting of 10 mM NH_4Ac in ACN-H_2O (30:70, v/v) pH 6.0 (A) and 1 mM NH_4Ac in ACN-H_2O (30:70, v/v) pH 10.5 (B) was delivered to a Biobasic AX column (50 x 2.1 mm ID, 5 µm, Thermo Fisher Scientific Inc, Waltham, MA, USA). A guard cartridge (10 x 2.1 mm ID, 5 µm) was used to protect the analytical column. The eluent pH was increased and the NH_4Ac concentration was decreased in mobile phase B relative to mobile phase A to obtain a good separation of the mono-, di-

and triphosphates [23]. 25 µL injections were carried out using the autosampler thermostated at 4 °C. The total runtime was 10 min. The autosampler needle was rinsed before and after aspiration with 400 µL of MeOH.

During the first 3 and last 4 minutes the eluate was directed to waste using the divert valve on the mass spectrometer. Ionization was performed using an electrospray ionization (ESI) source operating in the positive ion mode, equipped with a fused silica capillary (0.10 mm ID × 0.19 mm OD). The ESI probe was positioned at mark B and the distance from the sweep cone was set at 0.75 inch. The left-right position was set in the middle. The sheath and auxiliary gas were set at 37 and 10 arbitrary units (au) respectively with the ion sweep gas set at 1.0 au (all N_2). The collision gas (Argon) pressure was set at 2.0 mTorr. The sprayvoltage was 4500 V. The capillary was heated to 375 °C. A 0.7 full width half mass (FWHM) resolution (unit resolution) of the hyperquads was used for all transitions. The source collision induced dissociation (CID) was not used. The scan parameters are listed in Table 2. Data was acquired using Xcalibur 2.0 and processed using LCQuan 2.5 software (Thermo Fisher Scientific Inc).

Table 1. HPLC stepwise gradient for the WAXLC-MS/MS experiments

Time (min)	Flow rate (mL/min)	Mobile phase A* (%)	Mobile phase B** (%)
0	0.25	90	10
0.50	0.25	90	10
0.51	0.25	50	50
1.75	0.25	50	50
1.76	0.25	0	100
6.50	0.25	0	100
6.60	0.50	90	10
9.50	0.25	90	10
10.0	0.25	90	10

* Mobile phase A: 10 mM NH_4Ac in ACN-H_2O (30:70, v/v) pH 6.0

** Mobile phase B: 1 mM NH_4Ac in ACN-H_2O (30:70, v/v) pH 10.5

Table 2. Scan parameters of the Finningan TSQ Quantum ultra triple quadrupole mass spectrometer

Component	Parent ion (m/z)	Product ion (m/z)	Tube lens offset (au)	Scantime (s)	Collision energy (au)
2CdAMP	366	170	95	0.20	14
2CdADP	446	170	104	0.20	16
2CdATP	526	170	121	0.20	21
*CMP	336	119	70	0.10	25
*CDP	416	119	119	0.10	30
*CTP	496	119	126	0.10	35

Preparation of stock and working solutions

Only 2CdATP was commercially available. To obtain 2CdADP and 2CdAMP two stock solutions of 1 mg/mL 2CdATP in water were incubated in a water bath at 90°C for 4.25 h. The forced thermal degradation was monitored on the HPLC-UV system described under instrumentation. The

final concentrations of the nucleotides were determined on the HPLC-UV system using cladribine as external standard. The obtained solutions were diluted 100-fold with water. These separate sets of working solutions were used to prepare calibration and quality control samples for validation and quantification.

A 1 µg/mL *CTP stock solution was prepared in water and incubated in a water bath at 90°C for 3 h to obtain a mixture of *CTP, *CDP and *CMP (Figure 1). A volume of 750 µL of the mixture was diluted to 10 mL with water (IS working solution). All solutions were stored at -70°C.

Control incubated optimem and cell lysate

A volume of 750 µL of a 3×10^5 Madin-Darby canine kidney II (MDCKII) cells/mL suspension was plated on a 12-well Costar trans-well system. The cells were grown in Dulbecco's modified Eagle's medium (DMEM) supplemented with 10% fetal calf serum and penicillin/streptomycin for 5 days to form a confluent polarized monolayer. After washing with phosphate-buffered saline (PBS) incubation without 2CdA was performed in Optimem without serum. After incubation of the cells the Optimem from the apical and basolateral side was harvested (blank incubated apical and basolateral Optimem). The Optimem samples were stabilized by adding 30% of MeOH (blank stabilized apical and basolateral Optimem).

The cells were washed with ice-cold PBS. The membranes were cut from the well and transferred into a 1.5 mL Eppendorf cup and 500 µL of ice cold 70% MeOH was added to the membranes to lyse the cells and precipitate proteins. The samples were vortex mixed for 30 s followed by automatic shaking for 15 min at 1250 rpm (Labinco, Breda, The Netherlands). After centrifugation for 5 min at 15 000 *g* at 4°C the supernatant was used to prepare validation samples.

Preparation of calibration standards and validation samples

Blank stabilized apical Optimem was used to prepare calibration standards and validation samples.

Because a mixture of the three analytes was used to spike the calibration standards, these standards were prepared at several levels to cover the different ranges of interest of the analytes. The concentration levels used to construct the calibration curves were: 1.11, 1.38, 2.08, 2.77, 5.54, 13.8, 20.8 and 27.7 nM (2CdAMP); 0.550, 2.75, 4.12, 5.50, 11.0, 27.5, 41.2 and 55.0 nM (2CdADP); and 1.31, 2.61, 3.92, 5.23, 10.5, 26.1, 39.2 and 52.3 nM (2CdATP). These ranges were determined during the pre-validation based on the accuracy and precision values at the lower limit of quantification (LLOQ) of the different nucleotides.

Validation samples of the mixture were prepared at four levels: 1.37, 1.71, 13.7 and 25.7 nM (2CdAMP); 0.703, 3.52, 28.1 and 52.8 nM (2CdADP); and 1.73, 3.45, 27.6 and 51.8 nM (2CdATP).

All calibration standards and validation samples were prepared on an ice/water bath. Aliquots of 100 µL were stored at -70°C in 1.5 mL Eppendorf cups until analysis.

Sample preparation

Before analysis samples were allowed to thaw and climatize on an ice/water bath. The samples were vortexed for 10 s and centrifuged for 5 min at 15 000 *g* and 4°C to prevent particulates from entering the LC system. A volume of 10 µL of IS working solution was added to 100 µL of the cold supernatant and, after vortex mixing for 10 s, the mixture was transferred into an autosampler vial.

Validation procedures

A full validation was performed for the quantification of cladribine nucleotides in stabilized Optimem. A limited validation format was applied to the assay for the determination of the nucleotides in cell lysate using calibration standards in stabilized Optimem and validation samples in cell lysate.

Linearity

The calibration standards were prepared and analyzed in duplicate in three separate analytical runs. Deviations of the back-calculated concentrations from the nominal concentrations should be within ±20%. No more than 25% of the calibration standards were allowed to be rejected from the calibration curve. The coefficient of variation (CV) should be less than 20%.

Accuracy and precision

Validation samples at six levels in stabilized Optimem were analyzed in three analytical runs. Validation samples in cell lysate were analyzed in a single analytical run. For each compound accuracy and precision were assessed at four levels. The validation samples were quantified using calibration standards in stabilized Optimem injected before and after the validation samples. The differences between the nominal and the determined concentration were used to calculate the intra- (stabilized Optimem and cell lysate) and inter-assay (stabilized Optimem) accuracies. Inter-assay performance in cell lysate was monitored in duplo at three levels during three analytical runs. CVs were used to assess the precision of the method. All accuracies and CVs should be within ±20% and less than 20%, respectively.

Specificity and selectivity

Specificity and selectivity were determined in stabilized basolateral and apical Optimem and in cell lysate. Double blank (no IS added) and blank (only IS added) samples were checked for interferences. Samples spiked at

the LLOQ level were analyzed and the deviation from the nominal concentration was determined.

Ion suppression and recovery

For the determination of the ion suppression in stabilized Optimem the signal intensities of 2CdAMP (1.71, 13.7 and 25.7 nM), 2CdADP (3.52, 28.1 and 52.8 nM) and 2CdATP (3.45, 27.6 and 51.8 nM) in stabilized basolateral and apical Optimem were compared to the signal intensities of the analytes spiked to methanol/water (30:70, v/v) at the same levels.

To assess the ion suppression in cell lysate the signal intensities of 2CdAMP, 2CdADP and 2CdATP in cell lysate were compared to the signal intensities of the analytes in methanol/water (70:30, v/v) all spiked at the same concentrations as the stabilized Optimem.

The recovery was determined by spiking cells at two concentration levels (2CdAMP: 1.71 nM and 25.7 nM; 2CdADP: 3.52 nM and 52.8 nM; 2CdATP: 3.45 and 51.8 nM) before and after lysis and comparing the signals. Ion suppression and recoveries were determined in triplicate. Since the cells were all cultured under the same conditions the number of cells per well can be considered equal; at least 2.25×10^5 cells per sample.

Carry over

Carry over was assessed by injecting a blank sample (stabilized Optimem or cell lysate) after an upper limit of quantification (ULOQ) sample. Carry over of the analytes should be less than 20% of the peak area of a lower limit of quantification (LLOQ) sample. Carry over of the internal standards should be less than 5% of the internal standard peak area in a spiked sample.

Stability

All stability experiments in biomatrix were performed in triplicate at concentrations of 1.71 and 25.7 nM (2CdAMP); 3.52 and 52.8 nM (2CdADP); and 3.45 and 51.8 nM (2CdATP). Analytes were considered stable in biomatrix if the determined concentrations did not deviate more than ±20% from the concentration determined at time zero.

Stability was determined in stabilized Optimem and in cell lysate after two freeze/thaw cycles from nominally -70°C to 0°C (ice/water bath) (only in stabilized Optimem) and after 6 h at 0°C (ice/water bath). Reinjection reproducibility of the processed samples was assessed by reinjecting the calibration samples and the validation samples at 1.71, 13.7 and 25.7 nM (2CdAMP); 3.52, 28.1 and 52.8 nM (2CdADP); and 3.45, 27.6 and 51.8 nM (2CdATP) after 24 h in the autosampler (4°C).

Working solutions were considered stable if the determined concentrations did not deviate more than ±5% from the concentration determined at time zero. Stability of the working solutions was assessed by storing three aliquots of the solution at 20-25°C for 24 h. After dilution the

WAXLC/MS/MS signals were compared with the signals of freshly prepared diluted working solution.
Long-term stability of the nucleotide stock solution was determined by requantification of the stock using the HPLC-UV method described in the Experimental section.

Application of the assay

MDCKII cells were incubated with 10 µM 2CdA added to the basal compartment. Apical and basolateral Optimem samples were collected and cells were cut from the wells and lysed after 1, 2, 3 and 4 h as described for control incubated Optimem and cell lysate.

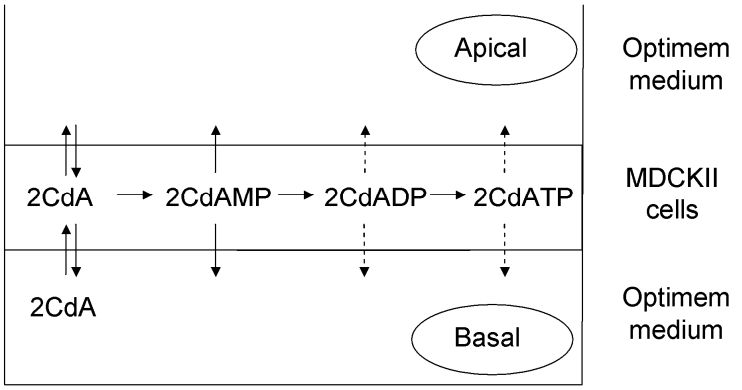

Figure 2. Schematic representation of the cladribine metabolism in a transwell system with cladribine added to the basal compartment.

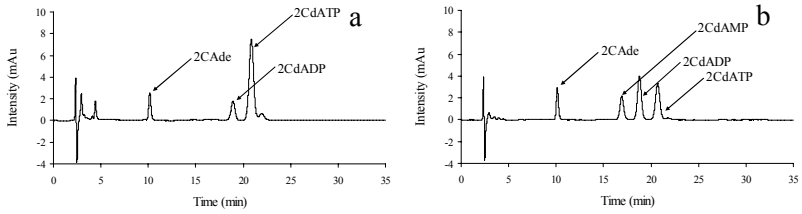

Figure 3. HPLC-UV chromatogram of a 2CdATP solution before (a) and after 4.25 hours at 90 °C(b)(2CdA elutes at 27.3 min, but is not present in examples).

Results and discussion

HPLC-UV

The development of the assay for 2CdAMP, 2CdADP and 2CdATP started with the HPLC-UV system using TEA as ion-pairing reagent [12;25]. The lack of sensitivity and the presence of interfering peaks in Optimem however demanded the design of a more sensitive and selective technique for biological samples.

The HPLC-UV system, on the other hand, proved to be very useful for the characterization of the reference nucleotide mixture. A chromatogram of the 2CdATP stock before and after a 4.25 hour incubation is shown in Figure 3. 2CdAMP and 2CdADP are formed during incubation. The fourth peak is the base 2-chloroadenine (2CAde), which is formed after cleavage of the N-glycosidic bond [12;26-28]. Nucleosides and nucleotides have identical UV absorption characteristics since they share the exact same chromophore. Since the system is isocratic, 2CdA, 2CdAMP, 2CdADP and 2CdATP, though eluting at different times, will have an identical molar absorptivity allowing an external quantification based on a 2CdA standard.

The purity of the 2CdATP reference compound was assessed using the HPLV-UV system. The 2CdATP standard that we obtained contained 2CdADP (7%), 2CAde (6%) and unidentified impurities besides 2CdATP(86%). On the certificate of analysis however, a >97% HPLC purity was claimed. Other authors have also seen impurities in nucleotide standards and emphasized the importance of determining the purity after purchase [18].

Mass spectrometry

Although the phosphate moieties of nucleotides are strong acidic and the pH of mobile phase B is basic (pH 10.5), the most intense signals were obtained operating the mass spectrometer in the positive ion mode. A fragment of the protonated base (Figure 1) was the most abundant product ion for all three nucleotides. This product ion at *m/z* 170 is the same as previously reported for cladribine [29;30]. An MS/MS mass spectrum of 2CdATP is depicted in Figure 4. Although the chlorine substitution on the base increases its basicity, leading to increased protonation, the neutral charge of the phosphate moiety is unexpected. Other groups have used the positive ion mode for the detection of nucleotides as well [19;23;31]. Masking of the negative charge on the phosphate groups by the ion pairing reagent DMHA has been proposed by Fung et al [31] as an explanation for the sensitivity in the positive ion mode. No DMHA or other ion pairing reagent is however present in the mobile phases of this method. Possibly the formation of hydrogen bonds within the molecule lowers the acidity in the gas phase leading to stabilization of the neutralized phosphate moiety.

Besides sensitivity, selectivity is also better in the positive ion mode. In the negative mode the pyrophosphate moiety (*m/z* 159) is the most abundant fragment for nucleoside di- and triphosphates. Quantification using this phosphate fragment would therefore rely solely on the first quadrupole for selectivity. Taking into account that most nucleoside di- and triphosphates elute in the same timeframe using the described system, detection using the positive ion mode is preferable. Another noticeable difference between both polarities is the difference in in-source dissociation of the triphosphate to the diphosphate. Using the negative ion mode in-source dissociation of 2CdATP into 2CdADP causes a signal in the 2CdADP transition at the retention time of 2CdATP. This in-source dissociation is lacking in the positive ion mode. A chromatographic separation of the triphosphate and diphosphate is therefore not essential. To improve signal intensity in the positive mode of the acidic compounds in the basic mobile phase post column addition of acetic acid was investigated. The signal intensity was however not increased further. The internal standards could be ionized in the positive ion mode as well. As for the cladribine nucleotides a protonated fragment of the base was the most abundant ion in the product ion scan.

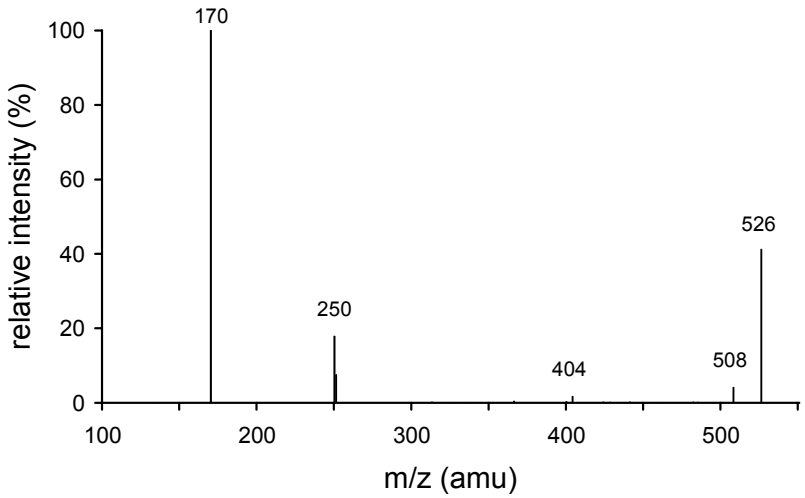

Figure 4. MS/MS spectrum of 2CdATP from $[M+H]^+$ at m/z 526

During method development it was noticed that the variance in signal intensity increased over 10-fold at lower concentrations while the peaks still had a very high signal to noise ratio. The internal standards did not correct for this variance. Using flow injections and continuous infusion the same effect was seen. All source parameters including polarity were then reassessed but no improvement in the variance was achieved. Increasing the amount of organic phase in the mobile phase to improve spray performance also did not change the high variance in the signal. Nucleotides are known to complexate with metals [32]. Complexation of nucleotides with various metal components of analytical systems has been associated with loss of analyte and peak tailing. The stainless steel electrospray capillary can be a major contributor to these effects [29]. We did not rule out the possibility that this phenomenon also influenced signal stability. Installing a new stainless steel electrospray capillary in the ESI source did not improve signal stability nor did addition of phosphate or EDTA to the mobile phase to occupy the binding sites on the inner surface of the capillary. Replacement of the stainless steel capillary with a fused silica electrospray capillary, however, led to an increased sensitivity and a significantly lower variance in signal at very low concentrations of the analytes. The peaks of the analytes at the LLOQ (Figure 5) show a very high signal to noise ratio suggesting the possibility of lowering the LLOQ. An increase in variance however then becomes again the limiting factor for further lowering the LLOQ of this assay.

Chromatography

Representative chromatograms of the nucleotides at the LLOQ level are shown in Figure 5. The commercially available 2-chloro-adenosine triphosphate, which is used as internal standard by others [33] in similar assays is potentially a very good internal standard because of the structural similarities with 2CdA. The compound was, however, not chosen because metabolic conversion from 2CdA to 2-chloro-adenosine triphosphate could not be ruled out [34]. We chose to use stable isotopically labelled cytidine nucleotides as internal standards. Although the analytes contain a purine base and the internal standards contain a pyrimidine base the compounds elute at the same time. The internal standards will therefore correct for matrix effects similar to stable isotopically labelled cladribine nucleotides [23].

Sample pretreatment

Since the Optimem medium was not supplemented with serum no sample cleanup was required to remove proteins. Therefore, our aim was to develop a method based on the direct injection of Optimem. During

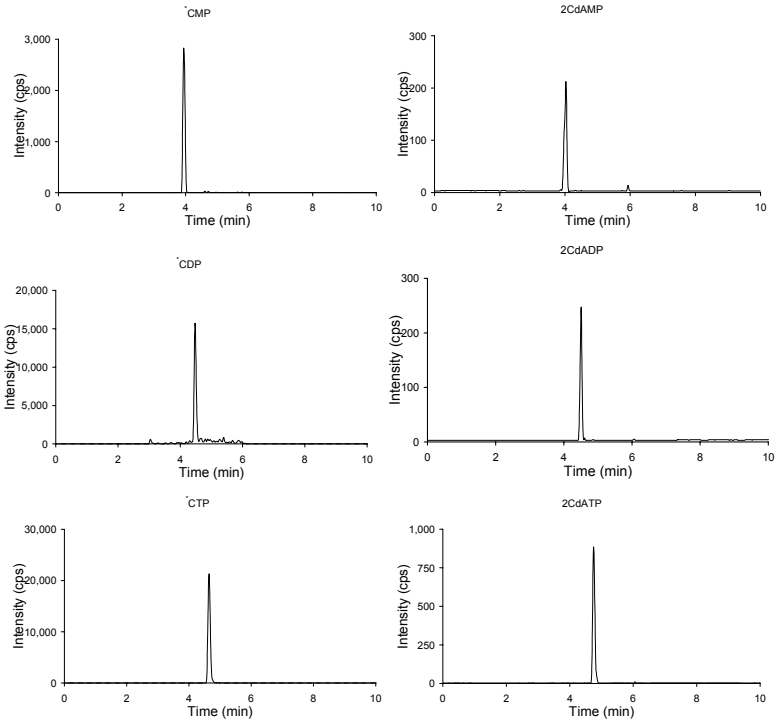

Figure 5. Representative chromatograms of 2CdAMP (1.11 nM, 4.02 min), 2CdADP (0.550 nM, 4.51 min), 2CdATP (1.31 nM, 4.75 min) at the LLOQ and of their internal standards *CMP (3.94 min), *CDP (4.47 min) and *CTP (4.65 min) in stabilized Optimem.

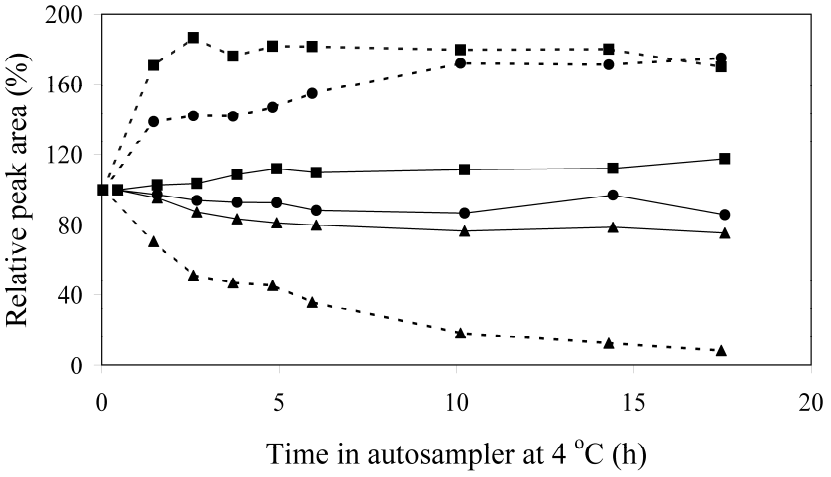

Figure 6. Stability of 2CdAMP (●), 2CdADP(■) and 2CdATP (▲) in apical Optimem (dashed lines) and stabilized apical Optimem (solid lines) in the autosampler (4 °C)

method development, however, we noticed a strong decrease in 2CdATP concentration and a strong increase in 2CdAMP and 2CdADP concentrations in blank incubated Optimem spiked with the analytes. Figure 6 shows the signals of 2CdAMP, 2CdADP and 2CdATP spiked to blank incubated Optimem during storage in the autosampler thermostatted at 4°C. When spiked to blank Optimem which had not been used to incubate cells 2CdAMP, 2CdADP and 2CdATP were stable. *CMP, *CDP and *CTP increased and decreased similarly and in this way corrected for the effect. A stable sample was however required to prevent degradation of 2CdATP before internal standard addition and to prevent 2CdATP concentrations diminishing below the limit of quantification. Moreover, if only 2CdAMP or 2CdADP is present in an Optimem sample the degradation of *CTP into *CMP and *CDP would lower the analyte/internal standard ratio resulting in an underestimation of the concentration. The decrease in triphosphates and increase in monophosphates and diphosphates are most likely caused by degradation of triphosphates into mono- and diphosphates. Since this conversion is not seen in blank Optimem we hypothesized that the degradation was caused by enzyme activity leaking from the cells during incubation in Optimem. (Pyro)phosphatases can be responsible for these reactions. We added phosphatase inhibitor cocktail set II to blank incubated Optimem before spiking it with the analytes. This cocktail set contains inhibitors of both alkaline and acid phosphatase. Addition of the cocktail set did however not influence the degradation rate. Addition of MeOH, on the other hand, did inhibit the conversion. Addition of 30% of MeOH almost completely inhibited the conversion of 2CdATP into 2CdAMP and 2CdADP (Figure 6) with an acceptable dilution. In cell lysate, which contains 70% MeOH, conversion of 2CdATP into 2CdAMP and 2CdADP was not observed

Validation procedures

Linearity

A weighting factor of the reciprocal of the squared concentration was used to construct the calibration curves. The accuracies of the back-calculated concentrations were between -6.89 and 5.54% (2CdAMP), -8.98 and 6.52% (2CdADP) and -8.80 and 9.60% (2CdATP). The CVs were less than 14.7% (2CdAMP), 10.1% (2CdADP) and 10.9% (2CdATP). Mean correlation coefficients (r^2) were 0.978, 0.990 and 0.987 for 2CdAMP, 2CdADP and 2CdATP, respectively.

Accuracy and precision

Tables 3, 4 and 5 summarize the intra- and inter-assay performance of the assay in stabilized Optimem and in cell lysate for the tested concentration levels. All intra- and interday accuracies and precisions were within ±20%.

Specificity and selectivity

No interferences were seen in the chromatograms from blank cell lysate, stabilized apical or basolateral Optimem at the retention times of the analytes. An interference was seen in the *CDP transition in every sample including blanks. This interference could be suppressed by using freshly prepared mobile phase. The interference could clearly be distinguished from the analyte peak and was always less than 5% of the internal standard peak area. The accuracies of the stabilized basolateral Optimem spiked at the LLOQ were -2.92, 7.54 and -9.83% for 2CdAMP, 2CdADP and 2CdATP, respectively. Thus the specificity and selectivity of this assay are satisfactory.

Ion suppression and recovery

The ion suppression data of 2CdAMP (25.7 nM), 2CdADP (52.8 nM), 2CdATP (51.8 nM) and their internal standards is presented in Table 6. The observed ion suppression was comparable at the three tested concentrations. The differences in ion suppression between the nucleotides might be caused by co eluting constituents of the Optimem medium. The ion suppression in cell lysate is less pronounced. The differences in ion suppression between blank incubated Optimem and cell lysate are similar for the analytes and their internal standard. The internal standards therefore correct for the effect of the different matrices allowing accurate quantification. The standard method for extraction of nucleotides from cells is acid precipitation with trichloroacetic or perchloric acid. Cladribine is however not stable in an acidic environment [26;28].[Moreover, the involatile salts cause ion suppression and pollute the mass spectrometer. Because lysis with an organic solvent and water gives similar recoveries [35;36], and is widely used in comparable assays, we have chosen to use 70% MeOH as lysis solution. The recoveries with 70% MeOH are given in Table 7.

Carry over

Carry over increased with the number of phosphates in the chemical structure and was 0.00, 9.08 and 9.44% of the area of a LLOQ sample in stabilized Optimem for 2CdAMP, 2CdADP and 2CdATP. In cell lysate only 2CdATP showed carry over, which was 10.8% of the area of a LLOQ-sample. Carry over of the internal standard was less than 1% for all internal standards in stabilized Optimem and cell lysate.

Stability

The stability data are presented in Table 8. The table shows the concentrations determined at t=0 and after the indicated periods under several conditions. By using stabilized Optimem, samples can be pretreated and analyzed without degradation of 2CdATP into 2CdAMP.

Table 3. Assay performance data for 2CdAMP, 2CdADP and 2CdATP in stabilized Optimem (n=5 for each run, n=15 for total)

Run	Compound	Nominal concentration (nM)	Measured concentration (nM)	Accuracy (% dev. from nominal)	Precision (% CV)
1	2CdAMP	1.37	1.47	7.09	9.40
2			1.62	18.1	11.4
3			1.37	-0.146	15.8
Total			1.48	8.35	13.5
1		1.71	1.95	13.9	16.4
2			1.77	3.74	12.2
3			1.58	-7.49	19.2
Total			1.77	3.39	17.2
1		13.7	13.5	-1.31	5.11
2			15.8	15.3	8.92
3			15.9	16.4	11.1
Total			15.1	10.1	11.3
1		25.7	27.3	6.15	13.8
2			29.2	13.5	6.01
3			28.5	10.8	18.1
Total			28.3	10.2	12.8
1	2CdADP	0.703	0.611	-13.1	18.0
2			0.674	-4.13	8.04
3			0.668	-5.04	13.1
Total			0.651	-7.42	13.2
1		3.52	4.21	19.7	5.09
2			4.19	18.9	2.25
3			3.43	-2.50	5.92
Total			3.94	12.0	10.4
1		28.1	30.0	6.62	4.42
2			27.6	-1.78	6.08
3			25.9	-7.76	9.42
Total			27.8	-0.973	8.77
1		52.8	52.0	-1.55	4.69
2			50.4	-4.47	9.03
3			51.0	-3.41	13.1
Total			51.1	-3.14	8.94
1	2CdATP	1.73	1.82	5.43	11.7
2			1.66	-4.28	11.3
3			1.84	6.36	11.9
Total			1.77	2.50	11.8
1		3.45	3.47	0.522	5.75
2			2.84	-17.7	12.5
3			3.90	13.1	9.31
Total			3.40	-1.37	15.8
1		27.6	28.9	4.57	5.92
2			32.2	16.7	5.78
3			31.1	12.5	3.84
Total			30.7	11.3	6.74
1		51.8	58.2	12.3	4.65
2			60.4	16.7	4.01
3			60.9	17.6	7.79
Total			59.9	15.5	5.73

Table 4. Intra-assay performance data for 2CdAMP, 2CdADP and 2CdATP in cell lysate (n=5)

Compound	Nominal concentration (nM)	Measured concentration (nM)	Accuracy (% dev. from nominal)	Precision (%CV)
2CdAMP	1.37	1.63	19.0	5.04
	1.71	2.04	19.3	15.9
	13.7	15.9	16.1	15.7
	25.7	28.0	8.79	9.85
2CdADP	0.703	0.617	-12.1	18.6
	3.52	3.79	7.78	13.6
	28.1	29.7	5.84	3.87
	52.8	54.9	4.02	6.57
2CdATP	1.73	1.46	-15.7	9.84
	3.45	3.10	-10.2	8.64
	27.6	27.7	0.290	2.03
	51.8	48.3	-6.68	5.15

Table 5. Inter-assay performance data for 2CdAMP, 2CdADP and 2CdATP in cell lysate (3 analytical runs, n=6 for total)

Compound	Nominal concentration (nM)	Measured concentration (nM)	Accuracy (% dev. from nominal)	Precision (%CV)
2CdAMP	1.71	1.85	8.19	16.4
	13.7	12.8	-6.33	4.29
	25.7	23.2	-9.79	10.4
2CdADP	3.52	3.20	-9.04	17.5
	28.1	27.4	-2.55	3.60
	52.8	48.5	-8.11	4.17
2CdATP	3.45	4.02	16.4	14.9
	27.6	32.2	16.6	4.13
	51.8	58.6	13.1	5.06

Table 7. Recovery of 2CdAMP, 2CdADP and 2CdATP after lysis of MDCKII cells with 70% MeOH (n=3)

Compound	Concentration (nM)	Recovery (%)	CV (%)
2CdAMP	1.71	98.9	5.74
	25.7	106	7.28
2CdADP	3.52	85.0	4.54
	52.8	92.7	7.94
2CdATP	3.45	86.5	10.2
	51.8	101	3.50

Table 6. Ion suppression of 2CdAMP (25.7 nM), 2CdADP (52.8 nM), 2CdATP (51.8 nM) and their internal standards (n = 3)

Matrix	2CdAMP		*CMP		2CdADP		*CDP		2CdATP		*CTP	
	Peak area (counts)	CV (%)	Peak area (counts)	CV (%)	Peak area (counts)	CV (%)	Peak area (counts)	CV (%)	Peak area (counts)	CV (%)	Peak area (counts)	CV (%)
MeOH:H_2O (30:70, v/v)	1.24E+05	8.18	4.32E+04	2.13	3.47E+05	4.41	1.50E+05	5.67	3.97E+05	4.96	1.92E+05	8.85
MeOH:H_2O (70:30, v/v)	1.25E+05	5.46	3.99E+04	11.2	3.16E+05	19.2	1.41E+05	16.2	3.74E+05	15.8	1.90E+05	12.3
Stabilized apical Optimem	9.79E+04	3.54	3.15E+04	1.03	3.02E+05	3.08	1.29E+05	6.54	2.21E+05	5.99	1.33E+05	4.35
Stabilized basolateral Optimem	1.03E+05	2.23	3.24E+04	13.2	3.07E+05	1.88	1.43E+05	1.70	2.51E+05	6.95	1.47E+05	7.75
Lysate	1.21E+05	5.79	3.61E+04	12.7	2.83E+05	21.3	1.24E+05	18.6	3.38E+05	21.0	1.77E+05	17.2
	Ion suppression (%)		Ion suppression (%)		Ion suppression (%)		Ion suppression (%)		Ion suppression (%)		Ion suppression (%)	
Stabilized apical Optimem	21.0		27.1		13.0		14.0		44.3		30.7	
Stabilized basolateral Optimem	16.9		25.0		11.5		4.67		36.8		23.4	
Cell lysate	3.20		9.52		10.4		12.1		9.63		6.84	

Table 8. Stability data of 2CdAMP, 2CdADP, 2CdATP, *CMP, *CDP and *CTP (n=3 for all values except for the stock solution (n=4))

Matrix	Condition	Compound	Initial conc (nM) /(*counts*)	Found conc (nM) /(*counts*)	Dev. (%)
Water (stock solution)	-70 °C, 6.5 months	2CdAMP	1380	1385	0.362
		2CdADP	2708	2750	1.57
		2CdATP	2510	2615	4.18
Water (working solution)	20-25 °C, 24 h	2CdAMP	*2.63x10^5*	*2.75x10^5*	4.56
		2CdADP	*8.11x10^5*	*8.48x10^5*	4.56
		2CdATP	*6.97x10^5*	*7.03x10^5*	0.909
		*CMP	*1.28x10^4*	*1.32x10^4*	2.86
		*CDP	*6.64x10^4*	*6.36x10^4*	-4.32
		*CTP	*7.38x10^4*	*7.27x10^4*	-1.45
Stabilized Optimem*	-70 °C, 11 days	2CdAMP	1.71**	1.94	13.5
			25.7**	25.1	-2.20
		2CdADP	3.52**	2.90	-17.6
			52.8**	47.4	-10.2
		2CdATP	3.45**	3.66	6.18
			51.8**	53.7	3.73
	2 freeze/ thaw cycles, 70 °C	2CdAMP	1.76	1.59	-9.64
			27.6	30.3	9.78
		2CdADP	4.09	4.78	16.9
			51.0	55.6	9.16
		2CdATP	3.39	2.75	-18.8
			57.9	52.2	-9.85
	Ice-water, 6 h	2CdAMP	1.38	1.41	2.17
			24.7	25.7	3.91
		2CdADP	4.06	4.42	8.87
			55.1	51.4	-6.71
		2CdATP	2.87	2.90	1.05
			65.7	60.1	-8.57
	Autosampler (4 °C) reinjection 24 h	2CdAMP	1.76	2.03	15.0
			13.5	12.2	-9.41
			27.6	30.1	8.97
		2CdADP	4.17	3.77	-9.52
			29.8	26.2	-12.1
			51.0	48.4	-5.04
		2CdATP	3.39	2.85	-16.0
			28.6	28.6	0.117
			57.9	59.9	3.57
Cell lysate	-70 °C, 1 month	2CdAMP	2.20	2.04	-7.13
			28.0	27.3	-2.50
		2CdADP	3.40	3.22	-5.29
			49.6	48.2	-2.89
		2CdATP	3.51	3.29	-6.26
			47.8	46.0	-3.84
	Ice-water, 6 h	2CdAMP	1.56	1.50	2.56
			26.7	30.2	13.2
		2CdADP	3.69	3.39	-8.05
			55.1	51.4	-6.71
		2CdATP	2.87	2.90	1.05
			65.7	60.1	-8.57
	Autosampler (4 °C), reinjection 24 h	2CdAMP	2.20	1.89	-14.1
			16.1	16.1	0.00
			28.0	28.4	1.31
		2CdADP	3.84	4.14	7.82
			29.4	32.3	9.99
			56.1	58.2	3.68
		2CdATP	3.19	3.29	3.13
			27.3	25.7	-6.10
			47.5	44.4	-6.60

* Blank apical Optimem containing 30% MeOH
** Nominal values

Application of the assay

Figure 7 shows the 2CdAMP, 2CdADP and 2CdATP concentration in cell lysate after incubation for 4 h with 10 µM 2CdA added at the basolateral side. Figure 8 shows the 2CdAMP concentration in basolateral Optimem during incubation with 10 µM 2CdA added at the basolateral side. 2CdADP and 2CdATP were not detected in Optimem samples. Analysis of the Optimem samples using the HPLC-UV method described in the Experimental section showed that almost all (~95%) of the added cladribine was present as non-phosphorylated cladribine in apical and basolateral Optimem. The exact number and volume of the cells are not known so concentrations cannot be expressed as nanomoles per cell or nM in cells. The concentration is therefore expressed as nM in lysate after lysing the cells in 500 µL 70% MeOH. After validation the methodology described should be applicable to other matrices such as peripheral blood mononuclear cells (PBMCs) as well.

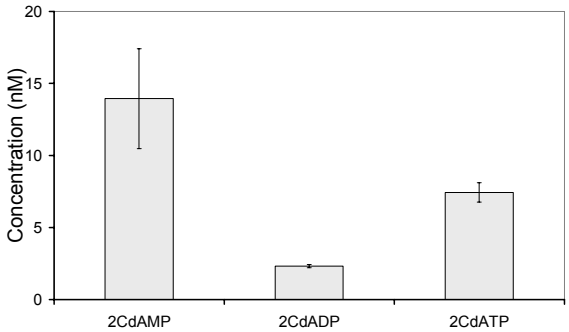

Figure 7. Concentration of 2CdAMP, 2CdADP and 2CdATP in MDCKII cell lysate after 4 hours incubation with 2CdA (10 µM added to the basal compartment)(values are means ± standard deviation, n=2)

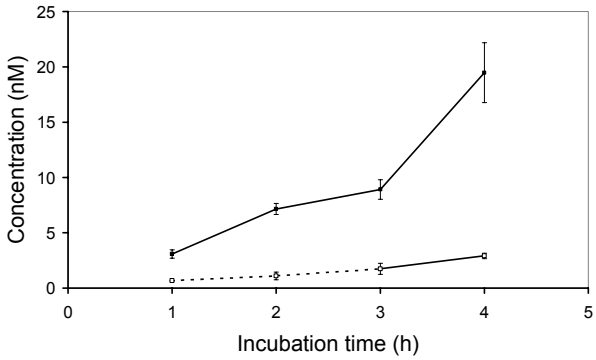

Figure 8. Concentration of 2CdAMP in basolateral(■) and apical(□) Optimem during an incubation with 2CdA (10 µM added to the basal compartment)(values are means ± standard deviation, n=2)(parts of the curve below the LLOQ (1.59nM) are depicted as dashed lines)

Conclusion

A method was developed and validated for the quantitative determination of 2CdAMP, 2CdADP and 2CdATP in cells and Optimem medium. The validated dynamic ranges in Optimem medium and cell lysate were 1.11-27.7, 0.550-55.0 and 1.31-52.3 nM respectively. The described method is >150-fold more sensitive than the method described by Reichelova et al [12] which had an LLOQ of 200 nM. Optimem samples required stabilization with 30% MeOH to prevent conversion of 2CdATP into 2CdADP and 2CdAMP. The method was successfully applied to characterize cladribine nucleotide transport in MDCKII cells.

References

[1] W. Kong, K. Engel, J. Wang, Curr. Drug Metab 5 (2004) 63.
[2] E. S. Arner, Leuk. Lymphoma 21 (1996) 225.
[3] J. Liliemark, Clin. Pharmacokinet. 32 (1997) 120.
[4] S. Seto, C. J. Carrera, M. Kubota, D. B. Wasson, D. A. Carson, J. Clin. Invest 75 (1985) 377.
[5] W. R. Hartman, P. Hentosh, Mol. Pharmacol. 65 (2004) 227.
[6] F. Albertioni, S. Lindemalm, V. Reichelova, B. Pettersson, S. Eriksson, G. Juliusson, J. Liliemark, Clin. Cancer Res. 4 (1998) 653.
[7] L. Jordheim, C. M. Galmarini, C. Dumontet, Curr. Drug Targets. 4 (2003) 443.
[8] J. D. Schuetz, M. C. Connelly, D. Sun, S. G. Paibir, P. M. Flynn, R. V. Srinivas, A. Kumar, A. Fridland, Nat. Med. 5 (1999) 1048.
[9] G. Jedlitschky, B. Burchell, D. Keppler, J. Biol. Chem. 275 (2000) 30069.
[10] G. Reid, P. Wielinga, N. Zelcer, M. De Haas, L. Van Deemter, J. Wijnholds, J. Balzarini, P. Borst, Mol. Pharmacol. 63 (2003) 1094.
[11] J. Liliemark, G. Juliusson, Clin. Cancer Res. 1 (1995) 385.
[12] V. Reichelova, F. Albertioni, J. Liliemark, J. Chromatogr. B Biomed. Appl. 682 (1996) 115.
[13] J. T. Slusher, S. K. Kuwahara, F. M. Hamzeh, L. D. Lewis, D. M. Kornhauser, P. S. Lietman, Antimicrob. Agents Chemother. 36 (1992) 2473.
[14] B. L. Robbins, B. H. Waibel, A. Fridland, Antimicrob. Agents Chemother. 40 (1996) 2651.
[15] A. Darque, G. Valette, F. Rousseau, L. H. Wang, J. P. Sommadossi, X. J. Zhou, Antimicrob. Agents Chemother. 43 (1999) 2245.
[16] C. Solas, Y. F. Li, M. Y. Xie, J. P. Sommadossi, X. J. Zhou, Antimicrob. Agents Chemother. 42 (1998) 2989.
[17] J. D. Moore, G. Valette, A. Darque, X. J. Zhou, J. P. Sommadossi, J. Am. Soc. Mass Spectrom. 11 (2000) 1134.
[18] T. King, L. Bushman, P. L. Anderson, T. Delahunty, M. Ray, C. V. Fletcher, J. Chromatogr. B 831 (2006) 248.
[19] R. L. Claire, III, Rapid Commun. Mass Spectrom. 14 (2000) 1625.
[20] A. Pruvost, F. Becher, P. Bardouille, C. Guerrero, C. Creminon, J. F. Delfraissy, C. Goujard, J. Grassi, H. Benech, Rapid Commun. Mass Spectrom. 15 (2001) 1401.
[21] R. Tuytten, F. Lemiere, W. V. Dongen, E. L. Esmans, H. Slegers, Rapid Commun. Mass Spectrom. 16 (2002) 1205.
[22] Y. Q. Xia, M. Jemal, N. Zheng, X. Shen, Rapid Commun. Mass Spectrom. 20 (2006) 1831.
[23] G. Shi, J. T. Wu, Y. Li, R. Geleziunas, K. Gallagher, T. Emm, T. Olah, S. Unger, Rapid Commun. Mass Spectrom. 16 (2002) 1092.
[24] S. A. Veltkamp, M. J. Hillebrand, H. Rosing, R. S. Jansen, E. R. Wickremsinhe, E. J. Perkins, J. H. Schellens, J. H. Beijnen, J. Mass Spectrom. 41 (2006) 1633.
[25] T. Uesugi, K. Sano, Y. Uesawa, Y. Ikegami, K. Mohri, J. Chromatogr. B Biomed. Sci. Appl. 703 (1997) 63.
[26] S. Lindemalm, F. Albertioni, J. Liliemark, Anticancer Drugs 8 (1997) 445.
[27] V. Reichelova, J. Liliemark, F. Albertioni, J. Pharm. Biomed. Anal. 13 (1995) 711.
[28] A. Tarasiuk, J. Skierski, Z. Kazimierczuk, Arch. Immunol. Ther. Exp. (Warsz.) 42 (1994) 13.
[29] M. D. Moyer, T. Johannsen, R. J. Stubbs, J. Pharm. Biomed. Anal. 17 (1998) 45.
[30] W. N. Wu, L. A. McKown, M. D. Moyer, W. Cheung, Xenobiotica 34 (2004) 591.
[31] E. N. Fung, Z. Cai, T. C. Burnette, A. K. Sinhababu, J. Chromatogr. B 754 (2001) 285.
[32] H. Sigel, R. Griesser, Chem. Soc. Rev. 34 (2005) 875.
[33] F. Becher, A. Pruvost, C. Goujard, C. Guerreiro, J. F. Delfraissy, J. Grassi, H. Benech, Rapid Commun. Mass Spectrom. 16 (2002) 555.

[34] J. Bierau, R. Leen, A. H. Gennip, H. N. Caron, A. B. Kuilenburg, J. Chromatogr. B 805 (2004) 339.
[35] M. K. Grob, K. O'Brien, J. J. Chu, D. D. Chen, J. Chromatogr. B 788 (2003) 103.
[36] S. Palmer, S. Cox, J. Chromatogr. A 667 (1994) 316.

Chapter 2.3

Simultaneous quantification of emtricitabine and tenofovir nucleotides in peripheral blood mononuclear cells using weak anion-exchange liquid chromatography coupled with tandem mass spectrometry

Robert S Jansen, Hilde Rosing, Wiete Kromdijk, Rob ter Heine, Jan HM Schellens and Jos H Beijnen

Submitted for publication

Abstract

Emtricitabine (FTC) and tenofovir (TFV) are currently the most prescribed antiretroviral drugs for treatment of human immunodeficiency virus (HIV) infection. These drugs require intracellular phosphorylation to become active. This article describes the development and validation of an assay for the simultaneous quantification of FTC mono-, di- and triphosphate (FTC-MP, -DP and -TP), TFV and TFV mono- and diphosphate (TFV-MP and -DP) in peripheral blood mononuclear cells.
Reference compounds and internal standards were obtained by thermal degradation of FTC-TP, TFV-DP, stable isotope-labeled TFV-DP and stable isotope-labeled cytosine triphosphate. Cells were lysed in methanol:water (70:30, v/v) and the extracted nucleotides were analyzed using weak anion-exchange chromatography coupled with tandem mass spectrometry. Calibration ranges in PBMC lysate from 0.727-36.4, 1.33-66.4 and 1.29-64.6 nM for FTC-MP, FTC-DP and FTC-TP and from 1.51-75.6, 1.54-77.2 and 2.54-127 nM for TFV, TFV-MP and TFV-DP, respectively, were validated. Accuracies were within -10.3 and 16.7% deviation at the lower limit of quantification at which the coefficients of variation were less than 18.2%. At the other tested levels accuracies were within -14.3 and 9.81% deviation and the coefficients of variation lower than 14.7%. The stability of the compounds was assessed under various analytically relevant conditions. The method was successfully applied to clinical samples.

Introduction

Emtricitabine (2',3'-dideoxy-5-fluoro-3'-thiacytidine; FTC; figure 1) and tenofovir (TFV; figure 1) are a nucleoside and a nucleotide reverse transcriptase inhibitor (NRTI and NtRTI), respectively. These drugs are the most commonly backbone of antiretroviral therapy, which is used against human immunodeficiency virus (HIV) infections. A combination of both agents with the non-nucleoside reverse transcriptase inhibitor efavirenz has recently been approved as the first once-daily, single pill combination therapy against HIV.

Both analogs require intracellular phosphorylation to become active. In cells, the nucleoside analog FTC is first phosphorylated to its monophosphate (FTC-MP) by deoxycytidine kinase after which it is converted further to its di- and triphosphate (FTC-DP and FTC-TP; figure 1).

The acyclic nucleotide analog TFV, on the other hand, already contains a phosphate moiety. To increase the bioavailability and cell penetration, this polar molecule is administered as a disoproxil fumarate prodrug (TDF) that first requires hydrolization to TFV. Subsequently, TFV is phosphorylated intracellularly to its mono- and diphosphate (TFV-MP and TFV-DP; figure 1) containing 2 and 3 phosphate groups in total, respectively. FTC-TP and TFV-DP are the active metabolites that inhibit viral reverse transcriptase, thereby inhibiting viral replication.

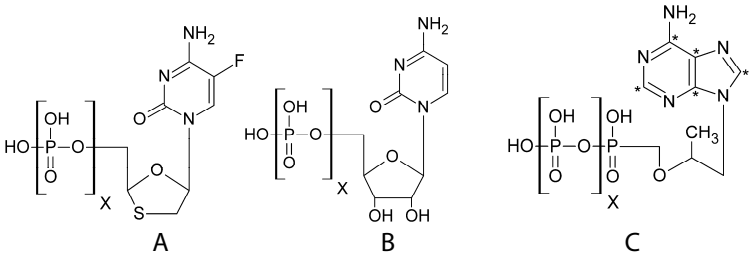

Figure 1. Chemical structures of FTC (A), cytosine (B) and TFV (C)(X=0) and their mono- (X=1), di- (X=2) and triphosphate (X=3). The asterisks indicate ^{13}C-atoms in *TFV internal standards.

For FTC and TFV, plasma drug levels are less informative because the intracellular pharmacokinetics of the phosphorylated metabolites are different from the plasma pharmacokinetics of the parent compounds. The plasma half-lifes of FTC and TFV are, for example, 8-10 [1] and 14 [2] hours, whereas intracellular half-lifes of 39 [1] and 150 [3] hours have been observed for FTC-TP and TFV-DP, respectively. Moreover, metabolite levels are subject to inter-individual variation and intracellular drug-drug interactions [4]. It is important to measure these analytes because low triphosphate levels can cause viral resistance, whereas high levels have been associated with treatment toxicity [5]. Determination of lower phosphates can give valuable information on their intracellular

pharmacokinetics. Thus, monitoring of intracellular FTC and TFV nucleotide levels will give more insight in the pharmacology of FTC and TFV.

FTC-TP and TFV-DP have indirectly been determined in peripheral blood mononuclear cells (PBMCs) after dephosphorylation, using high performance liquid chromatography with ultraviolet (HPLC-UV) [6] and mass spectrometric (LC-MS) detection [7].

Direct LC-MS determination of FTC-TP and TFV-DP has been performed using the ion-pairing agents tetrabutylammonium [1;3;4;8-11] and dimethylhexylamine [12-16] and weak anion-exchange liquid chromatography (WAXLC-MS/MS) [17]. Although some of these methods also include TFV and/or TFV-MP [4;10-12], none include FTC-MP or FTC-DP.

In this paper we describe the development and validation of a method for the quantification of FTC-MP, -DP and -TP in combination with TFV, TFV-MP and TFV-DP in human PBMCs.

Table 1. HPLC stepwise gradient for the WAXLC-MS/MS experiments

Time (min)	Flow rate (mL/min)	Mobile phase A[a] (%)	Mobile phase B[b] (%)
0	0.25	90	10
0.50	0.25	90	10
0.51	0.25	50	50
1.75	0.25	50	50
1.76	0.25	0	100
6.50	0.25	0	100
6.60	0.50	90	10
9.50	0.25	90	10
10.0	0.25	90	10

[a] 10 mM ammonium acetate in acetonitrile-water (30:70, v/v) pH 6.0
[b] 1 mM ammonium acetate in acetonitrile-water (30:70, v/v) pH 10.5

Table 2. Settings for the API4000 triple quadrupole mass spectrometer

Compound	Precursor ion (m/z)	Product ion (m/z)	Declustering potential (V)	Collision energy (V)
FTC-MP	328	130	45	20
*CMP	336	119	45	20
FTC-DP	408	130	62	35
*CDP	416	119	62	35
FTC-TP	488	130	75	29
*CTP	496	119	75	29
TFV	288	176	126	35
*TFV	293	181	126	35
TFV-MP	368	270	76	27
*TFV-MP	373	275	76	27
TFV-DP	448	270	86	37
*TFV-DP	453	275	86	37

Materials and methods

Chemicals

FTC and TFV were purchased from Sequoia Research products (Pangbourne, UK). $^{13}C_9$,$^{15}N_3$(U)-labeled cytidine triphosphate (*CTP; figure 1) was purchased from Buchem BV (Apeldoorn, The Netherlands), whereas $^{13}C_5$-labeled TFV-DP (*TFV-DP, figure 1) was obtained from Moravek (Brea, CA, USA). Unlabeled FTC-TP and TFV-DP were kindly provided by Gilead Sciences Inc. (Foster city, CA, USA).

Methanol and acetonitrile were obtained from Biosolve Ltd (Amsterdam, The Netherlands) and distilled water was obtained from B Braun (Melsungen, Germany). Ammonium acetate, aqueous ammonia 25%, glacial acetic acid, tetrabutylammonium dihydrogenphosphate, potassium dihydrogen phosphate were all from Merck (Darmstadt, Germany).

Instrumentation

HPLC-UV experiments were performed on an Agilent 1100 series liquid chromatograph system (Agilent technologies, Palo Alto, CA, USA) consisting of a binary pump, in-line degasser, autosampler, column oven and UV detector. Data were acquired using Chromeleon 6.50 software (Dionex corp., Sunnyvale, CA, USA).

The mobile phases consisted of 10 mM tetrabutylammonium dihydrogenphosphate with 70 mM potassium dihydrogen phosphate (mobile phase A) and methanol (mobile phase B). A mobile phase mixture containing 7.5% (v/v) B was delivered isocratically to a Synergi hydro-RP column (150 X 2.0 mm ID, 4 µm particles; Phenomenex, Torrance, CA, USA) with a flow of 0.25 mL/min to separate the analytes. FTC and FTC-MP were only separated using 100% mobile phase A delivered to two Synergi hydro-RP columns (150+150 X 2.0 mm ID, 4 µm particles). A volume of 10 µL was injected using the autosampler thermostated at 4°C. Absorption was measured at 280 nm (FTC) and 259 nm (TFV).

LC-MS/MS analyses were also performed on an Agilent 1100 series liquid chromatograph system consisting of a binary pump, in-line degasser and autosampler but with an API4000 triple quadrupole mass spectrometer (Applied Biosystems, Foster city, CA, USA) for detection.

Mobile phase A (10 mM ammoniumacetate in acetonitrile/water (30:70 v/v) pH 6.0) and B (1 mM ammoniumacetate in acetonitrile/water (30:70 v/v) pH 10.5) were delivered to a Biobasic AX column (50 x 2.1 mm ID, 5 µm particles; Thermo Fisher Scientific Inc, Waltham, MA, USA) with a 10 mm guard cartridge as presented in table 1. Before each injection the needle was washed with methanol for 40 seconds. Samples were kept at 4 °C in the autosampler tray and a 25 µL injection volume was applied. The switching valve directed the eluate to waste during the first 3 and last 2 minutes of the run. Ionization was performed using a turbo V ion source

operated in the positive ionization mode at a voltage of 5500 V and 550°C. The curtain gas (N_2) was set at 10 arbitrary units, whereas gas 1 and 2 (zero air) were set at 70 and 50 arbitrary units, respectively. Scans of 50 ms were performed for each compound at unit resolution. The compound dependent scan conditions are summarized in table 2. Data were acquired and processed using Analyst 1.5 software (Applied Biosystems).

Preparation of reference and internal standard stock and working solutions

Aqueous solutions of FTC-TP, *CTP, TFV-DP and *TFV-DP were incubated in a water bath at 90°C. The thermal degradation of the compounds into lower phosphates was monitored using the HPLC-UV system described in section 2.2. Mixtures containing similar amounts of FTC, *C, TFV and *TFV nucleotides were obtained after 5, 4.25, 3 and 2 hours, respectively. The content of these nucleotide mixtures was determined using HPLC-UV. Two FTC and two TFV reference solutions were prepared from separate weightings. The peak areas obtained by injecting these references solutions in three-fold were compared to those obtained by injecting the nucleotide solutions with unknown concentrations in three-fold. The mixtures of FTC and TFV nucleotides were finally mixed and diluted in water to obtain working solutions. Likewise, the *C nucleotides were mixed with the *TFV nucleotides and diluted in water to obtain the internal standard working solution. All solutions were stored at -70°C.

Isolation and lysis of PBMCs

Blank PBMCs were isolated from human leukocyte buffy coat (Sanquin, Amsterdam, the Netherlands) as previously described [18]. Clinical samples were obtained by drawing 8 mL whole blood in a cell preparation tube (BD Vacutainer CPT; BD, Franklin lakes, NJ, USA). After centrifugation at 1500 g for 30 minutes the PBMCs were collected and washed twice with cold phosphate buffered saline (PBS). The number of cells isolated was determined using a Cell-Dyn 4000 haematology analyzer (Abbott Diagnostics, Abbott Park, IL, USA). Blank PBMCs were directly lysed in methanol:water (70:30, v/v)(22.5 X 10^6 PBMCs/mL), whereas clinical samples were stored at -20°C as a cell pellet and lysed in 200 µL methanol:water (70:30, v/v) before analysis.

Preparation of calibration, validation and stability samples

Six non-zero calibration standards (CALs) and validation samples (VSs) at the lower limit of quantitation (LLOQ), low, mid and high level (table 3) were freshly prepared in blank PBMC lysate before each analytical run.
Stability samples (SSs) were prepared at the low and high level by spiking blank PBMC lysate with working solution (1.5% or less of the total volume).

Aliquots of 100 µL of these solutions were stored at the test conditions and treated as unknowns before processing and analysis.

Sample processing

Unknowns and blank lysates were vortex mixed for 10 seconds. To 90 µL of the suspensions, 10 µL of working solution (CALs and VSs) or water (unknowns) was added. Internal standard working solution (5 µL) was then added at a concentration of approximately 3 nM for *CMP, *CDP and *CTP and of 10-15 nM for *TFV, *TFV-MP and *TFV-DP. Finally, the samples were again vortex mixed, centrifuged for 5 minutes at 23,100 g and transferred to an autosampler vial.

Validation procedures

Linearity

The calibration standards were prepared and analyzed in duplicate in three separate analytical runs. Deviations of the back-calculated concentrations from the nominal concentrations should be within ±20% at the LLOQ and within ±15% at the other levels. No more than one third of the calibration standards were allowed to be rejected from the calibration curves.

Accuracy and precision

Validation samples at 4 levels were analyzed in 5-fold in 3 analytical runs. For each compound the accuracy and precision values were assessed. The differences between the nominal and the determined concentration were used to calculate the intra- and inter-assay accuracies. The coefficients of variation (CV) were calculated to assess the precision of the method. Deviations and precisions should be within ±15% and less than 15%, respectively, except at the LLOQ where they should be within ±20% and less than 20%, respectively.

Specificity and selectivity

Specificity and selectivity were determined in PBMC lysate from 5 different individuals. Double blank (no internal standard added) samples were checked for analyte and internal standard interferences. Samples spiked at the LLOQ level were analyzed and the deviation from the nominal concentration should be within ±20%.

Matrix effect and recovery

Lysate containing 0, 25, 50, 75, 100 and 125 X 10^6 PBMCs/mL (corresponding to 0, 5, 10, 15, 20 and 25 X 10^6 PBMCs per sample) was prepared in methanol:water (70:30, v/v) using PBMCs isolated from a single donor buffy coat. These suspensions were used to prepare validation samples at the mid level as described in section 2.6. Each PBMC concentration was processed and analyzed in triplicate.

Carry over

Carry over was assessed by injecting a blank sample after the highest calibration standard. Carry over of the analytes should be less than 20% of the peak area of a sample at the LLOQ. Carry over of the internal standards should be less than 5% of the internal standard peak area in a spiked sample.

Stability

Stability of the stock solutions was assessed after 5 hours storage at 20-25 °C using the HPLC-UV system. Stock solutions were considered stable if the determined concentrations did not deviate more than ±5% from the concentration determined at time zero. Stability in lysate was determined after 6 hours storage at 20-25°C. Moreover, we assessed the reinjection reproducibility of the processed samples by reinjecting the calibration samples and the validation samples at the low and high level after 24 hours in the autosampler at 4 °C. Analytes were considered stable in biomatrix if the determined concentrations did not deviate more than ±15% from the concentration determined at time zero. All stability experiments were performed in triplicate.

Application of the assay

Using the described method, PBMCs were isolated from a patient treated with 200 mg FTC and 245 mg TDF once-daily for 3 years, who switched to a single once-daily tablet also containing 200 mg FTC and 245 mg TDF. Samples were collected 4, 8 and 12 months after therapy switch. The analytical result, expressed as nM in PBMC lysate, was finally multiplied with the lysate sample volume to obtain the absolute amount of the analytes in a sample. This amount was then divided by the number of cells present in the sample to obtain the amount of analyte per 10^6 PBMCs.

Results and discussion

Reference standards

Because some analytes were not commercially available we thermally degraded FTC-TP, *CTP, TFV-DP and *TFV-DP into mixtures of their lower phosphates as described in the experimental section. Since the chromophores of a nucleoside and its nucleotides are identical we could quantify the obtained mixtures on the isocratic HPLC-UV systems, using reference FTC and TFV material. The thus obtained solutions contained 32.7, 59.8, and 58.2 µM (FTC-MP, -DP and -TP, respectively), 68.1, 69.4 and 115 µM (TFV, TFV-MP and -DP, respectively). The *TFV internal standards did not cause a signal in the mass transitions of their unlabeled variants, indicating sufficient isotopic purity. Stable isotope-labeled FTC nucleotides were not commercially available. Therefore we used the nucleotides of the stable isotope-labeled structural analog cytosine.

WAXLC-MS/MS

Up-front fragmentation can cause the degradation of higher phosphates into lower phosphates before entering the mass analyzers. Therefore, separation between mono-, di- and triphosphates is necessary for their correct quantification. Separation was achieved by applying a pH gradient to a weak anion-exchange column, thereby decreasing the anion-exchange capacity of the column and separating the nucleotides [19]. Figure 2 shows typical chromatograms of a sample spiked at the LLOQ. The effect of the up-front fragmentation is clearly visible as peaks in the mass transition TFV at the retention time of TFV-MP and TFV-DP (figure 2). The sensitivity was similar using the negative and the positive ionization mode for all analytes except TFV, which was ionized more efficiently in the positive ionization mode. Although the detection of these phosphate-containing analytes is intuitively expected to be more sensitive in the negative ionization mode, we and others showed the effective ionization and superior selectivity in the positive ionization mode [14;20]. This superior selectivity is achieved because more selective fragments are formed. For the nucleotides of the pyrimidines FTC and *C, the protonated base was the most abundant fragment for each nucleotide. The loss of a mono- and diphosphate moiety most likely results in the m/z 270 fragment of TFV-MP and TFV-DP, whereas cleavage of the ether bond resulted in a fragment including the base (m/z 176) for TFV.

Validation procedures

Linearity

The calibration curves were constructed using linear regression of the analyte-internal standard ratio with a $1/x^2$ weighting factor. The deviations of the mean back-calculated concentrations from nominal were between -1.98 and 3.89%, -3.58 and 4.94% and -3.51 and 3.79% for FTC-MP, FTC-DP and FTC-TP, respectively. Likewise, the deviations were between -1.56 and 1.43%, -1.47 and 2.01% and -3.15 and 2.89% for TFV, TFV-MP and TFV-DP, respectively. The coefficients of variance were lower than 13.1% and correlation coefficients (r) were better than 0.990 for all analytes.

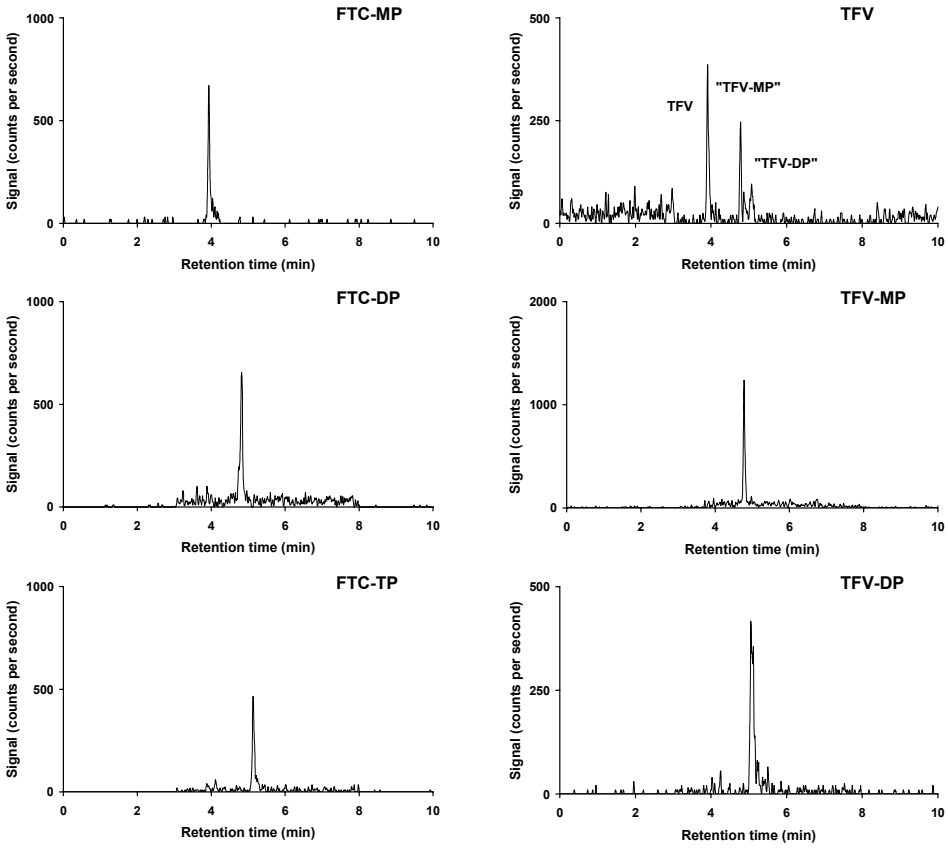

Figure 2. Chromatograms of a sample spiked at the LLOQ level, containing 0.727 (FTC-MP), 1.33 (FTC-DP), 1.29 (FTC-TP), 1.51 (TFV), 1.54 (TFV-MP) and 2.54 nM (TFV-DP). "TFV-MP"and "TFV-DP" indicate the peaks in the TFV mass transition caused by up-front fragmentation of TFV-MP and TFV-DP to TFV.

Accuracy and precision

In table 3 the inter-assay performance is summarized for the tested concentration levels. Likewise, the intra-assay accuracies and precisions were between -10.3 and 16.7% deviation and lower than 17.8% CV for all analytes at the LLOQ level, whereas the intra-assay accuracies and precisions were between -14.3 and 9.81% deviation and lower than 14.7% CV for all analytes at the other concentrations. Therefore, the accuracy and precision of the method comply to commonly accepted criteria for bioanalytical method validation [21].

Specificity and selectivity

No interferences were observed in the chromatograms from blank PBMC lysate at the retention times of the analytes or internal standards. Moreover, the accuracies of the samples spiked at the LLOQ ranged from -18.0-19.7% deviation from nominal. Thus, the specificity and selectivity of this assay are satisfactory.

Matrix effect and recovery

The number of PBMCs isolated can vary per sample. Moreover, this factor is very important for the matrix effect and recovery [22]. Therefore, the matrix effect and recovery was determined at several cell concentrations including the normal range of 5-20 X 10^6 PBMCs per sample [22].
Figure 3 shows the matrix effect and recovery for FTC-TP. Similar results were obtained for all other analytes. As observed for similar analytes, the absolute analyte signals decreased at higher cell amounts [22]. This can be due to absorption to cell debris (recovery) or ion-suppression caused by co-eluting cell constituents eluting at the same time as the analytes (matrix effect). The internal standards, however, corrected well for this effect. The analyte-internal standard ratios determined in cell-containing samples were between 88.7 and 112% of those determined in the cell-free samples, showing the robustness of the assay towards number of isolated cells.

Carry over

Carry over was less than 17.1% of the area of an LLOQ sample for all analytes and less than 4.35% of the internal standard area of a spiked sample for all internal standards. Therefore, carry over of the analytes and internal standards was acceptable.

Stability

The stability data are presented in table 4. The table shows the concentrations determined at time zero and after the indicated periods under several conditions. The concentrations determined after storage under the test conditions did not deviate more than ±5% for the stock

Table 3. Inter-assay performance data for FTC and TFV nucleotides in PBMC lysate

Compound (calibration range)	Nominal concentration (nM)	Inter-assay accuracy (% DEV)	Inter-assay precision (% CV)
FTC-MP	0.727	-4.57	15.1
(0.727-36.4 nM)	2.27	-12.4	11.0
	4.54	0.793	13.2
	24.2	-0.634	8.37
FTC-DP	1.33	-0.902	10.8
(1.33-66.4 nM)	4.15	-3.37	7.99
	8.30	0.00803	6.92
	43.1	-0.139	10.1
FTC-TP	1.29	-1.79	12.2
(1.29-64.6 nM)	4.04	-11.4	10.2
	8.08	1.39	9.48
	43.1	-2.41	10.7
TFV	1.51	5.74	18.2
(1.51 -75.6 nM)	4.73	-7.37	10.7
	9.46	-3.81	9.79
	50.4	-2.76	8.42
TFV-MP	1.54	-1.86	12.9
(1.54-77.2 nM)	4.82	-4.70	11.6
	9.65	-2.00	10.6
	51.4	-4.40	10.5
TFV-DP	2.54	6.33	12.6
(2.54-127 nM)	7.95	-4.82	11.1
	15.9	4.11	9.55
	84.8	-3.59	10.7

DEV: deviation from nominal
CV: Coefficient of variation

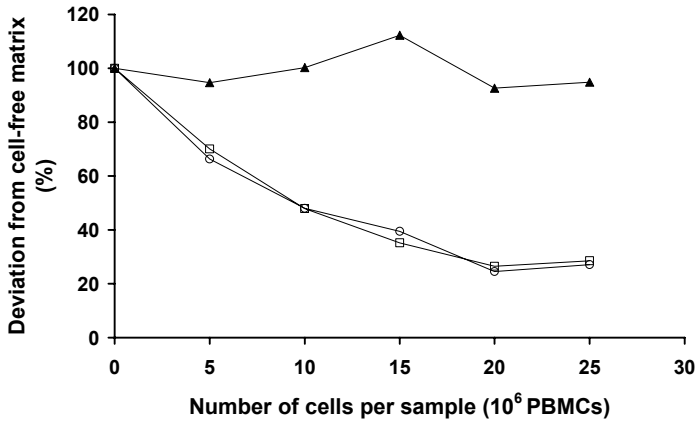

Figure 3. Matrix effect plus recovery for FTC-TP (□) and *CTP(○), and the analyte-internal standard ratio(▲) in samples containing different amounts of PBMCs.

Table 4. Stability data of the analytes in working solutions and biomatrix

Matrix	Condition	Analyte	Initial conc (nM/*μM*)	Found conc (nM/*μM*)	Deviation (%)
Water (stock solution)	5 hours, 20-25°C	FTC-MP	*32.7*	*33.3*	1.83
		FTC-DP	*59.8*	*60.7*	1.51
		FTC-TP	*58.2*	*59.1*	1.55
		TFV	*68.1*	*70.9*	4.11
		TFV-MP	*69.4*	*71.9*	3.60
		TFV-DP	*115*	*115*	0.00
PBMC lysate	6 hours, 20-25°C	FTC-MP	2.29	2.21	-3.35
			21.2	23.8	12.4
		FTC-DP	4.00	3.77	-5.59
			41.3	38.9	-5.65
		FTC-TP	3.54	3.05	-13.9
			37.9	38.0	0.264
		TFV	3.78	4.45	10.7
			43.7	48.3	10.7
		TFV-MP	4.57	5.01	9.62
			46.7	48.0	2.79
		TFV-DP	7.31	8.18	11.9
			74.9	71.3	-4.81
Final extract	24 hours reinjection, autosampler (4°C)	FTC-MP	2.02	2.21	8.58
			24.2	21.3	-13.5
		FTC-DP	3.97	3.58	-10.9
			41.6	47.7	12.7
		FTC-TP	3.39	3.38	-0.494
			40.0	44.2	9.58
		TFV	4.20	3.84	-9.38
			50.1	48.3	-3.73
		TFV-MP	4.62	4.22	-9.64
			50.0	51.8	3.41
		TFV-DP	7.21	6.94	-3.89
			86.5	76.5	-13.1

solutions and not more than ±15% for the biological samples indicating acceptable stability. Long term stability experiments are currently ongoing.

Application of the assay

The determined nucleotide levels are depicted in figure 4. All analytes were detected in the samples. The levels of FTC-TP were low, but in the range of previously reported values [1]. The sparse data on FTC-MP and FTC-DP show comparable FTC-MP, FTC-DP and FTC-TP levels, although FTC-MP and FTC-DP levels are relatively high in these samples [6].
Like the FTC nucleotide levels, the levels of TFV and its metabolites were low, but in the range of previously reported values [3;7;16]. TFV and its metabolites have, to the best of our knowledge, never simultaneously been determined in clinical samples, but *in vitro* experiments by others showed several different TFV:TFV-MP:TFV-DP ratios at similar concentrations [4;10;11]. Finally, the FTC nucleotides do not show a trend in time, whereas the levels of TFV and its mono and diphosphate increase over the sampling period of 8 months, indicating slow intracellular accumulation.

Conclusions

A sensitive method for the simultaneous quantification of FTC-MP, -DP and -TP, and TFV, TFV-MP and -DP has been developed and validated. Assuming a mean of 10 million PBMCs per sample the LLOQ of the method is 14.5, 26.6 and 25.9 fmol/10^6 PBMCs for FTC-MP, FTC-DP and FTC-TP and 30.3, 30.9 and 50.9 fmol/10^6 PBMCs for TFV, TFV-MP and TFV-DP, respectively. The method requires minimal sample pretreatment and is the first for the simultaneous quantitation all 6 analytes.

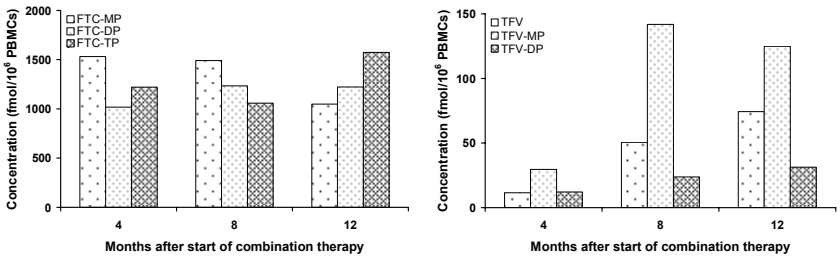

Figure 4. Analyte levels in PBMCs from a patient on treatment with once-daily truvada (containing 200 mg FTC and 245 mg TDF).

References

[1] L. H. Wang, J. Begley, C. R. St, III, J. Harris, C. Wakeford, F. S. Rousseau, AIDS Res. Hum. Retroviruses 20 (2004) 1173.

[2] P. Barditch-Crovo, S. G. Deeks, A. Collier, S. Safrin, D. F. Coakley, M. Miller, B. P. Kearney, R. L. Coleman, P. D. Lamy, J. O. Kahn, I. McGowan, P. S. Lietman, Antimicrob. Agents Chemother. 45 (2001) 2733.

[3] T. Hawkins, W. Veikley, R. L. Claire, III, B. Guyer, N. Clark, B. P. Kearney, J. Acquir. Immune. Defic. Syndr. 39 (2005) 406.

[4] K. Borroto-Esoda, J. E. Vela, F. Myrick, A. S. Ray, M. D. Miller, Antivir. Ther. 11 (2006) 377.

[5] D. J. Back, D. M. Burger, C. W. Flexner, J. G. Gerber, J. Acquir. Immune. Defic. Syndr. 39 Suppl 1 (2005) S1.

[6] A. Darque, G. Valette, F. Rousseau, L. H. Wang, J. P. Sommadossi, X. J. Zhou, Antimicrob. Agents Chemother. 43 (1999) 2245.

[7] T. King, L. Bushman, J. Kiser, P. L. Anderson, M. Ray, T. Delahunty, C. V. Fletcher, J. Chromatogr. B 843 (2006) 147.

[8] R. L. Claire, III, Rapid Commun. Mass Spectrom. 14 (2000) 1625.

[9] Bartley, S, Begley, JA., and Clark, TN., Proceedings of the 55th ASMS conference on mass spectrometry and allied topics (2007).

[10] W. E. Delaney, A. S. Ray, H. Yang, X. Qi, S. Xiong, Y. Zhu, M. D. Miller, Antimicrob. Agents Chemother. 50 (2006) 2471.

[11] A. S. Ray, F. Myrick, J. E. Vela, L. Y. Olson, E. J. Eisenberg, K. Borroto-Esodo, M. D. Miller, A. Fridland, Antivir. Ther. 10 (2005) 451.

[12] T. Lynch, G. Eisenberg, M. Kernan, Nucleosides Nucleotides Nucleic Acids 20 (2001) 1415.

[13] Kuklenyik, Z, Martin, A, Pau, C, Garcia-Lerma, G, Heneine, W, Pirkle, J, and Barr, J, Proceedings of the 56th ASMS conference on mass spectrometry and allied topics (2008).

[14] A. Pruvost, F. Theodoro, L. Agrofoglio, E. Negredo, H. Benech, J. Mass Spectrom. 43 (2008) 224.

[15] L. Durand-Gasselin, D. Da Silva, H. Benech, A. Pruvost, J. Grassi, Antimicrob. Agents Chemother. 51 (2007) 2105.

[16] A. Pruvost, E. Negredo, H. Benech, F. Theodoro, J. Puig, E. Grau, E. Garcia, J. Molto, J. Grassi, B. Clotet, Antimicrob. Agents Chemother. 49 (2005) 1907.

[17] Delinsky, DC, Hernandez-Santiago, B., and Schinazi, RF, Proceedings of the 54th ASMS conference on mass spectrometry and allied topics (2006).

[18] S. A. Veltkamp, M. J. Hillebrand, H. Rosing, R. S. Jansen, E. R. Wickremsinhe, E. J. Perkins, J. H. Schellens, J. H. Beijnen, J. Mass Spectrom. 41 (2006) 1633.

[19] G. Shi, J. T. Wu, Y. Li, R. Geleziunas, K. Gallagher, T. Emm, T. Olah, S. Unger, Rapid Commun. Mass Spectrom. 16 (2002) 1092.

[20] R. S. Jansen, H. Rosing, C. J. de Wolf, J. H. Beijnen, Rapid Commun. Mass Spectrom. 21 (2007) 4049.

[21] U.S Food and Drug Administration: Centre for Drug Evaluation and Research: Guidance for Industry: Bioanalytical Method Validation. 2001.

[22] F. Becher, A. Pruvost, J. Gale, P. Couerbe, C. Goujard, V. Boutet, E. Ezan, J. Grassi, H. Benech, J. Mass Spectrom. 38 (2003) 879.

Chapter 2.4

Retention studies of 2′-2′-difluoro-deoxycytidine and 2′-2′-difluoro-deoxyuridine nucleosides and nucleotides on porous graphitic carbon: Development of a liquid chromatography-tandem mass spectrometry method

Robert S Jansen, Hilde Rosing, Jan HM Schellens and Jos H Beijnen

Journal of Chromatography A
Volume 1216, Issue 15, Pages 3168-74
2009

Abstract

The development of a method for the separation of 2′-2′-difluorodeoxycytidine (gemcitabine, dFdC), 2′-2′-difluorodeoxyuridine (dFdU) and their mono-, di- and triphosphates using a porous graphitic carbon column (Hypercarb), without ion-pairing agent, is described. The retention of dFdC and dFdU could be controlled with an organic modifier (acetonitrile, CH_3CN) and the retention of the anionic nucleotides with an eluting ion (bicarbonate). Separation of all analytes was achieved using a 0-25 mM ammonium bicarbonate gradient in CH_3CN-H_2O (15:85, v/v). Under these conditions, however, very long re-equilibration times were required. Injection of an acidic solution (100 µL 10 % formic acid in H_2O, v/v; 2.65 M) after running a gradient directly restored the separation capabilities of the column. Still, separation between the analytes slowly deteriorated over a period of months. These problems were solved by preconditioning the column with a pH buffered hydrogen peroxide (H_2O_2) solution (0.05% H_2O_2 in 15 % CH_3CN-H_2O (15:85, v/v), pH 4) before starting an analytical run. The oxidation of the stationary phase with H_2O_2 prevented its slow reduction, which most likely caused the decreasing retention times. The analytes were detected using tandem mass spectrometry.

Introduction

Gemcitabine (2′-2′-difluorodeoxycytidine, dFdC, figure 1) is a nucleoside analog widely used in the treatment of various solid tumors. After administration, intracellular enzymes phosphorylate dFdC into its mono- (dFdCMP), di- (dFdCDP) and finally triphosphate (dFdCTP). dFdCDP inhibits the enzyme ribonucleotide reductase whereas dFdCTP is incorporated into DNA causing cell death [1]. The ubiquitous enzyme cytidine deaminase rapidly deaminates dFdC into 2′-2′-difluorodeoxyuridine (dFdU, figure 1), which is relatively inactive [2]. Recently dFdU mono-, di- and triphosphate (dFdUMP, dFdUDP and dFdUTP) were detected in different cells from mice [3] and dFdUTP in white blood cells from patients [4] receiving dFdC. Moreover, in vitro experiments showed that dFdUTP was incorporated into DNA and RNA and inhibited cell proliferation [2]. Monitoring dFdC, dFdU and their metabolites in white blood cells or tumor tissue from patients may shed more light on the activity and toxicity of dFdC and the role of the dFdU nucleotides therein, but requires a method for their selective analysis.

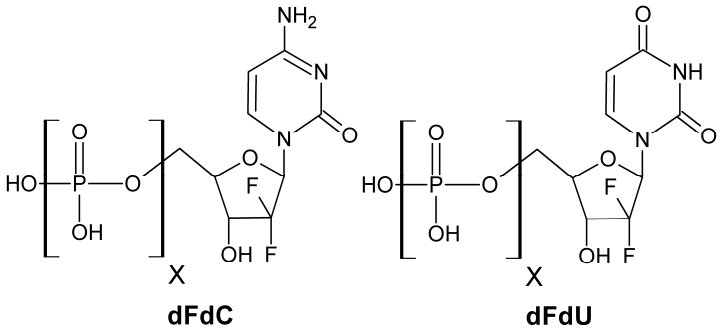

Figure 1. Chemical structures of the nucleosides dFdC and dFdU (X=0), and their mono- (X=1), di- (X=2) and triphosphates (X=3).

Methods for the intracellular analysis of nucleosides and nucleotides used in human immunodeficiency virus (HIV) therapy have recently been reviewed by Lai et al [5]. Many other methods have, however, been developed for the intracellular determination of anti-cancer and naturally occurring nucleosides and nucleotides. The methods can be divided into indirect and direct approaches. Indirect approaches are based on separation and isolation of the mono-, di- and triphosphates on a strong anion-exchange solid phase extraction (SPE) column and subsequent dephoshorylation of the nucleotides into the nucleosides, which can then be analyzed using regular reversed phase methods [6]. Because of the

extensive sample pre-treatment and multiple analyses per sample, indirect approaches are labour- and instrument time-intensive.
Direct approaches do not require dephosphorylation, but chromatographic separation of the nucleotides is essential because higher phosphates can degrade into lower phosphates in the ion source of the mass spectrometer (MS). Separation of nucleotides is relatively easy using ion-pairing agents and salt gradients. MS detection in combination with these chemicals is, however, problematic because of their low volatility and ability to cause ion-suppression. Therefore low amounts of regular ion-pairing agents [7-9] or volatile ion-pairing agents [10-12] have been used. Others used weak ion-exchange chromatography [13-15] or hydrophilic liquid interaction chromatography (HILIC) on amino [16] or titania [17] columns. A porous graphitic carbon (PGC) column was recently used for the separation of several sugars and sugar mono- and diphosphates [18]. Adenosine, guanosine, cytidine and uridine nucleosides and nucleotides were separated using a PGC column with diethylamine (DEA) added to the mobile phase as ion-pairing reagent [19].
dFdC and dFdU only differ 1 Da in molecular weight and have very similar MS fragmentation patterns. dFdC molecules containing a naturally occurring ^{13}C- or ^{15}N-isotope (about 11 % of the dFdC molecules) will therefore have the mass of dFdU and produce a signal in the dFdU mass transition. Likewise dFdCMP, dFdCDP and dFdCTP produce a signal in the dFdUMP, dFdUDP and dFdUTP mass transition. As a consequence, separation between the dFdC and dFdU nucleosides, mono-, di- and triphosphates is pivotal for their simultaneous determination.
Although separation of cytidine and uridine nucleosides and nucleotides is possible with selected HILIC and ion-pairing methods, they require long run times and often lack base-line separation [16;20]. Base line separation, though, was achieved within 15 minutes for the most of the 16 nucleosides and nucleotides analyzed on a PGC column with DEA added to the mobile phase [19]. We could, however, not separate all analytes using the method and peaks showed considerable peak tailing.
No existing method fulfilled our need for separation of dFdC and dFdU nucleosides and nucleotides with MS detection. The similarity between the cytidine and uridine moiety of the molecules on the one hand and the considerable difference in charge between the phosphate moiety of the molecules on the other hand, make the separation in a single run analysis particularly challenging. Because of the unique retention properties and ability to retain polar and ionic analytes we explored the potential of PGC to achieve separation of these analytes.
PGC consists of flat sheets of hexagonally arranged carbon atoms. The material is produced by heating silica gel impregnated with a phenol-formaldehyde resin up to 2500°C in an inert atmosphere [21]. The obtained stationary phase can be used over a broad pH range (1-14), at high

temperatures (>500°C), and is compatible with solvents and chemicals that cannot be used with conventional HPLC columns [22]. Various interactions occur between the stationary phase surface, mobile phase components and solutes [23;24]:

1) Hydrophobic or dispersive interactions with the apolar graphite surface and hydrophilic mobile phase. This property makes the material behave like strong reversed phase material.

2) Electronic interactions with the polarizable graphite surface. Polar or polarizable analytes cause a charge-induced dipole at the graphite surface causing retention of negatively charged analytes [25]. Functional groups present at the edge of the carbon sheets have also been associated with these electronic interactions [26].

3) Steric interactions caused by the planar nature of the graphite surface. The contact area between analyte and stationary phase influences the retention time making separations between stereoisomers possible [27;28].

4) Redox interactions. PGC can act as oxidizing or reducing agent towards analytes [29-31]. Moreover the redox state of the material influences the retention of analytes [32;33].

Because of the different retention mechanisms separation between compounds with a wide range in polarity can be achieved. Although PGC has unique retention properties and has been commercially available as a stationary phase since 1988, relatively few analytical methods using this material have been published. Most of these methods use a gradient of an organic modifier on bare PGC for the analysis of polar analytes [22;23]. A small number of articles describe the analysis of ionic compounds using PGC but these methods often employ ion-pairing agents [34-36] or adsorbed column modifiers [37-39] in combination with an organic modifier. Only a few methods use bare PGC without any ion-pairing agent in the ion-interaction mode [18;26;28;40-44].

Possibly the unpredictable chromatographic behaviour of compounds on the material and the lack of understanding of retention mechanisms have limited the number of applications. We found, however, the column material to be very useful for the separation of dFdC and its metabolites. This article describes the development of the chromatographic system for the analysis of dFdC, dFdU and their nucleotides with MS detection.

Experimental

Chemicals

dFdC hydrochloride, dFdCMP, dFdCDP dFdCTP, dFdU, dFdUMP, dFdUDP and dFdUTP were kindly provided by Eli Lilly and Company (Indianapolis, USA). Acetonitrile (CH_3CN) was obtained from Biosolve Ltd. (Amsterdam, The Netherlands). Distilled water (H_2O) was obtained from B Braun (Melsungen, Germany). All other solvents or chemicals were analytical grade or better and originated from Merck (Darmstadt, Germany).

Instrumentation

HPLC-UV experiments were performed on an Agilent 1100 series liquid chromatograph system (Agilent technologies, Palo Alto, CA, USA) consisting of a binary pump, an inline degasser, autosampler, column oven and UV detector. Absorption was measured at 260 nm and data were acquired with Chromeleon 6.50 software (Dionex corp., Sunnyvale, CA, USA).

HPLC-MS experiments were performed using a Thermo Fischer TSQ Quantum Ultra™ mass spectrometer (Thermo Fisher Scientific Inc., Waltham, MA, USA) with a Shimadzu LC system (Shimadzu, Kyoto, Japan) consisting of a SIL-HTc autosampler with SCL-10A^{vp} systemcontroller, two LC20-AD Prominence pumps, a FCV-11AL valve unit, a DGU-20A5 inline degasser unit and a CTO-20AC column oven. Ionization of the analytes was performed with an electrospray ionization (ESI) source with a tension of 4500 V for both the positive and negative ion mode. Electrical grounding was achieved with the standard grounding union of the ESI source. MS scan parameters are listed in table 1. Data were acquired using Xcalibur 2.0 software (Thermo Fisher Scientific Inc., Waltham, MA, USA).

Table 1. Scan parameters of the TSQ quantum ultra triple quadrupole mass spectrometer.

Compound	Parent ion (m/z)	Product ion (m/z)	Collision energy (V)	Polarity
dFdC	264	112	17	+
dFdU	263	111	20	-
dFdCMP	344	246	17	+
dFdUMP	345	247	18	+
dFdCDP	424	326	14	+
dFdUDP	425	327	13	+
dFdCTP	504	326	26	+
dFdUTP	505	247	28	+

Chromatographic conditions

All chromatographic experiments were performed using Hypercarb columns (100 mm x 2.1 mm, 5 µm particle size; Thermo Fisher Scientific Inc., Waltham, MA, USA) thermostated at 45 °C. A flow of 0.25 mL/min was used in all experiments. 1 µL injections of a mixture of the analytes in H_2O were performed to assess their retention. The dead volume of the chromatographic systems was determined by injecting tetrahydrofuran.

Isocratic elutions to assess retention behaviour as a function of the amount of organic modifier and eluting ion were performed on the HPLC-UV system. The column was conditioned at each test condition for one hour prior to analysis.

Gradient chromatography was carried out on the HPLC-UV (reconditioning experiments) and HPLC-MS system using the final conditions, unless described otherwise. CH_3CN-H_2O (20:80, v/v) was used in mobile phases A and B in all experiments except the experiments on preconditioning of PGC before the start of an analytical run.

For the reconditioning experiments 100 µL of H_2O, diluted formic acid (CHOOH) (10 % in H_2O, v/v; 2.65 M), hydrofluoric acid (HF) (0.1 M) or sodium iodate ($NaIO_3$) (25 mM) was injected between each analytical injection.

The final conditions were as follows: before each analytical run the column was treated (30 minutes, 0.25 mL/min) with preconditioning buffer consisting of 1 mM ammonium acetate (NH_4Ac) in CH_3CN-H_2O (15:85, v/v) with 0.05 % hydrogen peroxide (H_2O_2) and with the pH adjusted to 4 with glacial acetic acid (CH_3COOH). Next, gradient chromatography was started. Mobile phase A consisted of 1 mM NH_4Ac in CH_3CN-H_2O (15:85, v/v) with the pH adjusted to 5 with glacial CH_3COOH. Mobile phase B consisted of 25 mM ammonium bicarbonate (NH_4HCO_3) in CH_3CN-H_2O (15:85, v/v). The mobile phases were delivered at a flow of 0.25 mL/min with the following gradient: 0-0.1 min: 0% B, 0.1-2.0 min: 0-100% B, 2.0-12 min: 100% B, 12-15 min: 0 % B. Between each analytical injection 100 µL diluted CHOOH (10% in H_2O, v/v; 2.65 M) was injected in a flow of 0% B with the column outlet directed to the waste for 5 minutes. The steps required for a successful analytical run are summarized in table 2.

Table 2. Summary of steps required for the separation of dFdC, dFdU and their nucleotides on PGC.

Step	Mobile phase	Time	Injection
1. Preconditioning	Preconditioning buffer	30 min	-
2. Gradient elution	Gradient mobile phase A and B	15 min	25 µL sample
3. Reconditioning	Mobile phase A	5 min	100 µL diluted CHOOH
Steps 2 and 3 are repeated for each sample			

Results and discussion

Elution characteristics of PGC

Assay development was started based on a method published by Xing et al., who used a PGC stationary phase and DEA as ion-pairing agent to separate 16 nucleosides and nucleotides [19]. We could, however, not separate all the dFdC and dFdU nucleotides with this system and peaks showed considerable tailing. Moreover, the use of DEA reduced the sensitivity for some analytes.

Then the PGC column was used without an ion-paring agent. Carboxylic acids are commonly used as eluting ions [40]. An effective, and commonly used eluting ion is trifluoroacetic acid (TFA). TFA is, however, known to cause severe ion suppression when used in combination with MS detection [19]. Ammonium formate and acetate have also been used to elute nucleotides, but the nucleotides showed peak tailing when DEA was not added [19].

Because PGC behaves similar to anion-exchange stationary phases the use of a stronger, but volatile, anion as eluting ion was explored. Bicarbonate (HCO_3^-) ions have an elution strength higher than phosphate ions on anion-exchange columns and show even more elution strength on PGC [38;43]. Moreover, HCO_3^- ions are MS-compatible and, as was shown recently, reduce peak tailing caused by interactions between stainless steel surfaces and the phosphate groups of nucleotides [45]. Although HCO_3^- is in acid-base equilibrium with H_2CO_3 ($H_2O + CO_2$) and CO_3^{2-} under the tested conditions, it will be referred to as HCO_3^- throughout the text.

We first assessed the effect of an organic modifier on the retention of the analytes. In figure 2 the capacity factors k′ of dFdC, dFdU and their nucleotides are plotted against the amount of CH_3CN in the mobile phase containing 1 mM NH_4HCO_3 and 1 mM ammonia (NH_4OH) (pH 9.1). Both dFdC and dFdU, showed a conventional elution pattern governed by hydrophobic interactions. The nucleotides, however, showed U-shaped elution curves indicating mixed retention effects.

Using CH_3CN-H_2O (20:80, v/v) both nucleosides were baseline separated. The CH_3CN concentration was therefore fixed at 20% and different NH_4HCO_3 concentrations were tested for their ability to elute the analytes. In figure 3 the capacity factors of the analytes are plotted against the amount of NH_4HCO_3 in the mobile phase. The capacity factor of the two nucleosides was hardly affected by the NH_4HCO_3 concentration. This is in agreement with the retention being governed by hydrophobic interactions. With the amount of CH_3CN fixed, the column behaved like an ion-exchange column for the nucleotides with decreasing retention at an increasing concentration of eluting ion. The temperature of the column only had a minor effect on the chromatography. A temperature of 45°C

was chosen since slightly better peak shapes were obtained. A steep gradient of NH_4HCO_3 in a fixed CH_3CN concentration was most effective in eluting and separating all compounds with acceptable peak shape and run time. Purine nucleosides and nucleotides could be eluted using the same approach but required more or stronger organic modifiers like isopropanol or tetrahydrofuran.

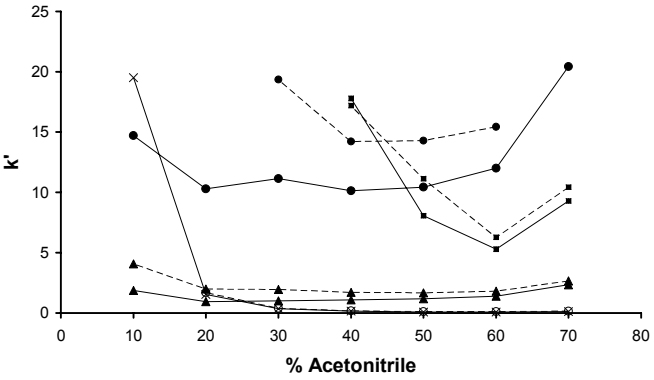

Figure 2. Capacity factor k' of dFdC (X, solid line), dFdU (O, dotted line), dFdCMP (▲, solid line), dFdUMP (▲, dotted line), dFdCDP (●, solid line), dFdUDP (●, dotted line, dFdCTP (■, solid line) and dFdUTP (■, dotted line) versus the percentage of acetonitrile mixed with 1 mM NH_4HCO_3 and 1 mM NH_4OH (pH 9.1). dFdU did not elute within the monitored time at 10 % acetonitrile.

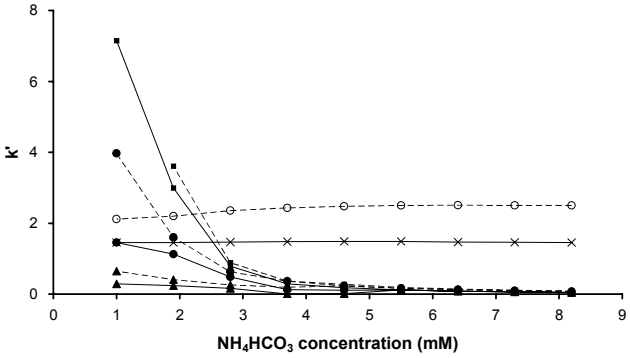

Figure 3. Capacity factor k' of dFdC (X, solid line), dFdU (O, dotted line), dFdCMP (▲, solid line), dFdUMP (▲, dotted line), dFdCDP (●, solid line), dFdUDP (●, dotted line, dFdCTP (■, solid line) and dFdUTP (■, dotted line) versus the amount of NH_4HCO_3 present in the mobile phase (CH_3CN-H_2O (20:80, v/v) with 1 mM NH_4OH).

The use of HCO_3^- as eluting ion on bare PGC is relatively unexplored.
HCO_3^- has been used on PGC before by others, but CH_3CN gradients were used for elution [46-49]. Using only HCO_3^-, Chambers et al. concluded that a bare PGC column does not have a high anion-exchange capacity because 0.90 mM CO_3^{2-}/ 0.85 mM HCO_3^- (pH 10.3) eluted a set of 7 common anions near the void volume [38].
Recently, however, combined organic modifier - HCO_3^- (0-210 mM [43]) and - CH_3COO^- (0-700mM [43] and 0-490 mM [50]) gradients were used for the separation of ι- and κ–carrageenan oligosaccharides on PGC with evaporative light scattering detection. Pabst et al also showed that nucleotides were retained on PGC and that elution of these analytes was possible with CH_3CN and HCO_3^- [49]. Our experiments show that, after conditioning, PGC columns have sufficient anion-exchange capacity and that HCO_3^- ions are very effective in eluting anionic analytes from the column.

Reconditioning of PGC during an analytical run

Using a steep gradient of HCO3- and a fixed percentage of CH3CN in the mobile phase all nucleosides and nucleotides were separated within 15 minutes. Direct analysis of a second sample was, however, not possible because of a loss in retention of the nucleotides (table 3, problem 1). The effect was most dramatic for the triphosphates, whereas the retention of nucleosides remained almost unaffected. Long re-equilibration (30-60 minutes) with mobile phase A was required before a next successful separation could be achieved. Other methods using eluting ion gradients on PGC also required long re-equilibration times [18;42], even up to 2 hours [43;44].
Interestingly, we found that after a 100 µL injection of diluted CHOOH (10 % in H_2O, v/v; 2.65 M) the separation properties of the column were restored. Identical injections with H_2O did not result in fast reconditioning of the column. We hypothesized that two effects could cause the loss in retention: 1) HCO_3^- ions strongly bound to the active sites inactivate the electronic properties of the PGC, or 2) the pH (= 8.2) of mobile phase B changes the ion affinity of the PGC. When formate ions pass the PGC material they may act as eluting ions thus displacing the HCO_3^- ions and restoring the separation properties. On the other hand, the acidity of the diluted CHOOH (pKa = 3.74, pH = 1.59) could be responsible for the observed effect. To differentiate between these two mechanisms diluted HF and $NaIO_3$ were injected between analyses. HF has a pKa similar to CHOOH (pKa = 3.15), but the F^- ion is a very weak eluting ion [40]. $NaIO_3$, on the other hand, is not acidic but IO_3^- is a relatively strong eluting ion [40]. After injections with HF the separation capacity was maintained, whereas the analytes were not separated after IO_3^- injections. It was therefore concluded that diluted CHOOH restored the separation capabilities of PGC

due to its low pH. The low pH could either 1) cause a reaction of protons with the strongly bound HCO_3^- ions resulting in CO_2 and H_2O formation, or 2) change the ion affinity of the stationary phase. To differentiate between these two possible mechanisms we used phosphate, which unlike HCO_3^- is stable at low pH, as eluting ion. Diluted CHOOH injections were, however, still required when phosphate was used as eluting ion. We therefore concluded that the acidity of the diluted CHOOH changes the ion affinity of the PGC and in that way restores its separation capability. Possibly injections of acid solutions could decrease the re-equilibration time of the previously mentioned methods as well [18;42-44].

Table 3. Overview of problems encountered during method development and their solutions.

Problem	Solution
1. Loss of separation capabilities after running a gradient	Reconditioning PGC with diluted CHOOH
2. Decrease of retention times over a period of months	Preconditioning PGC with 0.05 % H_2O_2
3. Slow stabilization of retention times after starting an analytical run	Preconditioning PGC at pH 4

The redox state of PGC

During further method development a slow, but progressive, decrease in retention times mainly affecting the charged nucleotides was noticed (table 3, problem 2). The decrease in retention undermined the separation, required because of isotope and up-front fragmentation signals, of the analytes (table 4, figure 4).

Several articles describe slow changes in retention time and peak efficiencies occurring over hours to months [26;33;38;49;51;52]. Koivisto et al [51] speculated that a rearrangement of "amorphous" PGC layers might be responsible for the observed effects. In other articles the changes have been related to the redox state of PGC material [26;32;33;52]. Oxidation of PGC seems to increase positive surface charge and thus retention of anions. Reduction of the material, on the other hand, causes a decrease in retention of anions [32]. The redox properties of PGC have been quantified by Törnkvist et al. who performed a redox titration with PGC and permanganate and concluded that 0.1 % of PGC material is oxidizable [33]. The origin of the redox properties is unclear but the presence of oxidizable groups at the end of the graphite sheets has been associated with the effect. Shibukawa et al. determined the anion-exchange capacity of an oxidized PGC column and concluded that 0.030 % of the column is charged [32]. They concluded that the redox and anion-exchange sites may be identical. The found percentages are in the same order of magnitude as the 0.4 % of carbon edge atoms with unsatisfied valencies calculated by Knox and Ross [24], and the 0.14 % oxygen content

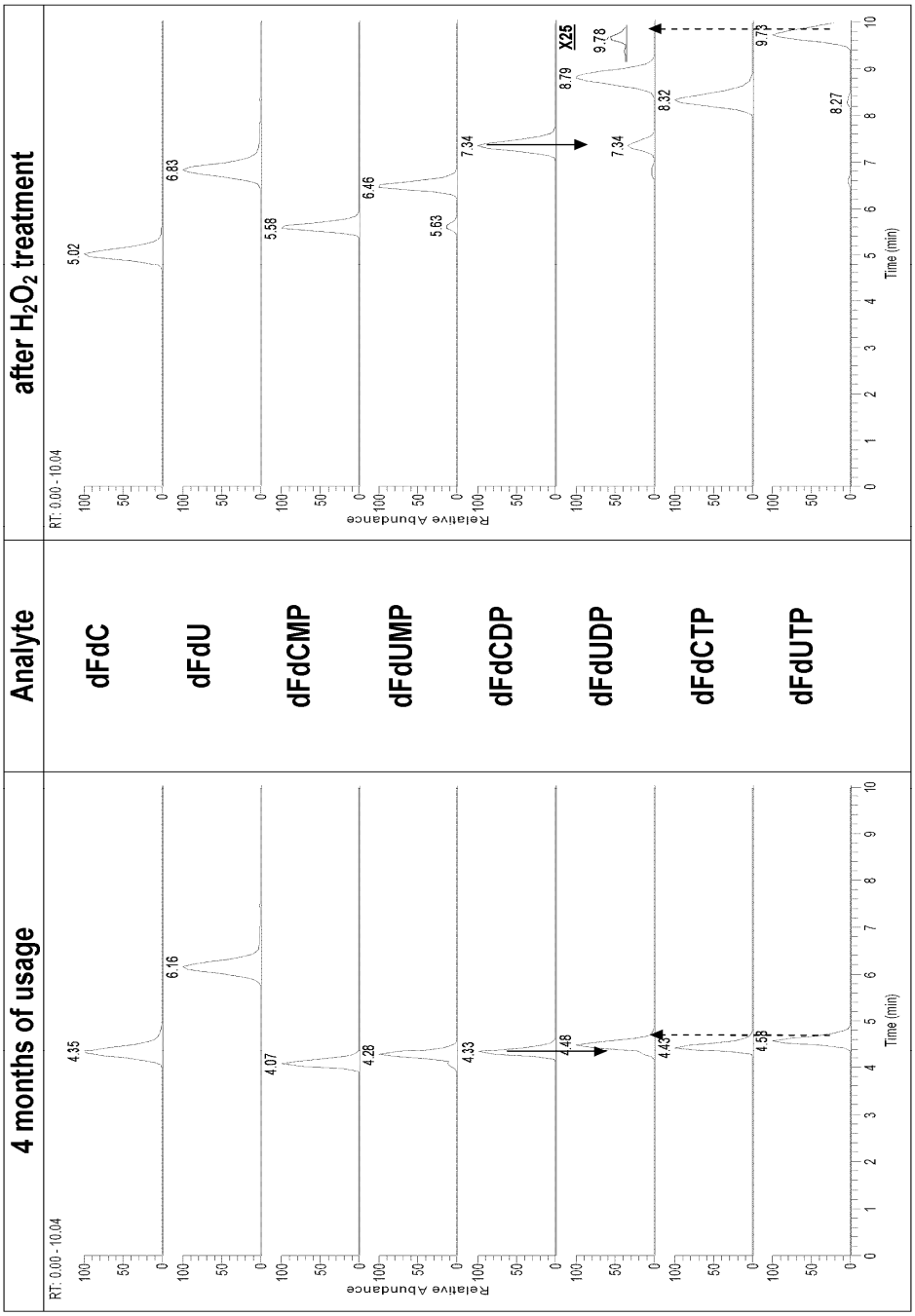

Figure 4. HPLC-MS chromatograms of dFdC, dFdU and their nucleotides on a PGC column after 4 months of usage without preconditioning and after subsequent H_2O_2 treatment. The arrows indicate the ^{15}N- and ^{13}C-isotope signal (solid line) and up-front fragmentation (dotted line, Y-axis zoomed 25 times) with dFdUDP as example.

attributed to phenol, carbonyl, carboxylic acid, lactone and quinone groups in PGC material [53].
Changes in the redox state of the column can be caused by electric tension over the conducting PGC column, caused by the tension applied in the ESI source [49;52]. Our column was, however, grounded, and the retention times of the analytes were similar on the HPLC-UV system where no voltages were applied. Slow oxidation or reduction can also be caused by unknown constituents of the mobile phase or samples [32].
We reasoned that a similar mechanism could be responsible for the slow decrease in retention time and loss of separation observed in our study. Indeed, treating the column with H_2O_2 immediately increased the retention of the analytes (figure 4). Reduction of the column with sodium thiosulphate, on the other hand, resulted in a dramatic further decrease in retention (table 2).
The use of oxidizing agents to restore and to maintain the redox state of the column was then explored. H_2O_2 was sufficiently strong to restore the column properties and is volatile. Direct addition of H_2O_2 to the mobile phase, however, decreased retention times, and the chromatography deteriorated after addition of H_2O_2 to the diluted CHOOH injections. The column was therefore preconditioned with mobile phase A containing 0.05% H_2O_2 before the start of an analytical run. The effect of the treatment persists for at least 60 analytical injections. In this way the PGC remains in the oxidized state and retention properties are maintained.
Rinne et al. have reported on the oxidizing capabilities of PGC [31]. They analyzed a set of four oxidation-sensitive catecholamines using PGC. No oxidation was observed using mobile phases consisting of H_2O, CH_3CN and CH_3COOH. Extensive oxidation was, however, seen after contamination of the PGC column with small amounts of pentafluoropropionic acid (PFPA), which was used as an ion-pairing agent on a pre-column. They argued that strong acids like PFPA could oxidize the graphite to ionic graphite salts in the presence of oxidizing agents. Addition of reductive agents to the mobile phase, however, did not prevent oxidation of the analytes. This raises the question whether the injections of diluted CHOOH used in our method cause oxidation of the graphite surface resulting in increased retention of the analytes. However, the fact that long re-equilibration with mobile phase A without any buffer also resulted in recovery of the retention characteristics does not support this theory. In addition, in a few months of time, a change in retention times was observed despite injections of diluted CHOOH during the analytical runs. The diluted CHOOH injections thus did not stop the slow reduction of the column, which could, on the other hand, be prevented using H_2O_2 in the preconditioning solvent before the start of an analytical run.

Preconditioning of PGC before the start of an analytical run

Although final retention times were stable and sufficiently long using the H_2O_2 pretreatment and reconditioning with formic acid, 10-20 gradient runs were required to reach stable retention times within an analytical run (table 3, problem 3). Preconditioning the column with a mobile phase of a controlled pH before analysis had a profound effect on the retention times at the start of the analytical run. After preconditioning the column with a pH lower than 4, retention times decreased until constant retention times were obtained. Conversely, after preconditioning the column with a pH higher than 4, the retention times increased until the same constant retention times were reached. After preconditioning the column with mobile phase A adjusted to pH 4 before analysis, however, retention times were stable almost directly (figure 5). The reproducibility of the preconditioning was confirmed on a second day.

The mobile phase used to oxidize the column before use was therefore adjusted to pH 4 (preconditioning buffer). Because the pH had a strong effect on the retention times the pH in mobile phase A was controlled by adding 1 mM NH_4Ac and adjusting the pH to 5.

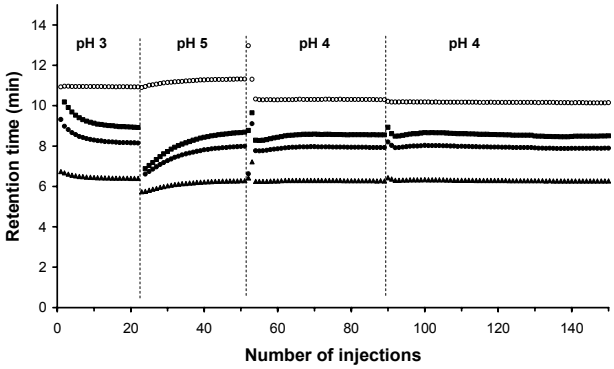

Figure 5. The effect of the pH of the preconditioning mobile phase on the retention of dFdU (O), dFdUMP(▲), dFdUDP(●) and dFdUTP(■). Experiments were performed on four separate days, as indicated by the dotted lines.

Table 4. Retention times of dFdC, dFdU and their nucleotides on a PGC column at different moments during method development.

Description	dFdC	dFdU	dFdCMP	dFdUMP	dFdCDP	dFdUDP	dFdCTP	dFdUTP
	Retention time (min)							
1 month method development	4.25	6.50	8.09	9.11	10.42	11.35	11.34	11.98
4 months method development	4.35	6.16	4.07	4.28	4.33	4.48	4.43	4.58
After oxidation	5.02	6.83	5.58	6.46	7.34	8.79	8.32	9.73
After reduction	4.56	6.16	3.92	4.12	4.17	4.28	4.27	4.43

pH considerations

The pH of the mobile phase had a significant effect on the retention of the polar analytes. The pH affects the degree of ionization of both the analyte and HCO_3^- ions. In this way the pH also influences the retention of analytes and strength of eluting ions. Additionally, the pH has an effect on PGC, which became apparent after preconditioning the column with mobile phases of different pH and after injecting acid solutions.

The effect of pH on the PGC enables the column to be used in different ways, similar to weak ion-exchange chromatography [13]. Firstly, elution of analytes is possible by using a pH gradient. Analytes can be loaded onto the column at a low pH and eluted from the column at high pH. A second approach is to control the electronic interaction capacity of the PGC by controlling the pH. At high pH values the PGC has a low electronic interaction capacity, and only low concentrations of eluting ion are required to elute the analytes from the column, thereby reducing ion suppression with MS detection.

Most likely the injections with diluted CHOOH and the preconditioning of the column at pH 4 before starting an analytical run are not required if the pH of mobile phase A is lowered. However, HCO_3^- is not stable in an acidic environment in which it reacts to form CO_2 and H_2O. If the pH of mobile phase A would be lowered, large volumes of CO_2 gas would be formed upon mixing of mobile phase A with mobile phase B. To prevent formation of CO_2 upon injecting diluted CHOOH the developed gradient ends with 3 minutes 0 % mobile phase B. Possibly other, acid-stable, eluting ions can be used as well, enabling the use of the pH effect to its full extent.

Conclusion

An LC-MS/MS method for the separation of dFdC and dFdU and their mono-, di- and triphosphates has been developed. In contrast to previously published methods, the analytes are completely separated within 15 minutes. Injections of a volume of 100 µL diluted CHOOH resulted in fast recovery of column properties after running a gradient where otherwise long re-equilibration was required. The effect is based on the acidity of the CHOOH, although the exact mechanism, through alteration of the redox state or another mechanism, remains unclear. The redox state and pH were also found to be of extreme importance for stable retention of the nucleotides and were controlled using a pH buffered H_2O_2 solution. Although the importance of controlling the redox state of PGC columns was stressed before [32;33], no applications have been described putting theory into practice. The retention of the nucleosides is governed by the amount of organic modifier, whereas the retention of the nucleotides is controlled by the amount of eluting ion. Using the described chromatographic system a bioanalytical assay for the analytes can be developed. With minor adjustments, the developed method may not only be applicable to other cytidine analogs with uridine metabolites like cytarabine and PSI-6130 but also to purine nucleosides and their nucleotides.

References

[1] W. Plunkett, P. Huang, Y. Z. Xu, V. Heinemann, R. Grunewald, V. Gandhi, Semin. Oncol. 22 (1995) 3.

[2] S. A. Veltkamp, D. Pluim, M. A. van Eijndhoven, M. J. Bolijn, F. H. Ong, R. Govindarajan, J. D. Unadkat, J. H. Beijnen, J. H. Schellens, Mol. Cancer Ther. 7 (2008) 2415.

[3] S. A. Veltkamp, D. Pluim, O. van Tellingen, J. H. Beijnen, J. H. Schellens, Drug Metab Dispos. 36 (2008) 1606.

[4] S. A. Veltkamp, R. S. Jansen, S. Callies, D. Pluim, C. M. Visseren-Grul, H. Rosing, S. Kloeker-Rhoades, V. A. Andre, J. H. Beijnen, C. A. Slapak, J. H. Schellens, Clin. Cancer Res. 14 (2008) 3477.

[5] J. Lai, J. Wang, Z. Cai, J. Chromatogr. B 868 (2008) 1.

[6] T. King, L. Bushman, P. L. Anderson, T. Delahunty, M. Ray, C. V. Fletcher, J. Chromatogr. B 831 (2006) 248.

[7] R. L. Claire, III, Rapid Commun. Mass Spectrom. 14 (2000) 1625.

[8] T. Hawkins, W. Veikley, R. L. Claire, III, B. Guyer, N. Clark, B. P. Kearney, J. Acquir. Immune. Defic. Syndr. 39 (2005) 406.

[9] J. E. Vela, L. Y. Olson, A. Huang, A. Fridland, A. S. Ray, J. Chromatogr. B 848 (2007) 335.

[10] A. Pruvost, F. Becher, P. Bardouille, C. Guerrero, C. Creminon, J. F. Delfraissy, C. Goujard, J. Grassi, H. Benech, Rapid Commun. Mass Spectrom. 15 (2001) 1401.

[11] E. N. Fung, Z. Cai, T. C. Burnette, A. K. Sinhababu, J. Chromatogr. B 754 (2001) 285.

[12] F. Becher, D. Schlemmer, A. Pruvost, M. C. Nevers, C. Goujard, S. Jorajuria, C. Guerreiro, T. Brossette, L. Lebeau, C. Creminon, J. Grassi, H. Benech, Anal. Chem. 74 (2002) 4220.

[13] G. Shi, J. T. Wu, Y. Li, R. Geleziunas, K. Gallagher, T. Emm, T. Olah, S. Unger, Rapid Commun. Mass Spectrom. 16 (2002) 1092.

[14] S. A. Veltkamp, M. J. Hillebrand, H. Rosing, R. S. Jansen, E. R. Wickremsinhe, E. J. Perkins, J. H. Schellens, J. H. Beijnen, J. Mass Spectrom. 41 (2006) 1633.

[15] R. S. Jansen, H. Rosing, C. J. de Wolf, J. H. Beijnen, Rapid Commun. Mass Spectrom. 21 (2007) 4049.

[16] S. U. Bajad, W. Lu, E. H. Kimball, J. Yuan, C. Peterson, J. D. Rabinowitz, J. Chromatogr. A 1125 (2006) 76.

[17] T. Zhou, C. A. Lucy, J. Chromatogr. A 1187 (2008) 87.

[18] C. Antonio, T. Larson, A. Gilday, I. Graham, E. Bergstrom, J. Thomas-Oates, J. Chromatogr. A 1172 (2007) 170.

[19] J. Xing, A. Apedo, A. Tymiak, N. Zhao, Rapid Commun. Mass Spectrom. 18 (2004) 1599.

[20] R. L. Cordell, S. J. Hill, C. A. Ortori, D. A. Barrett, J. Chromatogr. B 871 (2008) 115.

[21] J. Knox, B. Kaur, G. R. Millward, J. Chromatogr. 352 (1986) 3.

[22] C. K. Lim, Adv. Chromatogr. 32 (1992) 1.

[23] T. Hanai, J. Chromatogr. A 989 (2003) 183.

[24] P. Ross and J. H. Knox, in E. Grushka and P. R. Brown (Editors), Advances in chromatography, Marcel Dekker Inc, New York, 1997, p. 73.

[25] G. H. Gu, C. K. Lim, J. Chromatogr. 515 (1990) 183.

[26] T. Takeuchi, T. Kojima, T. Miwa, J. High Resolut. Chromatogr. 23 (2000) 590.

[27] Y. Q. Xia, M. Jemal, N. Zheng, X. Shen, Rapid Commun. Mass Spectrom. 20 (2006) 1831.

[28] C. Elfakir, M. Dreux, J. Chromatogr. A 727 (1996) 71.

[29] M. Shibukawa, A. Unno, T. Miura, A. Nagoya, K. Oguma, Anal. Chem. 75 (2003) 2775.

[30] K. Saitoh, K. Koichi, F. Yabiku, Y. Noda, M. D. Porter, M. Shibukawa, J. Chromatogr. A 1180 (2008) 66.
[31] S. Rinne, A. Holm, E. Lundanes, T. Greibrokk, J. Chromatogr. A 1119 (2006) 285.
[32] M. Shibukawa, H. Terashima, H. Nakajima, K. Saitoh, Analyst 129 (2004) 623.
[33] A. Tornkvist, K. E. Markides, L. Nyholm, Analyst 128 (2003) 844.
[34] P. Chaimbault, K. Petritis, C. Elfakir, M. Dreux, J. Chromatogr. A 870 (2000) 245.
[35] T. Okamoto, A. Isozaki, H. Nagashima, J. Chromatogr. A 800 (1998) 239.
[36] M. Gennaro, E. Marengo, V. Gianotti, J. Liq. Chromatogr. Related Technol. 23 (2000) 2599.
[37] H. Nagashima, T. Okamoto, J. Chromatogr. A 855 (1999) 261.
[38] S. D. Chambers, C. A. Lucy, J. Chromatogr. A 1176 (2007) 178.
[39] J. Knox, Q. Wan, Chromatographia 42 (1996) 83.
[40] C. Elfakir, P. Chaimbault, M. Dreux, J. Chromatogr. A 829 (1998) 193.
[41] J. P. Mercier, P. Morin, M. Dreux, A. Tambute, J. Chromatogr. A 849 (1999) 197.
[42] S. Mazan, G. Cretier, N. Gilon, J. M. Mermet, J. L. Rocca, Anal. Chem. 74 (2002) 1281.
[43] A. Antonopoulos, P. Favetta, W. Helbert, M. Lafosse, J. Chromatogr. A 1147 (2007) 37.
[44] A. Antonopoulos, B. Herbreteau, M. Lafosse, W. Helbert, J. Chromatogr. A 1023 (2004) 231.
[45] Y. Asakawa, N. Tokida, C. Ozawa, M. Ishiba, O. Tagaya, N. Asakawa, J. Chromatogr. A 1198-1199 (2008) 80.
[46] T. Oguma, S. Tomatsu, A. M. Montano, O. Okazaki, Anal. Biochem. 368 (2007) 79.
[47] N. G. Karlsson, B. L. Schulz, N. H. Packer, J. M. Whitelock, J. Chromatogr. B 824 (2005) 139.
[48] R. P. Estrella, J. M. Whitelock, N. H. Packer, N. G. Karlsson, Anal. Chem. 79 (2007) 3597.
[49] M. Pabst, F. Altmann, Anal. Chem. 80 (2008) 7534.
[50] A. Antonopoulos, P. Favetta, M. Lafosse, W. Helbert, J. Chromatogr. A 1059 (2004) 83.
[51] P. Koivisto, M. Stefansson, Chromatographia 57 (2003) 37.
[52] A. Tornkvist, S. Nilsson, A. Amirkhani, L. M. Nyholm, L. Nyholm, J. Mass Spectrom. 39 (2004) 216.
[53] L. M. Ponton, M. D. Porter, J. Chromatogr. A 1059 (2004) 103.

Chapter 2.5

Simultaneous quantification of 2′-2′-difluoro-deoxycytidine and 2′-2′-difluoro-deoxyuridine nucleosides and nucleotides in white blood cells using porous graphitic carbon chromatography coupled with tandem mass spectrometry

Robert S Jansen, Hilde Rosing, Jan HM Schellens and Jos H Beijnen

Submitted for publication

Abstract

A novel assay for the simultaneous quantification of the widely used anticancer agent 2'-2'-difluoro-deoxycytidine (gemcitabine; dFdC), its deaminated metabolite 2'-2'-difluoro-deoxyuridine (dFdU) and their mono-, di- and triphosphates (dFdCMP, dFdCDP, dFdCTP, dFdUMP, dFdUDP and dFdUTP) in peripheral blood mononuclear cells (PBMCs) is described. Separation of all 8 compounds was achieved within 15 minutes using a porous graphitic carbon column (Hypercarb) with a gradient from 0 to 25 mM ammonium bicarbonate in acetonitrile-water (15:85, v/v). Calibration ranges in PBMC lysate from 4.29 to 429, 29.0 to 2900, 31.4 to 3140 and 36.9 to 3690 nM for dFdC, dFdCMP, dFdCDP and dFdCTP and from 42.1 to 4210, 25.4 to 2540, 43.2 to 4320 and 52.7 to 5270 nM for dFdU, dFdUMP, dFdUDP and dFdUTP, respectively, were validated. Accuracies were within 80.0-120 % at the lower limit of quantification (LLOQ) and the precisions were less than 20.0 %. At the other tested levels accuracies were within 85.0-115 % and precisions less than 15.0 %. Mixtures of $^{13}C,^{15}N_2$-labeled dFdC and dFdU nucleotides were synthesized and used as internal standards. Whole blood samples showed extensive ongoing dFdC metabolism when stored at room temperature, but not on ice-water, which made the addition of enzyme inhibitors unnecessary. Stock solutions and samples were stable under all analytically relevant conditions. The method was successfully applied to clinical samples.

Introduction

Gemcitabine (2′-2′-difluorodeoxycytidine, dFdC, figure 1) is a nucleoside analog 2′-, 2′-Difluoro-deoxycytidine (dFdC, gemcitabine, Figure 1) is a pyrimidine nucleoside analog widely used in the therapy of various solid tumors. In whole blood, dFdC is rapidly deaminated by cytidine deaminase (CDA) to 2′-, 2′-difluoro-deoxyuridine (dFdU, Figure 1), which is relatively inactive [1;2]. dFdC is, however, also taken up into cells where it is phosphorylated into its mono-, di- and triphosphate (dFdCMP, dFdCDP and dFdCTP). dFdCDP inhibits ribonucleotide reductase, whereas dFdCTP inhibits DNA synthesis and causes cell death [3].

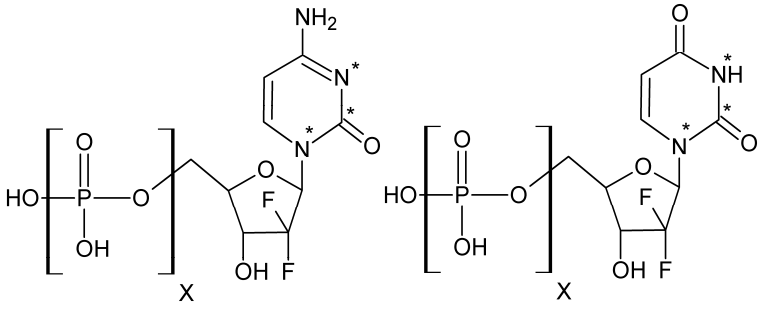

Figure 1. Chemical structures of the nucleosides dFdC and dFdU (X=0), and their mono- (X=1), di- (X=2) and triphosphates (X=3). The asterisks indicate the position of ^{13}C- and ^{15}N-atoms in the internal standards.

Recently the formation of the mono-, di- and triphosphate of dFdU (dFdUMP, dFdUDP and dFdUTP) was discovered [2;4;5]. These nucleotides can be formed by direct phosphorylation of dFdU, or via deamination of dFdCMP by deoxycytidine monophosphate deaminase (dCMPD) and subsequent phosphorylation. The metabolism of dFdC is depicted in Figure 2. dFdUMP is a thymidylate synthase inhibitor [6] and dFdUTP is incorporated into DNA and RNA [2]. Monitoring dFdC, dFdU and their metabolites in cells is pivotal to improve the understanding of the complex intracellular pharmacology of dFdC and may shed more light on the role of the dFdU metabolites in dFdC therapy.

The determination of low levels of nucleotides is, however, analytically challenging. For many years, anion-exchange and ion-pairing methods have been applied to separate nucleosides and nucleotides. However, the use of salts and ion-pairing agents with low volatility hampers their direct application with MS detection.

Both indirect and direct methods that circumvent this problem have been developed [7].

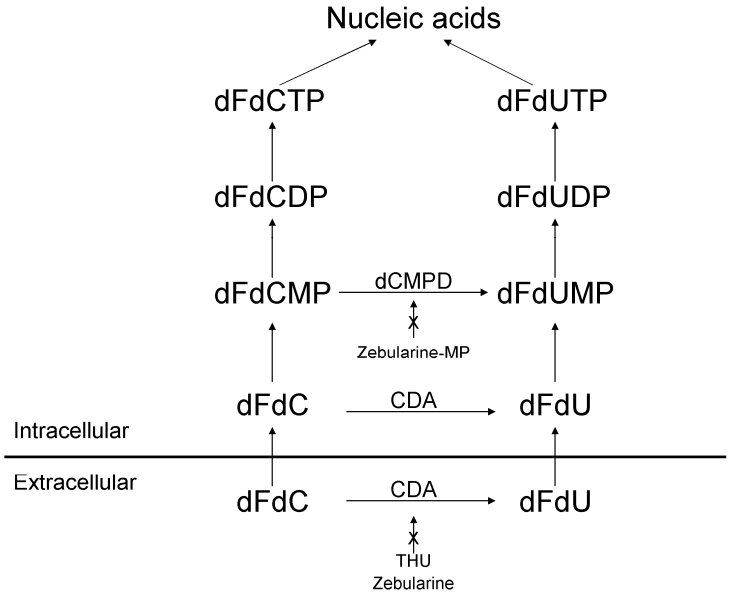

Figure 2. Schematic representation of the metabolism of dFdC.

Indirect methods consist of a dephosphorylation step, after which the obtained nucleoside has been quantified using a radioimmunoassay (RIA) [8;9], liquid chromatography with ultraviolet (LC-UV) [10;11] or mass spectrometric (LC-MS) [12;13] detection.

Several direct approaches have been developed. Weak anion exchange liquid chromatography (WAXLC) with a pH gradient [14-16] and methods using volatile [17-23], or low levels of involatile, ion-pairing agents [24-26] have been applied for the analysis of nucleotides with MS detection. Separations of nucleosides and nucleotides using porous graphitic carbon (PGC) [27-29] and titania [30] columns have also been described.

Although many methods to quantify dFdCTP in cells have been published [2;15;31-36], only three have been thoroughly validated [15;32;33]. dFdCTP has been quantified in PBMCs using anion exchange liquid chromatography [32] and simultaneous determination of dFdCDP and dFdCTP was achieved using an ion-pairing method [33]. Both methods, however, employed UV detection and have high lower limits of quantification (LLOQ) (dFdCTP: 0.4 µM [32]; dFdCDP: 0.31 µM and dFdCTP: 0.46 µM [33], respectively). A sensitive WAXLC-MS/MS assay with an LLOQ of 2.0 nM was developed and validated in our laboratory for the quantification of dFdCTP in PBMCs [15].

None of these methods, however, describe the simultaneous quantification of dFdC, and its mono-, di- and triphosphate nucleotides, let alone in combination with dFdU and its mono-, di- and triphosphate forms. dFdC and dFdU differ only 1 amu in molecular weight and share a similar fragmentation pattern. A dFdC molecule containing a naturally occurring ^{13}C- or ^{15}N-isotope (about 11 % of the dFdC molecules) will

therefore have the same parent mass as dFdU and produce a signal in the dFdU mass transition. Consequently, the same is true for dFdCMP-dFdUMP, dFdCDP-dFdUDP and dFdCTP-dFdUTP. Moreover up-front fragmentation of higher phosphates into lower phosphates causes interfering signals when higher phosphates elute. Because the analytes can not be fully distinguished with the MS, chromatographic separation of the analytes is crucial. Separation of the analytes is, however, particularly demanding because of the large difference in polarity of the analytes on the one hand, and the great similarities between dFdC and dFdU congeners on the other hand.

Although separation of cytidine and uridine nucleosides and nucleotides has been achieved with selected MS compatible PGC [27], HILIC [37] and ion-pairing methods [38], most require long run times without, or only marginally, achieving base-line separation.

Here we present a new method capable of separating and quantitating dFdC, dFdU and their nucleotides in PBMCs in a single analytical run. PGC is known for its ability to separate very similar analytes such as diastereomers [39], as well as very dissimilar analytes such as positive and negative ions [40]. PGC is, however, also notorious for its unpredictable and non-reproducible retention properties [41-45].

Nevertheless, a PGC column was selected on which the nucleotides were separated and eluted with an ammonium bicarbonate (NH_4HCO_3) gradient, whereas the nucleosides were separated and eluted with isocratic acetonitrile (CH_3CN). By controlling the redox state of the PGC, in combination with proper column cleaning, we were able to obtain a reproducible separation [46]. To achieve an optimal assay performance we synthesized a mixture of stable isotope-labeled nucleotides from ^{13}C, $^{15}N_2$-labeled dFdC and dFdU to serve as internal standards.

In summary, this is the first publication describing the validation of a method for the simultaneous quantification of dFdC, dFdU and their mono-, di- and triphosphate in PBMCs using a PGC column and MS/MS detection. Moreover, the first data on the combined concentrations of these analytes in PBMCs from a patient receiving dFdC are presented.

Experimental

Chemicals

dFdC hydrochloride, dFdCMP, dFdCDP dFdCTP, dFdU, dFdUMP, dFdUDP and dFdUTP were kindly provided by Eli lilly and company (Indianapolis, IN, USA). Stable isotope (^{13}C, $^{15}N_2$) labeled dFdC and dFdU (Figure 1) were obtained from Toronto Research Chemicals (North York, Canada). Tetrahydrouridine (THU) and zebularine were from Calbiochem (Darmstadt, Germany). Methanol (CH_3OH) and acetonitrile (CH_3CN) were obtained from Biosolve Ltd (Amsterdam, The Netherlands) and distilled water (H_2O) was obtained from B Braun (Melsungen, Germany). Ficoll-Paque plus density gradient was purchased from GE Healthcare (Chalfont St. Giles, United Kingdom) and cell preparation tubes (CPTs) (BD Vacutainer CPT) were from BD (Franklin lakes, NJ, USA). All other solvents or chemicals were of analytical grade or better and originated from Merck (Darmstadt, Germany).

Synthesis of nucleotides

Mixtures of ^{13}C,$^{15}N_2$-labeled dFdC (*dFdC, *dFdCMP, *dFdCDP and *dFdCTP) and dFdU (*dFdU, *dFdUMP, *dFdUDP and *dFdUTP) internal standards (ISs) were synthesized from *dFdC and *dFdU. About 50 µmoles of nucleoside were dissolved in 2.5 mL trimethylphosphate. dFdC hydrochloride required gentle heating over a flame to dissolve. Proton sponge (1,8-bis(dimethylamino)naphthalene) (100 µmoles) was added and the mixture was cooled on ice. A large excess (16 equivalents) of phosphorous oxychloride was then added dropwise after which the mixture was stirred at room temperature for 3.5 (*dFdC) and 7 (*dFdU) hours. After adding an excess (20 equivalents) of cold tributylammonium phosphate and tributylamine (250 µM in dimethylformamide), the reaction mixture was poured into 15 mL cold 1 M triethylammonium bicarbonate. The solution was lyophilized and then dissolved in water before storage at -70°C.

Reference standards

Because the HPLC-UV system is isocratic and nucleosides have the same chromophore as its nucleotides, we could quantitate the nucleotide stock solutions based on the nucleoside stocks with known concentrations [16].
HPLC-UV analysis of the synthesized IS mixtures showed that the *dFdC nucleotides mixture contained 318, 411, 483 and 562 µM *dFdC, *dFdCMP, *dFdCDP and *dFdCTP respectively. Likewise, the *dFdU nucleotides mixture contained 350, 194, 175 and 259 µM *dFdU, *dFdUMP, *dFdUDP and *dFdUTP respectively. Other reaction products were observed on the HPLC-UV system, but did not interfere with the LC-MS/MS analysis. As expected, the ISs eluted at the exact same time as the analytes (not shown). No signal was observed in the analyte windows upon elution of

their labeled IS, indicating sufficient isotopic purity. The main impurities found in the unlabeled nucleotide stocks were 8.53 and 3.37 % diphosphate peaks of the dFdCTP and dFdUTP peak areas respectively and 1.99 and 0.85 % monophosphate peaks of the dFdCDP and dFdUDP peak areas respectively.

Instrumentation

HPLC-UV experiments were performed on an Agilent 1100 series liquid chromatograph system (Agilent technologies, Palo Alto, CA, USA) consisting of a binary pump, an in-line degasser, autosampler, column oven and UV detector. Data were acquired using Chromeleon 6.50 software (Dionex corp., Sunnyvale, CA, USA).

The mobile phase consisted of 10 mM tetrabutylammonium dihydrogenphosphate with 70 mM potassium dihydrogen phosphate in CH_3OH-H_2O (16:84, v/v) and was delivered isocratically to a Synergi hydro-RP column (150 X 2.0 mm ID, 4 µm particles; Phenomenex, Torrance, CA, USA) with a flow of 0.25 mL/min. A volume of 10 µL was injected using the autosampler thermostated at 4 °C. Absorption was measured at 268 nm (dFdC) and 258 nm (dFdU) during 30 minutes.

LC-MS/MS experiments were performed using a Thermo Fischer TSQ Quantum Ultra mass spectrometer (Thermo Fisher Scientific Inc, Waltham, MA, USA) with a Shimadzu LC system (Shimadzu, Kyoto, Japan) consisting of a SIL-HTc autosampler with SCL-10A^{vp} systemcontroller, two LC20-AD Prominence pumps, a FCV-11AL valve unit, a DGU-20A5 in-line degasser unit and a CTO-20AC column oven. Ionization was performed using the electrospray ionization (ESI) source equipped with a metal needle to which 4500 V was applied in both the positive and the negative ion mode. The sheath and auxiliary were set at 49 and 25 arbitrary units (au) respectively with the ion sweep gas set at 2.0 au (all N_2). The capillary temperature was set at 300°C and the collision gas (argon) at 0.5 mTorr. Scans of 50 ms were performed at unit resolution. The compound dependent scan parameters are shown in Table 1. Data were acquired using Xcalibur 2.0 software and processed using LCQuan 2.5 software (Thermo Fisher Scientific Inc., Waltham, MA, USA).

A Hypercarb column (100 X 2.1 mm ID, 5 µm particles, Thermo Fisher Scientific Inc, Waltham, MA, USA) was equipped with a Hypercarb guard column (10 X 2.1 mm ID, 5 µm) to protect the analytical column and was thermostated at 45 °C. Before an analytical run (about 60 samples) the column was treated (30 minutes, 0.25 mL/min) with preconditioning buffer consisting of 1 mM ammonium acetate (NH_4CH_3COO) in CH_3CN-H_2O (15:85, v/v) with 0.05 % hydrogen peroxide (H_2O_2) and with the pH adjusted to 4 with glacial acetic acid (CH_3COOH). The autosampler needle was rinsed before and after aspiration with 200 µL CH_3OH. After the injection of 25 µL sample, gradient chromatography was started. Mobile phase A consisted of 1 mM NH_4CH_3COO in CH_3CN-H_2O (15:85, v/v) with the pH adjusted to 5 with glacial CH_3COOH. Mobile phase B consisted of 25 mM ammonium

bicarbonate (NH_4HCO_3) in CH_3CN-H_2O (15:85, v/v). The mobile phases were delivered at a flow of 0.25 mL/min with the following gradient: 0-0.1 min: 0 % B, 0.1-2.0 min: 0-100 % B, 2.0-12 min: 100 % B, 12-15 min: 0 % B. During the first 4.5 minutes the eluate was directed to waste. Between each analytical injection 100 µL diluted CHOOH (10 % in H_2O, v/v; 2.65 M) was injected in a flow of 0 % B with the column outlet directed to the waste for 5 minutes. After each analytical batch the column was back-flushed with about 20 column volumes tetrahydrofuran before storage on mobile phase A.

Table 1. Scan parameters of the TSQ Quantum Ultra triple quadrupole mass spectrometer.

Compound	Parent ion (m/z)	Product ion (m/z)	Skimmer offset (V)	Tube lens offset (V)	Collision energy (V)	Polarity
dFdC	264	112	18	87	17	+
*dFdC	267	115	18	87	17	+
dFdU	263	111	14	52	20	-
*dFdU	266	114	14	52	20	-
dFdCMP	344	246	15	119	17	+
*dFdCMP	347	249	15	119	17	+
dFdUMP	345	247	21	101	18	+
*dFdUMP	348	250	21	101	18	+
dFdCDP	424	326	16	128	14	+
*dFdCDP	427	329	16	128	14	+
dFdUDP	425	327	14	140	13	+
*dFdUDP	428	330	14	140	13	+
dFdCTP	504	326	14	140	26	+
*dFdCTP	507	329	14	140	26	+
dFdUTP	505	247	10	146	28	+
*dFdUTP	508	250	10	146	28	+

Preparation of stock and working solutions

Stock solutions of dFdC, dFdCMP, dFdCDP, dFdCTP, dFdU, dFdUMP, dFdUDP and dFdUTP were prepared at 1 mg/mL in water. Nucleoside stocks were prepared in duplicate and the nucleotide stocks in singular. The content and purity of all nucleotide standards were determined in three-fold on the HPLC-UV system using nucleoside reference standards. One mixture of the stocks was prepared for the calibration standards (CALs) and one for the preparation of the validation- and stability samples (VSs and SSs). For the preparation of SSs working solutions were prepared from stock solution containing only one analyte. All solutions were further diluted in H_2O to obtain working solutions. The synthesized mixtures of labeled IS were quantitated likewise and diluted in water to 12.7, 16.4, 19.3, 22.5, 28.0, 15.5, 14.0 and 20.7 µM for *dFdC, *dFdCMP, *dFdCDP, *dFdCTP, *dFdU, *dFdUMP, *dFdUDP and *dFdUTP respectively (IS working solution). All solutions were stored at -70 °C.

Stability during sample collection

Whole blood (citrate phosphate dextrose anticoagulated) from a single healthy donor was incubated with 10 µM dFdC at 37°C for 1.5 hour. Aliquots of 8 mL whole blood were transferred to CPTs, stored at room temperature and centrifuged (without cooling, for 20 minutes at 1,700 g) directly and after 0.5, 1, and 3 hours (singular). Furthermore, aliquots of 14 mL of the incubated whole blood were transferred to tubes on ice containing 150 µL H_2O, THU (10 mg/mL), or zebularine (10 mg/mL). The samples were stored on ice and processed as patient samples directly (3-fold) and after 0.5, 1, and 3 hours (singular). From these samples plasma was also collected in which dFdC and dFdU was determined using a previously published method [47]. Erythrocytes were collected from a single sample processed at time zero.

Isolation and lysis of PBMCs

The PBMCs were isolated and processed to a cell pellet as described previously [15]. In brief, a buffy coat collected from whole blood (15 mL) was resuspended in phosphate buffered saline (PBS) and layered over Ficoll-Paque plus density gradient. After centrifugation the PBMCs were collected and washed with PBS. The thus obtained pellet was resuspended in 70 µL PBS and a 10 µL aliquot was taken for a cell count using a haematology analyser (Cell-Dyn 1700; Abbott Diagnostics, Abbott Park, IL, USA) or a DNA assay with Hoechst 33258 (Bio-Rad DNA quantitation kit). A 60 µL-aliquot of the remaining cell suspension was added to 140 µL cold CH_3OH, vortex mixed for 1 minute and stored as a suspension at -70 °C until analysis. Alternatively, samples lysed with perchloric acid ($HClO_4$) as described previously [15] could be used. A 100 µL aliquot of the $HClO_4$ lysate was treated with 5 µL 47 % KOH solution upon which a $KClO_4$ precipitate was formed. The sample was then centrifuged at 23,100 g for 10 minutes and the supernatant was stored at -70 °C.

For the preparation of blanks, blank human leukocyte buffy coat (Sanquin, Amsterdam, the Netherlands) from 500 mL whole blood was diluted to 500 mL with PBS and further treated as whole blood. The obtained blank PBMC suspension was diluted to 70-75 X 10^6 PBMCs/mL with PBS before lysis. The thus obtained blank lysate suspension was either stored as such (blank PBMC lysate suspension for the stability samples and the partial validation in PBMC lysate suspension) or centrifuged for 5 minutes at 23,100 g after which the supernatant was transferred to new containers (blank PBMC lysate supernatant). All blanks were stored at -70 °C.

Spiking of calibration standards, validation samples and stability samples

Eight non-zero CALs and VSs at the LLOQ, low, mid and high level (Table 2) were freshly prepared in blank PBMC lysate supernatant before each analytical run. SSs were prepared separately for each analyte at the mid

level by spiking 3 mL blank PBMC lysate suspension with aqueous working solution (1 % or less of the total volume). Aliquots of 100 µL of these solutions were stored at the test conditions and treated as unknowns before processing/analysis. Dilution samples were prepared in blank PBMC lysate suspension at a concentration of 5 times the upper limit of quantification (ULOQ). Samples were diluted ten times with blank PBMC lysate supernatant before analysis.

Sample processing

Unknowns and blank lysates were kept on ice-water and vortex mixed for 10 seconds. To 90 µL of the supernatant or suspension, 10 µL of working solution (CALs and VSs) or H_2O (unknowns) was added. After the addition of 5 µL IS working solution the samples were vortex mixed, centrifuged for 5 minutes at 23,100 g, and transferred to an autosampler vial. The loss of volume when mixing the PBS and CH_3OH (60 µL cell suspension plus 140 µL CH_3OH results in an end volume which is 97 % of the sum of both volumes) was corrected for when determining the concentrations in patient samples. The analytical result, expressed as nM in PBMC lysate, was finally multiplied with the total lysate sample volume (194 µL) to obtain the absolute amount of the analytes. This amount, originally present in 60 µL cell suspension in PBS was then divided by six times the amount of cells present in 10 µL of the same cell suspension to obtain the amount of analyte per 10^6 PBMCs.

Validation procedures

Matrix effect and recovery

Suspensions containing 0, 75, 150, 300 and 600 X 10^6 cells/mL were prepared in PBS using PBMCs freshly isolated from a single donor buffy coat . Aliquots of 50 µL of these suspensions were spiked with 10 µL PBS (post-lysis spike) or working solution (pre-lysis spike) containing all analytes in PBS (final concentration at the mid level). The suspension containing 150 X 10^6 cells/mL was also spiked at the low and high level. The samples were then lysed with 140 µL CH_3OH and 90 µL of the suspension, or supernatant after centrifugation, was spiked with 10 µL of PBS (pre-lysis spike) or working solution (post-lysis spike). Finally, IS working solution (5 µL) was added to each sample before or after centrifugation, directly preceding the analysis. Each samples was processed and analyzed in triplicate.

Linearity

In agreement with the FDA guidelines for bioanalytical method validation [48], the calibration standards were prepared and analyzed in duplicate in three separate analytical runs. Deviations of the back-calculated concentrations from the nominal concentrations should be within ±15.0 % and within ±20.0 % at the LLOQ. The coefficient of variation should be less

than 20.0 % at the LLOQ level. No more than 33 % of the calibration standards were allowed to be rejected from the calibration curve, which should contain at least one sample at the LLOQ and the ULOQ.

Accuracy and precision

VSs prepared at 4 levels in blank PBMC lysate supernatant were analyzed in three analytical runs (N=5 per run). Additionally, a single run was performed with validation samples prepared at 4 levels in blank PBMC lysate suspension (N=5). The deviations from the nominal concentrations were used to calculate the intra- and inter-assay accuracies. Intra-assay and inter-assay (100 % X (standard deviation of overall mean/overall mean)) coefficients of variation (CVs) were used to assess the precision of the method. All accuracies should be within 85-115 % and CVs should be less than 15.0 % except at the LLOQ where the accuracies should be within 80-120 % and CVs less than 20.0 % according to the FDA guidelines for bioanalytical method validation [48].

To assess the accuracy and precision above the ULOQ, dilution samples prepared at 5-fold the ULOQ were diluted 10-fold with blank PBMC lysate supernatant in 5-fold. The 10-fold dilution was considered validated if the determined concentrations did not deviate more than 15.0 % from the nominal concentration, with CVs of 15.0 % or less.

Specificity and selectivity

Specificity and selectivity were determined using 6 batches of blank PBMC [48]. Double blank (no IS added) samples were checked for interferences. Samples spiked at the LLOQ level were analyzed and the deviation from the nominal concentration was determined, which should be within ±20.0 %.

Carry over

Carry over was assessed by injecting a blank sample after a ULOQ sample. The analyte peak area in the blank should be less than 20.0 % of the peak area of an LLOQ sample. Carry over of the IS should be less than 5.00 % of the IS peak area in a spiked sample.

Stability

Stability of the separate analyte stock solutions was assessed by storing three aliquots of each stock at 20-25 °C for 24 hours. Long term stability (-70°C) was determined by re-assaying the stock solutions using the HPLC-UV method described in the experimental section. Stock solutions were considered stable if the determined concentrations did not deviate more than ±5 % from the concentration determined at time zero.

Stability in blank PBMC lysate supernatant was determined after 5 hours on ice-water. Reinjection reproducibility of the processed samples was assessed by reinjecting the calibration and stability samples after 24 hours

in the autosampler (4 °C). Analytes were considered stable in biomatrix if the determined concentrations did not deviate more than ±15.0 % from the concentration determined at time zero.

Application of the assay

The described method was applied to samples obtained from a patient with ovarian cancer at the end of, and 1, 2, 8 and 24 hours after a 450 mg/m^2 intravenous dFdC infusion over 45 minutes. Analytes were extracted from PBMCs using $HClO_4$, and the number of cells isolated was determined using DNA quantitation.

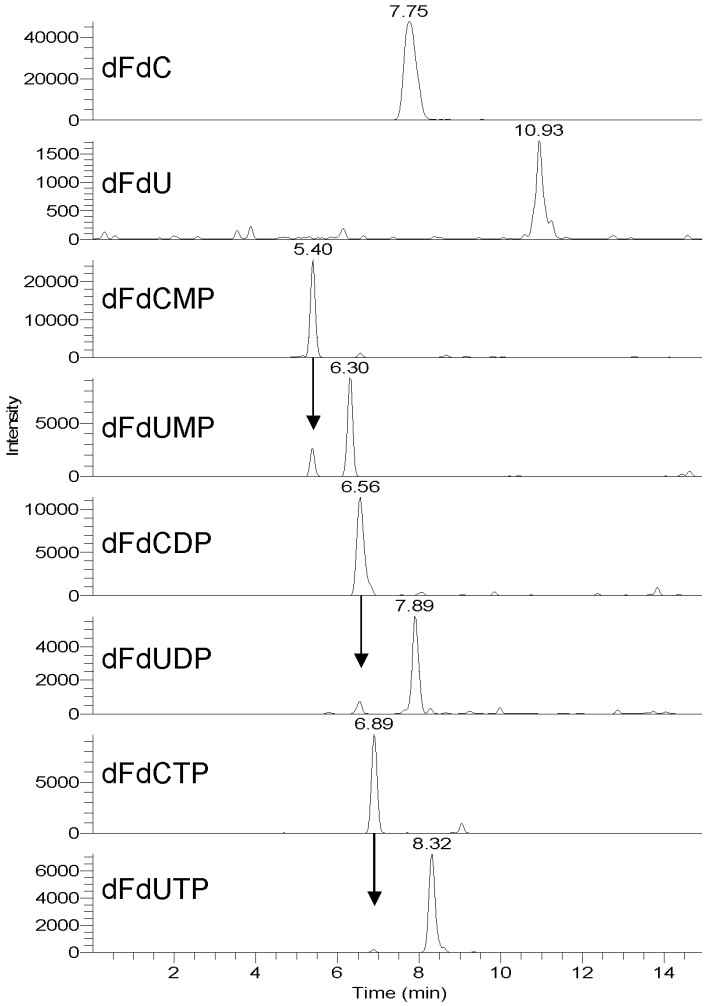

Figure 3. Representative chromatograms of a calibration sample at the LLOQ, containing dFdC (4.29 nM), dFdU (42.1 nM), dFdCMP (29.0 nM), dFdUMP (25.4 nM), dFdCDP (31.4 nM), dFdUDP (43.2 nM), dFdCTP (36.9 nM) and dFdUTP (52.7 nM). The arrows indicate the signals of dFdC nucleotides (containing a naturally occurring ^{13}C- or ^{15}N-isotope) in the mass transitions of the dFdU nucleotides.

Results and discussion

Chromatography

Using the conditions described in the experimental section, all 8 analytes were separated within 15 minutes. Representative chromatograms of the analytes at the LLOQ level are depicted in Figure 3. The signals of dFdC nucleotides containing a ^{13}C or ^{15}N atom are clearly visible in the chromatograms of the dFdU nucleotides, but do not interfere with the quantification. The exceptional separation capabilities of the column were maintained by treating the column with H_2O_2 before each run and by injecting formic acid onto the column between each injection. The retention times of the analytes are determined by hydrophobic and electronic interactions [46]. All charged compounds will most likely be eluted from the column using the described gradient. With only 15 % CH_3CN in the mobile phase, more hydrophobic compounds will, on the other hand, be retained on the column and can slowly elute during later injections. The ion-suppression can thus be variable during the analysis of multiple samples. However, with stable isotope labeled ISs and proper column care, the system is reproducible and robust as shown by the presented validation.

Mass spectrometry

MS detection was performed in the positive ionization mode for all analytes except dFdU. Positive ionization, although counter-intuitive for these phosphoric acids, has been performed in nucleotide analysis before [16;21;24]. It has been suggested that the presence of an amino function causes this effect [21]. The fact that the dFdU nucleotides, which lack an amino function, could also be detected sensitively in the positive ionization mode does not support this theory. It is remarkable that dFdU gave the most intense signal using the negative ionization mode, whereas its nucleotides, bearing acidic phosphate groups, gave more intense signals in the positive ionization mode. Calculation of the gas-phase proton affinities by others showed that the phosphate group is actually the most likely site of protonation for uridine and thymidine monophosphates and that the proton affinity of some of these monophosphates is higher than that of its nucleoside [49].

Besides a higher sensitivity, the positive ionization mode also provides a higher selectivity against other nucleotides [21]. Nucleotide fragments produced in the negative ionization mode are often (pyro)phosphates, which are the same for every nucleotide. Moreover, the parent mass of nucleotides is often similar. The masses of the *dFdU nucleotides are for example the same as the adenosine-, deoxyguanosine- and zidovudine nucleotides [19]. These compounds would most likely have interfered with the detection if the negative ionization mode had been used.

Stability during sample collection

We assessed the stability of the analytes in whole blood samples to define the conditions under which the samples should be taken and for how long samples could be left before further sample pretreatment should be performed. To obtain a large number of identical samples we incubated whole blood from a single donor with dFdC. These *in vitro* spiked samples were then transferred to tubes containing water or key enzyme inhibitors on ice, or to CPTs at room temperature.

THU is a potent CDA inhibitor that is often applied to stabilize plasma dFdC and dFdU samples [47]. Zebularine is a CDA inhibitor as well, but its intracellularly formed monophosphate also inhibits dCMPD [50]. Moreover, we tested the applicability of CPTs for the cell isolation. Isolation of PBMCs from whole blood is easier, faster and gives higher yields using CPTs compared to isolation using Ficoll. Fast isolation can also be an advantage when analyzing unstable triphosphates [17;18]. CPTs have, therefore, often been used for the analysis of intracellular anti-HIV nucleotides [51]. However, the gel used in CPTs is temperature sensitive which prevents their use under cooled conditions. The samples collected in CPTs were therefore stored and processed at room temperature.

The *in-vitro* spiked samples mainly contained dFdCTP, low levels of dFdCDP and dFdUTP and trace amounts of dFdC (61.5, 6.40, 3.41 and 1.20 pmoles/million cells respectively (mean (N=3) at t=0, without inhibitor). The amount of dFdCTP and dFdUTP per million PBMCs is plotted against the storage time in Figure 4. In the samples stored at room temperature (CPTs) the amount of both triphosphates was relatively high at t=0, and the concentration increased even further upon storage. This increase was most likely caused by dFdC still entering the cell, followed by phosphorylation and deamination.

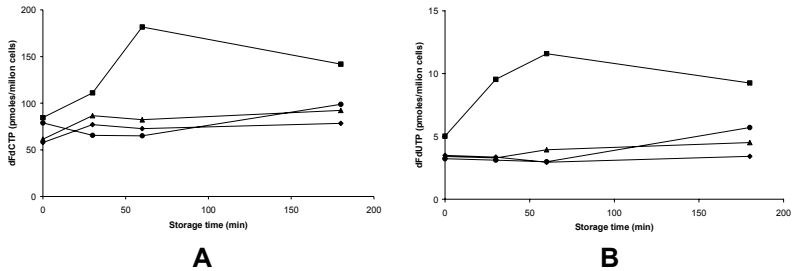

Figure 4. Effect of storage and PBMC isolation conditions and the addition of enzyme inhibitors on the concentration of dFdCTP (A) and dFdUTP (B) in PBMCs. Samples were stored and PBMCs were isolated at room temperature using CPTs, without the addition of an enzyme inhibitor (■), or samples were stored and PBMCs were isolated on ice-water using Ficoll-Paque with no enzyme inhibitor (▲), THU (●) or zebularine (♦). All further sample pretreatment was performed on ice-water.

The increase was much less pronounced when samples were stored on ice-water. The addition of inhibitors did not influence the intracellular nucleotide concentrations when samples were stored and processed on ice-water. Analysis of the plasma samples showed that both THU and zebularine effectively inhibited dFdC deamination into dFdU (1302;912.7 ng/mL without inhibitor, 1577;472.2 ng/mL with THU, and 1692;476.2 ng/mL dFdC;dFdU with zebularine (overall mean, N=6)). The difference of extracellular dFdC and dFdU levels was, however, not reflected by the intracellular analyte levels. Addition of a CDA or dCMPD inhibitor was therefore not necessary.
Another approach to prevent nucleosides from entering the cells is to inhibit the nucleoside transporters facilitating this transport by adding inhibitors like nitrobenzylthioinosine (NBMPR) or dipyridamole. Even with cellular uptake inhibited, other processes might, however, still change intracellular analyte levels. Based on the presented data, we chose to collect and process samples on ice, without addition of an enzyme inhibitor.
Samples with PBMCs isolated from whole blood always contain small amounts of erythrocytes and since phosphorylated nucleoside reverse transcriptase inhibitors (NRTI's) have been detected in erythrocytes [52] we tested for this possible interfering effect. We analysed erythrocytes collected from one of the *in-vitro* spiked samples as PBMCs, but none of the analytes was detected. Therefore, we did not perform an erythrocyte lysis step during PBMC isolation for this assay.

Validation

Matrix effect and recovery

The most important factor determining the matrix effect and recovery is the number of cells in a sample, which should therefore be part of a validation [51]. The number of cells varies per sample because of the different amounts of PBMCs in whole blood and variation in isolation yield. At first IS addition and the post-lysis spike was performed after centrifugation of the suspension obtained after cell lysis. The mean (N=3) analyte concentrations in the post-lysis spiked samples were between -10.2 % and +12.2 % of the nominal concentration for all analytes and all cell amounts. However, the concentrations determined for the pre-lysis spiked samples were only acceptable for the nucleosides and monophosphates, and not for the di- and triphosphates. The determined concentrations decreased with the number of PBMCs in the samples to deviations as high as -87.9 % and -81.9 % for dFdCTP and dFdUTP respectively in the sample with 30 million PBMCs. These determined concentrations of dFdC and its nucleotides are depicted in Figure 5A. Similar results were obtained for dFdU and its nucleotides.
Because all results were acceptable when the analytes were spiked to the supernatant of the centrifuged sample (Figure 5a) we concluded that the

number of PBMCs did not affect the chromatographic separation or MS detection. We reasoned that the loss of analytes spiked before lysis was due to absorption to cell debris. We therefore repeated the experiment but performed the post-lysis spike and IS addition with the cell suspension, before centrifugation of the sample. The loss of analyte could then be corrected for by the loss in ISs. The results for dFdC and its nucleotides are shown in Figure 5C. Although the determined concentration still decreased with an increasing number of cells, the deviations from the cell free results were within 15.0 % for all analytes in samples containing upto 15 million PBMCs. Similar results were obtained at the low and high level. Clinical samples from 16 mL whole blood typically yield 1-10 million PBMCs using the described isolation method.

These experiments show that addition of the IS solution before centrifugation is critical for obtaining accurate results. We chose to assess accuracy and precision over 3 analytical runs using cell-free supernatant for both calibration standards and validation samples. Additionally, we determined the accuracy and precision using cell suspensions for validation samples in a single run.

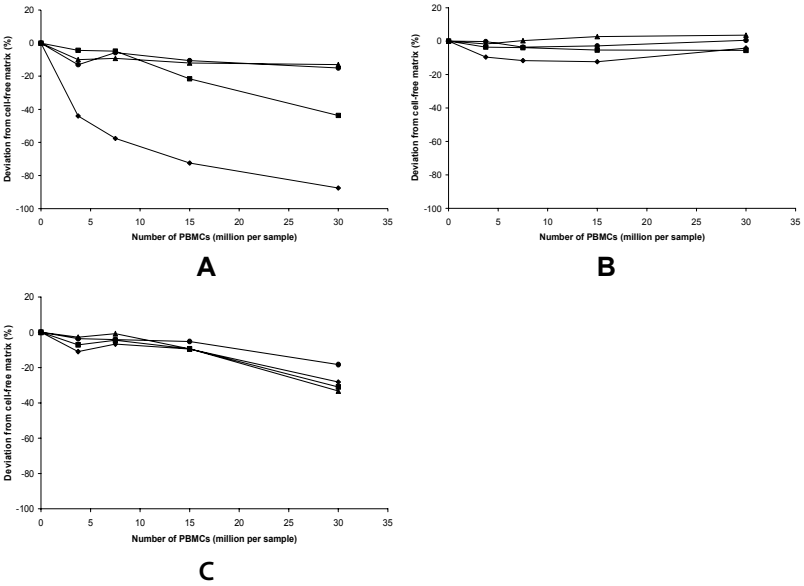

Figure 5. Determined dFdC (●), dFdCMP (▲), dFdCDP (■) and dFdCTP (♦) concentrations in samples containing different numbers of PBMCs. (A) Analytes added before lysis, ISs added after lysis and after centrifugation; (B) Analytes and ISs added after lysis and centrifugation; (C) Analytes added before lysis, ISs added before centrifugation (final condition).

Linearity

Calibration curves were constructed using linear regression of the analyte/IS ratio with a $1/x^2$ weighting factor. The mean accuracies of the back-calculated concentrations did not deviate more than -8.88 % and +13.0 % from the nominal concentrations for all compounds at all levels. Correlation coefficients were 0.991 or higher.

Accuracy and precision

In Table 2 the inter-assay performance using PBMC lysate supernatant is summarized. The intra-assay accuracies at the LLOQ were within 85.3 % and 119 % with a maximum intra-assay precision of 19.7 %. At the other levels the intra-assay accuracies ranged from 92.3 % to 109 % with a maximum intra-assay precision of 14.9 % (data not shown). Table 3 shows the intra-assay performance of the analytes in PBMC lysate suspension. Likewise, all accuracies and precisions were within the acceptance criteria [48].

The determined concentrations in the diluted samples deviated 7.77 % to -15.0 % from the nominal concentrations, with CVs of 11.2 % or lower. A 10-fold dilution of samples was therefore considered validated.

To assess the overall precision of the method (including the cell isolation, cell count, sample pretreatment and the final analysis), the samples to determine the stability during sample pretreatment that were taken at t=0, were processed in triplicate. The variation observed in these samples is the overall precision. The CVs for dFdC, dFdCDP, dFdCTP and dFdUTP were 25.7, 15.8, 3.42 and 15.7 % respectively.

Specificity and selectivity

No interferences were seen in the chromatograms from all blank cell lysates. The accuracies of the analytes spiked at the LLOQ were between 80.1 % and 120 % for all compounds, showing that the selectivity of this assay is satisfactory.

Carry over

Carry over was less than 14.0 % for all analytes and less than 2.28 % for the internal standards. The formic acid injections between analytical runs reduced the carry over that is often observed in nucleotide analyses [16].

Stability

The analytes were stable under the tested conditions as shown in Table 4. Moreover, an increase of lower phosphates caused by dephosphorylation of higher phosphates during storage was not observed in these separately spiked stability samples. Still, analyte levels higher than the levels validated here, might cause measurable concentrations of lower phosphates after degradation [53]. Data from samples containing

extremely high concentrations of analytes should therefore be interpreted with caution.

Application of the assay

In Figure 6 the concentrations of dFdC, dFdU, dFdCDP, dFdCTP and dFdUTP after an intravenous dFdC infusion at a dose of 450 mg/m^2 are presented. The intracellular nucleoside concentrations followed the trend seen in dFdC and dFdU plasma levels [54]: the highest levels of dFdC and dFdU were observed in the sample taken at the end of the dFdC infusion. At later time points only the dFdU concentration was above the LLOQ.

The highest levels of the nucleotides, on the other hand, were measured in the sample collected 2 hours after the end of the infusion. Others have reported peak values within 15 [55] and 30 minutes [54], but also after 1.5 [56] and about 3 hours [33] after the end of the infusion. The dFdUTP:dFdCTP ratio is relatively low compared to the ratio found after prolonged oral administration [4]. Possibly dFdUTP accumulates after multiple dosing. Although clearly present in some samples, dFdCMP, dFdUMP and dFdUDP were below the LLOQ in these samples.

PBMCs are obtained relatively easy, but are a surrogate matrix. This method can, however, also be used to quantify dFdC and its metabolites in tumor tissue. Moreover, the method can be used to determine dFdC, dFdU and their monophosphates, which are extruded from cells by drug efflux pumps, in plasma and urine.

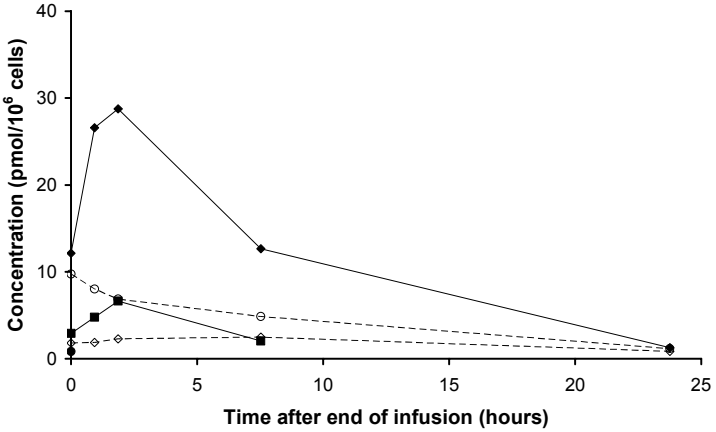

Figure 6. Concentration versus time curves of dFdC (●), dFdU (o), dFdCDP (■), dFdCTP (♦) and dFdUTP (◊) in PBMCs isolated from a patient with ovarian cancer after receiving 450 mg/m^2 dFdC intravenously over 45 minutes. Although peaks were observed, dFdCMP, dFdUMP and dFdUDP were below the LLOQ in these samples.

Table 2. Inter-assay performance data for dFdC, dFdU and their mono-, di- and triphosphate in PBMC lysate supernatant (N=15).

Compound (calibration range)	Nominal concentration (nM)	Inter-assay accuracy (%)	Inter-assay precision (% CV)
dFdC	4.29	99.2	7.89
(4.29-429 nM)	12.9	101	3.79
	129	101	2.64
	364	102	2.50
dFdCMP	29.0	103	12.5
(29.0-2900 nM)	87.0	98.7	9.05
	870	99.3	4.01
	2460	98.4	2.75
dFdCDP	31.4	103	14.0
(31.4-3140 nM)	94.2	99.1	11.4
	942	101	3.48
	2670	103	4.95
dFdCTP	36.9	97.5	15.8
(36.9-3690 nM)	111	97.4	11.3
	1110	103	2.72
	3140	104	3.28
dFdU	42.1	106	17.0
(42.1-4210 nM)	126	102	8.39
	1260	101	5.98
	3580	102	4.10
dFdUMP	25.4	96.5	17.1
(25.4-2540 nM)	76.2	98.5	12.0
	762	101	3.39
	2160	102	3.90
dFdUDP	43.2	102	17.9
(43.2-4320 nM)	129	103	11.0
	1290	104	6.05
	3670	103	4.76
dFdUTP	52.7	97.1	20.0
(52.7-5270 nM)	158	99.2	11.2
	1580	102	5.72
	4480	104	2.86

Table 3. Intra-assay performance data for dFdC, dFdU and their mono-, di-, and triphosphate in PBMC lysate suspension (N=5).

Compound (calibration range)	Nominal concentration (nM)	Intra-assay accuracy (%)	Intra-assay precision (% CV)
dFdC	4.29	82.3	4.57
(4.29-429 nM)	12.9	99.2	2.71
	129	98.6	2.18
	364	100	2.03
dFdCMP	20.0	88.4	17.2
(29.0-2900 nM)	87.0	97.8	9.81
	870	97.5	3.32
	2460	96.3	2.97
dFdCDP	31.4	102	18.6
(31.4-3140 nM)	94.2	97.1	11.8
	942	97.4	3.22
	2670	97.3	3.79
dFdCTP	36.9	98.8	19.7
(36.9-3690 nM)	111	91.4	6.59
	1110	96.0	5.12
	3140	94.2	2.92
dFdU	42.1	115	13.6
(42.1-4210 nM)	126	96.5	13.5
	1260	103	6.01
	3580	104	3.27
dFdUMP	25.4	109	19.6
(25.4-2540 nM)	76.2	114	9.39
	762	103	4.05
	2160	98.9	3.08
dFdUDP	43.2	97.1	18.9
(43.2-4320 nM)	129	99.2	14.5
	1290	102	4.49
	3670	99.3	4.72
dFdUTP	52.7	87.9	17.7
(52.7-5270 nM)	158	107	10.2
	1580	101	3.19
	4480	101	4.67

Table 4. Stability data of dFdC, dFdU and their mono-, di- and triphosphates (N=3)

Matrix	Condition	Analyte	Initial conc (nM/*mM*)	Found conc (nM/*mM*)	Dev. (%)
Water (stock solution)	20-25°C, 24 hours	dFdC	*3.84*	*3.74*	-2.60
		dFdCMP	*2.55*	*2.58*	1.07
		dFdCDP	*1.27*	*1.29*	1.54
		dFdCTP	*1.33*	*1.36*	1.92
		dFdU	*3.76*	*3.73*	0.798
		dFdUMP	*2.25*	*2.24*	-0.363
		dFdUDP	*1.49*	*1.50*	0.945
		dFdUTP	*1.58*	*1.60*	1.40
	-70°C, 3 months	dFdC	*3.79*	*3.84*	1.32
		dFdCMP	*2.55*	*2.58*	1.09
		dFdCDP	*1.27*	*1.28*	0.574
		dFdCTP	*1.33*	*1.37*	1.22
		dFdU	*3.79*	*3.84*	1.32
		dFdUMP	*2.25*	*2.28*	1.12
		dFdUDP	*1.49*	*1.47*	-1.06
		dFdUTP	*1.58*	*1.57*	-0.800
PBMC lysate	Ice-water, 5 hours	dFdC	128	126	-1.04
		dFdCMP	718	616	-14.2
		dFdCDP	969	992	2.37
		dFdCTP	1050	1020	-2.90
		dFdU	1240	1370	10.8
		dFdUMP	663	600	-9.60
		dFdUDP	1320	1280	-2.78
		dFdUTP	1480	1310	-11.5
	-70°C, 3 months	dFdC	128	115	-9.92
		dFdCMP	812	750	-7.68
		dFdCDP	969	830	-14.8
		dFdCTP	1050	1000	-4.18
		dFdU	1240	1230	-0.809
		dFdUMP	663	590	-11.0
		dFdUDP	1320	1130	-14.1
		dFdUTP	1560	1400	-10.2
Final extract	Autosampler (4°C), reinjection, 24 hours	dFdC	128	126	-1.31
		dFdCMP	812	747	-8.01
		dFdCDP	969	977	0.791
		dFdCTP	1050	1060	1.05
		dFdU	1240	1330	7.55
		dFdUMP	663	617	-6.93
		dFdUDP	1320	1240	-5.81
		dFdUTP	1560	1400	-10.2

Conclusion

The presented method is the first with which dFdC and its nucleotides, but also dFdU and its nucleotides, can be analyzed in a single analytical run and without the need of dephosphorylation. Expressed as pmol/million PBMCs the LLQ's are 0.208, 1.41, 1.52 and 1.79 for dFdC, dFdCMP, dFdCDP and dFdCTP and 2.04, 1.23, 2.10 and 2.56 for dFdU, dFdUMP, dFdUDP and dFdUTP respectively (assuming a mean PBMC yield of 4 million PBMCs per sample [15]).
The presented validation shows that, if important factors such as redox state and pH are controlled and if the column is cleaned after each analytical run, PGC can be used to develop a robust method with exceptional selectivity.
PBMCs should be collected and processed on ice, but the addition of a deaminase inhibitor is not required. Furthermore it is shown that IS addition should be performed before centrifugation of the cell lysate, to correct for absorption of the analytes to cell debris.
Finally, the method should be applicable to other deoxycytidine analogs and their deoxycytidine and deoxyuridine metabolites with minor adaptations. Concluding, this method provides a valuable tool to better understand the *in-vivo* pharmacology of dFdC.

References

[1] R. Grunewald, H. Kantarjian, M. Du, K. Faucher, P. Tarassoff, W. Plunkett, J. Clin. Oncol. 10 (1992) 406.

[2] S. A. Veltkamp, D. Pluim, M. A. van Eijndhoven, M. J. Bolijn, F. H. Ong, R. Govindarajan, J. D. Unadkat, J. H. Beijnen, J. H. Schellens, Mol. Cancer Ther. 7 (2008) 2415.

[3] W. Plunkett, P. Huang, V. Gandhi, Anticancer Drugs 6 Suppl 6 (1995) 7.

[4] S. A. Veltkamp, R. S. Jansen, S. Callies, D. Pluim, C. M. Visseren-Grul, H. Rosing, S. Kloeker-Rhoades, V. A. Andre, J. H. Beijnen, C. A. Slapak, J. H. Schellens, Clin. Cancer Res. 14 (2008) 3477.

[5] S. A. Veltkamp, D. Pluim, O. van Tellingen, J. H. Beijnen, J. H. Schellens, Drug Metab Dispos. 36 (2008) 1606.

[6] P. Ziemkowski, K. Felczak, J. Poznanski, T. Kulikowski, Z. Zielinski, J. Ciesla, W. Rode, Biochem. Biophys. Res Commun. 362 (2007) 37.

[7] J. Lai, J. Wang, Z. Cai, J. Chromatogr. B 868 (2008) 1.

[8] J. T. Slusher, S. K. Kuwahara, F. M. Hamzeh, L. D. Lewis, D. M. Kornhauser, P. S. Lietman, Antimicrob. Agents Chemother. 36 (1992) 2473.

[9] B. L. Robbins, B. H. Waibel, A. Fridland, Antimicrob. Agents Chemother. 40 (1996) 2651.

[10] A. Darque, G. Valette, F. Rousseau, L. H. Wang, J. P. Sommadossi, X. J. Zhou, Antimicrob. Agents Chemother. 43 (1999) 2245.

[11] C. Solas, Y. F. Li, M. Y. Xie, J. P. Sommadossi, X. J. Zhou, Antimicrob. Agents Chemother. 42 (1998) 2989.

[12] J. D. Moore, G. Valette, A. Darque, X. J. Zhou, J. P. Sommadossi, J. Am. Soc. Mass Spectrom. 11 (2000) 1134.

[13] T. King, L. Bushman, P. L. Anderson, T. Delahunty, M. Ray, C. V. Fletcher, J. Chromatogr. B 831 (2006) 248.

[14] G. Shi, J. T. Wu, Y. Li, R. Geleziunas, K. Gallagher, T. Emm, T. Olah, S. Unger, Rapid Commun. Mass Spectrom. 16 (2002) 1092.

[15] S. A. Veltkamp, M. J. Hillebrand, H. Rosing, R. S. Jansen, E. R. Wickremsinhe, E. J. Perkins, J. H. Schellens, J. H. Beijnen, J. Mass Spectrom. 41 (2006) 1633.

[16] R. S. Jansen, H. Rosing, C. J. de Wolf, J. H. Beijnen, Rapid Commun. Mass Spectrom. 21 (2007) 4049.

[17] A. Pruvost, F. Becher, P. Bardouille, C. Guerrero, C. Creminon, J. F. Delfraissy, C. Goujard, J. Grassi, H. Benech, Rapid Commun. Mass Spectrom. 15 (2001) 1401.

[18] F. Becher, A. Pruvost, C. Goujard, C. Guerreiro, J. F. Delfraissy, J. Grassi, H. Benech, Rapid Commun. Mass Spectrom. 16 (2002) 555.

[19] F. Becher, D. Schlemmer, A. Pruvost, M. C. Nevers, C. Goujard, S. Jorajuria, C. Guerreiro, T. Brossette, L. Lebeau, C. Creminon, J. Grassi, H. Benech, Anal. Chem. 74 (2002) 4220.

[20] G. Hennere, F. Becher, A. Pruvost, C. Goujard, J. Grassi, H. Benech, J. Chromatogr. B 789 (2003) 273.

[21] A. Pruvost, F. Theodoro, L. Agrofoglio, E. Negredo, H. Benech, J. Mass Spectrom. 43 (2008) 224.

[22] E. N. Fung, Z. Cai, T. C. Burnette, A. K. Sinhababu, J. Chromatogr. B 754 (2001) 285.

[23] R. Tuytten, F. Lemiere, W. V. Dongen, E. L. Esmans, H. Slegers, Rapid Commun. Mass Spectrom. 16 (2002) 1205.

[24] R. L. Claire, III, Rapid Commun. Mass Spectrom. 14 (2000) 1625.

[25] T. Hawkins, W. Veikley, R. L. Claire, III, B. Guyer, N. Clark, B. P. Kearney, J. Acquir. Immune. Defic. Syndr. 39 (2005) 406.

[26] J. E. Vela, L. Y. Olson, A. Huang, A. Fridland, A. S. Ray, J. Chromatogr. B 848 (2007) 335.

[27] J. Xing, A. Apedo, A. Tymiak, N. Zhao, Rapid Commun. Mass Spectrom. 18 (2004) 1599.
[28] C. Crauste, I. Lefebvre, M. Hovaneissian, J. Y. Puy, B. Roy, S. Peyrottes, S. Cohen, J. Guitton, C. Dumontet, C. Perigaud, J. Chromatogr. B Analyt. Technol. Biomed. Life Sci. (2009).
[29] M. Gouy, H. Fabre, M. Blanchin, S. Peyrottes, C. Périgaud, I. Lefebvre, Anal. Chim. Acta 566 (2006) 178.
[30] T. Zhou, C. A. Lucy, J. Chromatogr. A 1187 (2008) 87.
[31] R. Nishi, T. Yamauchi, T. Ueda, Cancer Sci. 97 (2006) 1274.
[32] R. W. Sparidans, M. Crul, J. H. Schellens, J. H. Beijnen, J. Chromatogr. B 780 (2002) 423.
[33] R. Losa, M. I. Sierra, M. O. Gion, E. Esteban, J. M. Buesa, J. Chromatogr. B 840 (2006) 44.
[34] A. W. Blackstock, H. Lightfoot, L. D. Case, J. E. Tepper, S. K. Mukherji, B. S. Mitchell, S. G. Swarts, S. M. Hess, Clin. Cancer Res. 7 (2001) 3263.
[35] v. H. Ruiz, V, G. Veerman, E. Boven, P. Noordhuis, J. B. Vermorken, G. J. Peters, Biochem. Pharmacol. 48 (1994) 1327.
[36] V. Heinemann, L. W. Hertel, G. B. Grindey, W. Plunkett, Cancer Research 48 (1988) 4024.
[37] S. U. Bajad, W. Lu, E. H. Kimball, J. Yuan, C. Peterson, J. D. Rabinowitz, J. Chromatogr. A 1125 (2006) 76.
[38] R. L. Cordell, S. J. Hill, C. A. Ortori, D. A. Barrett, J. Chromatogr. B 871 (2008) 115.
[39] Y. Q. Xia, M. Jemal, N. Zheng, X. Shen, Rapid Commun. Mass Spectrom. 20 (2006) 1831.
[40] G. H. Gu, C. K. Lim, J. Chromatogr. 515 (1990) 183.
[41] M. Pabst, F. Altmann, Anal. Chem. 80 (2008) 7534.
[42] A. Tornkvist, K. E. Markides, L. Nyholm, Analyst 128 (2003) 844.
[43] A. Tornkvist, S. Nilsson, A. Amirkhani, L. M. Nyholm, L. Nyholm, J. Mass Spectrom. 39 (2004) 216.
[44] T. Takeuchi, T. Kojima, T. Miwa, J. High Resolut. Chromatogr. 23 (2000) 590.
[45] S. Rinne, A. Holm, E. Lundanes, T. Greibrokk, J. Chromatogr. A 1119 (2006) 285.
[46] R. S. Jansen, H. Rosing, J. H. Schellens, J. H. Beijnen, J. Chromatogr. A 1216 (2009) 3168.
[47] L. D. Vainchtein, H. Rosing, B. Thijssen, J. H. Schellens, J. H. Beijnen, Rapid Commun. Mass Spectrom. 21 (2007) 2312.
[48] U.S Food and Drug Administration: Centre for Drug Evaluation and Research: Guidance for Industry: Bioanalytical Method Validation. 2001.
[49] K. B. Green-Church, P. A. Limbach, J. Am. Soc. Mass Spectrom. 11 (2000) 24.
[50] J. J. Barchi, Jr., D. A. Cooney, Z. Hao, Z. H. Weinberg, C. Taft, V. E. Marquez, H. Ford, Jr., J. Enzyme Inhib. 9 (1995) 147.
[51] F. Becher, A. Pruvost, J. Gale, P. Couerbe, C. Goujard, V. Boutet, E. Ezan, J. Grassi, H. Benech, J. Mass Spectrom. 38 (2003) 879.
[52] L. Durand-Gasselin, D. Da Silva, H. Benech, A. Pruvost, J. Grassi, Antimicrob. Agents Chemother. 51 (2007) 2105.
[53] M. Jemal, Y. Q. Xia, J. Pharm. Biomed. Anal. 22 (2000) 813.
[54] J. L. Abbruzzese, R. Grunewald, E. A. Weeks, D. Gravel, T. Adams, B. Nowak, S. Mineishi, P. Tarassoff, W. Satterlee, M. N. Raber, ., J. Clin. Oncol. 9 (1991) 491.
[55] R. Grunewald, H. Kantarjian, M. J. Keating, J. L. Abbruzzese, P. Tarassoff, W. Plunkett, Cancer Research 50 (1990) 6823.
[56] J. R. Kroep, G. Giaccone, D. A. Voorn, E. F. Smit, J. H. Beijnen, H. Rosing, C. J. van Moorsel, C. J. van Groeningen, P. E. Postmus, H. M. Pinedo, G. J. Peters, J. Clin. Oncol. 17 (1999) 2190.

Chapter 2.6

Protein versus DNA as a marker for peripheral blood mononuclear cell counting

Robert S Jansen, Hilde Rosing, Jan HM Schellens and Jos H Beijnen

Submitted for publication

Abstract

Quantitative analysis of intracellular analytes not only requires an accurate and precise assay for the quantitation of the analytes, but also for the quantitation of the number of cells in which they were determined. In this technical note we compare protein and DNA as markers for the number of peripheral blood mononuclear cells (PBMCs) isolated from whole blood. The protein content of samples was highly influenced by red blood cell contamination and was, therefore, a less suitable marker. The DNA-based method was unaffected by red blood cell contamination and was finally validated over a range from 10-300 million PBMCs/mL.

Introduction

The molecular targets of many drugs are not located in blood plasma or the exterior of cells, but rather inside cells. Plasma levels of these compounds can therefore be regarded only as a surrogate for the actual intracellular concentrations. Still, determination of plasma levels appears sufficient for most drugs because equilibrium exists between the plasma and intracellular drug concentration.

For some drugs and metabolites, however, the plasma concentrations are not in equilibrium with intracellular concentrations. This can be due to intracellular accumulation of the drug, or due to intracellular formation of metabolites.

The active metabolites of nucleoside analogs, which are used in anticancer, antiviral and immunosuppressive therapies, are only formed inside cells, and have a half-life that is much longer than that of their parent nucleoside in plasma. For these drugs, intracellular metabolite levels are much more informative than plasma prodrug levels [1].

Most assays for intracellular analytes use peripheral blood mononuclear cells (PBMCs) as matrix because of their role in the immune system and because their nucleoside metabolism is fully functional, as opposed to that of red blood cells and platelets.

Intracellular assays require an accurate and precise determination of the amount of analyte as well as of the number of cells in which it was determined. Many publications describe extensive validations of intracellular assays, but these validations generally do not include the cell counting step [2;3]. Moreover, separate validations of cell counting procedures are very sparse [4].Cell counting step can, however, be a considerable source of variability [5].

Since the accuracy and precision of the final result is composed of the accuracy and precision of the cell count and the final analysis, an accurate and precise cell counting method is pivotal to obtain correct results. PBMCs have been counted using a microscope, haemocytometer and protein and DNA determinations [2;4;6;7].

Here, we compare the Bradford protein determination [8] with a DNA determination using the fluorescent dye Hoechst 33258 [9] for counting the number of PBMCs in a sample. Moreover, we describe the validation of a DNA-based PBMC counting method.

Experimental

Cell isolation and preparation

Red blood cells were obtained by centrifuging whole blood for 5 min at 1500 g and collecting the precipitate. The cells were frozen, and the haemoglobin concentration was determined using a haematology analyzer (Cell-Dyn 4000; Abbott Diagnostics, Abbott Park, IL, USA).

For comparison of cell counting with a haemocytometer, the protein determination and the DNA determinations, 8 mL whole blood was collected in cell preparation tubes (BD Vacutainer CPT; BD, Franklin Lakes, NJ, USA). After centrifuging (20 min at 1500 g) the PBMCs were collected and washed with 15 mL phosphate buffered saline (PBS). The cells were finally resuspended in 70 µL PBS.

For the validation of the DNA-based cell counting assay, PBMCs were isolated from human leukocyte buffy coat (Sanquin, Amsterdam, the Netherlands) originating from 500 mL whole blood as previously described [7]. The obtained PBMC suspensions were diluted to the desired concentration with PBS, aliquoted in 10 µL volumes and stored at -70°C.

Cell count using a haemocytometer

The number of PBMCs and RBCs was determined in each sample using a Cell-Dyn 4000 haematology analyzer.

Protein determination

The total protein concentration in samples was determined using the Bradford protein assay (Bio-Rad protein assay, Bio-Rad, Hercules, CA, USA). Seven bovine serum albumine calibration standards were prepared in concentrations ranging from 50-1000 µg/mL. Calibration standards and unknowns were transferred (10 µL) to a 96-well microplate (BD microtest™, flat bottom; BD, Franklin Lakes, NJ, USA). All samples were processed in duplicate. After the addition of 250 µL dye reagent (Coomassie brilliant blue G-250), the absorption was directly measured at 590 nm using a microplate reader type EL340 (Bio-Tek Instruments Inc, Winooski, VT, USA).

DNA-based cell count

The DNA-based cell counting was performed using the fluorescent dye Hoechst 33258 (Bio-Rad DNA quantitation kit, Bio-Rad, Hercules, CA, USA). Seven PBMC calibration standards were prepared in concentrations ranging from 10-300 X 10^6 PBMCs/mL (determined using a haemocytometer). Moreover, validation PBMC suspensions were prepared from a second donor buffy coat at concentrations of approximately 10, 75 and 250 X 10^6 PBMCs/mL (determined using a haemocytometer). Calibration standards, validation samples and unknowns in PBS (all 10 µL)

were diluted with 750 µL water and sonicated for 30 minutes. A volume of 10 µL of this suspension was then transferred to a 96-well opaque microplate (Optiplate-96 F; Perkin Elmer, Waltham, MA, USA) in two-fold. After the addition of 300 µL dye (2 µg/mL Hoechst 33258 in assay buffer (2 M NaCl, 100 mM EDTA, 100 mM TRIS)) the microplate was measured 5 times during 0.1 s with excitation at 355 nm and emission at 460 nm using a Wallac Victor 1420 (Perkin Elmer, Waltham, MA, USA). The mean of the 5 measurements was used for the data processing.

Data processing

Calibration curves were constructed using Excel 2003 software (Microsoft, Redmond, WA, USA). For the protein determination, we used a quadratic fit with $1/x^2$ weighting, because absorption is not linear over the concentration range. For the DNA-based cell count we used a linear fit with $1/x^2$ weighting. Calibration standards were excluded if the deviation of the back-calculated concentration from the nominal concentration was more than ±15.0% or more than ±20.0% at the lower limit of quantification (LLOQ). No more than 25% of the calibration standards were allowed to be rejected from the calibration curve, which should contain at least one sample at the LLOQ and the upper limit of quantification (ULOQ). Samples were only reported if the results from the duplicate analyses did not deviate more than 15.0%.

Method comparison

Whole blood was collected from 4 individuals and PBMCs were isolated as described under "cell isolation". Of the final cell suspension, 20 µL aliquots were diluted 20-fold in PBS (haemocytometer) and water (protein determination), or 76-fold in water (DNA determination). The samples were repeatedly measured using each method.

Validation of DNA method

Linearity

Deviations of the back calculated concentrations from the nominal concentrations should be within ±20.0 at the LLOQ and within ±15.0% at the other levels. No more than one third of the calibration standards were allowed to be rejected from the calibration curve.

Inaccuracy and precision

The intra- and inter-assay inaccuracy and precision were determined by analyzing the validation samples at three levels in three separate runs (N=5 per run). The inaccuracy of the method was assessed comparing the determined cell count (DNA-based determination) with the reference cell count (haemocytometer). The coefficients of variation (CV) were calculated to assess the precision of the method. Inaccuracies and precisions should

be within ±15.0% and less than 15.0%, respectively, except at the LLOQ where they should be within ±20.0% and less than 20.0%, respectively.

Stability

Stability of the PBMC suspensions was assessed in 3-fold with samples containing 67.5 X 10^6 PBMCs/mL. Stability of non-lysed samples in PBS was assessed after 7 hours at ambient temperatures, and after 2 freeze(-70°C)-thaw cycles. Likewise, stability was tested in lysed samples after 2 hours at 20-25°C, and after 2 freeze(-70°C)-thaw cycles. Moreover, the re-assay reproducibility was assessed after storing a microplate for 4.5 hours at ambient temperatures, protected from light. The samples were considered stable if the found concentrations did not deviate more than 15.0% from the nominal or initial concentration.

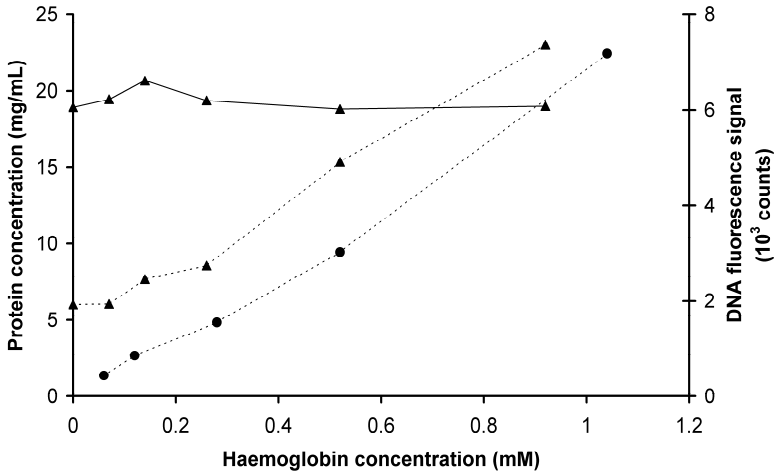

Figure 1. Effect of the haemoglobin concentration on the protein (dashed line) and DNA (solid line) concentration in samples with PBMCs (▲) and without PBMCs (●)

Results and discussion

In studies where we used the Bradford protein assay to correct for the number of cells isolated from clinical samples, a small number of samples contained exceptionally high protein levels. Visual inspection of these samples revealed a red discoloration. We reasoned that red blood cell contamination was the source of the high protein levels observed. Because red blood cells do not contain DNA, a DNA-based cell counting method was considered.

In preliminary experiments we investigated this possibly confounding factor more thoroughly by spiking red blood cells to neat solutions (without PBMCs) and to PBMC containing samples. Figure 1 clearly shows the impact that haemoglobin, a marker for red blood cell contamination, has on the amount of protein in a sample. A relatively low contamination already had a significant influence on the total protein concentration. A red blood cell lysis- and wash-step would improve the performance of the protein method, but requires extra sample handling. The DNA signals were, as expected, not influenced by the red blood cell contamination, making it more robust towards the inevitable red blood cell contamination. Therefore, the DNA-based cell counting was developed further.

DNA determination

The fluorescent dye Hoechst 33258 selectively binds to double stranded DNA, upon which the fluorescent signal and excitation wavelength shift [9]. Initially, we prepared Hoechst 33258 in assay buffer that was diluted 10 times. This, however, resulted in slowly increasing fluorescence signals, which kept increasing for up to 5 hours after addition. When using undiluted assay buffer, on the other hand, the signal rapidly increased, allowing direct analysis. Others have reported that high salt concentrations dissociate the DNA from proteins in crude cell extracts [9]. Cell lysis was performed in a relatively large volume of water. When smaller volumes were used, cell numbers in samples with a high PBMC concentration were underestimated, indicating incomplete dissolution of the DNA. Finally, we noticed variation in the final measurement of the microplate. To reduce this variation each well was measured five times.

Method comparison

We systematically compared the three described methods by applying each of them to PBMCs originating from 4 different individuals. The results of this comparison are presented in figure 2. With CVs lower than 10%, all methods showed a good precision. Moreover, high correlation coefficients were found between the cell number determined using the haemocytometer and the protein (0.959) and DNA-based results (0.995).

The slightly lower coefficient of correlation for the protein determination was most likely caused by variable red blood cell contamination. In agreement with our preliminary experiments, the samples containing relatively high amounts of red blood cells showed a relatively high protein concentration, whereas the DNA-based method remained unaffected. The cell numbers determined using the DNA-based method deviated 9.74-19.1% from the numbers determined using the haemocytometer.

Cell counting using a haemocytometer or microscope remain the reference methods. These methods, however, require intact cells and must therefore be performed before freezing the sample. Personnel trained for PBMC counting should thus be present when each sample is processed. Moreover, instruments and trained personnel should be available at each clinical site in case of multi-center studies. A standardized assay performed in a central laboratory reduces the need of instruments and personnel, and the concomitant analytical variation. Of the two markers tested, DNA proved to be the most appropriate for PBMC counting. Therefore, we validated the DNA-based PBMC counting method.

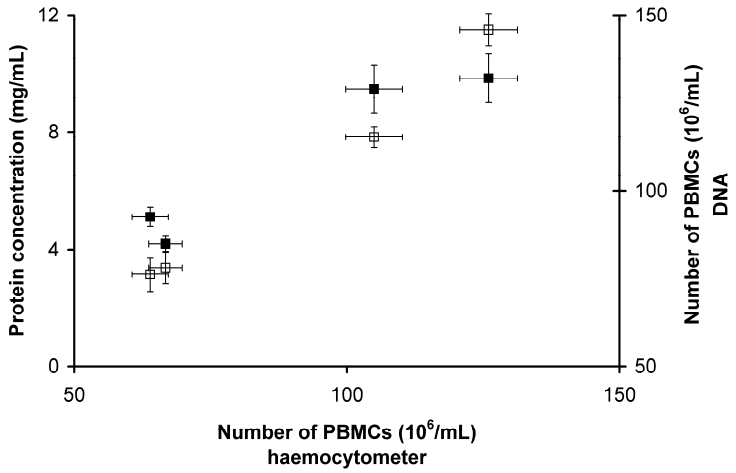

Figure 2. Protein concentration (■) and DNA-based PBMC count (□) versus cell count using haemocytometer. Data points are presented as mean (N=5 for protein determination and DNA-based cell count, N=3 for haemocytometer cell count) ± the standard deviations

DNA-based cell count validation

Linearity

The mean back-calculated deviations from the nominal concentrations of the calibration standards ranged from -6.75-3.35% and precision were better than 10.4% at all calibration levels. The correlation coefficients were 0.993 or better.

Inaccuracy and precision

The assay performance is presented in table 1. The determined mean PBMC concentrations deviated -5.72, 9.16 and -7.29% from the nominal concentration for the validation samples containing 14.2, 67.5 and 245 X 10^6 PBMCs/mL, respectively. All precisions were lower than 15.0%, except at the lowest validation sample, where it was lower than 20.0%. Concluding, both the inaccuracy and the precision of the method are satisfactory.

Stability

The stability of the samples under different conditions is summarized in table 2. Deviations of less than 15.0% were found, showing that the samples were stable under all tested conditions. Long-term stability tests are ongoing.

Table 2. Stability data of PBMC samples

Matrix	Condition	Nominal/*initial* concentration (10^6 PBMCs/mL)	Measured concentration (10^6 PBMCs/mL)	CV (%)	Dev (%)
PBS	7 h, ambient temperatures	67.5	70.7	2.62	4.69
(non-lyzed)	2 freeze(-70^{0}C)-thaw cycles	67.5	74.1	6.08	9.78
Water	2 h, ambient temperatures	67.5	73.2	0.993	8.52
(Lyzed)	2 freeze(-70^{0}C)-thaw cycles	67.5	64.1	8.99	-5.02
Re-assay reproducibility	4.5 h, ambient temperatures, protected from light	*78.9*	82.2	1.54	4.18

The described method should also be applicable to other types of cells as long as the amount of DNA per cell is identical to that of PBMCs. Results obtained from leukemic or other malignant cells should, thus, be interpreted with care because malignant cells often have an aberrant karyotype and thus contain an aberrant amount of DNA. Moreover, chemotherapeutic agents can cause a shift in the cell-cycle of dividing cells, thereby altering the amount of DNA per cell. This is, however, not a problem for healthy PBMCs, which are non-dividing.

Table 1. Assay performance of the DNA-based PBMC counting method

Run #	Replicate	PBMC concentration (10^6/mL)		
		14.2	67.5	245
1	1	18.2	82.5	243
	2	17.0	76.8	232
	3	15.5	77.3	233
	4	13.3	75.0	232
	5	15.4	76.4	232
2	1	11.4	74.5	235
	2	14.6	76.3	232
	3	12.7	72.3	230
	4	12.7	75.1	231
	5	8.22	73.6	228
3	1	14.2	69.0	226
	2	12.9	70.2	220
	3	12.3	65.3	210
	4	11.4	70.9	210
	5	11.0	70.0	213
Mean #1		15.9	77.6	234
Mean #2		11.9	74.4	231
Mean #3		12.4	69.1	216
Overall mean		13.4	73.7	227
Intra-assay inaccuracy #1 (% dev)		11.8	15.0	-4.33
Intra-assay inaccuracy #2 (% dev)		-16.0	10.2	-5.63
Intra-assay inaccuracy #3 (% dev)		-13.0	2.34	-11.9
Inter-assay inaccuracy (% dev)		-5.72	9.16	-7.29
Intra-assay precision #1 (% CV)		11.6	3.70	2.06
Intra-assay precision #2 (% CV)		19.8	2.03	1.12
Intra-assay precision #3 (% CV)		10.3	3.21	3.25
Inter-assay precision (% CV)		18.9	5.70	4.25

Conclusions

A DNA-based cell counting method is preferable over a protein-based method, because inevitable red blood cell contamination of PBMC samples severely influences the protein content. The described DNA-based method has been validated for the accurate and precise determination of the number of PBMCs present in a sample of isolated PBMCs. Crude cell suspensions could be used with minimal sample pretreatment, allowing fast analysis. The determination is not influenced by red blood cell contamination.

Acknowledgements

The authors would like to thank Joke Schol for her excellent technical assistance.

References

[1] J. F. Rodriguez Orengo, J. Santana, I. Febo, C. Diaz, J. L. Rodriguez, R. Garcia, E. Font, O. Rosario, P. R. Health Sci. J. 19 (2000) 19.
[2] T. King, L. Bushman, J. Kiser, P. L. Anderson, M. Ray, T. Delahunty, C. V. Fletcher, J. Chromatogr. B 843 (2006) 147.
[3] G. Shi, J. T. Wu, Y. Li, R. Geleziunas, K. Gallagher, T. Emm, T. Olah, S. Unger, Rapid Commun. Mass Spectrom. 16 (2002) 1092.
[4] H. Benech, F. Theodoro, A. Herbet, N. Page, D. Schlemmer, A. Pruvost, J. Grassi, J. R. Deverre, Anal. Biochem. 330 (2004) 172.
[5] D. Salmon-Ceron, R. Lassalle, A. Pruvost, H. Benech, M. Bouvier-Alias, C. Payan, C. Goujard, E. Bonnet, F. Zoulim, P. Morlat, P. Sogni, S. Perusat, J. M. Treluyer, G. Chene, Clin. Infect. Dis. 36 (2003) 1295.
[6] F. Becher, A. Pruvost, C. Goujard, C. Guerreiro, J. F. Delfraissy, J. Grassi, H. Benech, Rapid Commun. Mass Spectrom. 16 (2002) 555.
[7] S. A. Veltkamp, M. J. Hillebrand, H. Rosing, R. S. Jansen, E. R. Wickremsinhe, E. J. Perkins, J. H. Schellens, J. H. Beijnen, J. Mass Spectrom. 41 (2006) 1633.
[8] M. M. Bradford, Anal. Biochem. 72 (1976) 248.
[9] C. Labarca, K. Paigen, Anal. Biochem. 102 (1980) 344.

Chapter 3

Pharmacology
of nucleoside analogs

Chapter 3.1

Contribution of the drug transporter ABCG2 (breast cancer resistance protein) to resistance against anticancer nucleosides

Cocky JF de Wolf, Robert S Jansen, Hiroaki Yamaguchi, Marcel de Haas, Koen van de Wetering, Jan Wijnholds, Jos H Beijnen and Piet Borst

Molecular Cancer Therapeutics
Volume 7, Issue 9, Pages 3092-102
2008

Abstract

We have studied the potential contribution of ABCG2 (breast cancer resistance protein) to resistance to nucleoside analogs. In cells transfected with DNA constructs resulting in overexpression of human or mouse ABCG2, we found resistance against cladribine, clofarabine, fludarabine, 6-mercaptopurine, and 6-mercaptopurine riboside in both MDCKII and HEK293 cells and against gemcitabine only in HEK293 cells. With Transwell studies in MDCK cells and transport experiments with vesicles from Sf9 and HEK293 cells, we show that ABCG2 is able to transport not only the nucleotide CdAMP, like several other ATP-binding cassette transporters of the ABCC (multidrug resistance protein) family, but also the nucleoside cladribine itself. Expression of ABCG2 in cells results in a substantial decrease of intracellular CdATP, explaining the resistance against cladribine. The high transport rate of cladribine and clofarabine by ABCG2 deduced from Transwell experiments raises the possibility that this transporter could affect the disposition of nucleoside analogs in patients or cause resistance in tumors.

Introduction

Nucleoside, nucleotide, and nucleobase analog drugs are commonly used in the treatment of various types of cancer as well as in anti(retro)viral (HIV) therapy. Uptake and efflux of these drugs is mediated by equilibrative (uptake and efflux) transporters (SLC29 family) and concentrative (uptake) nucleoside transporters (SLC28 family) located in the plasma membrane [1;2]. Their cytotoxic action requires conversion into nucleotides and often incorporation into DNA. Whereas resistance of retroviruses against these analog is usually due to modification of the substrate specificity of the viral reverse transcriptase, resistance of cancer cells is mainly due to interference with nucleoside uptake [1] or decreased conversion of nucleoside into nucleoside monophosphate by nucleoside kinases [3;4].

A new potential mechanism for nucleoside analog resistance was discovered by Schuetz et al. [5], who showed that a lymphoid cell line selected for zidovudine resistance highly overexpressed the gene for multidrug resistance protein 4 (ABCC4). Experiments with transfected cells overexpressing transporter gene constructs subsequently showed that both ABCC4 and ABCC5 (multidrug resistance protein 5) can cause resistance to a range of nucleoside analogs and to the thiopurines 6-mercaptopurine (6-MP) and thioguanine [5-15]. Invariably, resistance was due to the ability of ABCC4 and ABCC5 to extrude the nucleoside monophosphates from the resistant cells rather than the nucleoside or nucleobase analogs themselves or the corresponding nucleoside diphosphates and triphosphates. Whether ABCC4 and ABCC5 contribute to resistance in human patients remains to be seen. The low affinity of these transporters for nucleoside monophosphate analogs makes this doubtful [10;11], but more studies are required for a definitive conclusion [12].

ABCC4 and ABCC5 belong to the C subfamily of the ATP-binding cassette (ABC) transporters. One other member of this large subfamily of organic anion transporters, ABCC11, is also able to mediate resistance to some nucleobase and nucleoside analogs [16]. In addition, several groups recently reported that an ABC transporter from the G family, the ABCG2 (breast cancer resistance protein), is able to cause cellular resistance to various nucleoside analogs, such as the antiretroviral compounds zidovudine, lamivudine [17;18], and PMEA [19] and the antileukemic purine analog [8-^{3}H]2-chloro-2′-deoxyadenosine (cladribine, 2-CdA) [19]. ABCG2 transports a wide range of xenotoxins (reviewed in refs. [20-22]) and endogenous metabolites, such as riboflavin [23]. It is present in the apical membrane of many tissues, such as the bile canalicular membrane of hepatocytes in the liver, the syncytiotrophoblasts in the placenta, the microvessel endothelium at the blood brain barrier, and the villi in the intestine [20-23]. This location makes ABCG2 an important determinant of the pharmacodynamics and thus efficacy of administered drugs that are a substrate of ABCG2 [20-23].

In the work of Wang et al. [17;18], resistance to zidovudine caused by ABCG2 was shown to be due to reduced drug accumulation in the cells, but the nature of the metabolite exported was not defined. As we have shown that ABCG2, like ABCC4 and ABCC5 [6;24-27], is able to transport cyclic GMP [28], this raised the possibility that ABCG2 is also able to export nucleotide analogs, like ABCC4 and ABCC5 do. To characterize the transport specificity of ABCG2 for nucleoside and nucleobase analog drugs, we determined ABCG2-mediated resistance to a panel of clinically relevant drugs. In two independent cell lines, we found that ABCG2 mediated high-level resistance against cladribine, clofarabine, and mercaptopurine (6-MP) among several other drugs that were tested. Of these drugs, we chose cladribine as a model substrate for further analysis of the transported substrate(s). We show here that ABCG2 transports the intact nucleoside, cladribine, as well as the monophosphate metabolite.

Materials and methods

Materials

2-CdA, [8-^{3}H]2-chloro-2′-dAMP (2-CdAMP), and [8-^{14}C]6-MP were purchased from Moravek Biochemicals. [^{14}C]inulin and [3′,5′,7-^{3}H]methotrexate were purchased from GE Healthcare. 2-Chloro-2′-deoxy-2′-fluoro-β-d-adenosine (clofarabine) and [8-^{14}C]clofarabine were a gift from GenZyme. Ko143 was a gift from Dr. A. Schinkel (The Netherlands Cancer Institute). Rat anti-mouse ABCG2 antibody, BXP-53, was a gift from Dr. G.L. Scheffer (Free University Amsterdam). Rabbit anti-rat IgG horseradish peroxidase was obtained from DAKO. All culture reagents were obtained from Invitrogen. All other chemicals and reagents were purchased from Sigma-Aldrich.

Synthesis of 2-CdAMP

2-CdAMP was synthesized using a previously described phosphorylation method with modifications [29;30]. In brief, 0.1 mmol dried 2-CdA (Sequoia Research Products) was dissolved in 2.5 mL trimethylphosphate together with 0.15 mmol 1,8-bis(dimethylamino) naphthalene (Proton Sponge). The reaction was carried out on ice water. Phosphorous oxychloride (0.4 mmol) was added dropwise to the stirred solution. After 2 h, the reaction mixture was poured into 20 mL of 1 mol/L triethylammonium bicarbonate solution (pH 8.5). The reaction yield was 69%. The solvents were evaporated under reduced pressure and the remaining semisolid was washed twice with diethylether. After reconstitution in water, 100 µL volumes of the product were injected onto a Biosep DEAE-PEI column (75 × 7.8 mm, 7 µm; Phenomenex) and chromatographed using an ammonium bicarbonate gradient (0-360 mmol/L) at 0.5 mL/min. The UV absorption of the eluate was monitored at 264 nm and the fractions containing 2-CdAMP were collected and lyophilized twice. High-performance liquid chromatography (HPLC)-mass spectrometry analysis of the product on a weak anion exchange column coupled to a Quantum Ultra mass spectrometer (Thermo Fisher Scientific) operated in the positive ion mode [31] confirmed the identity of the product (*m/z* 366 $(M + H)^{+}$). The purity of the product was 96% as determined by HPLC-UV [31]. Solutions of the final product in water were quantitated using HPLC-UV [31] and stored at −70°C.

Cell culture and transduction

Wild-type (WT) Madin-Darby canine kidney (MDCKII) cells and MDCKII cells stably transduced with human ABCG2 [32] or mouse Abcg2 [33] were described before and were kindly provided by Dr. A. Schinkel. Additionally, human embryonic kidney (HEK293) cells were stably transduced with the retroviral LZRS-IRES-GFP expression vector [34] containing the cDNA for

either human ABCG2 or mouse Abcg2 as described previously [32]. After expansion, clones were screened for expression of (functional) ABCG2/Abcg2 by determination of increased resistance to mitoxantrone in a cytotoxicity assay and by immunoblot analysis. Membrane localization was determined by immunocytochemistry. All cell lines were cultured in DMEM, which contained 10% FCS and was supplemented with 100 units/mL penicillin/streptomycin.

Immunoblot analysis

Membrane vesicles (20 µg protein) were fractionated on a denaturing 7.5% polyacrylamide slab gel and transferred onto a nitrocellulose membrane. After blocking for 1 h in PBS containing 1% nonfat dry milk, 1% bovine serum albumin, and 0.05% Tween 20, the membrane was incubated for 1 h at room temperature with the specific antibody. ABCG2 and Abcg2 were detected with the monoclonal antibody BXP-53 (1:400; ref. [35]). As secondary antibody, horseradish peroxidase-conjugated rabbit anti-rat IgG was used at a dilution of 1:1,000. Enhanced chemiluminescence was used for detection by incubating the membrane for 1 min with freshly mixed 1.25 mmol/L 3-aminophtalhydrazide, 0.2 mmol/L *p*-coumaric acid, and 0.01% (v/v) H_2O_2 in 0.1 mol/L Tris (pH 8.5).

Semiquantitative PCR

Total RNA was isolated from cell cultures using Trizol reagent (Invitrogen) according to the manufacturer's recommendations. Total RNA (2 µg) was reverse transcribed using SuperScript II reverse transcriptase and random hexamers (Invitrogen). One-sixtieth of the cDNA was used in the PCR analysis. ABCG2/Abcg2 transcript levels were determined by densitometric measurement of PCR product using Syngene densitometric software tools and normalized to the internal standard, β-actin. Degenerate ABCG2/Abcg2 primers, 5′-CTTACAGTTCTCAGCAGCTC-3′ and 5′-ATGGAGAAGATGATTGTTCG-3′, were used to generate a PCR product of 309 bp spanning exons 4 to 7. For canine β-actin (MDCKII cells), the following primers were used, 5′-CGGCACCAGGGCGTGATG-3′ and 5′-GCCTGGATGGCCACATACATGG-3′, to generate a PCR product of 299 bp. For human β-actin (HEK293 cells), the following primers were used, 5′-AGGCACCAGGGCGTGATG-3′ and 5′-GCCTGGATAGCAACGTACATGG-3′, to generate a PCR product of 299 bp.

Cytotoxicity assay

A colorimetric assay using a sulforhodamine B reaction was adapted for a quantitative measurement of cell growth and viability following the technique described by Skehan et al. [36]. First, the density at which cells displayed a linear growth rate over a period of 4 days was determined for each cell line. Cells were seeded in 96-well microtiter plates, at 3,000 per well in aliquots of 100 µL, and were allowed to attach to the plate surface

by growing them in a drug-free medium for 18 h. Afterward, dilution series of drugs were added to the cells in aliquots of 100 µL (dissolved in medium). After 4 days of exposure, the cytotoxicity was measured by the sulforhodamine B methodology for all drugs, except for CPT11 and mitoxantrone. Briefly, cells were fixed by adding 25 µL cold 50% (w/v) trichloroacetic acid and incubating for 60 min at 4°C. Plates were washed with tap water and dried. Sulforhodamine B solution [50 µL; 0.4% (w/v) in 1% acetic acid] was added to each microtiter well and incubated for 10 min at room temperature. Unbound sulforhodamine B was removed by washing with 1% acetic acid. Plates were air-dried and bound stain was dissolved with 10 mmol/L Tris unadjusted for pH. Absorbance was read on an automated spectrophotometric plate reader (Tecan) at a single wavelength of 490 nm. The relative resistance was calculated as the ratio of 50% inhibition of growth (IC_{50}) of the resistant cell line to the IC_{50} of the parental cell line. For CPT11 and mitoxantrone, cytotoxicity was quantified by cell counting and trypan blue exclusion. Cells were seeded in 24-well culture plates at 2.2×10^3 per well in 500 µL aliquots. After 4 days of exposure to a concentration range of either CPT11 or mitoxantrone, cells were trypsinized and resuspended into a single-cell suspension in PBS. Cell suspensions were counted on an automatic cell counter (Casy 1; Schärfe System).

Transepithelial transport assay

Transepithelial transport assays were done as described previously [37]. Radiolabeled drug was added to the medium at either the basolateral or apical compartment after which extrusion of radiolabel in the opposite compartment was measured through time over a period of 4 h. The amount of label in the medium was quantified by liquid scintillation counting (Beckman Coulter). Parallel assays with unlabeled cladribine were done from which total medium and cell lysate were harvested after 4 h and analyzed for cladribine and metabolite contents by HPLC-UV and HPLC-tandem mass spectrometry, respectively. Cell lysates were prepared in 70% methanol.

HPLC-UV and HPLC-tandem mass spectrometry

A reverse-phase ion pairing HPLC-UV method was developed to analyze cladribine and its anabolites [31]. Although cladribine and its anabolites were separated using the method, the monophosphate, diphosphate, and triphosphate could not be determined due to the low levels present and interference of growth medium. This method was therefore used only to determine cladribine levels. Briefly, samples (10 µL) were injected onto a Gemini C18 column (150 × 4.6 mm, 3 µm; Phenomenex) thermostated at 45°C. The sample was eluted using a 0.2 mL/min isocratic flow of a triethylamine phosphate [pH 6.75; prepared by mixing 0.1 mol/L triethylamine and 0.09 mol/L phosphoric acid (pH 6.75)] containing 10%

methanol. UV absorption was measured at 265 nm. The lower limit of quantitation was 20 nmol/L 2-CdA.

For the determination of cladribine monophosphate, diphosphate, and triphosphate, a more sensitive and specific weak anion exchange HPLC method coupled to tandem mass spectrometry was developed and validated [31]. Samples were spiked with a mixture of internal standards and a volume of 25 µL was injected onto a BioBasic AX column (50 × 2.1 mm, 5 µm; Thermo Fisher Scientific). A 0.25 mL/min binary gradient of 10 mmol/L ammonium acetate in water/acetonitrile (70:30, v/v; pH 6.0; solvent A) and 1 mmol/L ammonium acetate in water/acetonitrile (70:30, v/v; pH 10.5; solvent B) was used to separate the nucleotides. The following gradient was used: 0 to 0.5 min 10% solvent B, 0.51 to 1.75 min 50% solvent B, 1.76 to 6.5 100% solvent B, 6.5 to 6.6 min linear to 10% solvent B, and 6.6 to 10 min 10% solvent B. A Quantum Ultra mass spectrometer (Thermo Fisher Scientific) operated in the positive ion mode was used to monitor specific mass transitions of each analyte (2-CdATP *m/z* 525.9→170, 2-CdADP *m/z* 445.9→170, and 2-CdAMP *m/z* 365.9→170). The validated range was 1.11 to 27.7, 0.550 to 55.0, and 1.31 to 52.3 nmol/L for 2-CdAMP, 2-CdADP, and 2-CdATP, respectively.

Vesicular uptake assay

Inside-out membrane vesicles were prepared from *Spodoptera frugiperda* insect cells (Sf9) and HEK293 cells overproducing human ABCG2 and mouse Abcg2 as described previously [38] with the following modification. The final homogenization and vesicular storage buffer for HEK293 cells was 10 mmol/L Tris-HCl (pH 7.4) instead of 50 mmol/L Tris-HCl/250 mmol/L sucrose (pH 7.4). ATP-dependent transport of radiolabeled compounds into inside-out membrane vesicles was measured using the rapid filtration technique as described previously [38] with the following modifications. Vesicular uptake buffer for incubations with Sf9 vesicles consisted of 50 mmol/L Tris-HCl (pH 7.4)/250 mmol/L sucrose. For incubations with HEK293 vesicles, the vesicular uptake buffer was 10 mmol/L Tris-HCl (pH 7.4). High-throughput filtration assays were done in Multiscreen$_{HTS}$ FB 96-well filter plates on the Millipore Multiscreen$_{HTS}$ vacuum manifold (Millipore). Filters were washed four times with 200 µL PBS and the radioactivity retained on the filter was counted by liquid scintillation counting.

Statistical analysis

A two-sided Student's *t* test was used to determine the statistical significance between experimental groups.

Results

ABCG2/Abcg2 RNA and protein levels in transfected MDCKII and HEK293 cells

In addition to the available MDCKII cells overexpressing human ABCG2 [32] and mouse *Abcg2* [33], we constructed HEK293 cells overexpressing these transporter genes to extend the range of cells available for resistance studies. The continued expression of *ABCG2/Abcg2* was routinely checked by Western protein blot analysis and was stable over at least 20 cell culture passages. ABCG2/Abcg2 was located at the apical membrane in a monolayer of polarized MDCKII-cells and at the membrane of HEK293 cells as determined by immunohistochemistry (results not shown).

As shown in Supplementary Fig. S1A, cells making mouse Abcg2 produced a more prominent band on Western blots than cells making human ABCG2 and the mouse band also migrated more slowly through polyacrylamide gels. The difference in migration is due to a difference in N-linked glycosylation: after deglycosylation with endoglycosidase F, the two proteins comigrated as expected based on their estimated open reading frames, 656 (ABCG2; ref. [39]) and 657 (Abcg2; ref. [40]) amino acids, respectively (results not shown). The difference in the intensity of the ABCG2 and Abcg2 band could be due to a higher affinity of the antibody for the mouse protein, as this was used to raise the BXP-53 antibody [35]. To check expression levels, transcript levels were analyzed by semiquantitative PCR with degenerate ABCG2/Abcg2 primers (Supplementary Fig. S1B). Approximately 2-fold more Abcg2 transcripts were calculated to be present in cDNA prepared from both a confluent and a log-phase cell culture from the MDCKII-mAbcg2 clone than in the MDCKII-hABCG2 clone, whereas similar transcript amounts were calculated for HEK293-mAbcg2 and HEK293-hABCG2 cells. Hence, the apparent difference in protein levels in Supplementary Fig. S1A is not reflected in transcript levels in Supplementary Fig. S1B.

Resistance to Nucleoside and Nucleobase Analogs Mediated by Human and Mouse ABCG2/Abcg2

Table 1 summarizes our results of the effects of ABCG2 and Abcg2 on cellular resistance to nucleoside and nucleobase analogs used in treatment of cancer. For comparison, resistance to the classic ABCG2 substrates mitoxantrone and CPT11 and to the antiviral nucleotide analog bis-POM-PMEA was determined. In general, resistance levels found were higher for *Abcg2*-transfected cells than for *ABCG2*-transfected cells and for MDCKII cells than for HEK293 cells. Notable exceptions were found, however. Whereas we did not find any resistance to gemcitabine in MDCKII cells, substantial resistance to this drug was found in the transfected HEK293 cells.

Table 1

A. Growth inhibition of MDCKII, MDCKII-hABCG2, and MDCKII-mAbcg2 cells by nucleoside, nucleotide and nucleobase analogs

Drug	WT	hABCG2		mAbcg2	
	IC_{50} (SE)	IC_{50} (SE)	RF	IC_{50} (SE)	RF
Mitoxantrone	0.02 (0.01)	0.20 (0.06)	12.1 *	1.69 (0.25)	100.9 ***
CPT11	0.02 (0.00)	0.02 (0.00)	0.9	0.07 (0.01)	3.9 *
Cladribine	0.51(0.03)	2.02 (0.32)	4 ***	13.47 (2.06)	26.5 ***
Clofarabine	0.45 (0.06)	2.79 (0.45)	6.2 ***	34.36 (7.60)	76.3 ***
Fludarabine	139.9 (18.1)	491.6 (142.2)	3.5 *	835.7 (226.1)	6 *
Gemcitabine	0.19 (0.02)	0.16 (0.02)	0.8	0.12 (0.01)	0.6 *
6-MP riboside	13.9 (0.8)	139.2 (0.9)	10 ***	206.4 (15.3)	14.8 **
Thioguanine riboside	10.0 (0.7)	21.4 (0.7)	2.1 *	5.4 (0.5)	0.5 *
6-MP	29.5 (1.6)	2938.7 (415.3)	99.5 ***	5318.6 (543.5)	180.1 ***
Thioguanine	25.4 (1.1)	37.0 (3.7)	1.5 *	31.4 (3.4)	1.2
5-Fluorouracil	1.75 (0.38)	1.75 (0.06)	1	0.76 (0.10)	0.43 *
bis-POM-PMEA	13.40 (1.49)	36.80 (5.01)	2.8 **	53.48 (1.62)	4 ***

B. Growth inhibition of HEK293, HEK293-hABCG2, and HEK293-mAbcg2 cells by nucleoside, nucleotide and nucleobase analogs

Mitoxantrone	0.06 (0.01)	0.11 (0.01)	1.8 *	0.38 (0.07)	6.1 **
CPT11	0.01 (0.00)	0.02 (0.00)	1.8 **	0.02 (0.00)	2.6 ***
Cladribine	0.64 (0.21)	2.62 (0.46)	4.1 **	3.71 (0.49)	5.8 **
Clofarabine	0.37 (0.10)	0.88 (0.11)	2.4 *	1.78 (0.21)	4.8 ***
Fludarabine	54.85 (11.6)	90.71 (2.7)	1.7 *	85.83 (2.8)	1.6 *
Gemcitabine	0.02 (0.01)	0.06 (0.01)	3.7 *	0.05 (0.00)	3.4 **
6-MP riboside	0.74 (0.11)	2.86 (0.29)	3.9 **	2.11 (0.24)	2.9 **
Thioguanine riboside	0.42 (0.6)	0.83 (0.16)	2.0 *	0.66 (0.09)	1.6
6-MP	1.66 (0.19)	7.01 (1.87)	4.2 *	6.02 (1.03)	3.6 **
Thioguanine	1.03 (0.04)	2.23 (0.37)	2.0 *	2.27 (0.17)	2.2 **
5-Fluorouracil	4.97 (1.48)	4.66 (0.51)	0.9	4.43 (0.61)	0.9
bis-POM-PMEA	0.81 (0.15)	1.85 (0.05)	2.3 **	8.20 (0.44)	10.1 ***

The IC_{50} values are mean ± SE (µmol/L) drug of three to six experiments in triplicate. Cellular protein was stained and quantified by the sulforhodamine B colorimetric assay as described in the Materials and Methods, except for mitoxantrone and CPT11. Cytotoxicity of these drugs was quantified by cell counting and trypan blue exclusion. Statistical significance was calculated with an unpaired two-tailed Student's *t*-test; * $p<0.05$, ** $p<0.01$, *** $p<0.001$.

Transport of cladribine and clofarabine by ABCG2/Abcg2 through MDCKII monolayers

Figure 1A shows the effect of the presence of human or mouse ABCG2 on the transport of radioactive cladribine and clofarabine through monolayers of MDCKII cells. Nearly 30% of the radioactivity associated with [3H]cladribine goes through the monolayer in WT cells and the rate of transport is the same in both directions. Uptake of both cladribine and clofarabine into cells is known to be mediated mainly by the equilibrative nucleoside transporter ENT1 and the concentrative nucleoside transporter CNT3 and to a lesser extent also by ENT2 and CNT2 [41;42]. Diffusion through the membrane is probably minimal, as transport of [3H]cladribine

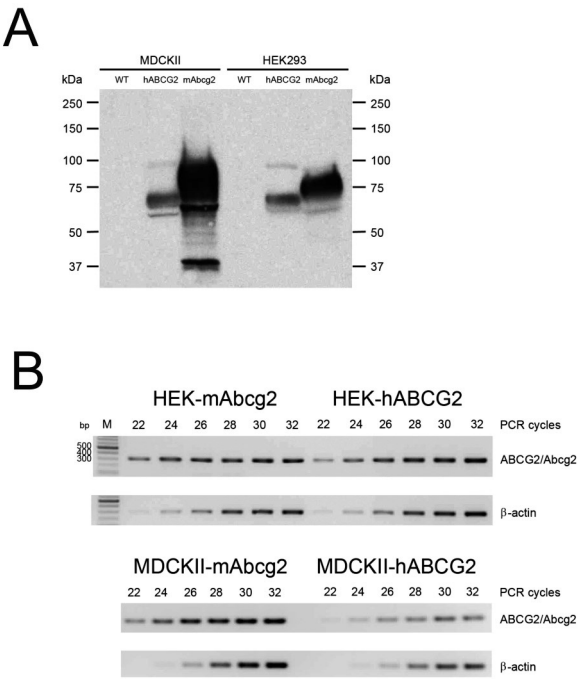

Supplementary Fig. 1 Overexpression of ABCG2/Abcg2 in MDCKII and HEK293 cells (A) Western Blot analysis of ABCG2/Abcg2 expression. 20 µg protein was loaded per lane. ABCG2/Abcg2 detection with antibody BXP-53, equal loading was confirmed by Ponceau staining. (B) Semiquantitative PCR on cDNA from HEK293 and MDCKII cells overexpressing either ABCG2 or Abcg2. Analysis was also performed on the parental cell lines and did not result in PCR product. PCR products were analysed using the Syngene software. The amount of α-actin PCR product within a cell line (HEK293 or MDCKII) was used to calculate the difference in relative expression of ABCG2 and Abcg2.High resistance was found against the purine analogs cladribine, clofarabine, and 6-MP. Resistance against 6-MP was especially high in MDCKII cells, with 100-fold (ABCG2) and 180-fold (Abcg2) resistance ($P < 0.001$), respectively. Resistance was much less in the transfected HEK293 cells, 4.2-fold ($P < 0.05$) and 3.6-fold ($P < 0.01$), respectively (Table 1B). In both cell lines, increased resistance mediated by ABCG2/Abcg2 was also found for 6-MP riboside.

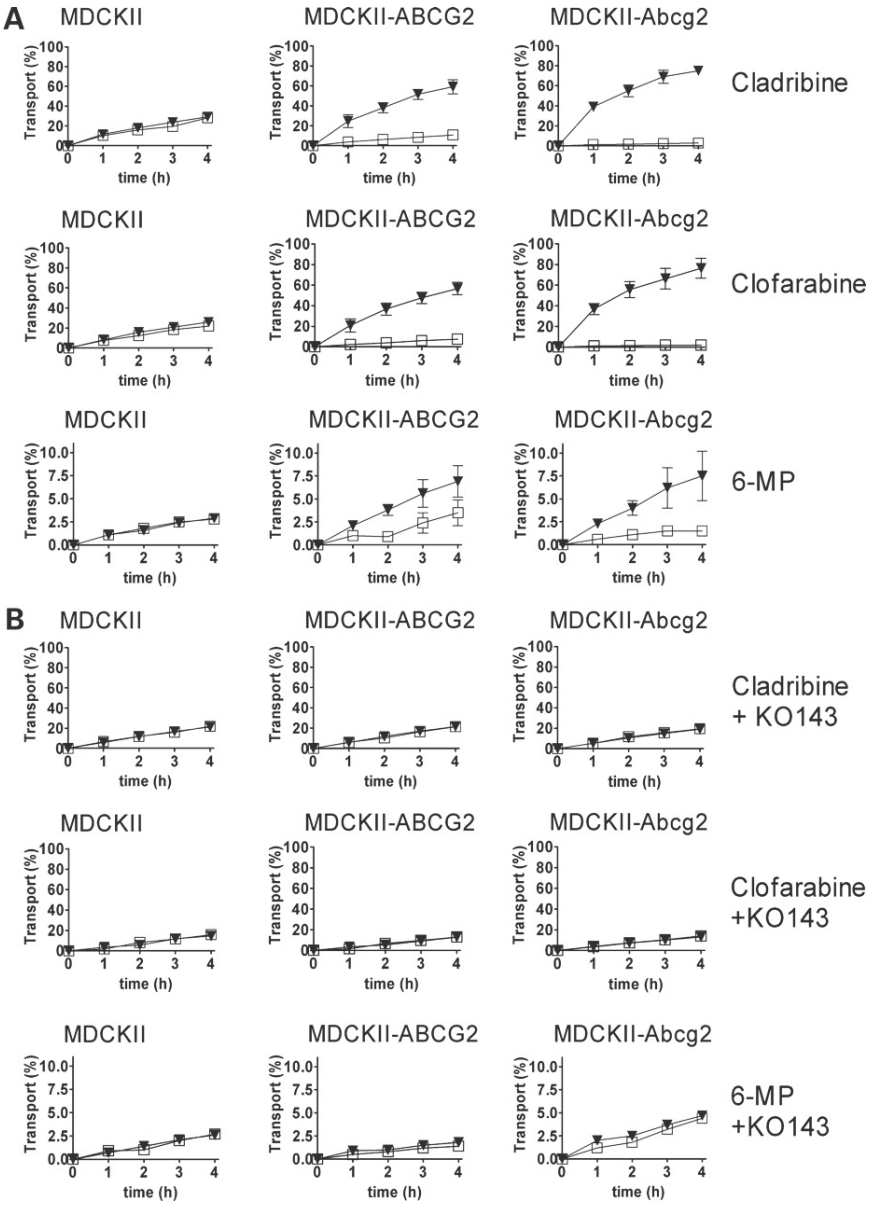

Figure 1. Transport of cladribine and clofarabine by human ABCG2 and mouse Abcg2. A, monolayers of MDCKII-parental, MDCKII-mAbcg2, and MDCKII-hABCG2 were incubated with 1 µmol/L cladribine or clofarabine for 4 h. At t = 0, drug was added to the apical or basal compartment and the percentage transport was calculated from the amount of radioactive label appearing in the opposite compartment. Mean ± SE of two experiments in duplicate. B, cell cultures were preincubated for 2 h with 1 µmol/L Ko143 in both compartments before addition of 1 µmol/L drug at t = 0 to either apical or basal side. Mean of a representative experiment in duplicate. Samples were taken at t = 1, 2, 3, and 4 h. ▾, basal to apical transport; □, apical to basal transport

through the monolayer was inhibited >90% by excess cold clofarabine (results not shown). The presence of ABCG2/Abcg2 in the apical membrane increased transport in the apical direction and decreased transport in the basal direction. These effects were completely blocked by addition of 1 μmol/L of the specific ABCG2 inhibitor Ko143 [43] to the cell culture medium (Fig. 1B). We have shown previously that resistance to nucleoside or nucleobase analogs caused by the ABC transporters ABCC4 and ABCC5 is due to transport of the corresponding nucleoside monophosphates formed in the cell [10]. To determine which form of cladribine is transported by ABCG/Abcg2, we used a recently developed HPLC-tandem mass spectrometry method that can separate cladribine and cladribine monophosphate, diphosphate, and triphosphate [31].

We analyzed the medium and cell lysates from 4 h Transwell transport assays in which 10 μmol/L cladribine was added to either the medium at the basolateral or the apical side of the MDCKII monolayer. The results of these experiments are summarized in Fig. 2 and Table 2.

The striking result is that more than 99% of the transported compounds were identified as cladribine under all conditions. Whereas parental cells effluxed similar amounts of cladribine apically and basolaterally, the presence of ABCG2 or Abcg2 in the cells increased efflux at the apical side and reduced basolateral efflux to minimal values. Only low levels of 2-CdAMP were formed intracellularly, even in parental MDCKII cells, suggesting that deoxycytidine kinase levels are low in these cells. Nevertheless, the increased appearance of 2-CdAMP in the apical medium from ABCG2/Abcg2-overexpressing cells compared with WT MDCKII cells (Table 2A) indicated that 2-CdAMP is a substrate of ABCG2/Abcg2. The possibility that 2-CdAMP levels were underestimated due to 2-CdAMP dephosphorylation by extracellular 5′-nucleotidases after extrusion from the cell was excluded by addition of 5′-nucleotidase inhibitors to the medium: Addition of high concentrations (100 μmol/L) of the inhibitors AMP-PCP and ARL67156 had no effect on 2-CdAMP levels (results not shown). No CdADP or CdATP was detectable in the medium and these compounds are presumably not transported by ABCG2/Abcg2. In WT cells, 2-CdAMP was effluxed more into the basolateral than into the apical medium, suggesting the presence of an endogenous transporter at the basolateral membrane, which is capable of 2-CdAMP transport. This could be a member of the ABCC family, as efflux was inhibited >90% by 100 μmol/L indomethacin, a general inhibitor of ABCC-type transporters (results not shown; ref. [44].

The 2-CdAMP efflux observed is a complex function of the rate of cladribine transport and the side of the monolayer to which cladribine is added. In the ABCG2-transfected cells, apical efflux of cladribine is moderately increased, but there is still sufficient 2-CdAMP formed in the cell (Fig. 2C and D; Table 2) to allow ABCG2 to substantially increase 2-CdAMP efflux relative to WT cells at the apical side, without influencing efflux at the basolateral side (Fig. 2B). In the Abcg2-transfected cells, the apical efflux of cladribine is strongly increased. This appears to result in

such a reduced level of intracellular cladribine—intracellular cladribine concentrations were consistently below the limit of detection and could therefore not be measured—that transport of cladribine from apical to basolateral virtually ceases (Fig. 2A; Table 2). As a consequence, also 2-CdAMP synthesis is reduced, explaining why the apical efflux of 2-CdAMP relative to ABCG2-transfected cells is reduced and why basolateral efflux is nearly abolished.

The side at which cladribine is added to the monolayer affects the amount of 2-CdAMP effluxed into the basolateral medium. In both ABCG2- and Abcg2-transfected cells, more 2-CdAMP tends to come out basolaterally when cladribine is added basolaterally than when it is added apically (ABCG2 cells: 23.5 versus 8.8 pmol, P = 0.1; Abcg2 cells: 3.4 versus 0.7 pmol, P = 0.002). This indicates that the presence of ABCG2/Abcg2 in the apical membrane results in a locally low intracellular cladribine concentration near the apical membrane.

Table 2. Levels of cladribine and metabolites in medium and cell lysates of MDCKII, MDCKII-ABCG2, and MDCKII-Abcg2 cells after a 4 h transepithelial transport assay

MDCKII	WT	ABCG2	Abcg2
A			
Apical Medium			
Cladribine	1348.4 ± 108.7	2794.7 ± 108.8	4480.2 ± 753.8
CdAMP	3.4 ± 1.1	22.4 ± 6.6	12.1 ± 3.3
Basolateral Medium			
Cladribine	5963.2 ± 166.9	4484.6 ± 167.1	3533.1 ± 655.8
CdAMP	19.7 ± 6.3	23.5 ± 6.9	3.4 ± 0.4
Lysate			
CdAMP	6.6 ± 0.7	2.6 ± 1.0	0.4 ± 0.1
CdADP	1.5 ± 0.2	0.5 ± 0.2	0.0 ± 0.0
CdATP	4.2 ± 0.5	1.3 ± 0.5	0.2 ± 0.0
B			
Basolateral Medium			
Cladribine	1270.2 ± 37.4	357.9± 78.8	56.1 ± 11.0
CdAMP	11.1 ± 2.8	8.8 ± 3.4	0.7 ± 0.0
Apical Medium			
Cladribine	5966.4 ± 60.5	6874.3 ± 237.7	7269.6 ± 176.8
CdAMP	7.2 ± 2.2	21.6 ± 10.2	9.3 ± 1.4
Lysate			
CdAMP	5.6 ± 0.4	1.6 ± 0.5	0.3 ± 0.1
CdADP	1.1 ± 0.1	0.3 ± 0.1	0.0 ± 0.0
CdATP	3.4 ± 0.3	0.8 ± 0.3	0.1 ± 0.1

A) Cladribine (750 µl, 10 µmol/L) was added to the basolateral compartment at t=0, B) Cladribine (750 µl, 10 µmol/L) was added to the apical compartment at t=0. Cladribine and metabolites were measured and quantified as described in materials and methods. Values are mean ± SE (in pmol) of three independent experiments in duplicate.

If cladribine is added at the apical side, drug entering the cell is immediately pumped out. If it is added at the basolateral side, it has to diffuse through the cell to the apical membrane before it can be pumped out, thereby setting up a diffusion gradient within the cell with higher cladribine concentrations near the basolateral membrane and hence more 2-CdAMP synthesis than near the apical membrane.

Because the cytotoxic effect of cladribine mainly results from its conversion into 2-CdATP and its subsequent incorporation into DNA, it is important to note that the 2-CdATP concentrations in the ABCG2/Abcg2-transfected cells are much lower than in the WT cells explaining the substantial resistance to cladribine observed in these cells (Fig. 2C and D; Table 1).

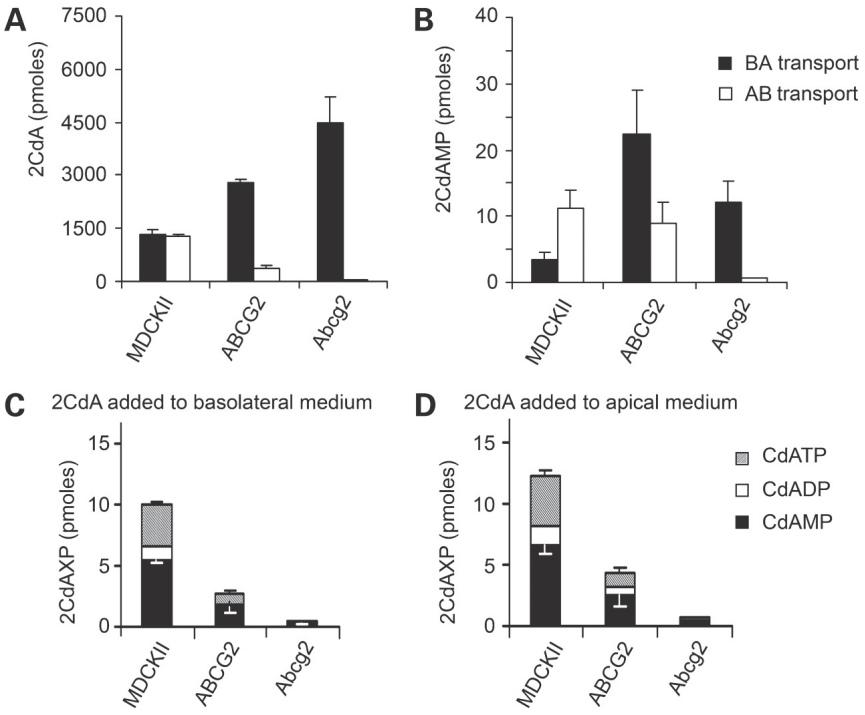

Figure 2. Transport and appearance of cladribine and its metabolites in medium and cell lysate 10 µmol/L (7,500 pmol) cladribine was added to the apical or basolateral medium of monolayer cultures of MDCKII-parental, MDCKII-mAbcg2, or MDCKII-hABCG2 cells for 4 h after which the amount of effluxed (**A**) cladribine (2-CdA) or (**B**) cladribine monophosphate (2-CdAMP) was determined in medium in the opposite compartment. No cladribine diphosphate or triphosphate was detected in medium. The intracellular appearance of the cladribine metabolites: 2-CdAMP (▪), 2-CdADP (□), and 2-CdATP ( ), in incubations in which cladribine was added either (**C**) basolaterally or (**D**) apically was also determined. Intracellular cladribine levels were under the detection limit of 20 nmol/L, which equals 9 pmol/lysate.

Because over 99% of total transported substrate was cladribine, we determined the apparent affinity (Km) of ABCG2 for cladribine from net transport curves with radiolabeled substrate (Fig. 4): transport in MDCKII-ABCG2/Abcg2 monolayers minus that in MDCKII parental monolayers. This affinity is only very approximate, as the cladribine concentration in the medium is only distantly related to the intracellular cladribine concentration seen by the transporter. ABCG2 had a higher affinity for cladribine than the murine orthologue (80 ± 7 versus 248 ± 26 µmol/L). On the other hand, the velocity of cladribine transport by Abcg2 was much higher than that of ABCG2 with Vmax values of 121 ± 4 versus 17 ± 0.5 nmol (monolayer) 4 h−1. We think that the possible difference in the amount of ABCG2/Abcg2 in the cell membrane (Supplementary Fig. S1) is not enough to explain this difference in velocity and that the Abcg2 present may be more active.

To test whether other ABC transporters can transport cladribine as well, additional Transwell assays were conducted with MDCKII monolayers overexpressing the genes for ABCC transporters 1 to 5 as well as ABCB1. We did not find an increased efflux of [3H]cladribine to the apical (ABCB1, ABCC2) or basolateral (ABCC1, ABCC3, ABCC4, and ABCC5) medium in any of these cell lines (result not shown). From these experiments, we infer that none of these ABC-transporters transport cladribine.

Vesicular Transport of Cladribine and 2-CdAMP by ABCG2/Abcg2

To determine kinetic variables for the transport of cladribine and 2-CdAMP by ABCG2/Abcg2, we tested both substrates in vesicular transport by vesicles from Sf9 or HEK293 cells overexpressing ABCG2 or Abcg2. No transport was observed with [^{3}H]cladribine. Presumably, cladribine is transported into the vesicles but leaks out through equilibrative nucleoside transporters or by passive diffusion. We therefore tested cladribine transport in an indirect fashion by determining its ability to competitively inhibit uptake of [^{3}H]methotrexate into Sf9 vesicles.

The experiments were done at pH 7.4 rather than at pH 5.5, where transport rates are higher [45], to make the results obtained comparable with those of the Transwell experiments done at pH 7.4. The affinity of Abcg2 for methotrexate, not determined previously, proved to be similar to that of ABCG2 at about 2 mmol/L, in line with published data [45-47]. Similar values were obtained with Sf9 (Fig. 4A) and HEK293 (Fig. 4B) vesicles. Cladribine inhibited methotrexate transport in a competitive fashion, inhibition being higher at 0.5 than at 4 mmol/L methotrexate. Human ABCG2 was much more inhibited than the murine Abcg2, the apparent inhibitory constants K_i being about 50 and 300 to 400 µmol/L (Fig. 4). This is in agreement with the Transwell experiments in which the apparent K_m of ABCG2 for cladribine was much lower than of Abcg2 (Fig. 3).

Obtaining kinetic variables for CdAMP uptake was unexpectedly complicated. At low CdAMP concentrations, vesicles from WT Sf9 cells bound significant amounts of [^{3}H]CdAMP and this apparent accumulation was not prevented by addition of nonhydrolyzable ATP analogs (not shown). The nature of this association of [^{3}H]CdAMP with the vesicles is not known. To assess transport by ABCG2, we corrected all values for CdAMP accumulation by ABCG2-Sf9 and Abcg2-Sf9 vesicles with the values obtained with WT vesicles. With these corrections, CdAMP uptake by ABCG2/Abcg2 was linear for about 10 min (not shown) and transport was saturable as shown in Supplementary Fig. S2. At the high CdAMP concentrations required for saturation, the values are inaccurate because of the relatively low specific radioactivity of the [^{3}H]CdAMP available. Hence, only approximate values for the kinetic variables can be deduced. For ABCG2, we find in Sf9 cells in three experiments a K_m of about 148 µmol/L (range, 126-165) and a V_{max} of about 775 pmol/mg protein/min (range, 578-984). For the Abcg2, data are even less accurate, and in two experiments, we find an average K_m of about 0.5 mmol/L and a V_{max} of 0.4 nmol/mg protein/min. Compared with other ABCG2 substrates, these rates of transport are substantial, but the affinity for this substrate is relatively low.

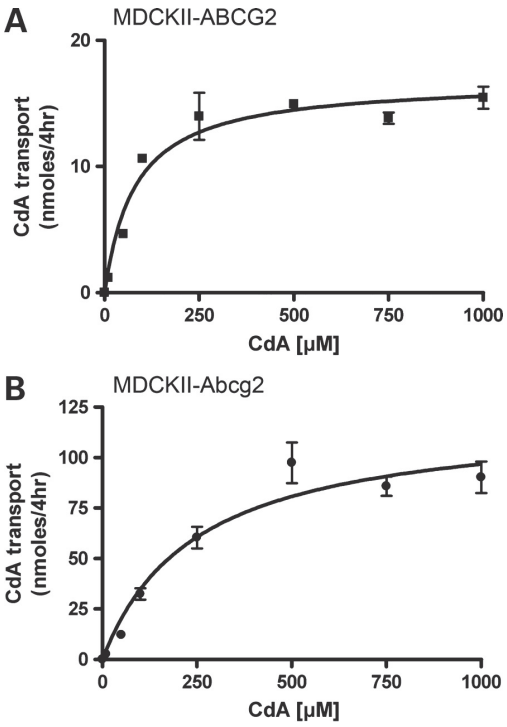

Figure 3. Transport of [3H]cladribine by human ABCG2 and mouse Abcg2. Monolayers of MDCKII-parental, MDCKII-mAbcg2, and MDCKII-hABCG2 cells were incubated with increasing concentrations of cladribine for 4 h. At t = 0, drug was added to the apical or basal compartment and the percentage transport was calculated from the amount of radioactive label appearing in the opposite compartment. Values are net transport (transport measured in apical medium from ABCG2/Abcg2-overexpressing cells minus transport measured in apical medium from parental cells). Mean ± SE of two experiments in duplicate.

Transport of 6-MP by Human and Mouse ABCG2/Abcg2

ABCG2/Abcg2 conferred increased resistance in cytotoxicity assays to both 6-MP and 6-MP riboside in both cell lines tested, MDCKII and HEK293 (Table 1). Also, the directional transport of [^{14}C]6-MP in epithelial transport assays with monolayers of MDCKII cells was higher in the basal to apical direction in ABCG2/Abcg2-overexpressing cells than in WT cells and this increased rate was reduced to WT levels on addition of the ABCG2-specific inhibitor Ko143 (results not shown). Preliminary HPLC data indicate that 6-MP riboside as well as the monophosphate metabolite, tIMP, is transported by ABCG2/Abcg2 (unpublished data).

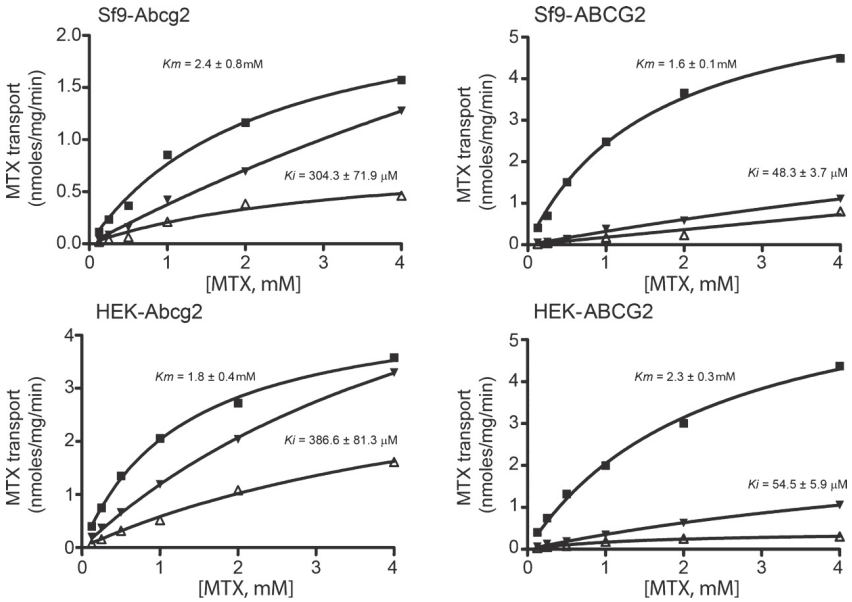

Figure 4. Kinetics of cladribine transport by human ABCG2 and mouse Abcg2. Competition by a fixed concentration of cladribine of transport of increasing concentrations of [3H]methotrexate by Abcg2 and ABCG2 in vesicular uptake studies with vesicles prepared from Sf9 insect cells or HEK cells. The concentrations of added cladribine were 0 μmol/L (▪), 500 μmol/L (▾), and 1,000 μmol/L (▵).

Discussion

We have found that ABCG2 can cause resistance to several nucleobase and nucleoside analogs used in cancer chemotherapy in addition to its effect on the antiretroviral nucleosides zidovudine and lamivudine [17;18]. Remarkably, ABCG2 transports not only the nucleoside monophosphate metabolite of cladribine—in analogy with other ABC transporters that can cause resistance to nucleobase and nucleoside analogs [6;11;12;14]—but also cladribine itself. Presumably, this holds also for (some of) the other nucleoside analogs affected by ABCG2, such as clofarabine, fludarabine, and 6-MP riboside. Our preliminary results for 6-MP confirm this assumption (unpublished data). Moreover, while our work was being finished, Pan et al. [48] reported evidence that the antiretroviral nucleosides zidovudine and abacavir are transported as nucleosides as well by Abcg2.

In the cell clones used here, transport of cladribine by Abcg2 was more effective than by ABCG2. Presumably, this is due to a higher catalytic activity of Abcg2 than ABCG2, as the affinity of Abcg2 for cladribine seems to be lower rather than higher than that of ABCG2 (Figs. 3 and 4). The results in Table 2 indicate that, at high transport rates of ABCG2/Abcg2, the effects on nucleoside transport contribute more to resistance than the effects on transport of 2-CdAMP: in the Abcg2 transfectant, intracellular 2-CdAMP is reduced 16-fold relative to WT cells. This cannot be due to increased 2-CdAMP transport, because both apical and basolateral efflux of 2-CdAMP are actually decreased relative to the ABCG2 transfectant. This implies that high concentrations of Abcg2 can reduce intracellular cladribine concentrations to such an extent that synthesis of 2-CdAMP is lowered. This is quite an accomplishment of Abcg2 given the high rate at which cladribine enters the cells via nucleoside transporters.

Obviously, the potential effect of the presence of ABCG2/Abcg2 on toxicity of cladribine to cells must depend on the ability of several metabolic processes to compete with export of cladribine/2-CdAMP by the transporter: the rate of influx of cladribine via nucleoside transporters, the rate of conversion of cladribine into 2-CdAMP by cytosolic deoxycytidine kinase and mitochondrial deoxyguanosine kinase [4], and the conversion into 2-CdADP and 2-CdATP, which can be the rate-limiting step in 2-CdATP synthesis [49]. It is of interest that ABCG2/Abcg2 appears to transport clofarabine at least as efficiently as cladribine (Fig. 1; Table 1). Clofarabine has clinical advantages over cladribine and fludarabine, because it can be administered orally (reviewed in ref. [50]. ABCG2 is prominently present in the apical membrane of the intestinal epithelium and is known to interfere with drug uptake [21-23]. It will be of interest to test in Abcg2−/− mice [20] whether Abcg2 affects oral availability of clofarabine.

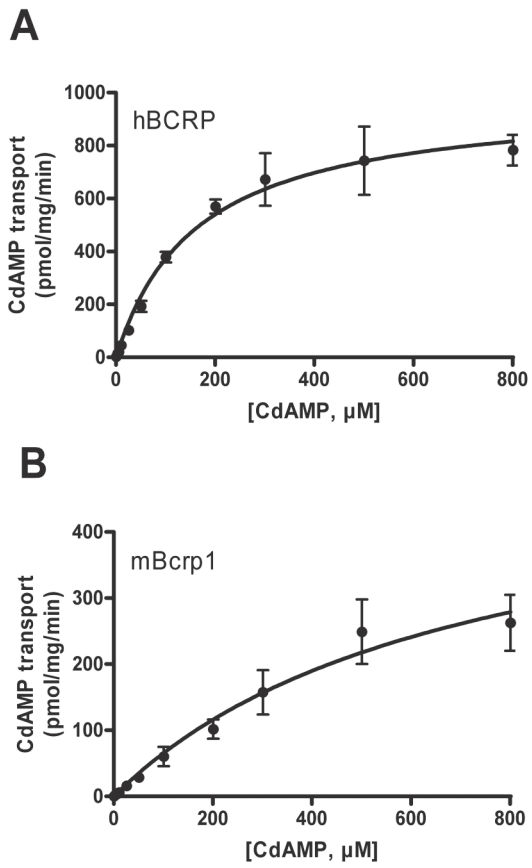

Supplementary Fig. 2 Vesicular Uptake of CdAMP by ABC transporters. A. Uptake of CdAMP by vesicles from ABCG2-Sf9 cells as function of CdAMP concentration. Vesicles were incubated with 3H-CdAMP for 6 min. and uptake was measured as described in the Methods section. The values presented are average ± SD and corrected for uptake by wild-type cell vesicles in the presence of ATP. B. As A, but Abcg2-Sf9 vesicles.

References

[1] J. Zhang, F. Visser, K. M. King, S. A. Baldwin, J. D. Young, C. E. Cass, Cancer Metastasis Rev. 26 (2007) 85.
[2] M. Podgorska, K. Kocbuch, T. Pawelczyk, Acta Biochim. Pol. 52 (2005) 749.
[3] M. Staub and S. Eriksson, in G. J. Peters (Editor), Deoxycytidine analogs in cancer therapy, Humana press, Totowa, 2006, p. 29.
[4] B. Munch-Petersen and J. Piskur, in G. J. Peters (Editor), Deoxycytidine analogs in cancer therapy, Humana press, Totowa, 2006, p. 53.
[5] J. D. Schuetz, M. C. Connelly, D. Sun, S. G. Paibir, P. M. Flynn, R. V. Srinivas, A. Kumar, A. Fridland, Nat. Med. 5 (1999) 1048.
[6] Z. S. Chen, K. Lee, G. D. Kruh, J. Biol. Chem. 276 (2001) 33747.
[7] M. Adachi, G. Reid, J. D. Schuetz, Adv. Drug Deliv. Rev. 54 (2002) 1333.
[8] O. Turriziani, J. D. Schuetz, F. Focher, C. Scagnolari, J. Sampath, M. Adachi, F. Bambacioni, E. Riva, G. Antonelli, Biochem. J. 368 (2002) 325.
[9] M. Adachi, J. Sampath, L. B. Lan, D. Sun, P. Hargrove, R. Flatley, A. Tatum, M. Z. Edwards, M. Wezeman, L. Matherly, R. Drake, J. Schuetz, J. Biol. Chem. 277 (2002) 38998.
[10] P. R. Wielinga, G. Reid, E. E. Challa, d. H. van, I, L. Van Deemter, M. De Haas, C. Mol, A. J. Kuil, E. Groeneveld, J. D. Schuetz, C. Brouwer, R. A. De Abreu, J. Wijnholds, J. H. Beijnen, P. Borst, Mol. Pharmacol. 62 (2002) 1321.
[11] G. Reid, P. Wielinga, N. Zelcer, M. De Haas, L. Van Deemter, J. Wijnholds, J. Balzarini, P. Borst, Mol. Pharmacol. 63 (2003) 1094.
[12] S. Pratt, R. L. Shepard, R. A. Kandasamy, P. A. Johnston, W. Perry, III, A. H. Dantzig, Mol. Cancer Ther. 4 (2005) 855.
[13] P. Borst and P. Wielinga, in G. J. Peters (Editor), Deoxycytidine analogs in cancer therapy, Humana press, Totowa, 2006, p. 109.
[14] T. Imaoka, H. Kusuhara, M. Adachi, J. D. Schuetz, K. Takeuchi, Y. Sugiyama, Mol. Pharmacol. 71 (2007) 619.
[15] J. Wijnholds, C. A. Mol, L. Van Deemter, M. De Haas, G. L. Scheffer, F. Baas, J. H. Beijnen, R. J. Scheper, S. Hatse, E. De Clercq, J. Balzarini, P. Borst, Proc. Natl. Acad. Sci. U. S. A 97 (2000) 7476.
[16] Y. Guo, E. Kotova, Z. S. Chen, K. Lee, E. Hopper-Borge, M. G. Belinsky, G. D. Kruh, J. Biol. Chem. 278 (2003) 29509.
[17] X. Wang, T. Furukawa, T. Nitanda, M. Okamoto, Y. Sugimoto, S. Akiyama, M. Baba, Mol. Pharmacol. 63 (2003) 65.
[18] X. Wang, T. Nitanda, M. Shi, M. Okamoto, T. Furukawa, Y. Sugimoto, S. Akiyama, M. Baba, Biochem. Pharmacol. 68 (2004) 1363.
[19] K. Takenaka, J. A. Morgan, G. L. Scheffer, M. Adachi, C. F. Stewart, D. Sun, M. Leggas, K. F. Ejendal, C. A. Hrycyna, J. D. Schuetz, Cancer Res. 67 (2007) 6965.
[20] A. E. van Herwaarden, A. H. Schinkel, Trends Pharmacol. Sci. 27 (2006) 10.
[21] B. Sarkadi, L. Homolya, G. Szakacs, A. Varadi, Physiol Rev. 86 (2006) 1179.
[22] R. W. Robey, O. Polgar, J. Deeken, K. W. To, S. E. Bates, Cancer Metastasis Rev. 26 (2007) 39.
[23] A. E. van Herwaarden, E. Wagenaar, G. Merino, J. W. Jonker, H. Rosing, J. H. Beijnen, A. H. Schinkel, Mol. Cell Biol. 27 (2007) 1247.
[24] G. Jedlitschky, B. Burchell, D. Keppler, J. Biol. Chem. 275 (2000) 30069.
[25] R. A. van Aubel, P. H. Smeets, J. G. Peters, R. J. Bindels, F. G. Russel, J. Am. Soc. Nephrol. 13 (2002) 595.
[26] P. R. Wielinga, d. H. van, I, G. Reid, J. H. Beijnen, J. Wijnholds, P. Borst, J. Biol. Chem. 278 (2003) 17664.
[27] G. Jedlitschky, K. Tirschmann, L. E. Lubenow, H. K. Nieuwenhuis, J. W. Akkerman, A. Greinacher, H. K. Kroemer, Blood 104 (2004) 3603.

[28] C. J. de Wolf, H. Yamaguchi, d. H. van, I, P. R. Wielinga, S. L. Hundscheid, N. Ono, G. L. Scheffer, M. De Haas, J. D. Schuetz, J. Wijnholds, P. Borst, FEBS J. 274 (2007) 439.
[29] T. Kovacs, L. Otvos, Tetrahedron Letters 29 (1988) 4525.
[30] B. Fischer, J. L. Boyer, C. H. Hoyle, A. U. Ziganshin, A. L. Brizzolara, G. E. Knight, J. Zimmet, G. Burnstock, T. K. Harden, K. A. Jacobson, J. Med. Chem. 36 (1993) 3937.
[31] R. S. Jansen, H. Rosing, C. J. de Wolf, J. H. Beijnen, Rapid Commun. Mass Spectrom. 21 (2007) 4049.
[32] P. Pavek, G. Merino, E. Wagenaar, E. Bolscher, M. Novotna, J. W. Jonker, A. H. Schinkel, J. Pharmacol. Exp. Ther. 312 (2005) 144.
[33] J. W. Jonker, J. W. Smit, R. F. Brinkhuis, M. Maliepaard, J. H. Beijnen, J. H. Schellens, A. H. Schinkel, J. Natl. Cancer Inst. 92 (2000) 1651.
[34] F. Michiels, R. A. van der Kammen, L. Janssen, G. Nolan, J. G. Collard, Methods Enzymol. 325 (2000) 295.
[35] J. W. Jonker, M. Buitelaar, E. Wagenaar, M. A. Van Der Valk, G. L. Scheffer, R. J. Scheper, T. Plosch, F. Kuipers, R. P. Elferink, H. Rosing, J. H. Beijnen, A. H. Schinkel, Proc. Natl. Acad. Sci. U. S. A 99 (2002) 15649.
[36] P. Skehan, R. Storeng, D. Scudiero, A. Monks, J. McMahon, D. Vistica, J. T. Warren, H. Bokesch, S. Kenney, M. R. Boyd, J. Natl. Cancer Inst. 82 (1990) 1107.
[37] P. Breedveld, N. Zelcer, D. Pluim, O. Sonmezer, M. M. Tibben, J. H. Beijnen, A. H. Schinkel, O. van Tellingen, P. Borst, J. H. Schellens, Cancer Res. 64 (2004) 5804.
[38] N. Zelcer, T. Saeki, G. Reid, J. H. Beijnen, P. Borst, J. Biol. Chem. 276 (2001) 46400.
[39] R. Allikmets, L. M. Schriml, A. Hutchinson, V. Romano-Spica, M. Dean, Cancer Res. 58 (1998) 5337.
[40] J. D. Allen, R. F. Brinkhuis, J. Wijnholds, A. H. Schinkel, Cancer Res. 59 (1999) 4237.
[41] V. L. Damaraju, S. Damaraju, J. D. Young, S. A. Baldwin, J. Mackey, M. B. Sawyer, C. E. Cass, Oncogene 22 (2003) 7524.
[42] K. M. King, V. L. Damaraju, M. F. Vickers, S. Y. Yao, T. Lang, T. E. Tackaberry, D. A. Mowles, A. M. Ng, J. D. Young, C. E. Cass, Mol. Pharmacol. 69 (2006) 346.
[43] J. D. Allen, A. van Loevezijn, J. M. Lakhai, d. van, V, O. van Tellingen, G. Reid, J. H. Schellens, G. J. Koomen, A. H. Schinkel, Mol. Cancer Ther. 1 (2002) 417.
[44] M. P. Draper, R. L. Martell, S. B. Levy, Br. J. Cancer 75 (1997) 810.
[45] P. Breedveld, D. Pluim, G. Cipriani, F. Dahlhaus, M. A. van Eijndhoven, C. J. de Wolf, A. Kuil, J. H. Beijnen, G. L. Scheffer, G. Jansen, P. Borst, J. H. Schellens, Mol. Pharmacol. 71 (2007) 240.
[46] E. L. Volk, E. Schneider, Cancer Res. 63 (2003) 5538.
[47] Z. S. Chen, R. W. Robey, M. G. Belinsky, I. Shchaveleva, X. Q. Ren, Y. Sugimoto, D. D. Ross, S. E. Bates, G. D. Kruh, Cancer Res. 63 (2003) 4048.
[48] G. Pan, N. Giri, W. F. Elmquist, Drug Metab Dispos. 35 (2007) 1165.
[49] N. E. Van den, S. Cardoen, F. Offner, F. Bontemps, Int. J. Oncol. 27 (2005) 1113.
[50] V. Gandhi and W. Plunkett, in G. J. Peters (Editor), Deoxycytidine analogs in cancer therapy, Humana press, Totowa, 2006, p. 153.

Chapter 3.2

Oral Administration of Gemcitabine in Patients with Refractory Tumors: A Clinical and Pharmacologic Study

Stephan A Veltkamp, Robert S Jansen, Sophie Callies, Dick Pluim, Carla M Visseren-Grul, Hilde Rosing, Susanne Kloeker-Rhoades, Valerie AM Andre, Jos H Beijnen, Christopher A Slapak and Jan HM Schellens

Clinical Cancer Research
Volume 14, Issue 11, Pages 3477-86
2008

Abstract

Purpose: To determine the toxicity, tolerability, pharmacokinetics, pharmacodynamics, and preliminary antitumor activity of oral gemcitabine (2',2'-difluorodeoxycytidine; dFdC) in patients with cancer.

Experimental Design: Patients with advanced or metastatic cancer refractory to standard therapy were eligible. Gemcitabine was administered p.o. starting at 1 mg once daily using dose escalation with three patients per dose level. Patients received one of two dosing schemes: (a) once daily dosing for 14 days of a 21-day cycle or (b) every other day dosing for 21 days of a 28-day cycle. Pharmacokinetics were assessed by measuring concentrations of dFdC and 2',2'-difluorodeoxyuridine (dFdU) in plasma and gemcitabine triphosphate in peripheral blood mononuclear cells, and pharmacodynamics by measuring the effect on T-cell proliferation.

Results: Thirty patients entered the study. Oral gemcitabine was generally well-tolerated. The maximum tolerated dose was not reached. Mainly moderate gastrointestinal toxicities occurred except for one patient who died after experiencing grade 4 hepatic failure during cycle two. One patient with a leiomyosarcoma had stable disease during 2 years and 7 months. Systemic exposure to dFdC was low with an estimated bioavailability of 10%. dFdC was highly converted to dFdU, probably via first pass metabolism and dFdU had a long terminal half-life (~89 h). Concentrations of dFdCTP in peripheral blood mononuclear cells were low, but high levels of gemcitabine triphosphate, the phosphorylated metabolite of dFdU, were detected.

Conclusions: Systemic exposure to oral gemcitabine was low due to extensive first-pass metabolism to dFdU. Moderate toxicity combined with hints of activity warrant further investigation of the concept of prolonged exposure to gemcitabine.

Introduction

Gemcitabine (2',2'-difluorodeoxycytidine; dFdC) is used in the treatment of patients with various solid tumors [1;2]. It is currently formulated in an i.v. solution (Gemzar) and usually administered as 30-minute infusion at a dose of 1,000 to 1,250 mg/m^2 on days 1 and 8 of a 21-day or days 1, 8, and 15 of a 28-day cycle. Gemcitabine is taken up into cells by nucleoside transporters [3] and is intracellularly phosphorylated to gemcitabine monophosphate by deoxycytidine kinase (EC 2.7.1.74) and subsequently converted by other kinases into its active diphosphate and triphosphate (dFdCTP) forms [1;4]. dFdCTP competes with the natural substrate dCTP for incorporation into DNA, thereby inhibiting DNA synthesis [5;6] and blocking cells in the early S phase of the cell cycle [7]. In addition, gemcitabine diphosphate inhibits ribonucleotide reductase [8] ultimately resulting into depletion of dCTP pools and enhanced incorporation of dFdCTP into DNA. Moreover, gemcitabine can potentiate its own cytotoxic effect via other pathways [6;9]. Besides, dFdC is extensively deaminated by cytidine deaminase (EC 3.5.4.5; ref. [9]) into 2',2'-difluorodeoxyuridine (dFdU), which has been reported to be present mainly in liver of humans and kidney of mice [10]. Clinical studies showed that dFdU has a long terminal half-life ($t_{1/2}$, ~50 h) and is largely excreted in the urine (>90% of the dose; ref. [11]).

Preclinical studies showed that the efficacy and tolerability of gemcitabine was highly dose schedule dependent [1;12]. Clinical studies suggested that protracted or continuous administration of i.v. gemcitabine results in higher antitumor activity in cancer patients [13;14]. dFdCTP levels have been measured in peripheral blood mononuclear cells (PBMC) and leukemic cells of patients treated with i.v. gemcitabine to investigate the pharmacokinetics of gemcitabine [15-17]. Intracellular exposure to dFdCTP and its incorporation into DNA increased with the gemcitabine concentration [5] and dFdCTP accumulation correlated with gemcitabine cytotoxicity [18-20]. Pharmacodynamics of gemcitabine can be explored by measuring the effect on T-cell proliferation, which was shown to be inhibited by gemcitabine at low nanomolar concentrations [21;22].

It was postulated that continuous treatment with oral gemcitabine might be efficacious in human malignancies and that p.o. dosing would be more convenient for patients than i.v. administration. Oral gemcitabine showed antitumor activity against human colon, lung, and prostate tumor xenografts in mice after once daily dosing for 14 days (0.5-3 mg/kg) and every other day dosing for seven doses (1.25-10 mg/kg)(unpublished data). Marginal hematologic toxicity and dose-responsive intestinal lesions and enteropathy were found in mice after single oral gemcitabine administration at high doses [23].

Based on the promising antitumor activity in several human tumor xenografts and the marginal hematologic toxicity in preclinical models, a

phase I study was started to investigate the feasibility of oral gemcitabine at a continuous dosing schedule in patients with advanced solid tumors. The following dosing schedules were investigated: once daily dosing for 14 days of a 21-day cycle (part A) or every other day dosing for 21 days of a 28-day cycle (part B). Because of the observation of dose-limiting intestinal lesions in mice [23], a starting dose of 0.6 mg/m^2/day corresponding to 1 mg/day was chosen for part A.

The objectives of this study were to determine the following: (*a*) the toxicity, tolerability, and maximum tolerated dose (MTD); (*b*) preliminary antitumor activity; and (*c*) the pharmacokinetics and pharmacodynamics of oral gemcitabine for both dosing schedules.

Patients and methods

Eligibility

Patients with histologically or cytologically confirmed advanced and/or metastatic cancer for which no treatment of higher priority existed were eligible. Other eligibility criteria were as follows: age of ≥18 y, performance status of ≤2 on the Eastern Cooperative Oncology Group scale, and an estimated life expectancy of ≥3 mo. Previous chemotherapy, hormonal therapy, and radiotherapy had to be discontinued for at least 4 wk before study entry and 6 wk in the case of mitomycin-C or nitrosourea. Patients had to have adequate bone marrow function, defined as absolute neutrophil count of ≥1.5 x 10^9/L, platelets of ≥100 x 10^9/L, and hemoglobin of ≥5.6 mmol/L, and adequate renal and hepatic function defined as serum creatinine of ≤1.5 of the upper limit of normal (ULN), serum bilirubin of ≤1.5 times of the ULN, and alanine transaminase (ALT) and aspartate transaminase (AST) of ≤2.5 times of the ULN (or ≤5 of times the ULN in the case of tumor involvement in the liver). The study protocol was approved by the local Medical Ethics Committee and all patients had to give written informed consent.

Treatment plan and study design

Patients started with gemcitabine once daily for 14 d of a 21-day cycle (part A). Gemcitabine was p.o. administered as capsule(s) with one glass of tap water within 1 h after breakfast. Cohorts of three patients per dose level were used. A low flat starting dose of 1 mg and the introduction of 1 wk of rest were chosen based on the preclinical toxicology studies and criteria by DeGeorge et al [24]. If no dose-limiting toxicity (DLT) was reported in the first three patients at any dose level, the dose was escalated. Dose levels were initially set at 2, 4, 8, 12, 15, and 20 mg. If one DLT occurred, three additional patients were enrolled at that dose level. DLTs were defined as any of the following events occurring during the first treatment cycle and related to study treatment: any grade 4 hematologic toxicity lasting longer than 5 d, or grade 3 or grade 4 nonhematologic toxicity (except for untreated nausea and vomiting). The MTD was defined as one dose level below the dose level at which two of six patients experienced a DLT. By protocol, part B was planned to start upon identification of the MTD in part A. In part B, patients were to receive oral gemcitabine every other day for 21 d of a 28-day cycle. The starting dose in part B was planned to be at the established MTD for part A because toxicity in part B was expected to be milder. Subsequently, dose escalation proceeded to the next dose levels. An additional six patients were planned to be treated at the dose level determined to be the MTD for part B.

Drug formulation

Gemcitabine (LY188011) was provided by Eli Lilly and Company as capsules containing gemcitabine as hydrochloride salt equivalent to 1, 5, or 15 mg of gemcitabine. The capsules were stored in the refrigerator at 2°C to 8°C

Patient evaluation and follow-up

Pretreatment evaluation included a complete medical history and physical examination, vital signs, electrocardiogram, chest X-ray, hematology (hemoglobin, WBC, platelets, neutrophils, and lymphocytes), serum chemistry (bilirubin, alkaline phosphatase, AST, ALT, blood urea nitrogen, creatinine, calcium, glucose, total protein, albumin, sodium, and potassium), and pregnancy test (if indicated). Before each cycle, the physical examination and vital signs were repeated, hematology and serum chemistry were checked, and any concomitant medication was noted. During each cycle, hematology was checked on day 7 and 14 in part A and day 7, 14, and 21 in part B (±3 d). Serum chemistry was checked on day 7 in part A and day 14 in part B (±3 d). All toxicities were graded according to the Common Toxicity Criteria version 2.0. If hematologic toxicity (absolute neutrophil count is $<1.0 \times 10^9$/L for 5 d or platelets are $<50 \times 10^9$/L) or nonhematologic toxicity (grade 3/4, excluding nausea and vomiting) was observed within a cycle, the dose was reduced or was held until recovery and retreatment was allowed according to protocol. No new cycle of gemcitabine was allowed unless the absolute neutrophil count was $\geq 1.0 \times 10^9$/L and platelets were $\geq 100 \times 10^9$/L. If treatment was held for longer than 3 wk for toxicity reasons, the patient had to be removed from the study. Dose adjustments had to take into account the capsule strengths available (1, 5, and 15 mg), and therefore, dose reductions had to be rounded down to the nearest increment. Tumor assessments were done by radiological imaging and/or tumor measurement of palpable or visible examination at baseline and day 1 of every other cycle and were evaluated according to the RECIST criteria [25].

Analysis of dFdC and dFdU in plasma

Blood samples were collected during cycle 1 on day 1 and 2 at 0.5, 1, 2/3, 4, 6, 8, and 24 h after oral gemcitabine administration. On day 14 (part A) and 21 (part B) samples were collected at the following time points: predose, 0.5, 1, 2, 4, 6, 8, 24, 48 to 72 h, and 7 d (day 21 of 28; ± 1 day) after p.o. intake of gemcitabine. Blood samples of 3 mL of venous blood were drawn into sodium-heparinized tubes containing 500 µg tetrahydrouridine and immediately centrifuged at 4°C for 5 min at 1,500 x *g*. Plasma was collected and stored at −20°C until analysis. Analytic standards of dFdC and dFdU and $[^{13}C_2][^{15}N_3]$-dFdC and $[^{13}C_4][^{15}N_2]$-dFdU (internal standards) were obtained from Eli Lilly. Plasma samples were vortex mixed and centrifuged at 2,000 x *g* for 5 min, and 100 µL of plasma were transferred into a 2.0 mL

well of a 96-wells plate. The same was done for the analytical standards, quality controls, and blank plasma. Three-hundred µL of Milli-Q were transferred to blank plasma and 300 µL of internal standards working solution were added to the samples. An OASIS column for solid-phase extraction was conditioned by 500 µL methanol and 500 µL Milli-Q. The samples with internal standards were mixed 5 times, transferred to the extraction plate, and washed with 500 µL Milli-Q. Then, dFdC, dFdU, and internal standards were eluted with 200 µL methanol. The eluate was collected and evaporated until dryness under nitrogen at 65°C for 45 min. Samples were reconstituted in 200 µL Milli-Q, vortex mixed, centrifuged at 2,000 x *g* for 5 min, and the supernatant was collected. Separation of the analytes was done by reversed phase high pressure liquid chromatography using an Ace 5 C18 HL column maintained at room temperature. The mobile phase consisted of a mixture of water (A) and methanol with 1% formic acid (B) using the following gradient: t = 0: 100% A; t = 0.25 min: 25% B; t = 2.0 min: 100% B; and t = 3.0 min: 100% A. The injection volume was 20 µL and the total run time was 4 min. The analytes were quantified using a tandem mass spectrometer with a turbo V ionspray source operating in the positive ion mode. The ionspray voltage was kept at 3.5 kV with a source temperature of 650°C. The following mass-to-charge (*m/z*) transitions were monitored: *m/z* 264 to 112 for dFdC, *m/z* 265 to 113 for dFdU, *m/z* 269 to 117 for $[^{13}C_2][^{15}N_3]$-dFdC, and *m/z* 271 to 119 for $[^{13}C_4][^{15}N_2]$-dFdU. The interassay accuracy for dFdC ranged from 0.1% to 6.5% and the interassay precision ranged from 2.0% to 3.7%, whereas for dFdU, the interassay accuracy ranged from –1.2% to 6.9% and the interassay precision ranged from 1.3% to 6.8%. The lower and upper limit of quantification of both dFdC and dFdU in human plasma were 0.5 and 500 ng/mL, respectively.

Analysis of dFdCTP in PBMCs

Blood samples were collected during cycle 1 on day 1 and 14 (part A) or 21 (part B) at 1, 4, 8, and 24 h and on day 21 (part A) or 28 (part B; ± 1 day) after p.o. administration of gemcitabine. Blood samples of 15 mL of venous blood were drawn in sodium-heparinized tubes, centrifuged at 4°C for 5 min at 1,500 x *g*, PBMCs were isolated, and dFdCTP concentrations were determined as described previously using our validated liquid chromatography-tandem mass spectrometry assay [26]. The lower limit of quantification of dFdCTP in PBMCs was 0.277 ng/mg protein corresponding to 0.047 ng/10^6 cells (94 fmol per 10^6 cells).

To investigate whether dFdUTP, the triphosphate form of dFdU, was formed in PBMCs, the *m/z* transition of 503 to 159 was monitored. Blank human PBMCs were added to the reference compound dFdUTP and the response ratio (including ion suppression and mass spectrometry response) was determined. We compared the response ratio of dFdCTP to internal standards with dFdUTP to internal standards and used this factor to quantify the response ratios in the PBMC samples based on the dFdCTP

to internal standards calibration curve. Internal standards, dFdCTP, and dFdUTP had similar elution times.

T-cell proliferation assay

An explorative functional T-cell proliferation assay was used to characterize the effect of the treatment on T-cell proliferation in patients as a pharmacodynamic surrogate marker for bone marrow toxicity and or activity of oral gemcitabine. T-cell proliferation index (PI) of both CD_4^+ and CD_8^+ T cells was determined during cycle 1. In brief, samples were taken on day 1 (predose), on day 14 (part A) and 21 (part B) 1 h after p.o. dosing, and on day 21 (part A) and 28 (part B; ±1 day). Samples of healthy volunteers were taken as a control. For each sample, 16 mL whole blood was collected in BD Vacutainer CPT tubes with sodium citrate, and after centrifugation, PBMCs were isolated and resuspended in medium. Cells were counted, and 0.5×10^6 PBMCs in 1 mL were plated in 9 wells of a 24-well plate; 3 wells were used for flow cytometry settings, 2 for internal positive control, and 4 wells for the samples (2 of these wells were precoated with anti-CD3 to stimulate T-cell proliferation). Cells were cultured for 3 d. Then, 10 µL of anti–CD4-FITC and anti–CD8-phycoerythrin antibody were added to 500 µL of the samples. After washing and centrifugation, cells were taken up in 450 µL washing buffer. A volume of 50 µL of flow count beads was added to all samples. Both CD_4^+ and CD_8^+ T cells were counted within 1 h using fluorescent-activated cell sorting. The PI was calculated by the ratio of cell number after stimulation and cell number without stimulation of proliferation.

Pharmacokinetics/pharmacodynamics analysis

The pharmacokinetic variables of dFdC and dFdU in plasma, and of dFdCTP and dFdUTP in PBMCs were determined by noncompartmental analysis using WinNonLin version 5.0.1. The area under the plasma concentration time curve up to 24 h (AUC_{0-24}) was determined and up to the last measured concentration-time point extrapolated to infinity ($AUC_{0-\infty}$) using the trapezoidal method. The maximal observed drug concentration (C_{max}) was obtained directly from the experimental data. The $t_{1/2}$ was determined for dFdU. PI values of T cells were calculated as described above. The pharmacokinetic variables were reported as median and range. Statistical analysis was done with SPSS version 12.1.1. Paired Student's *t* tests were applied on the log-transformed values of the pharmacokinetic variables to investigate the differences between day 14 (part A) or 21 (part B) and day 1. ANOVA and Bonferoni *post hoc* tests were conducted to investigate any differences in PI between day 1, 14, and 21 (part A) and 1, 21, and 28 (part B). Differences were considered to be statistically significant at *P* value of <0.05.

A Bayesian analysis using WinBUGS version 1.4 was applied to the dFdC pharmacokinetic data. The model fitted was a two-compartment

disposition pharmacokinetics model with first-order absorption rate constant. The distribution of the pharmacokinetics variables in the population was assumed to be log normal. Previously reported pharmacokinetics variables after i.v. gemcitabine 500 to 3,600 mg/m^2 in 353 patients were used as informative priors for the total and intercompartmental clearance, and the central and peripheral volume of distribution [11;27]. These studies with i.v. gemcitabine 1,000 mg/m^2 as 30 min infusion showed a median C_{max} of dFdC of 40,000 ng/mL (range, 28,000-52,000 ng/mL) and indicated a dose and time-independent clearance of dFdC and dFdU. In addition, cytidine deaminase has a reported K_m for gemcitabine of 290 ± 20 µmol/L corresponding to 76,850 ± 5,300 ng/mL [28]. These data indicate no saturation of cytidine deaminase after i.v. administration of gemcitabine at clinical doses.

Results

Patient characteristics, dose-levels tested, and main drug-related toxicities.

Thirty patients were treated in this study and their characteristics are presented in Table 1 . The following dose-levels of gemcitabine were tested: 1, 2, 4, 6, and 8 mg (part A) and 8, 12, 16, and 20 mg (part B). Oral gemcitabine was generally well-tolerated without any DLTs, except for one patient treated with 8 mg daily gemcitabine as described below. All patients were evaluable for safety. Toxicity data are presented in Table 2 . The most prominent drug-related nonhematologic toxicities were nausea (37% of patients) and vomiting (30% of patients). Hematologic toxicity was mild and did not exceed Common Toxicity Criteria grade 2.

In part A, a total of 39 drug related adverse events were experienced by 11 of 18 patients; 74% of these were ≤grade 2. In part B, 19 adverse events were experienced by 6 of 12 patients; all ≤grade 2 (Table 2). Of these 58

Table 1. Patient characteristics

		n
Gender	Male	21
	Female	9
Age	Median	58
	Range	24-73
Race	Caucasian	28
	Hispanic	1
	Other	1
Tumor types	Colon	2
	Adenocarcinoma of unknown primary	3
	Sarcoma	5
	Lung adenocarcinoma	1
	Prostate	4
	Rectum	2
	Cholangiocarcinoma	1
	Ovarian	3
	Cervical	1
	Pappilary adenocarcinoma	1
	Pancreas adenocarcinoma	2
	Vater's papil	1
	Parotis gland adenocarcinoma	1
	Squamous cell carcinoma	1
	Mesothelioma	1
	Melanoma	1
Performance status	0	3
	1	21
	2	6
Previous therapy	Hormonal therapy	4
	Radiotherapy	16
	Surgery	22
	Chemotherapy	26

Table 2. Drug-related toxicities: maximum grade across all cycles per dosing regimen and dose-level.

Adverse events		Part A						Part B				
Dose-levels (mg)		1	2	4	6	8	Total	8	12	16	20	Total
No. of patients evaluable		3	3	6	3	3	18	3	3	3	3	12
Hematologic	CTC Grade											
Anemia	1	1	0	0	0	0	1	0	0	0	0	0
	2	0	0	0	0	1	1	0	0	0	0	0
Leucocytopenia**	1	0	0	1	0	0	1	0	0	1	0	1
Neutropenia**	1	0	0	0	0	0	0	0	0	1	0	1
Thrombocytopenia**	1	0	0	1	0	1	2	1	0	1	0	2
Non-hematologic												
Vomiting	1	0	1	0	0	0	1	0	0	0	2	2
	2	0	0	0	0	2	2	1	0	0	0	1
	3	1	0	2	0	0	3	0	0	0	0	0
Nausea	1	0	1	2	0	1	4	1	1	1	1	4
	2	0	0	0	0	0	0	0	0	0	1	1
	3	0	0	1	0	1*	2	0	0	0	0	0
Fatigue	1	0	1	0	1	0	2	0	0	0	0	0
	2	0	0	1	0	1	2	0	0	0	0	0
	3	0	0	0	0	1*	1	0	0	0	0	0
Anorexia	1	0	0	0	0	0	0	0	0	0	1	1
	3	0	0	0	0	1*	1	0	0	0	0	0
DIC	3	0	0	0	0	1*	1	0	0	0	0	0
Diarrhea	1	1	1	0	0	0	2	0	0	0	0	0
	2	0	0	2	0	0	2	0	0	0	0	0
Constipation	1	1	0	1	0	0	2	0	0	0	0	0
	2	0	0	1	0	0	1	0	0	0	0	0
Abdominal pain	1	0	0	0	1	0	1	0	0	0	0	0
	2	0	0	0	0	0	0	0	0	1	0	1
Headache	2	0	0	0	0	0	0	0	0	0	1	1
GI (other)	2	0	0	0	0	0	0	0	0	0	1	1
Renal (other)	2	0	1	0	0	0	1	0	0	0	0	0
Stomatitis/pharyngitis	2	0	0	1	0	0	1	0	0	0	0	0
Alopecia	1	0	0	0	0	0	0	0	1	0	0	1
Fever	1	0	0	1	0	0	1	0	0	0	0	0
Myalgia	1	0	0	0	0	0	0	0	0	0	1	1
Neuropathy	1	0	0	1	0	0	1	0	0	0	0	0
Rigors	1	0	0	0	0	0	0	0	0	0	1	1
Elevated AST	4	0	0	0	0	1*	1	0	0	0	0	0
Elevated ALT	4	0	0	0	0	1*	1	0	0	0	0	0
Elevated creatinine	2	0	1	0	0	0	1	0	0	0	0	0

Data are reported as number of patients

DIC, disseminated intravascular coagulation; GI, gastrointestinal; AST, aspartate transaminase; ALT, alanine transaminase.

* Grade 3/4 toxicities in the single patient with severe hepatic and renal failure.

** Not designated as drug related on the case report form

observed adverse events, 55% were grade 1, 28% were grade 2, and 17% were grade 3 and 4 (corresponding to 4 patients in part A). Gastrointestinal-related toxicities (i.e., vomiting, nausea, abdominal pain, constipation, diarrhea, and anorexia) corresponded to 53% and 50% of the grade 1 and grade 2 adverse events, respectively. In part A, 54% of the toxicities were gastrointestinal related of which 52% were grade 2/3, and in part B, 53% were gastrointestinal related of which 30% were grade 2/3.

Fourteen patients experienced one or more serious adverse events, of which only 4 patients in part A (1 at 1 mg, 2 at 4 mg, and 1 at 8 mg) experienced serious adverse events related to the study drug. For three of these patients, the nature of these serious adverse events were vomiting and nausea and were not considered DLTs. A 68-year-old male with an adenocarcinoma of unknown primary (ACUP) treated once daily with 8 mg oral gemcitabine was considered to have a toxic death. The first cycle was almost uneventful. However, 9 days after the initiation of the second cycle, he developed fever (temperature, 38.8°C), followed by the following DLTs: grade 4 liver and kidney failure with rapid steep increases in ALT (2,424 U/L) and AST (2,781 U/L), γ-GT (237 U/L), lactate dehydrogenase (3,360 U/L), ureum (24, 6 mmol/L), and creatinine (200 μmol/L); grade 3 fatigue; nausea; anorexia; and grade 3 disseminated interstitial coagulation. All cultures were negative. Ultrasound of liver and kidney showed normal caliber of liver and biliary ducts, with however, an aberrant corticomedullar differentiation and a strongly reduced blood flow in the left kidney. Treatment with oral gemcitabine and comedication (simvastatin, irbesartan/hydrochloorthiazide, oxazepam, and omeprazol) were stopped, and the patient was given i.v prednisone 1 mg/kg. Despite this, his clinical situation deteriorated, and 5 days later, the patient died. Obduction revealed severe toxic induced liver necrosis, which was likely related to the study drug. Other possible causes for severe liver toxicity, such as viral infections (hepatitis B and C), liver metastasis, and alcohol abuse were excluded and an interaction between gemcitabine and comedication was unlikely.

Due to this lethal toxicity, the dose of the other patient on 8 mg daily treatment was deescalated to 4 mg, and this dose level was expanded by inclusion of 3 extra patients. Review of safety and pharmacokinetic data of the first 18 patients enrolled in five dose levels (1, 2, 4, 6, and 8 mg) in part A led to the pharmacologically driven decision to stop enrollment in part A in the absence of a MTD. The exposure to dFdC and dFdCTP was low and variable at all dose levels. It was expected that the dosing schedule in part B would allow higher doses of oral gemcitabine to be safely administered, possibly leading to increased dFdC exposure. Dose escalation in part B was carried out from 8 to 12, 16, up to 20 mg and stopped at that level in the absence of a MTD because of the low systemic exposure to dFdC and dFdCTP.

Response

Twenty-seven of the 30 patients were evaluable for response. The total number of cycles of therapy completed by all patients was 112. Seven patients (23%) had stable disease and 20 patients (67%) developed progressive disease. Of the 7 patients with stable disease, 5 subjects were treated in part A at the dose levels of 2 mg (n = 1), 4 mg (n = 2), 6 mg (n = 1), and 8 mg (n = 1), and 2 subjects were treated in part B at the dose levels of 12 mg (n = 1) and 16 mg (n = 1). The patients with stable disease had the following tumor types: leiomyosarcoma (1x; 39 cycles), cholangiocarcinoma (1x; 2 cycles), ovarian carcinoma (1x; 4 cycles), ACUP (2x; 2 and 2 cycles each), adenocarcinoma of the pancreas (1x; 8 cycles), and adenocarcinoma of the parathyroid gland (1x; 6 cycles). One female with advanced leiomyosarcoma who had been treated with doxorubicin and ifosfamide received 2 mg oral gemcitabine once daily for 14 days of a 3-weekly cycle. She tolerated the therapy well with only a few delays in the start of new treatment cycles due to 2- to 3-fold increased liver enzyme values that were also present before start of therapy [at start: AST, 66 U/L (ULN, 40 U/L); ALT, 124 U/L (ULN, 45 U/L)]. She had stable disease for 27 cycles of therapy and then had to switch to 5 mg every other day for 21 days of a 4-weekly cycle because the supply of 1 mg capsules was exhausted. She received another 12 cycles of therapy. After having stable disease for 39 cycles, the therapy was stopped because she developed increased liver enzyme values (AST, 180 U/L; ALT, 246 U/L), which was likely caused by oral gemcitabine. Treatment had to be held for >3 weeks as a result of the increased liver function tests, and the patient was required by protocol to stop study treatment. She was on study for 2 years and 7 months. Concentrations of dFdC and dFdU in plasma and levels of dFdCTP in PBMCs during cycle 1 were comparable with those of the other patients.

Pharmacokinetics/pharmacodynamics of gemcitabine

Blood sampling was done in all 30 patients. The pharmacokinetic variables of dFdC, dFdU, dFdCTP, and dFdUTP are shown in Table 3A and B. Concentration versus time profiles are depicted in Fig. 1 , and C_{max} values are shown in Fig. 2 . Systemic exposure to dFdC was low at all dose levels due to extensive first-pass metabolism to dFdU, and no dose-dependent increase in exposure to dFdC was observed (Figs. 1 and 2). For dFdC, C_{max} values are presented only because AUC and $t_{1/2}$ could not be precisely calculated. Median bioavailability of gemcitabine was estimated at 10% (range, 5-17%). Because the study was terminated, it was decided not to give the patients a low dose of i.v. gemcitabine that was planned at the end of the study for calculation of the bioavailability of oral gemcitabine.

The systemic exposure to dFdU increased with dose after single and multiple administration and showed accumulation after once daily and every other day dosing of oral gemcitabine (Figs. 1 and 2).

Table 3A. Pharmacokinetic variables of dFdC and dFdU in plasma and dFdCTP and dFdUTP in PBMCs after once-daily dosing of oral gemcitabine (Part A).

Variable Dose levels (mg)	1	2	4	6	8
Day 1					
Number of evaluable patients	3	3	6	3	3
dFdC					
C_{max} (ng/mL)	1.1	0.6 (0.5 - 0.7)	1.6 (0.7 - 7.7)	0.8 0.6 – 1.1)	2.3 0.6 – 3.5
dFdU					
C_{max} (ng/mL)	13 (13-15)	27 (25-31)	60 (46-90)	88 (53-113)	127 (111-137)
AUC_{0-24} (h*ng/mL)	277 (76-320)	471 (379-487)	1139 (957-1609)	1709 (1146-2022)	2379 (2338-2889)
dFdCTP					
C_{max} (ng/mg protein)	0.41 (0.33 - 0.48)	0.9 (0.6 - 1.3)	1.3 (0.3 - 4.1)	1.7 (0.5-2.0)	3.3 (1.4-4.8)
AUC_{0-24} (h*ng/mg protein)	5.0 (1.3 - 8.7)	4.3 (2.9 - 5.7)	19 (0.2 - 45)	26 (0.2-28)	36 (19-63)
dFdUTP					
C_{max} (ng/mg protein)	0.9 (0.7-1.0	0.7 (0.4-0.9)	2.1 (1.2-33)	5.9 (1.5-7.4)	4.6 (4.1-6.2)
AUC_{0-24} (h*ng/mg protein)	13 (8.0-18	4.7 (4.4-4.9)	38 (16-178)	97 (27-131)	64 (42-88)
Day 14					
Number of evaluable patients	2	3	5	3	2
dFdC					
C_{max} (ng/mL)	n.a.	n.a.	1.7 (0.7-7.2)	1.4	4.4 (2.7-6.2)
dFdU					
C_{max} (ng/mL)	78 (57-99)	107 (40-121)	325 (246-374)	368 (320-499)	631 (620-645)
AUC_{0-24} (h*ng/mL)	1695 (1216-2173)	2147 (653-2353)	7002 (5055-7480)	8473 (6971-11538)	13747 (13119-14375)
$t_{1/2}$ (h)	106 (81-130)	46 (16-157)	89 (58-146)	209 (58-249)	101 (86-115)
dFdCTP					
C_{max} (ng/mg protein)	0.7 (0.5-0.9	1.1 (0.9-1.1)	2.7 (0.9-9.9)	3.1 (1.5-4.7)	4.1 (3.2-5.0)
AUC_{0-24} (h*ng/mg protein)	2.2 (1.7-2.7)	6.8 (0.6-15)	29 (13-87)	28 (22-33)	40 (31-49)
dFdUTP					
C_{max} (ng/mg protein)	1.3 (1.1-1.5	3.3 (2.2-4.4)	9.0 (5.0-18)	13 (6-13)	28 (17-39)
AUC_{0-24} (h*ng/mg protein)	23 (20-25	55 (40-71)	143 (107-281)	129 (101-228)	467 (240-694)

Data are presented as median and range. N.a., not available; individual values are given if n < 3.

Table 3B. Pharmacokinetic variables of dFdC and dFdU in plasma and dFdCTP and dFdUTP in PBMCs after every other day-dosing of oral gemcitabine (Part B).

Variable Dose levels (mg)	8	12	16	20
Day 1				
Number of evaluable patients	3	3	3	3
dFdC				
C_{max} (ng/mL)	1.6 (0.7-2.5)	3.5 (2.0-6.7)	2.7 (1.8-6.6)	6.8 (2.6-12)
dFdU				
C_{max} (ng/mL)	150 (117-155)	221 (151-301)	373 (311-532)	333 (286-469)
AUC_{0-24} (h*ng/L)	2582 (2280-3292)	3736 (2991-6472)	7833 (6804-7896)	6207 (5167-6797)
dFdCTP				
C_{max} (ng/mg protein)	2.2 (1.4-2.5)	6.5 (1.3-8.2)	2.6 (1.9-5.8)	4.3 (1.1-4.7)
AUC_{0-24} (h*ng/mg protein)	24 (7.0-40)	69 (23-87)	14 (12-68)	15 (4.3-72)
dFdUTP				
C_{max} (ng/mg protein)	3.0 (2.4-3.8)	4.0 (2.5-5.0)	7.7 (4.3-11)	n.a.
AUC_{0-24} (h*ng/mg protein)	47 (41-69)	38 (28-47)	76 (48-151)	n.a.
Day 21				
Number of evaluable patients	3	3	3	3
dFdC				
C_{max} (ng/mL)	6.3 (1.9-6.3)	2.2 (2.1-5.8)	1.7 (0.6-4.1)	2.3 (1.6-6.2)
dFdU				
C_{max} (ng/mL)	365 (303-445)	746 (488-908)	974 (757-1078)	825 (791-1134)
AUC_{0-24} (h*ng/mL)	14125 (11245-16432)	24823 (17496-29066)	33235 (24471-36547)	32552 (21435-39674)
$t_{1/2}$ (h)	84 (79-103)	80 (76-104)	48 (34-59)	49 (39-79)
dFdCTP				
C_{max} (ng/mg protein)	1.7 (1.5-2.9)	4.7 (1.6-9.5)	3.4 (2.9-3.8)	1.4 (1.2-4.5)
AUC_{0-24} (h*ng/mg protein)	26 (6.7-62)	72 (26-130)	20 (13-32)	18 (7.5-29)
dFdUTP				
C_{max} (ng/mg protein)	5.2 (4.8-8.7)	11 (6.2-15)	14	n.a.
AUC_{0-24} (h*ng/mg protein)	151 (97-438)	211 (112-310)	248	n.a.

Data are presented as median and range. N.a., not available; individual values are given if n<3

This is explained by the long $t_{1/2}$ of dFdU. As expected, accumulation of dFdU was approximately twice as high after once daily (≈5- to 6- fold) compared with every other day dosing (≈2.5- to 3-fold; Fig. 2).
From the pharmacokinetics of i.v. gemcitabine, it is known that almost all of the administered gemcitabine dose (>90%) is excreted into the urine as dFdU [11]; hence, the fraction of the total gemcitabine dose that is converted into dFdU (F_m) is almost 1. The pharmacokinetics data for dFdU, after oral gemcitabine administration, support the estimation of an apparent dFdU clearance (Cl/($F*F_m$) = Dose/AUC; F = bioavailability) of 0.5 L/h and of a $t_{1/2}$ of 89 h. With F_m being close to 1, the apparent clearance of dFdU can be considered as Cl/F. After i.v. gemcitabine, the $t_{1/2}$ of dFdU is ≈ 50 hours and Cl/F is ≈1 to 2 L/h. The differences in Cl/F and $t_{1/2}$ of dFdU after oral and i.v. administration of gemcitabine show that first-pass metabolism is the rate-limiting step in the pharmacokinetics of dFdU after p.o. administration; hence, dFdC is metabolized in the liver and dFdU is slowly released into the systemic circulation. Thus, the pharmacokinetics of dFdU after p.o. administration of gemcitabine is indicative of a "flip-flop" phenomenon.

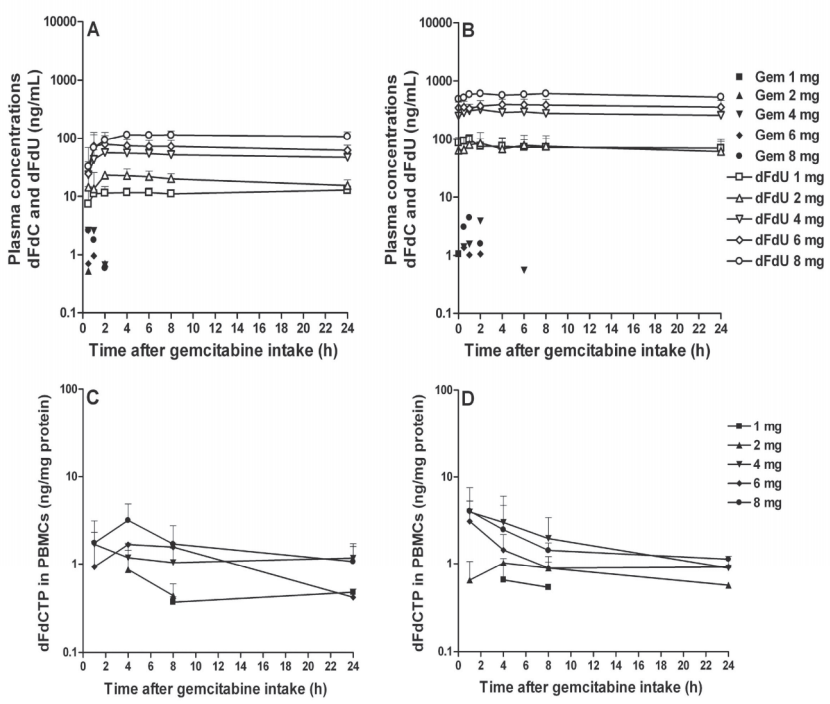

Figure 1. Concentration versus time curves of dFdC (ng/mL) and dFdU (ng/mL) in plasma on day 1 (A) and 14 (B) and of dFdCTP in PBMCs (ng/mg protein) on day 1 (C) and 14 (D) after daily administration of oral gemcitabine. Points, mean on a semilogarithmic scale; bars, SD.

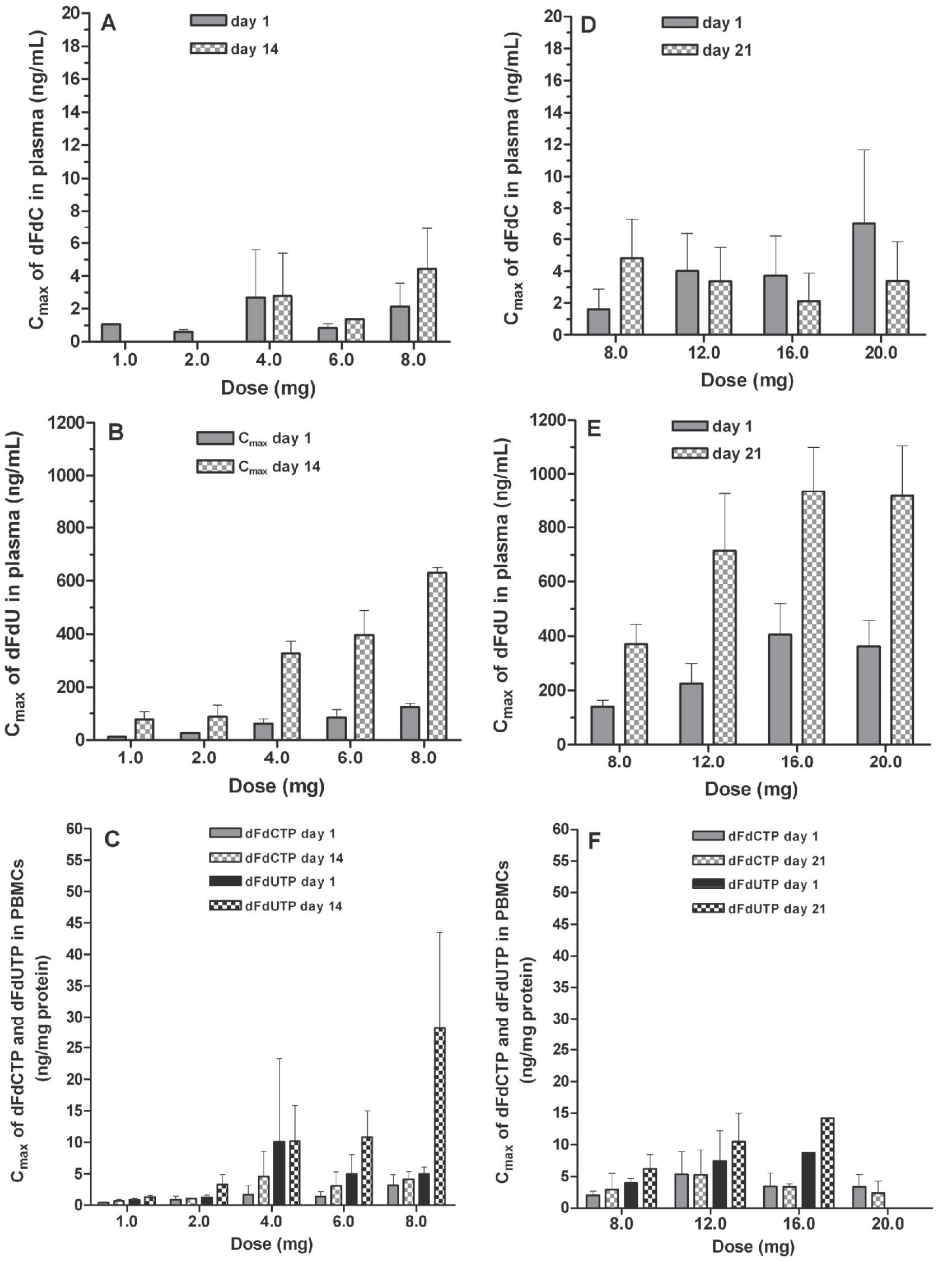

Figure 2. C_{max} of dFdC, dFdU, dFdCTP, and dFdUTP in Part A (A-C) and Part B (D-F) on day 1 and day 14 (Part A) and day 1 and 21 (Part B) after oral administration of gemcitabine. Columns, mean; bars, SD.

Concentrations of dFdCTP in PBMCs were detectable by our sensitive assay up to 24 hours after p.o. administration of low-dose gemcitabine. The C_{max} of dFdCTP slightly increased with dose (Fig. 2) but showed high interpatient variability. The mean AUC of dFdCTP in PBMCs (part A+B) was 32 h*ng/mg protein (~12.8 h*pmol per 10^6 cells) after single p.o. administration of 8 mg gemcitabine.

We hypothesized that dFdUTP was formed after administration of gemcitabine. Indeed, a significant peak eluting just after the dFdCTP peak was detected and dFdUTP eluted at the same retention time as the peak in the patient samples. Exposure to dFdUTP was higher compared with dFdCTP at almost all dose levels. C_{max} and AUC of dFdUTP increased with dose of oral gemcitabine (Table 3 and Fig. 2; dFdUTP levels were available for all patients, except for the patients at the 20 mg dose level). The mean value of the dose normalized AUC of dFdUTP (AUC dFdUTP/gemcitabine dose) for all dose levels in part A after single dosing on day 1 (11 h*ng/mg protein) and multiple dosing on day 14 (35 h*ng/mg protein) was significantly higher ($P = 0.001$) than the dose normalized AUC of dFdCTP on day 1 (4.0 h*ng/mg protein) and day 14 (6.2 h*ng/mg protein).

The PI values of CD_4^+ and CD_8^+ T cells showed high interpatient variability. We recently determined that in cultured T cells from healthy volunteers ($n = 42$), the mean PI values of CD_4^+ and CD_8^+ T cells were 3.6 ± 1.9 and 3.2 ± 1.8, respectively (unpublished data). In this study, no significant effects of oral gemcitabine on T-cell PI were found, consistent with the low hematologic toxicity and low systemic exposure to gemcitabine. In part A, for example, the mean PI of CD_4^+ cells altered from 3.4 ± 2.6 on day 1 (predose) to 3.0 ± 2.6 on day 14 and to 3.9 ± 3.5 on day 21 ($P = 0.714$).

Discussion

In this clinical study, we administered gemcitabine p.o. to patients with advanced solid tumors for the first timeOverall, oral gemcitabine at low dose levels was well-tolerated. The study was discontinued mainly because of the unfavorable pharmacokinetics of dFdC. More precisely, once daily administration for 14 days of oral gemcitabine at a dose of 8 mg (corresponding to a 225-fold lower dose compared with i.v. gemcitabine 1,000 mg/m^2) resulted in the following mean systemic exposures: dFdC C_{max} of 4.4 ng/mL (~5,700-fold lower compared with i.v. gemcitabine), dFdU AUC_{0-24} of 13.8 x 10^3 h*ng/mL (~25-fold lower compared with i.v. gemcitabine), and dFdCTP AUC_{0-24} of 40 h*ng/mg protein or 13.5 h*pmol per 10^6 PBMCs (~100- to 200-fold lower compared with i.v. gemcitabine). After single i.v. gemcitabine, dFdCTP AUC_{0-24} values of ~1,400 h*pmol per 10^6 PBMCs [29-31] and a cumulative dFdCTP AUC >3 weeks of 9,700 h*pmol per 10^6 PBMCs have been reported [11]. These data illustrate the significant difference in pharmacokinetics of gemcitabine after p.o. and i.v. administration.

The main pattern of toxicity observed in this study is gastrointestinal toxicity, whereas hardly any hematologic toxicity was observed, probably consistent with the low systemic exposure to dFdC. The incidence of gastrointestinal-related toxicity was similar between part A and part B, although the severity seemed to be less in part B (every other day) compared with part A (once daily). In the single patient in part A with lethal liver and kidney toxicity, exposure levels to dFdC, dFdU, and dFdCTP were comparable with those of other patients. However, the exposure to dFdUTP in this patient was high, with an AUC of 694 h*pmol/mg protein on day 14, compared with the other patients, in which AUC levels ranged from 20 to 270 h*pmol/mg protein after multiple daily dosing.

The study was terminated before the MTD was achieved because of the unfavorable pharmacokinetics of oral gemcitabine (low exposure to dFdC and dFdCTP and long $t_{1/2}$ of dFdU) and the lethal liver toxicity observed in one patient. We hypothesized that there was a relationship between the pharmacokinetics findings and toxicity of oral gemcitabine. Therefore, we carried out preclinical studies to investigate cytotoxicity, uptake, metabolism, and biodistribution of dFdC, dFdU, and phosphorylated metabolites. In brief, in HepG2 cells, the IC_{50} values of dFdC and dFdU were ~1 nmol/L (~0.3 ng/mL) and 2.5 µmol/L (~660 ng/mL; ref. [32]), respectively, after 14 days of drug exposure, comparable with the concentrations found in patients in this study. Furthermore, we discovered that dFdUTP is formed (via deamination of gemcitabine monophosphate to dFdUMP and via phosphorylation of dFdU) and incorporated into DNA and RNA [33]. The long $t_{1/2}$ of dFdU and its accumulation in patients after continuous oral gemcitabine administration might result in pharmacologically relevant concentrations for prolonged periods of time,

and dFdU might contribute to the activity/toxicity of gemcitabine (e.g., by incorporation of dFdUTP into nucleic acids). Of note, accumulation of arabinofuranosyladenine-uridine triphosphate in leukemic blasts has been reported after treatment with cytarabine (1-β-D-arabinofuranosylcytosine) 0.5 g/m^2/h administered as 2- or 4-hour infusion [34].
The best response was stable disease in seven patients with a median duration of three cycles in six of seven patients. Remarkably, the patient with advanced leiomyosarcoma had stable disease during 39 cycles of therapy after low dose oral gemcitabine. Second-line treatment with single agent i.v. gemcitabine was shown to be active in patients with leiomyosarcoma [35;36].
In conclusion, this is the first study that tested oral administration of gemcitabine in patients. It shows that the systemic exposure to dFdC was low due to extensive first-pass metabolism to dFdU, which must be overcome to successfully deliver gemcitabine p.o. We discovered for the first time the formation of dFdUTP in PBMCs of patients. Recently, different approaches have been attempted to decrease deamination of dFdC to dFdU, such as coupling a long chain fatty acid or an isoprenoid chain of squalene to the terminal amino group of dFdC [37;38], thereby protecting it from deamination by cytidine deaminase. Whether these strategies might ultimately lead to higher intracellular concentrations of dFdC and its active phosphorylated metabolites, possibly leading to an increased cytotoxicity, has to be further elucidated

References

[1] L. W. Hertel, G. B. Boder, J. S. Kroin, S. M. Rinzel, G. A. Poore, G. C. Todd, G. B. Grindey, Cancer Res. 50 (1990) 4417.
[2] S. Noble, K. L. Goa, Drugs 54 (1997) 447.
[3] J. R. Mackey, S. Y. Yao, K. M. Smith, E. Karpinski, S. A. Baldwin, C. E. Cass, J. D. Young, J. Natl. Cancer Inst. 91 (1999) 1876.
[4] V. Heinemann, L. W. Hertel, G. B. Grindey, W. Plunkett, Cancer Research 48 (1988) 4024.
[5] P. Huang, S. Chubb, L. W. Hertel, G. B. Grindey, W. Plunkett, Cancer Res. 51 (1991) 6110.
[6] V. Heinemann, Y. Z. Xu, S. Chubb, A. Sen, L. W. Hertel, G. B. Grindey, W. Plunkett, Cancer Res. 52 (1992) 533.
[7] R. Grunewald, H. Kantarjian, M. Du, K. Faucher, P. Tarassoff, W. Plunkett, J. Clin. Oncol. 10 (1992) 406.
[8] V. Heinemann, Y. Z. Xu, S. Chubb, A. Sen, L. W. Hertel, G. B. Grindey, W. Plunkett, Mol. Pharmacol. 38 (1990) 567.
[9] W. Plunkett, P. Huang, Y. Z. Xu, V. Heinemann, R. Grunewald, V. Gandhi, Semin. Oncol. 22 (1995) 3.
[10] G. W. Camiener, C. G. Smith, Biochem. Pharmacol. 14 (1965) 1405.
[11] L. Zhang, V. Sinha, S. T. Forgue, S. Callies, L. Ni, R. Peck, S. R. Allerheiligen, J. Pharmacokinet. Pharmacodyn. 33 (2006) 369.
[12] B. J. Braakhuis, G. W. Visser, I. Stringer, G. J. Peters, Eur. J. Cancer 27 (1991) 250.
[13] J. L. Abbruzzese, R. Grunewald, E. A. Weeks, D. Gravel, T. Adams, B. Nowak, S. Mineishi, P. Tarassoff, W. Satterlee, M. N. Raber, ., J. Clin. Oncol. 9 (1991) 491.
[14] M. Tempero, W. Plunkett, v. H. Ruiz, V, J. Hainsworth, H. Hochster, R. Lenzi, J. Abbruzzese, J. Clin. Oncol. 21 (2003) 3402.
[15] J. R. Kroep, G. Giaccone, D. A. Voorn, E. F. Smit, J. H. Beijnen, H. Rosing, C. J. van Moorsel, C. J. van Groeningen, P. E. Postmus, H. M. Pinedo, G. J. Peters, J. Clin. Oncol. 17 (1999) 2190.
[16] S. R. Patel, V. Gandhi, J. Jenkins, N. Papadopolous, M. A. Burgess, C. Plager, W. Plunkett, R. S. Benjamin, J. Clin. Oncol. 19 (2001) 3483.
[17] J. M. Buesa, R. Losa, A. Fernandez, M. Sierra, E. Esteban, A. Diaz, A. Lopez-Pousa, J. Fra, Cancer 101 (2004) 2261.
[18] V. W. van Haperen, G. Veerman, J. B. Vermorken, H. M. Pinedo, G. Peters, Biochem. Pharmacol. 51 (1996) 911.
[19] A. C. Verschuur, A. H. Van Gennip, R. Leen, A. B. Van Kuilenburg, Nucleosides Nucleotides Nucleic Acids 23 (2004) 1517.
[20] v. H. Ruiz, V, G. Veerman, E. Boven, P. Noordhuis, J. B. Vermorken, G. J. Peters, Biochem. Pharmacol. 48 (1994) 1327.
[21] E. Alvino, M. P. Fuggetta, M. Tricarico, E. Bonmassar, Anticancer Res. 18 (1998) 3597.
[22] R. Margreiter, M. Fischer, K. Roberts, T. Schmid, A. Hittmair, M. Schirmer, F. Geisen, M. Tiefenthaler, G. Konwalinka, Transplantation 68 (1999) 1051.
[23] Horton, N. D., Young, J. K., Perkins, E. J., and Truex, L. L., Am Assoc Cancer Res45 (2004) 486.
[24] J. J. DeGeorge, C. H. Ahn, P. A. Andrews, M. E. Brower, D. W. Giorgio, M. A. Goheer, D. Y. Lee-Ham, W. D. McGuinn, W. Schmidt, C. J. Sun, S. C. Tripathi, Cancer Chemother. Pharmacol. 41 (1998) 173.
[25] P. Therasse, S. G. Arbuck, E. A. Eisenhauer, J. Wanders, R. S. Kaplan, L. Rubinstein, J. Verweij, M. Van Glabbeke, A. T. van Oosterom, M. C. Christian, S. G. Gwyther, J. Natl. Cancer Inst. 92 (2000) 205.
[26] S. A. Veltkamp, M. J. Hillebrand, H. Rosing, R. S. Jansen, E. R. Wickremsinhe, E. J. Perkins, J. H. Schellens, J. H. Beijnen, J. Mass Spectrom. 41 (2006) 1633.

[27] U.S. Food and Drug Administration - Center for Drug Evaluation and Research: Oncology Tools Product Label Details for Prescribing Gemcitabine. http://www.accessdata.fda.gov/scripts/cder/onctools/prescribe.cfm?GN=gemcitabine . 1998.
[28] J. A. Gilbert, O. E. Salavaggione, Y. Ji, L. L. Pelleymounter, B. W. Eckloff, E. D. Wieben, M. M. Ames, R. M. Weinshilboum, Clin. Cancer Res. 12 (2006) 1794.
[29] J. M. Rademaker-Lakhai, M. Crul, D. Pluim, R. W. Sparidans, P. Baas, J. H. Beijnen, N. van Zandwijk, J. H. Schellens, Anticancer Drugs 16 (2005) 1029.
[30] C. J. van Moorsel, J. R. Kroep, H. M. Pinedo, G. Veerman, D. A. Voorn, P. E. Postmus, J. B. Vermorken, C. J. van Groeningen, W. J. van der Vijgh, G. J. Peters, Ann. Oncol. 10 (1999) 441.
[31] B. C. Kuenen, L. Rosen, E. F. Smit, M. R. Parson, M. Levi, R. Ruijter, H. Huisman, M. A. Kedde, P. Noordhuis, W. J. van der Vijgh, G. J. Peters, G. F. Cropp, P. Scigalla, K. Hoekman, H. M. Pinedo, G. Giaccone, J. Clin. Oncol. 20 (2002) 1657.
[32] Veltkamp, S. A., Ong, F. H., Bolijn, M. J., Garcia-Ribas, I., Beijnen, J. H., and Schellens, J. H., Naunyn Schmiedebergs Arch Pharmacol (2007) 145.
[33] Veltkamp, S. A., van Eijndhoven, M. A., Pluim, D., Bolijn, M. J., Jansen, R. S., Garcia-Ribas, I., Wickremsinhe, E. R., Beijnen, J. H., and Schellens, J. H., Am Assoc Cancer Res48 (2007) 366.
[34] V. Gandhi, Y. Z. Xu, E. Estey, Clin. Cancer Res. 4 (1998) 1719.
[35] K. Y. Look, A. Sandler, J. A. Blessing, J. A. Lucci, III, P. G. Rose, Gynecol. Oncol. 92 (2004) 644.
[36] N. Silvestris, D. Piscitelli, E. Crucitta, M. Fiore, M. De Lena, V. Lorusso, J. Chemother. 15 (2003) 507.
[37] F. Castelli, M. G. Sarpietro, M. Ceruti, F. Rocco, L. Cattel, Mol. Pharm. 3 (2006) 737.
[38] P. Couvreur, B. Stella, L. H. Reddy, H. Hillaireau, C. Dubernet, D. Desmaele, S. Lepetre-Mouelhi, F. Rocco, N. Dereuddre-Bosquet, P. Clayette, V. Rosilio, V. Marsaud, J. M. Renoir, L. Cattel, Nano. Lett. 6 (2006) 2544.

Chapter 3.3

Deoxyuridine analog nucleotides in deoxycytidine analog treatment: secondary active metabolites?

Robert S Jansen, Hilde Rosing, Jan HM Schellens and Jos H Beijnen

Submitted for publication

Abstract

Deoxycytidine analogs (dCa's) are nucleosides widely used in anti-cancer and anti-(retro)viral therapies. Intracellularly phosphorylated dCa anabolites are considered to be their main active metabolites. In this article the literature on the formation and pharmacological activity of deaminated dCa nucleotides is reviewed. Most dCa's are rapidly deaminated into deoxyuridine analogs (dUa's) which are only slowly phosphorylated and therefore relatively inactive. dUa nucleotides are, however, also formed via deamination of readily formed dCa monophosphates by deoxycytidine monophosphate deaminase (dCMPD) and subsequent phosphorylation. dUa-monophosphates can interact with thymidylate synthase (TS), whereas dUa-triphosphates can interfere with polymerases and are incorporated into nucleic acids. Administration of dCa's as monophosphate prodrugs and co-administration of the CDA inhibitor tetrahydrouridine (THU) do not prevent dUa nucleotide formation which is, on the other hand, influenced by the dose and dCMPD activity. It is concluded that formation of dUa nucleotides is a common phenomenon in treatment with dCa's and that these compounds may play a role in treatment outcome. We conclude that more attention should be given to these relatively unknown, but potentially important metabolites.

Introduction

Deoxycytidine analogs (dCa's) like ara-C and dFdC (figure 1) are extensively used in anti-cancer [1] but also in anti-viral therapies. Nucleoside analogs are prodrugs that require intracellular phosphorylation to become active (figure 2). dCa nucleosides enter the cell through nucleoside transporters after which they are converted into their monophosphate (dCaMP) by deoxycytidine kinase (dCK**;** EC 2.7.1.74). Subsequent phosphorylation results in formation of their di- (dCaDP) and finally triphosphate (dCaTP), which is the main active metabolite. dCa-triphosphates are substrate for, or inhibit DNA and RNA polymerases slowing down cell proliferation or viral replication.

Many dCa nucleosides are sensitive to intra- and extracellular deamination by the ubiquitous enzyme cytidine deaminase (CDA; EC 3.5.4.5), often resulting in relatively inactive deoxyuridine analogs (dUa). Deamination can also occur on the monophosphate level by deoxycytidine monophosphate deaminase (dCMPD; EC 3.5.4.12) resulting in dUa-monophosphates (dUaMP). Like dCaMP's these monophosphates can also be converted into their di- and triphosphates (dUaDP and dUaTP)(figure 2).

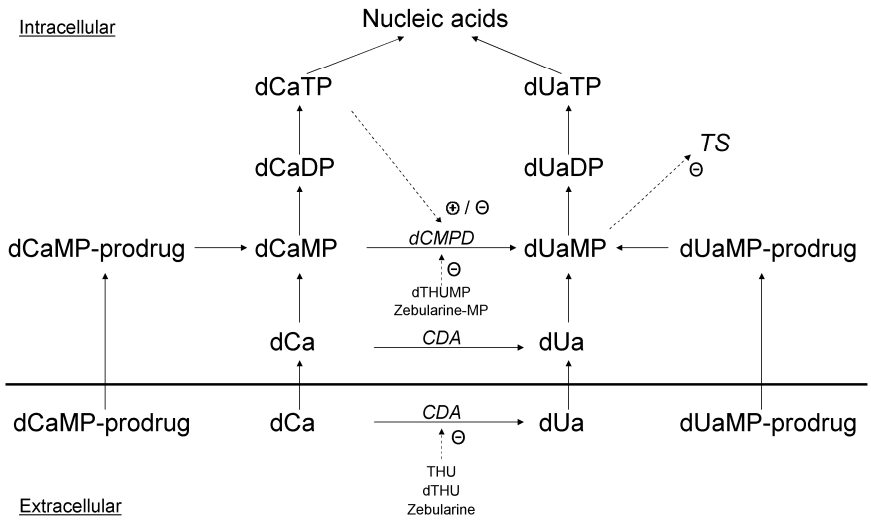

Figure 2. Metabolism of deoxycytidine analogs

Because most of the deaminated dCa's are relatively inactive if administered as nucleosides, deamination has often been considered an inactivation route [2;3]. Deoxyuridine analog nucleotides formed via different metabolic pathways can, however, contribute to the efficacy and toxicity of dCa nucleosides [4;5].
Recent discoveries in the pharmacokinetics of gemcitabine [6] and PSI-6130 [7] have drawn attention to the role of dUa nucleotides in dCa treatment. First, we review the literature related to the formation and formation route of dUa nucleotides after treatment with several registered and experimental dCa's (figure 1). The review is not exhaustive, but is limited to commonly used and recently developed dCa's. Secondly, the literature on the pharmacological activity of dUa's nucleotides is reviewed, looking at the pharmacology of dCa's from a different perspective.

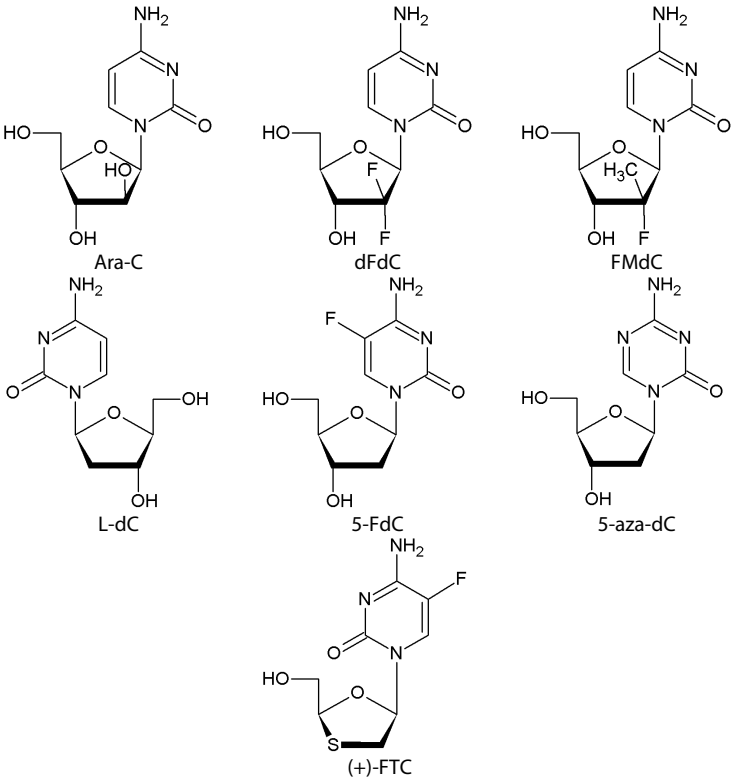

Figure 1. Chemical structures of deoxycytidine analogs

Formation of deoxyuridine analog nucleotides

Observed formation of deoxyuridine analog nucleotides

Ara-C (1-β-D-arabinofuranosylcytosine, cytarabine)(figure 1) is used in the treatment of haematological malignancies and is deaminated into ara-U (1-β-D-arabinofuranosyluracil) by CDA with an initial plasma half-life of 7-20 minutes [8]. Although ara-C is a cytidine analog, it resembles a 2'-deoxycytidine analog because the 2'-hydroxy group is in the unnatural arabino conformation. Already in the earliest *in vitro* investigations the formation of low amounts of ara-UMP and ara-UDP was shown (table I) [9]. In later work the formation of ara-UMP was confirmed [10;11], but although the possible formation of higher ara-U phosphates was reasoned and looked for, no ara-UDP or ara-UTP was found [10;12]. An analytical method for the determination of the major ara-C metabolites, including the uridine nucleotides, was published in 1996 by Braess et al [13]. Application of the assay to lymphoma cell lines incubated with [^{3}H]ara-C did, however, not result in measurable ara-UDP and ara-UTP levels. Two years later Gandhi et al. [14] showed the accumulation of ara-UTP in circulating blast cells of 6 patients with acute myeloid leukemia treated with ara-C. The intracellular ara-UTP peak concentrations ranged from 6-50 μM corresponding to 2.4-9.3% of the ara-CTP peak concentrations. These ara-CTP peak levels were reached at 0-0.5 hours after the end of the infusion whereas ara-UTP peak levels were reached 1-6 hours after the end of the infusion [14]. They confirmed their findings by incubating isolated leukemia blasts from patients with [^{3}H]ara-C.

dFdC (2', 2'-difluoro-2'-deoxycytidine, gemcitabine)(figure 1) is used in the treatment of various solid tumors. Like ara-C, dFdC is rapidly deaminated into dFdU (2', 2'-difluoro-2'-deoxyuridine) by CDA. In the first publication describing the cellular pharmacokinetics of dFdC only 0.7 % of 1 μM [^{14}C]dFdC was detected as dFdU nucleotide (table I) [15]. The formation of dFdUMP was noticed in a subsequent publication [16]. After incubating leukemia CCRF-CEM cells with dFdC for 2 hours, 11.9 % of the radioactivity could be attributed to dFdUMP. The formation of dFdUMP was, however, regarded as an inactivation route because formation would decrease dFdCTP levels. It was until 2008 that Veltkamp et al. noticed extensive accumulation of dFdUTP in white blood cells from patients receiving low doses of oral dFdC [17]. The mean value of the dose normalized area under the curve (AUC) of dFdUTP was 2.8-fold higher than dFdCTP on day 1 and increased to 5.6-fold on day 14 of a once-daily dosing schedule. Following these findings studies in mice [18] and cell cultures [6] were performed. In both studies the formation of dFdUTP was confirmed and low amounts of dFdUMP and dFdUDP were also detected. After multiple doses of oral and iv dFdC, dFdUTP accumulated especially in the liver, reaching AUC's up to

4.8-fold the dFdCTP AUC [18]. The intracellular half-life of dFdUTP was 7.0 hours in hepatoma cells compared to 12 hours for dFdCTP [6].

FMdC (β-D-2′-deoxy-2′-fluoro-2′-C-methylcytidine, PSI-6130)(figure 1) is a specific inhibitor of NS5B RNA polymerase used in the treatment of hepatitis C virus (HCV) infections [19]. The di-isobutyric acid ester prodrug of FMdC, R7128, is currently in phase I trials. Pharmacokinetic analysis of FMdC given iv and orally to rhesus monkeys showed extensive deamination into FMdU (β-D-2′-deoxy-2′-fluoro-2′-C-methyluridine, PSI-6206, RO2433) with mean serum half-lifes of 4.5 and 5.6 hours respectively [20]. As opposed to ara-UTP and dFdUTP, FMdUTP was discovered early in drug development (table I) [7]. After incubating primary human hepatocytes with [^{3}H]FMdC, FMdC and FMdU were mainly detected in the cells as nucleosides but also as their mono-, di- and triphosphates. Initially, the FMdC nucleotides were the most abundant, but after 24 hours of incubation the concentration of FMdU nucleotides exceeded those of the FMdC nucleotides. The effect was explained by determining the intracellular half-lifes of both triphosphates after washing the cells with drug-free medium. The mean half-life of FMdCTP was 4.7 hours, whereas the mean half-life of FMdUTP was 38.1 hours [7].

L-dC (β-L-2′-deoxycytidine, torcitabine)(figure 1) is the unnatural β-L isomer of deoxycytidine and specifically inhibits hepatitis B virus (HBV)-replication [21;22]. Its valine prodrug valtorcitabine has been tested in phase I/II clinical trials. Like other nucleosides in the β-L conformation, L-dC is not deaminated by CDA. Incubation of hepatoma cells and human hepatocytes, however, resulted in the formation of L-dU mono-, di- and triphosphate (table I). The relative amount of these nucleotides increased with longer incubation time. The L-dUTP:L-dCTP ratio, increased from 6% to 25% after incubating HepG2 cells for 2 and 24 hours [23]. Although the intracellular half-lives of L-dCTP and L-dUTP were not exactly determined, the half-life of L-dUTP appeared to be longer [22;23].

5-FdC (5-fluoro-2′-deoxycytidine)(figure 1) has shown *in vitro* [24] and *in vivo* [25] anti-tumor activity but never reached the market. Its effects are largely the same as 5-FU (5-fluorouracil), which is why formation of 5-FdUMP, the active metabolite of 5-FU, was reasoned. Therefore, as opposed to the previously mentioned compounds, deamination has always been considered an activation route of 5-FdC. Formation of 5-FdUMP was later confirmed in hepatoma cells (table I) [26] and formation of 5-FdUDP and 5-FdUTP in tumor-bearing mice [27]. Metabolites of 5-FdC cause both DNA hypomethylation and inhibition of thymidylate synthase (TS; EC 2.1.1.45) [4;28]. Recently the drug has entered phase I clinical trials in combination with the CDA inhibitor tetrahydrouridine (THU) aiming to increase the DNA hypomethylating effects [29].

Data has been published showing or suggesting conversion of several other dCa's into their dUaMP or into higher dUa phosphates. Some relevant examples are discussed below.

5-aza-dC (5-aza-2'-deoxycytidine, DAC, decitabine)(figure 1) has recently been approved by the FDA for the treatment of myelodysplastic syndrome (MDS) and is also used in the treatment of acute myeloid leukemia (AML). The recommended dose is 15 mg/m^2 given as a 3-hour iv infusion repeated every 8 hours during three days. It is rapidly deaminated by CDA with a half-life of 15-25 minutes [30]. 5-aza-dCTP is incorporated into DNA leading to inhibition of DNA methyltransferase. Thereby, 5-aza-dC causes hypomethylation and acts as an epigenetic agent. Early work with [^{3}H]5-aza-dC showed *in vivo* and *in vitro* formation of 5-aza-dUMP and possibly of higher phosphates (table I) [31]. After incubating leukemia cells with tritium-labeled 5-aza-dC for 1 hour Grant et al. assessed the radioactivity related to triphosphate metabolites [32]. Most radioactivity eluted after a cytidine triphosphate standard, but some activity eluted immediately after uridine triphosphate, indicating 5-aza-dUTP formation. To the best of our knowledge, 5-aza-dCTP nor 5-aza-dUTP or other related nucleotides have ever been analyzed in white blood cells from humans.

(+)-FTC ((+)-β-2',3'-dideoxy-5-fluoro-3'-thiacytidine)(figure 1) is the (+)-enantiomer the antiretroviral agent (-)-FTC (emtricitabine). Racivir, the enantiomeric mixture of (+)- and (-)-FTC, is currently in phase II studies. (-)-FTC is not susceptible to deamination, but the (+)-enantiomer is [33]. Moreover, (+)-FTUMP was detected in hepatoma cells after incubation with (+)-FTC (table I) [34].

Route of formation

There are two possible routes for the formation of dUa nucleotides: extra- or intracellular deamination of dCa's by CDA and subsequent phosphorylation of dUa's (route 1) and phosphorylation of dCa's into dCaMP and deamination into dUaMP by dCMPD (route 2). The routes of dUa nucleotide formation are depicted in figure 3 with ara-C as example. Several experiments have been performed to elucidate the route of formation of dUa nucleotides.

Formation of dUa nucleotides from extracellular dUa has been assessed by incubating cells with dUa. Gandhi et al. incubated leukemia blasts with [^{3}H]ara-U, but did not see ara-UTP formation [14]. Likewise, only negligible amounts of ara-U nucleotides were detected after [^{3}H]ara-U incubation of myeloid blasts, although small amounts of intracellular ara-U were found [11]. Muller et al, on the other hand, did see formation of ara-UMP, -DP and -TP [35]. After incubating mouse lymphoma cells with [^{3}H]ara-U only a very small amount of the radioactive label was taken up into the cells, but just 6.3 % of the radioactivity in the cells was attributed to ara-U, whereas 33.7%, 8.9% and 30.0 % was attributed to ara-UMP, -DP and -TP

respectively. Only small amounts of dUa nucleotides are thus formed after extracellular ara-U administration. Most likely, this is the cause of the low sensitivity of cells to ara-U compared to ara-C [11].
Similarly, dFdU was found to be about 10,000-fold [36] and 100,000-fold [6] less potent than dFdC. In hepatoma cells the dFdU mono-, di- and triphosphate accounted for 47%, 15% and 8% of the intracellular radioactivity after extracellular dFdU administration [6]. Again, however, the intracellular radioactivity accounted for only a very small part of the total added radioactivity. Furthermore, Veltkamp et al. showed that cells overexpressing human concentrative nucleoside transporter 1 (hCNT1) are more sensitive to dFdU [6]. On the other hand, Veltkamp et al showed that similar dFdC and dFdU amounts are taken up into MDCK-cells [6].
Finally, FMdU, was not active in hepatoma cells and in cell lines containing a HCV replicon [5;7;20].
Concluding, extracellular administration of the abovementioned dUa's does not lead to effective dUa nucleotide formation. This is, at least in part, caused by relatively poor cellular uptake.

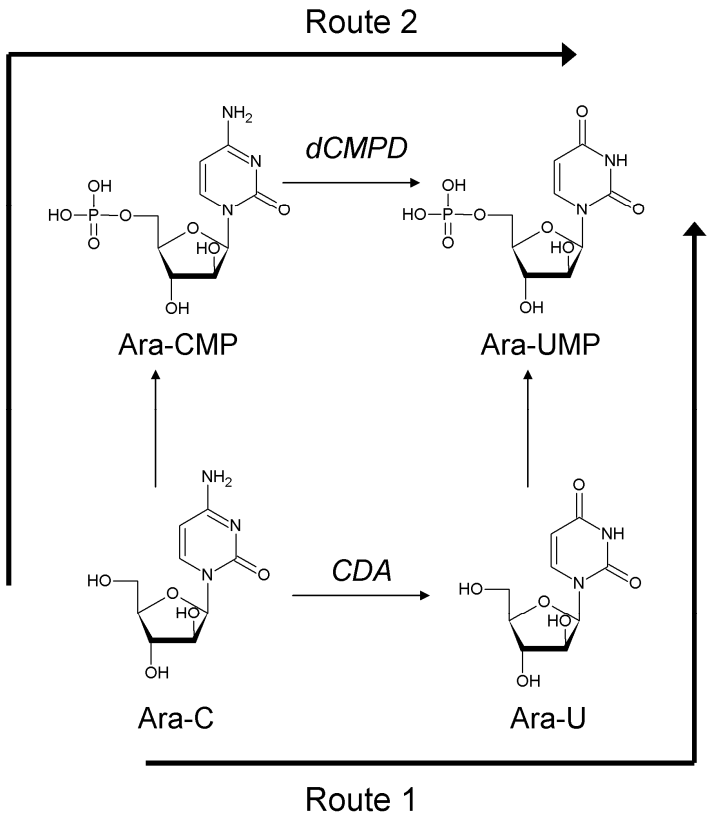

Figure 3. Routes of deoxyuridine analog nucleotide formation

Cellular uptake of the dUa is not required for dUa nucleotide formation if the dUa is formed intracellularly by dCa deamination. This conversion can be blocked with the CDA inhibitor tetrahydrouridine (THU)(figure 2). Blocking CDA in cells treated with 5-aza-dC indeed showed no 5-aza-dU formation. The 5-aza-UMP formation, however, only changed slightly [31]. In a similar experiment with ara-C, formation of ara-UTP was also unchanged or even increased [14]. Addition of THU to dFdC incubations does not prevent dFdU-TP formation either [6]. Finally, L-dU nucleotides were detected whereas L-dC is not a CDA substrate [23]. These results indicate that intracellular deamination of dCa's by CDA is not a pivotal step in dUa nucleotide formation.

Moreover, these studies indicate that dUa's are poor substrates for phosphorylation. This was confirmed for some compounds. Murakami et al showed that FMdU is not a substrate for uridine-cytidine kinase 1 (UCK-1), dCK or thymidine kinase 1 and 2 (TK1, TK2) [5]. Similarly, dFdU is not phosphorylated by TK1 [6;37] and only sparsely by TK2 [37]. Moreover, dFdU toxicity could be reversed by low amounts of dC, suggesting a very low affinity of dFdU for dCK [36], as was also mentioned by Plunkett et al [38].
For most of the dUa's, the combination of poor cellular uptake and slow subsequent phosphorylation make route 1 a less efficient route of dUa nucleotide formation.
Formation of dUa nucleotides via route 2 can be inhibited and thereby confirmed with the dCMPD inhibitors tetrahydrodeoxyuridine (dTHU) [39] and zebularine [40]. Indeed, treatment of blasts with dTHU inhibited ara-UTP formation 8-fold, whereas the ara-CTP accumulation increased with about 15% [14]. Moreover, the concentration of L-dU nucleotides was significantly reduced after dTHU incubation [23]. Treatment of cells with zebularine resulted in FMdUMP, -DP and -TP levels only 28%, 18% and 31% of the concentrations found in cells not treated with zebularine [5]. The FMdC nucleotide levels increased correspondingly. Finally, as opposed to THU, dTHU strongly increased the half-life of dFdCTP [16]. This was most likely caused by inhibiting deamination of dFdCMP formed from dFdCTP, which might otherwise be rephosphorylated into dFdCTP.
Activity of dCMPD towards dCaMP's was also confirmed *in vitro*. Deamination of 5-aza-dCMP [41] and (+)-FTCMP [34] was shown, and FMdCMP was indeed a substrate, although weak, for cloned human dCMPD [5].
Furthermore, the relative amount of ara-UMP in cells incubated with ara-C was correlated with the activity of dCMPD [11] and the intracellular half-life of ara-CTP showed a strong correlation with ara-UMP concentrations [11].
More evidence of formation via route 2 was given by synthesizing a FMdUMP prodrug, which delivered FMdUMP directly into cells (figure 2). Increasing cellular uptake and bypassing the first phosphorylation step of the nucleoside, FMdUTP was formed effectively [5]. It was also shown that FMdUMP was efficiently phosphorylated into its di- and triphosphate by

UMP-CMP-kinase (YMPK) and nucleoside diphosphate kinase (NDPK) [5]. Once dUaMP's are formed conversion into di- and triphosphates is likely, because enzymes that further phosphorylate the dUaMP's have a high catalytic activity for most nucleoside monophosphates [42].
An exception to the abovementioned nucleosides is 5-FdC. Unlike the other dUa's the 5-FdU, also called floxuridine, is effectively taken up into cells and phosphorylated by TK. 5-FdU nucleotides can therefore be formed via route 1 as well as via route 2 [4]. The same is true for other 5-substituted dCa's [43].

Concluding, most of the described dUa's are not taken up into cells effectively and/or are relatively poor substrates for phosphorylation (route 1). Therefore, only high exposure to these dUa's results in dUa nucleotide formation. Deamination of dCaMP's into their uridine congeners (route 2) followed by phosphorylation into dUaTP's is most likely the main route of dUa nucleotide formation.

Deoxycytidine monophosphate deaminase

Because deamination of dCaMP's is the main route of dUa nucleotide formation deoxycytidine monophosphate deaminase (dCMPD) is a key enzyme in the dUa nucleotide formation. dCMPD converts its natural substrate dCMP into dUMP and is highly regulated [44]. dCaMP's with substitutions at the 5-position of the cytosine base were still good substrates. Substitutions at the 2'-position were less well tolerated [45]. Still, dFdCMP was found to be a good substrate and ara-CMP a fair substrate [16;46]. Cytidine monophosphate, on the other hand, was not a good substrate [47]. Moreover, monophosphates of dCa nucleosides in the L-conformation (eg. apricitabine, lamivudine and emtricitabine) and dideoxy cytidine acted neither as substrates nor as inhibitors [46].
dCMPD activity is, however, influenced by several factors. The monophosphates GMP, dGMP and dUMP as well as several thymidine and uridine analog monophosphates are potent competitive inhibitors of its activity [44-46]. Moreover, the triphosphates dTTP and TTP inhibit dCMPD by allosteric interaction. dCTP, on the other hand, allosterically increases dCMPD activity [46;48]. Likewise, dCaTP's themselves can augment dCMPD activity as was shown for ara-CTP [44] and 5-aza-dCTP [41;49]. Other experiments, however, showed that ara-CTP and dFdCTP among other dCTP analogs could not activate [46], or in the case of dFdCTP, even inhibited dCMPD [16;50]. The direct or indirect inhibition of dCMPD and subsequent depletion of the dCTP pool competing for DNA incorporation has been proposed as a "self-potentiating" mechanism of dFdC [16].
Differences in dUa nucleotide formation between individuals might be explained by genetic variations in the dCMPD gene. Recently 29 polymorphisms were found in this gene. One non-synonymous polymorphism resulted in dCMPD with only 11% of the activity of wildtype enzyme [51].

Besides differences between patients there are also large intra-individual differences. dCMPD activity is high in normal rapidly dividing cells [52] and tumors [11;53;54]. The increased dCMPD activity has been used in the case of 5-FdC where increased conversion into cytotoxic 5-FdUMP in tumors was used as a selective targeting mechanism [25;26]. 5-FdUMP concentrations found in tumor tissue were between 45- and >5,400-fold higher compared to normal tissue. The higher phosphates F-dUDP and F-dUTP levels were also increased [27].

Although dCMPD plays a key-role in dUa nucleotide formation, its effect on the overall activity is unclear because 1) it increases the concentration of dUa nucleotides, but likewise 2) it increases the concentration of dU and dT nucleotides, the natural competitors of dUa nucleotides. Similarly it 3) decreases dCa nucleotide concentrations, and also 4) decreases the concentration of dC nucleotides, the natural competitors of dCa nucleotides. This ambiguity is illustrated by the fact that both decreased [49;55] and increased [56] dCMPD activity have been associated with resistance.

Table I. Formation of deoxyuridine analog nucleotides after deoxycytidine analog treatment

Parent compound	Status	Formation of deoxyuridine analog nucleotides (% of deoxycytidine congener)			Conditions	Ref.
		monophosphate	diphosphate	triphosphate		
Ara-C	Registered	0.35 µM (3.14%)	0.43 µM (1.33%)	2.9 µM (1.14%)	L1210 ascites cells, 51 µM, 20 min	[9]
		<5% RA	NT	NT	CLL-cells, 6.85 µM, 20 h	[10]
		10.6 % RA (707%)	0-0.5% RA (ND)	0.1-0.8% RA (ND)	Myeloblasts, 1 µM, 1 h	[11]
		5.5 % RA (367%)	0-0.5% RA (ND)	0.1-0.8% RA (ND)	Non-T myeloblasts	[11]
		ND	ND	6-50 µM (2.4-9.3%)	Blasts AML patients, 0.5g/m^2/h, 2/4 h	[14]
		ND	ND	2-41 µM (0.6 – 36.3 %)	Isolated leukemia blasts, 1-25 µM, 1 h	[14]
dFdC	Registered	0.7 % total dFdU nucleotides			CHO cells, 1 µM, 3 h	[15]
		15.3 % RA (1093%)	NT	NT	CCRF-CEM cells, 10 µM, 2 h	[16]
		11.9 % RA (2975%)	NT	NT	CCRF-CEM cells, 0.1 µM, 2 h	[16]
		ND	ND	11 h*ng/mg protein (275%)	PBMC's cancer patients, oral dosing, day 1	[17]
		ND	ND	35 h*ng/mg protein (565%)	PBMC's cancer patients, oral dosing, day 14	[17]
		Not calculated	Not calculated	14 h*pmol/g (87.5%)	PBMCs, oral dosing, 0.1 mg/kg(7qdx1d), $AUC_{0\text{-}8\ h}$	[18]
		Not calculated	Not calculated	16 h*pmol/g (106%)	PBMCs, iv dosing, 0.1 mg/kg(7qdx1d), $AUC_{0\text{-}8\ h}$	[18]
		6.7 h*pmol/mg protein (47.9%)	4.0 h*pmol/mg protein (9.09%)	5.0 h*pmol/mg protein (11.1%)	HepG2, 5 nM+THU, $AUC_{0\text{-}24\ h}$	[6]
		19 h*pmol/mg protein (12.8%)	8.6 h*pmol/mg protein (0.789%)	16 h*pmol/mg protein (0.948%)	HepG2, 500 nM+THU, $AUC_{0\text{-}24\ h}$	[6]
FMdC	Phase I	Yes (ND)	0.9 pmol/10^6 cells (~300%)	2.4 pmol/10^6 cells (171%)	Primary human hepatocytes, 2 µM , 24 h	[7]
		0.79 pmol/10^6 cells (122%)	4.79 pmol/10^6 cells (145%)	11.51 pmol/10^6 cells (99.8%)	Clone A cells, 5 µM , 48 h	[5]
L-dC	Phase I/II	6.73 pmol/10^6 cells (29.0%)	2.69 pmol/10^6 cells (26.4%)	18.2 pmol/10^6 cells (25.1%)	HepG2 cells, 10 µM , 24 h	[23]
		5.74 pmol/10^6 cells (20.8%)	3.93 pmol/10^6 cells (54.7%)	43.5 pmol/10^6 cells (48.3%)	Human hepatocytes, 10 µM , 24 h	[23]
5-FdC	Phase I	36.9 fmol/10^6 cells (103%)	ND	ND	HEp-2 cells, 0.1 µM, 30 min	[26]
		1,036 fmol/g tissue (128%)	5-FdUDP+5-FdUTP: 1,469 fmol/g tissue (1204 %)		Mice implanted tumor tissue, 12 mg/kg, 60 min	[27]
5-aza-dC	Registered	Detected,	ND	ND	Ehrlich ascitic tumor cells, 0.1 mM, 20 min	[31]
		but not quantitated (ND)			and mice, 0.2 µmole, 2 h	
		ND	ND	Unidentified peak (ND)	HL-60 cells, 5 µM, 1 h	[32]
(+)-FTC	Phase II	0.21 pmol/10^6 cells (1050%)	NT	NT	HepG2 derivative 2.2.15 (subclone P5A), 1 µM , 24 h	[34]

ND: Not determined, NT: Not detected, RA: radioactivity

Table II. Pharmacological activity of deoxyuridine analog nucleotides formed after deoxycytidine analog treatment

Compound	Enzyme (activity)	Incorporation DNA/RNA (competitor)	Remark	Ref.
Ara-UMP	Thymidylate (substrate)	-	Ara-TTP formation	[14]
dFdUMP	Thymidylate synthase (K_i app= 432.8 µM)	-	Determined dUMP as variable substrate	[60]
5-FdUMP	Thymidylate synthase (inhibitor)	-	Reviewed by Weckberger	[59]
Ara-UTP	DNA polymerase α (IC_{50} unknown) [65]	DNA (dTTP), inhibits further chain elongation		[65]
	DNA polymerase α (K_i=7.8 µM (dTTP), 10.4 µM (dUTP))	DNA (dTTP, dUTP)	No inhibition of RNA polymerases	[35]
	DNA polymerase β (K_i=12.1 µM (dTTP), 22.2 µM (dUTP))			
	DNA-directed DNA polymerase RSV (K_i=17.8 µM (dTTP), 28.8 µM (dUTP))			
	RNA-directed DNA polymerase RSV (K_i=3.4 µM (dTTP), 4.7 µM (dUTP))			
	DNA polymerase α (K_i=0.5 µM)	DNA (dTTP)		[64]
	DNA polymerase β (K_i=5.5 µM)			
	DNA polymerase γ (K_i=18 µM)			
dFdUTP	Unknown	DNA (unknown)	Similar incorporation as dFdCTP	[6]
		RNA (unknown)	at nucleoside IC_{50}'s	
FMdUTP	RNA polymerase NS5B (IC_{50}=0.52 µM, K_i=0.141 µM) [7]	RNA (UTP)	Blocks further chain elongation	[7]
L-dUTP	Woodchuck hepatitis virus DNA polymerase (IC_{50} = 5.26 µM)	DNA (unknown)		[21]
5-FdUTP	DNA polymerase α (K_m = 3.4 µM) and β(K_m = 15.4 µM)	DNA (dTTP)		[68]

Pharmacological activity of deoxyuridine analog nucleotides

Molecular pharmacology

Uridine analog monophosphates

Endogenous dUMP is a substrate for TS, which converts it into dTMP. Hence, analogs of dUMP are potential TS inhibitors. TS is a key enzyme in *de novo* dTMP synthesis and therefore a target in several cancer therapies [57].

Inhibition of TS is the main mechanism of action of 5-FU and its oral prodrug capecitabine. Their metabolite 5-FdUMP, which is also formed after 5-FdC administration, covalently binds to TS causing inhibition (table II) [58;59]. dUaMP analogs fluorinated at the 2'-position of the sugar moiety also show interactions with TS [60]. Some were substrates, but others, among which was dFdUMP, were only competitive inhibitors. Although the inhibitory potency of dFdUMP was relatively low, dFdC incubation did inhibit TS activity in several solid tumor cell lines by 90% [61]. The inhibitory activity of ara-UMP on TS has never been explored directly. Ara-C however inhibited TS activity after incubation of intact cells [62]. Moreover, the formation of ara-TTP indicates that ara-UMP is a TS substrate [14]. It can thus be concluded that dUaMP's can indeed be TS inhibitors.

Uridine analog triphosphates

Similar to other nucleoside triphosphates, dUaTP's can inhibit polymerases and can be incorporated into nucleic acids (table II). Incubation of mouse lymphoma cells with ara-U caused formation of ara-UMP, -DP and -TP, and inhibition of cell proliferation [35]. Ara-UMP was found in DNA as internucleotide indicating that the DNA chain could be elongated after incorporation. The direct effect of ara-UTP on different human and viral DNA- and RNA-polymerases was also assessed [35]. Ara-UTP inhibited incorporation of dTTP and dUTP at concentrations similar to those at which ara-CTP inhibits incorporation of dCTP [35;63]. Inhibition of DNA polymerase α, β and γ by ara-UTP was confirmed later [64].

The activity of ara-UTP was also investigated by Gandhi et al [65]. A DNA primer was extended based on 4 templates by DNA polymerase α in the presence of ara-CTP and ara-UTP and their natural competitors dCTP and dTTP. The dose dependent incorporation of ara-CTP and ara-UTP at C and T sites inhibited chain elongation at the incorporation site. Subsequent incorporation at a CT or TC sequence resulted in additive or synergistic inhibition. Polymerase α was inhibited at ara-UTP levels reached during ara-C therapy [14]. It can thus be concluded that ara-UTP is an additional active metabolite of ara-C. Besides a direct effect of ara-UTP, activity by

acting as a phosphate donor for ara-CTP formation has also been proposed [14].
dFdUTP activity was reasoned for the first time when incorporation of a dFdC metabolite into RNA was observed [66]. Incubation of cells with high concentrations of dFdU resulted in dFdUMP, dFdUDP and dFdUTP formation and toxicity (table II) [6]. Moreover, dFdUTP was incorporated into DNA and RNA and incorporation correlated with toxicity. When cells were incubated with dFdC or dFdU at their IC_{50}'s, comparable amounts of dFdCTP and dFdUTP were incorporated into DNA indicating similar intrinsic toxicity. Like ara-UTP, dFdUTP therefore seems to be an active metabolite as well.
The activity of FMdUTP was assessed using an HCV replicase assay and an HCV polymerase assay [7]. In the replicase assay the RNA synthesis by membrane associated HCV replication complexes was measured with and without FMdUTP. FMdUTP inhibited RNA synthesis with an IC_{50} of 1.19 μM compared to an IC_{50} of 0.34 μM for FMdCTP (table II). The direct effect of FMdUTP on HCV RNA polymerase was determined as well. Again FMdUTP showed similar activity compared to FMdCTP (IC_{50}'s of 0.52 μM and 0.13 μM respectively). Finally, the extension of an RNA primer by HCV polymerases using an RNA template was tested. FMdUMP was incorporated into RNA at uridine sites, after which further extension of the chain was blocked. A prodrug of FMdUMP has been used to deliver the compound into cells. As a prodrug the compound became a potent HCV replication inhibitor, elegantly showing the activity of the dUa nucleotides [5].
Although less potent than L-dCTP, L-dUTP effectively inhibited woodchuck hepatitis virus DNA polymerase [21], which is used as a model virus for human hepatitis B virus.
Finally, 5-FdU residues were detected in DNA after 5-FdC [28] and 5-FdU [67] treatment. The activity of 5-FdUTP as a metabolite of fluoropyrimidines was reviewed by Weckbecker [59;68].

Although the activity of the dUa nucleotides is generally less than their dCa congeners, the presented studies show that both dUaMP's and dUaTP's can have pharmacological activity.

Clinical pharmacology

Role of deoxyuridine analog nucleotides in deoxycytidine analog treatment

As shown previously in this review, dUa nucleotides are formed, and both dUaMP's and dUaTP's can have pharmacological activity. Their role in dCa treatment is, however, less clear.
The inhibitory capacity of FMdCTP and FMdUTP was tested on wild-type and mutated HCV RNA polymerase [5]. The mutation resulted in a 7.5 fold

resistance against FMdCTP but a 23.7 fold resistance against FMdUTP. These data show that the different metabolites can have different sensitivities towards mutations in polymerases. Possibly the presence of two active metabolites with different sensitivities towards mutations can increase the genetic barrier that a virus must overcome to become resistant [5]. This may be especially true in antiviral therapy where mutations in polymerases often confer resistance.
Treatment of cells with dFdU caused an arrest of cells in the early S-phase [6]. Moreover, dFdU shows cytotoxic [36] and radiosensitizing effects [69] at high concentrations *in vitro*. The dUa nucleotides responsible for this effect are most likely also formed during dCa therapy. Moreover, dCaTP's and dUaTP's are incorporated into nucleic acids at different sites thus increasing the chance of nucleotide analog incorporation. Subsequent incorporation of the nucleotide analogs leads to additional or synergistic activity [65]. The effects of dUa nucleotides can, however, also be very different from dCa nucleotides. As mentioned before 5-FdC metabolites cause both hypomethylation and inhibition of TS. These two activities are caused by 5-FdCTP and 5-FdUMP respectively.
Very little is known about the role of these nucleotides in toxicity. One patient has been described who developed lethal liver- and kidney-toxicity after treatment with oral dFdC. The dFdUTP levels found in PBMC's of this patient were exceptionally high, whereas dFdC, dFdU and dFdCTP levels were normal [17]. Concluding, the role of dUa nucleotides in dCa therapy is not clear, but an effect on effectivity and toxicity can be expected.

Dose

Short high-dose infusions have been compared with prolonged or multiple low dose infusion for several dCa's like decitabine [70], ara-C [71] and dFdC [72]. Prolonged exposure is thought to prevent saturation of triphosphate formation and can increase effectivity [72;73]. Prolonged infusion can, however, also alter dUa nucleotide accumulation.
Incubation of isolated leukemia blast from patients with increasing [^{3}H]-ara-C concentrations resulted in an increase of the relative ara-UTP amount from a mean of 2.0 % to a mean of 11.9 % [14]. Likewise, increasing the concentration at which hepatocytes from three donors were incubated resulted in increased relative FMdUTP concentrations [7].
Contrary to these findings, *in vitro* experiments with dFdC showed that the relative dFdUMP concentrations were higher after incubations with low dFdC concentrations [6;16]. After incubation with high concentrations only 0.94 % of the total recovered intracellular drug content was attributed to dFdU nucleotides, whereas this was 12 % after incubation at the low concentration [6]. The same effect, although less pronounced, was seen when mice were given dFdC intravenously either 7 times per day during one day, or once-daily during 7 days: the nucleotide levels were higher after 7 times during one day dosing, but the relative dFdUTP amount was lower [18].

The discrepancy between ara-C and FMdC on the one hand and dFdC on the other might be explained by the different effect of these nucleosides on dCMPD activity. dFdCDP is a ribonucleotide reductase inhibitor that thus decreases the dCTP concentration, which subsequently leads to lower dCMPD activity [50]. Moreover, dFdCTP itself might inhibit dCMPD, whereas ara-CTP is a dCMPD activator.
Concluding, the effect of the dose on dUa nucleotide concentration can differ between dCa's. High dFdC doses seem to decrease relative dFdU nucleotide levels whereas high ara-C and FMdC doses lead to higher relative dUa nucleotide concentrations.

Deaminase inhibitors

Since many dCa's are rapidly deaminated to dUa's in plasma, deaminase inhibitors have been used extensively to alter the kinetics of nucleosides.
THU is a CDA inhibitor and was used to prevent inactivation of and thus increase the exposure to iv 5-FdC [74] and ara-C [75] in patients. Moreover, the addition of THU increased the oral bioavailability of dFdC in mice from 10% to 40% [76]. The inhibition of deamination at the nucleoside level will, however, not prevent dUa nucleotide formation which are formed by deamination at the nucleotide level (route 2).
Inhibition of CDA has not only been used to prevent inactivation, but also to prevent unwanted activity of deaminated metabolites. After deamination by CDA, 5-FdC is effectively converted into dUa nucleotides (route 1). 5-FdC nucleotides act as DNA methyltransferase inhibitors, whereas the deaminated nucleotides have different pharmacological activities. Inhibition of 5-FdC deamination with THU has recently been used in a phase I study to prevent deaminated nucleotide related side effects [77]. Although 5-FdU plasma levels were much lower, 5-FdU nucleotide were most likely still formed intracellularly via route 2. Using this effect, the addition of THU to 5-FdC treatment has been used to target 5-FdUMP to dCMPD overexpressing tumors [25].
Thus, inhibition of CDA does not prevent dUa nucleotide formation, which are formed via route 2. Intracellular concentrations of all analog nucleotides should be determined to exactly determine the effect of THU co-administration.

Zebularine and dTHU inhibit both CDA and dCMPD. Zebularine and dTHU inhibit CDA [78] and are converted into their monophosphates, that inhibit dCMPD. Zebularine is also converted into an active triphosphate. Incubating replicon cells with zebularine before FMdC incubation lowered the EC_{90} from 4.9 uM to 2.1 uM. Zebularine itself showed no activity [5]. Likewise, addition of zebularine enhanced the antineoplastic activity of 5-aza-dC in murine fibroblast. The effect was caused by inhibition of deaminases and not by the antineoplastic effect of zebularine [79;80]. In contrast, 5-FdC toxicity decreased in HEp-2 cells after THU pre-incubation, but decreased even further after dTHU pre-incubation [25]. Still, Boothman

et al. showed that 5-FdC incorporation into DNA was increased 2-fold after THU co-administration and 25-fold after dTHU co-administration [26].

Concluding, CDA inhibition leads to higher dCa nucleotide concentrations, but does not prevent dUa nucleotide formation. Inhibition of dCMPD, on the other hand, does inhibit dUa nucleotide formation and can result in increased or, as in the case 5-FdC, decreased activity.

Prodrugs

Many chemical groups have been coupled to nucleosides to improve their pharmacokinetics. Cytarabine [81] and dFdC have, for example, been coupled to lipids [82;83], squalene [84] amino acids [85] and PEG [86] to decrease deamination by CDA and improve their oral bioavailability. Moreover, dCa's have been administered as phosphoramidate [87;88] or oligonucleotides [89] prodrugs to deliver them in cells as mono-phosphates, thereby bypassing cellular uptake and the first phosphorylation step (figure 2). Like the addition of CDA inhibitors these chemical modulations will, however, not prevent dUa nucleotide formation since the actual drugs are delivered in the activation pathway before or as the dCaMP. For example, uridine nucleotide formation was observed after incubating cells with the acyclic phosphonate prodrug of 5-aza-cytidine (hydroxy(phosphonomethoxy)propyl-5-aza-cytosine, HPMP-5-aza-C) [90]. Phosphoramidate prodrugs have also been prepared of dUa's [5;91]. Because the compounds are delivered intracellularly as dUaMP's any effect seen can be attributed solely to the dUa nucleotides. Finally, drug formulations containing ara-CTP, dFdCTP and 5-FdUTP have been prepared [92]. Since these analogs are released in the cell as triphosphate, their activity can be largely attributed to the administered triphosphate. However, breakdown to dCaMP and subsequent deamination might still result in dUa nucleotide formation [11]. Thus, depending on the prodrug mainly dUa-, mainly dCa- or both nucleotides will be formed.

Discussion

Formation of dUa nucleotides occurs after administration of several dCa's via deamination of dCaMP's by dCMPD. *In vitro* and *in vivo* activity has been shown for several dUaMP's and dUaTP's, but their exact role in dCa treatment remains unclear.

The question rises why so little attention has been given to these metabolites in the past. One of the reasons might be that the formation of dUa nucleotides is often low in preclinical studies. This might be caused by the relatively short incubation times, or low dCMPD activity in rodents and cell-lines. Moreover, dUa nucleotides can easily be overlooked or held for dCa nucleotides because the retention times on HPLC systems are very similar.

The formation and activity of dUa nucleotides should be taken into account when applying different treatment strategies such as prolonged low dosing, oral administration, (monophosphate-)prodrugs and co-administration with deamination inhibitors. Monitoring of the intracellular metabolites during these experiments can give more insight in the effect of these strategies on dUa nucleotide levels. Given the differences in metabolic conversion in different tissues these analyses should preferably be performed in the target tissue. A good understanding of the intracellular pharmacology is pivotal in the interpretation of results.

The presented studies show that formation and activity of dUa nucleotides has been established for some dCa's but less well or not for others. The exact role of dUa nucleotides in dCa therapy remains undefined and should be the subject of future investigations.

References

[1] A. Matsuda, T. Sasaki, Cancer Sci. 95 (2004) 105.
[2] L. Jordheim, C. M. Galmarini, C. Dumontet, Curr. Drug Targets. 4 (2003) 443.
[3] A. M. Bergman, H. M. Pinedo, G. J. Peters, Drug Resist. Updat. 5 (2002) 19.
[4] E. M. Newman, D. V. Santi, Proc. Natl. Acad. Sci. U. S. A 79 (1982) 6419.
[5] E. Murakami, C. Niu, H. Bao, H. M. Micolochick Steuer, T. Whitaker, T. Nachman, M. A. Sofia, P. Wang, M. J. Otto, P. A. Furman, Antimicrob. Agents Chemother. 52 (2008) 458.
[6] S. A. Veltkamp, D. Pluim, M. A. van Eijndhoven, M. J. Bolijn, F. H. Ong, R. Govindarajan, J. D. Unadkat, J. H. Beijnen, J. H. Schellens, Mol. Cancer Ther. 7 (2008) 2415.
[7] H. Ma, W. R. Jiang, N. Robledo, V. Leveque, S. Ali, T. Lara-Jaime, M. Masjedizadeh, D. B. Smith, N. Cammack, K. Klumpp, J. Symons, J. Biol. Chem. 282 (2007) 29812.
[8] A. Hamada, T. Kawaguchi, M. Nakano, Clin. Pharmacokinet. 41 (2002) 705.
[9] A. W. Schrecker, M. J. Urshel, Cancer Research 28 (1968) 793.
[10] T. C. Chou, Z. Arlin, B. D. Clarkson, F. S. Phillips, Cancer Res. 37 (1977) 3561.
[11] G. P. Jamieson, L. R. Finch, M. Snook, J. S. Wiley, Cancer Research 47 (1987) 3130.
[12] J. S. Wiley, J. Taupin, G. P. Jamieson, M. Snook, W. H. Sawyer, L. R. Finch, J. Clin. Invest 75 (1985) 632.
[13] J. Braess, J. Pfortner, C. C. Kaufmann, B. Ramsauer, M. Unterhalt, W. Hiddemann, E. Schleyer, J. Chromatogr. B Biomed. Appl. 676 (1996) 131.
[14] V. Gandhi, Y. Z. Xu, E. Estey, Clin. Cancer Res. 4 (1998) 1719.
[15] V. Heinemann, L. W. Hertel, G. B. Grindey, W. Plunkett, Cancer Research 48 (1988) 4024.
[16] V. Heinemann, Y. Z. Xu, S. Chubb, A. Sen, L. W. Hertel, G. B. Grindey, W. Plunkett, Cancer Res. 52 (1992) 533.
[17] S. A. Veltkamp, R. S. Jansen, S. Callies, D. Pluim, C. M. Visseren-Grul, H. Rosing, S. Kloeker-Rhoades, V. A. Andre, J. H. Beijnen, C. A. Slapak, J. H. Schellens, Clin. Cancer Res. 14 (2008) 3477.
[18] S. A. Veltkamp, D. Pluim, O. van Tellingen, J. H. Beijnen, J. H. Schellens, Drug Metab Dispos. 36 (2008) 1606.
[19] L. J. Stuyver, T. R. McBrayer, P. M. Tharnish, J. Clark, L. Hollecker, S. Lostia, T. Nachman, J. Grier, M. A. Bennett, M. Y. Xie, R. F. Schinazi, J. D. Morrey, J. L. Julander, P. A. Furman, M. J. Otto, Antivir. Chem. Chemother. 17 (2006) 79.
[20] G. Asif, S. J. Hurwitz, J. Shi, B. I. Hernandez-Santiago, R. F. Schinazi, Antimicrob. Agents Chemother. 51 (2007) 2877.
[21] M. L. Bryant, E. G. Bridges, L. Placidi, A. Faraj, A. G. Loi, C. Pierra, D. Dukhan, G. Gosselin, J. L. Imbach, B. Hernandez, A. Juodawlkis, B. Tennant, B. Korba, P. Cote, P. Marion, E. Cretton-Scott, R. F. Schinazi, J. P. Sommadossi, Antimicrob. Agents Chemother. 45 (2001) 229.
[22] D. N. Standring, E. G. Bridges, L. Placidi, A. Faraj, A. G. Loi, C. Pierra, D. Dukhan, G. Gosselin, J. L. Imbach, B. Hernandez, A. Juodawlkis, B. Tennant, B. Korba, P. Cote, E. Cretton-Scott, R. F. Schinazi, M. Myers, M. L. Bryant, J. P. Sommadossi, Antivir. Chem. Chemother. 12 Suppl 1 (2001) 119.
[23] B. Hernandez-Santiago, L. Placidi, E. Cretton-Scott, A. Faraj, E. G. Bridges, M. L. Bryant, J. Rodriguez-Orengo, J. L. Imbach, G. Gosselin, C. Pierra, D. Dukhan, J. P. Sommadossi, Antimicrob. Agents Chemother. 46 (2002) 1728.
[24] K. Mukherjee, C. Heidelberger, Cancer Res. 22 (1962) 815.
[25] J. A. Mekras, D. A. Boothman, L. M. Perez, S. Greer, Cancer Res. 44 (1984) 2551.
[26] D. A. Boothman, T. V. Briggle, S. Greer, Mol. Pharmacol. 27 (1985) 584.
[27] D. A. Boothman, T. V. Briggle, S. Greer, Cancer Res. 47 (1987) 2354.
[28] J. Kaysen, D. Spriggs, D. Kufe, Cancer Res. 46 (1986) 4534.

[29] J. H. Beumer, R. A. Parise, E. M. Newman, J. H. Doroshow, T. W. Synold, H. J. Lenz, M. J. Egorin, Cancer Chemother. Pharmacol. 62 (2008) 363.
[30] R. L. Momparler, Semin. Hematol. 42 (2005) S9.
[31] A. Cihak, Eur. J. Cancer 14 (1978) 117.
[32] S. Grant, F. Rauscher, III, J. Margolin, E. Cadman, Cancer Res. 42 (1982) 519.
[33] S. J. Hurwitz, M. J. Otto, R. F. Schinazi, Antivir. Chem. Chemother. 16 (2005) 117.
[34] M. T. Paff, D. R. Averett, K. L. Prus, W. H. Miller, D. J. Nelson, Antimicrob. Agents Chemother. 38 (1994) 1230.
[35] W. E. G. Muller, R. K. Zahn, Cancer Research 39 (1979) 1102.
[36] M. Tiefenthaler, F. Hohla, E. Irschick, E. Strasser-Wozak, N. Bacher, O. Muhlmann, W. Wein, G. Konwalinka, Immunobiology 207 (2003) 149.
[37] L. Wang, B. Munch-Petersen, S. A. Herrstrom, U. Hellman, T. Bergman, H. Jornvall, S. Eriksson, FEBS Lett. 443 (1999) 170.
[38] W. Plunkett, V. Gandhi, S. Chubb, B. Nowak, V. Heinemann, S. Mineishi, A. Sen, L. W. Hertel, G. B. Grindey, Nucleosides, Nucleotides and Nucleic Acids 8 (1989) 775.
[39] V. Heinemann, W. Plunkett, Biochem. Pharmacol. 38 (1989) 4115.
[40] J. J. Barchi, Jr., D. A. Cooney, Z. Hao, Z. H. Weinberg, C. Taft, V. E. Marquez, H. Ford, Jr., J. Enzyme Inhib. 9 (1995) 147.
[41] R. L. Momparler, M. Rossi, J. Bouchard, C. Vaccaro, L. F. Momparler, S. Bartolucci, Mol. Pharmacol. 25 (1984) 436.
[42] A. R. Van Rompay, M. Johansson, A. Karlsson, Pharmacol. Ther. 87 (2000) 189.
[43] De Clercq E FAU - Balzarini, J. F. Balzarini, J. F. Descamps, F. A. U. Huang GF, F. A. U. Torrence PF, D. F. Bergstrom, F. A. U. Jones AS, P. F. Serafinowski, G. F. Verhelst, R. T. Walker.
[44] P. H. Ellims, A. Y. Kao, B. A. Chabner, J. Biol. Chem. 256 (1981) 6335.
[45] W. R. Mancini, Y. C. Cheng, Mol. Pharmacol. 23 (1983) 159.
[46] J. Y. Liou, P. Krishnan, C. C. Hsieh, G. E. Dutschman, Y. C. Cheng, Mol. Pharmacol. 63 (2003) 105.
[47] P. H. Ellims, A. Y. Kao, B. A. Chabner, Mol. Cell Biochem. 57 (1983) 185.
[48] E. Scarano, G. Geraci, M. Rossi, Biochemistry 6 (1967) 192.
[49] R. L. Momparler, M. Rossi, J. Bouchard, S. Bartolucci, L. F. Momparler, C. A. Raia, R. Nucci, C. Vaccaro, S. Sepe, Adv. Exp. Med. Biol. 195 Pt B (1986) 157.
[50] Y. Z. Xu, W. Plunkett, Biochemical Pharmacology 44 (1992) 1819.
[51] J. A. Gilbert, O. E. Salavaggione, Y. Ji, L. L. Pelleymounter, B. W. Eckloff, E. D. Wieben, M. M. Ames, R. M. Weinshilboum, Clin. Cancer Res. 12 (2006) 1794.
[52] K. Ikenaka, M. Fukushima, H. Nakamura, M. Okamoto, T. Shirasaka, S. Fujii, Gann 72 (1981) 590.
[53] Y. Maehara, H. Nakamura, Y. Nakane, K. Kawai, M. Okamoto, S. Nagayama, T. Shirasaka, S. Fujii, Gann 73 (1982) 289.
[54] G. Giusti, C. Mangoni, B. De Petrocellis, E. Scarano, Enzymol. Biol. Clin. (Basel) 11 (1970) 375.
[55] B. R. Vincent, G. Buttin, Somatic. Cell Genet. 5 (1979) 67.
[56] P. H. Ellims, G. Medley, Leuk. Res. 8 (1984) 123.
[57] P. V. Danenberg, H. Malli, S. Swenson, Semin. Oncol. 26 (1999) 621.
[58] R. J. Langenbach, P. V. Danenberg, C. Heidelberger, Biochem. Biophys. Res. Commun. 48 (1972) 1565.
[59] G. Weckbecker, Pharmacol. Ther. 50 (1991) 367.
[60] P. Ziemkowski, K. Felczak, J. Poznanski, T. Kulikowski, Z. Zielinski, J. Ciesla, W. Rode, Biochem. Biophys. Res Commun. 362 (2007) 37.
[61] Ruiz, van Haperen, V, Veerman, G., Smid K., Pinedo, H. M., and Peters, G. J., Proceedings of the american association for cancer research36 (1995).
[62] G. B. FitzGerald, J. Ratliff, M. M. Wick, Anticancer Drug Des 1 (1987) 281.
[63] W. E. Muller, Z. I. Yamazaki, H. H. Sogtrop, R. K. Zahn, Eur. J. Cancer 8 (1972) 421.
[64] K. Ono, A. Ohashi, M. Ogasawara, A. Matsukage, T. Takahashi, C. Nakayama, M. Saneyoshi, Biochemistry 20 (1981) 5088.

[65] V. Gandhi, A. Chapman, Huang P, W. Plunkett, Proceedings of the american association for cancer research 34 (1993) 349.
[66] v. H. Ruiz, V, G. Veerman, J. B. Vermorken, G. J. Peters, Biochem. Pharmacol. 46 (1993) 762.
[67] P. V. Danenberg, C. Heidelberger, M. A. Mulkins, A. R. Peterson, Biochem. Biophys. Res. Commun. 102 (1981) 654.
[68] M. Tanaka, S. Yoshida, M. Saneyoshi, T. Yamaguchi, Cancer Res. 41 (1981) 4132.
[69] B. Pauwels, A. E. Korst, H. A. Lambrechts, G. G. Pattyn, C. M. de Pooter, F. Lardon, J. B. Vermorken, Cancer Chemother. Pharmacol. 58 (2006) 219.
[70] Y. Oki, E. Aoki, J. P. Issa, Crit Rev. Oncol. Hematol. 61 (2007) 140.
[71] W. Plunkett, J. O. Liliemark, E. Estey, M. J. Keating, Semin. Oncol. 14 (1987) 159.
[72] S. A. Veltkamp, J. H. Beijnen, J. H. Schellens, Oncologist. 13 (2008) 261.
[73] R. Grunewald, H. Kantarjian, M. J. Keating, J. L. Abbruzzese, P. Tarassoff, W. Plunkett, Cancer Research 50 (1990) 6823.
[74] J. H. Beumer, J. L. Eiseman, R. A. Parise, E. Joseph, J. L. Holleran, J. M. Covey, M. J. Egorin, Clin. Cancer Res. 12 (2006) 7483.
[75] W. Kreis, K. Chan, D. R. Budman, P. Schulman, S. Allen, L. Weiselberg, S. Lichtman, V. Henderson, J. Freeman, M. Deere, ., Cancer Res. 48 (1988) 1337.
[76] J. H. Beumer, J. L. Eiseman, R. A. Parise, E. Joseph, J. M. Covey, M. J. Egorin, Clin. Cancer Res. 14 (2008) 3529.
[77] J. H. Beumer, R. A. Parise, E. M. Newman, J. H. Doroshow, T. W. Synold, H. J. Lenz, M. J. Egorin, Cancer Chemother. Pharmacol. 62 (2008) 363.
[78] J. Laliberte, V. E. Marquez, R. L. Momparler, Cancer Chemother. Pharmacol. 30 (1992) 7.
[79] M. Lemaire, L. F. Momparler, N. J. Raynal, M. L. Bernstein, R. L. Momparler, Cancer Chemother. Pharmacol. (2008).
[80] M. Lemaire, L. F. Momparler, M. L. Bernstein, V. E. Marquez, R. L. Momparler, Anticancer Drugs 16 (2005) 301.
[81] A. Hamada, T. Kawaguchi, M. Nakano, Clin. Pharmacokinet. 41 (2002) 705.
[82] F. Castelli, M. G. Sarpietro, M. Ceruti, F. Rocco, L. Cattel, Mol. Pharm. 3 (2006) 737.
[83] C. M. Galmarini, F. Myhren, M. L. Sandvold, Br. J. Haematol. 144 (2009) 273.
[84] H. Khoury, A. Deroussent, L. H. Reddy, P. Couvreur, G. Vassal, A. Paci, J. Chromatogr. B 858 (2007) 71.
[85] C. P. Landowski, P. L. Lorenzi, X. Song, G. L. Amidon, J. Pharmacol. Exp. Ther. 316 (2006) 572.
[86] G. Pasut, F. Canal, V. L. Dalla, S. Arpicco, F. M. Veronese, O. Schiavon, J. Control Release 127 (2008) 239.
[87] W. Wu, J. Sigmond, G. J. Peters, R. F. Borch, J. Med. Chem. 50 (2007) 3743.
[88] S. C. Tobias, R. F. Borch, Mol. Pharm. 1 (2004) 112.
[89] C. B. Yoo, S. Jeong, G. Egger, G. Liang, P. Phiasivongsa, C. Tang, S. Redkar, P. A. Jones, Cancer Res. 67 (2007) 6400.
[90] L. Naesens, G. Andrei, I. Votruba, M. Krecmerova, A. Holy, J. Neyts, E. De Clercq, R. Snoeck, Biochem. Pharmacol. 76 (2008) 997.
[91] P. S. Ludwig, R. A. Schwendener, H. Schott, Eur. J. Med. Chem. 40 (2005) 494.
[92] C. M. Galmarini, G. Warren, E. Kohli, A. Zeman, A. Mitin, S. V. Vinogradov, Mol. Cancer Ther. 7 (2008) 3373.

Chapter 3.4

Decitabine triphosphate levels in peripheral blood mononuclear cells from patients receiving prolonged low-dose decitabine administration: a pilot study

Robert S Jansen, Hilde Rosing, Pierre W Wijermans, Ron J Keizer, Jan HM Schellens and Jos H Beijnen

Submitted for publication

Abstract

Decitabine is a nucleoside analog used in the epigenetic treatment of myelodysplastic syndrome. The compound requires intracellular conversion to its triphosphate to become active. Decitabine triphosphate has, however, never been quantified in patients. This article describes a method for the quantitative determination of decitabine triphosphate in peripheral blood mononuclear cells using liquid chromatography coupled to tandem mass spectrometry. The method was applied to samples from three patients receiving prolonged low-dose decitabine treatment. The data show that, in contrast with plasma decitabine levels, intracellular decitabine triphosphate accumulates during a treatment cycle of nine 15 mg/m^2 infusions. Moreover, the results suggest a relation between decitabine triphosphate levels and response to therapy. Furthermore, we searched for the presence of deaminated decitabine metabolites.

Introduction

Epigenetic therapy is a promising approach in cancer therapy because aberrant DNA methylation plays a role in many cancer types [1-3]. Decitabine (5-aza-2'-deoxycytidine, aza-dC; figure 1) is a classic epigenetic agent that is registered for treatment of patients with myelodysplastic syndrome. Aza-dC is a deoxycytidine (figure 1) analog which has a plasma half-life of only 15-25 minutes due to deamination to 5-aza-2'-deoxyuridine (aza-dU) [4]. After uptake in cells by nucleoside transporters, on the other hand, aza-dC is converted to its mono-, and subsequently di- and triphosphate (aza-dCMP, aza-dCDP and aza-dCTP, respectively). The metabolism of aza-dC is depicted in figure 2. The active metabolite aza-dCTP is incorporated into DNA leading to inhibition of DNA methyltransferases. Thereby, aza-dC causes global DNA hypomethylation. Moreover, specific tumor suppressor genes become hypomethylated, which results in their re-expression.

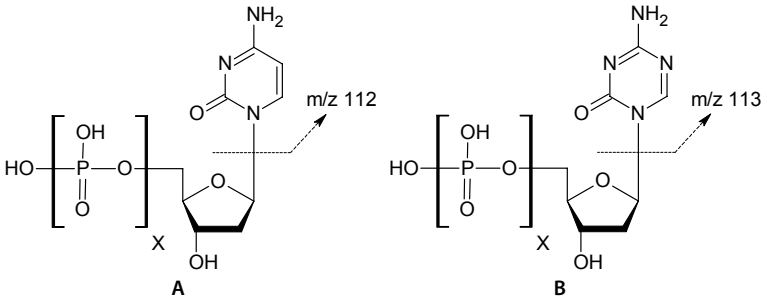

Figure 1. Molecular structure of deoxycytidine (dC) (A) and decitabine (B) (X=0) and their mono- (X=1), di- (X=2) and triphosphate (X=3). The arrows indicate the proposed fragmentation.

Based on classical maximum tolerated dose determinations, the drug was first tested at high (1500-2500 mg/m^2 per cycle) doses. Lower doses (100-150 mg/m^2 per cycle) were, however, later found to be effective as well, but without causing the myelosupppression observed at high doses [5;6]. The cytotoxic effect observed at higher doses reduces the hypomethylating effect, resulting in U-shaped dose-methylated DNA curves [7;8]. Thus, hypomethylation is the main effect at low doses, whereas high doses are cytotoxic [9]. This dual mechanism of action and the fact that the agent is S-phase specific, make that the dose schedule is of extreme importance.

For that reason various dosing schedules have been tested, ranging from long low-dose continuous [10] or intermittent [11] infusions to short, high-dose infusions [12]. Promising results have been obtained with low-dose infusions at a high intensity. Several of these dose schemes have been tested in relatively large clinical trials [13-16], leading to the registered

dosing scheme of 15 mg/m^2 administered as a 3-hour intravenous infusion repeated every 8 hours during 3 days.
Several pharmacokinetic and pharmacodynamic parameters have been determined to assess the effect of the different dosing schemes. Plasma aza-dC pharmacokinetic data is available [10;12;17-20], but only one study involves the recommended dose [21]. Global and specific gene methylation have been used as pharmacodynamic endpoints in many studies. Both approaches have, however, shown mixed correlations with clinical outcome [22-24].
Despite all these efforts, the optimal aza-dC dosing schedule remains a subject of debate [25;26]. Furthermore, some patients are, or become, resistant to aza-dC treatment [7;16].
For other nucleoside analogs, measurements of the active triphosphate have been used to determine optimal dosing schemes [27;28].Additionally, it has been suggested that aza-dC resistance is related to the lack of intracellular aza-dCTP formation [7]. Therefore, the determination of intracellular aza-dCTP is crucial to design an optimal dosing scheme as well as to detect and to understand the source of resistance to therapy.
Quantitative determination of aza-dC and its metabolites is, however, analytically challenging because of their instability and low concentrations [7;18;29;30]. As a result, data on the intracellular concentrations of aza-dCTP are extremely sparse [31]. Besides, these measurements were performed *in vitro* and in animals receiving high doses, whereas patients currently receive low doses of the drug.
Recently the formation of deaminated nucleotides has been shown in patients who were treated with the deoxycytidine analogs cytarabine and gemcitabine (2'-2'-difluorodeoxycytidine, dFdC) [32-34]. Moreover, these deaminated nucleotides possibly have pharmacological activity [35]. Cytarabine and gemcitabine use the same metabolic pathways as aza-dC (figure 2). Aza-dCMP is, for example, a substrate for deoxycytidine monophosphate deaminase (dCMPD) [36]. Indeed, early work with radioactive aza-dC showed *in vivo* and *in vitro* formation of the deaminated aza-dC monophosphate (aza-dUMP) and possibly of higher phosphates [37]. We hypothesised that deaminated nucleotides might also be formed during aza-dC therapy (figure 2).
In this article we present a sensitive method for the quantification of aza-dC nucleotides in peripheral blood mononuclear cells (PBMCs) using high performance liquid chromatography coupled with tandem mass spectrometry (HPLC-MS/MS). The method was used to determine intracellular aza-dCTP concentrations in PBMCs from patients with myelodysplastic syndrome for the first time. Furthermore, we have scouted for the presence of deaminated aza-dC nucleotides in plasma and PBMCs.

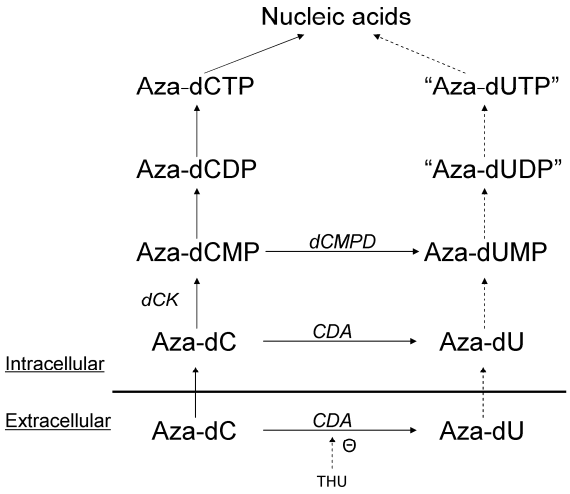

Figure 2. Schematic representation of the metabolism of aza-dC. Hypothesized metabolites are indicated by quotation marks. dCK: deoxycytidine kinase; CDA: cytidine deaminase; dCMPD: deoxycytidine monophosphate deaminase; THU: tetrahydrouridine.

Material and methods

Patients and dosing

All patients were diagnosed with myelodysplastic syndrome and received 15 mg/m^2 aza-dC, administered as a 4-hour intravenous infusion repeated every 8 hours during 3 days as previously described [16]. These treatment cycles were repeated every 6 weeks. A single sample was collected from patient 1 and 2 after the last (9th) infusion of the first cycle. Additional samples were collected only from patient 2 and 3 after infusion 3, 6 and 9 of cycle 5.

Patient sample collection

Blood samples (15-20 mL) were collected within 30 minutes after the end of the infusion, except the last sample from patient 3, which was collected 25 minutes before the end of the infusion. All samples were immediately placed on ice. A 10 mg/mL tetrahydrouridine solution was added (final concentration of 100 µg/mL) to the samples collected after the first cycle to prevent plasma *ex vivo* deamination of aza-dC [21;30].
The samples were centrifuged for 5 minutes at 1,500 g (4°C) to separate the plasma from the buffy coat containing the PBMCs. The plasma of the samples collected after the first cycle was stored at -70°C until analysis. The buffy coat was diluted in cold phosphate buffered saline (PBS) and layered over ficoll paque density gradient. After centrifugation during 20 minutes at 550 g (4°C) the PBMCs were collected and washed with cold PBS. The number of PBMCs isolated was determined, and the cells were finally suspended in PBS. Cold methanol was added (2.33 times the volume of the suspension) to lyse the cells and to extract the nucleotides. Finally, the samples were vortexed for 30 seconds and stored at -70°C until analysis. Blank PBMCs were isolated from donor buffy coat as previously described [38], and lysed with methanol as described above.

Ex vivo incubations

Blood was collected from two healthy volunteers. Aliquots of approximately 8 mL were incubated at 1, 10 or 100 µM aza-dC for 1 hour (batch 1) or at 1 and 100 µM for 5 hour (batch 2) at 37°C. The samples were then transferred to cell preparation tubes (BD Vacutainer CPT; BD, Franklin Lakes, NJ, USA) and centrifuged during 20 minutes at 1,500 g. The plasma and PBMCs were collected and processed further as described under "patient sample collection".

Aza-dC deamination

A solution containing 1 mg/mL aza-dC (Sigma, St. Louis, MO, USA) in 10 mM tris(hydroxymethyl)aminomethane (TRIS)-HCl buffer pH 7.5 was

treated with 20 µL (134 µg/mL) cytidine deaminase (Eli lilly and company, Indianapolis, IN, USA). The mixture was incubated at 37°C, and 10 µL samples were taken at time zero and after up to 1 hour. These samples were diluted with 90 µL methanol, centrifuged, and directly analyzed with the qualitative method described below.

Synthesis of aza-dC nucleotides

A mixture containing aza-dCMP, aza-dCDP and aza-dCTP was synthesized from aza-dC. About 25 µmole aza-dC was dissolved in 2.5 mL trimethylphosphate by brief gentle heating. Proton sponge (1,8-bis(dimethylamino)naphthalene) (50 µmoles) was added and the mixture was cooled on ice. A large excess (15 equivalents) of phosphorous oxychloride was then added dropwise over 6 minutes, after which the mixture was stirred at room temperature for 2.5 hours. After adding an excess (20 equivalents) of cold tributylammonium phosphate and tributylamine (250 µM in dimethylformamide) to the cooled reaction mixture, it was poured into 15 mL cold 1 M triethylammonium bicarbonate. The solution was lyophilized, redissolved in water and stored at -70°C.

The mixture was analyzed using the method for the qualitative analysis coupled to an LTQ mass spectrometer (MS) and photodiode array detector (both from Thermo Fisher Scientific Inc., Waltham, MA, USA). The synthesis products were identified by their m/z values (m/z 229, 309, 389 and 469 for aza-dC, aza-dCMP, aza-dCDP and aza-dCTP, respectively) and UV-absorption spectra (absorption maximum at 245 nm). Because nucleosides and nucleotides have an identical molar absorption, the products could be quantitated using UV-detection (245 nm), with an external aza-dC reference standard.

Sample preparation

Cell lysate and plasma samples were thawed on ice-water. To 90 µL of the samples, 5 µL water (unknown samples) or 5 µL diluted synthesized aza-dC nucleotide mixture (calibration standards) was added. Calibration standards were spiked with concentrations ranging from 1.20-120, 0.263-26.3 and 0.310-31.0 for aza-dCMP, aza-dCDP and aza-dCTP, respectively.

Stable isotope (^{13}C-$^{15}N_2$)-labelled dFdC, its deaminated metabolite 2'-2'-difluorodeoxyuridine (dFdU) and their nucleotides (5 µL) were added as internal standards. Finally the sample was centrifuged for 5 minutes at 23,100 g (4°C), and transferred to an autosampler vial.

Qualitative analysis of aza-dC, aza-dCMP, aza-dCDP and aza-dCTP and their deaminated metabolites

We recently developed a HPLC-MS/MS method to separate dFdC, dFdU and their mono-, di- and triphosphates compatible with MS detection [39].

With minor adaptations this method was used to screen for aza-dC, aza-dU and their mono-, di- and triphosphates in plasma and PBMCs. In brief, 25 µL processed sample was injected onto a porous graphitic carbon column (Hypercarb, 100 X 2.1 mm ID, 5 µm particles; Thermo Fisher Scientific Inc.). Separation was achieved using a gradient of 1 mM ammonium acetate in acetonitrile:water (15:85, v/v) pH 5 and 25 mM ammonium bicarbonate in acetonitrile:water (15:85, v/v), at a flow of 0.25 mL/min. Detection was performed using an API4000 triple quadrupole MS (Applied Biosystems, Foster city, CA, USA) using the transitions and polarities presented in table 1.

Quantitative analysis of aza-dCMP, aza-dCDP and aza-dCTP

The analysis of aza-dCMP, -DP and -TP in PBMC cell lysates was adapted from a method previously described for cladribine [40] and gemcitabine [38] nucleotides. In brief, 25 µL processed cell lysate was injected onto a weak anion exchange column (Biobasic AX column, 50 x 2.1 mm, 5 µm particles; Thermo Fisher Scientific Inc,). The analytes were separated using a fast gradient of 10 mM ammonium acetate in acetonitrile:water (30:70, v/v) pH 6.0 and 1 mM ammonium acetate in acetonitrile:water (30:70, v/v) pH 10.5, at a flow of 0.25 mL/min. Detection was performed with an API4000 triple quadrupole mass spectrometer operated in the positive ionization mode with the mass transitions presented in table 2.

Table 1. Mass transitions monitored with the API4000 triple quadrupole mass spectrometer for the qualitative analysis of aza-dC and it metabolites.

Compound	Parent ion (m/z)	Product ion (m/z)	Polarity
Aza-dC	229	113	+
Aza-dU	228	112	-
Aza-dCMP	309	113	+
Aza-dUMP	310	114	+
Aza-dCDP	389	113	+
Aza-dUDP	390	114	+
Aza-dCTP	469	113	+
Aza-dUTP	470	114	+

Table 2. Mass transitions monitored with the API4000 triple quadrupole mass spectrometer for the quantitative analysis of the aza-dC nucleotides.

Compound Name	Type	Parent ion (m/z)	Product ion (m/z)
dCMP	Interference	308	112
Aza-dCMP	Analyte	309	113
*dFdCMP	Internal standard	347	249
dCDP	Interference	388	112
Aza-dCDP	Analyte	389	113
*dFdCDP	Internal standard	427	329
dCTP	Interference	468	112
Aza-dCTP	Analyte	469	113
*dFdCTP	Internal standard	507	329

Results and discussion

Qualitative analysis of aza-dC, aza-dCMP, aza-dCDP and aza-dCTP and their deaminated metabolites

A qualitative method was developed to search for the presence of aza-dU and its mono-, di- and triphosphate. Deoxycytidines (dFdC and aza-dC and their nucleotides) cause a signal in the mass transition of their uridine variants (dFdU, aza-dU and their nucleotides) [39]. For correct detection of the uridine variants these analytes must, therefore, be separated chromatographically. Using the described HPLC system dFdC, dFdU and their nucleotides were all separated. The retention times of aza-dC and its nucleotides were very similar to those of dFdC and its nucleotides. Therefore, we assumed that aza-dU, aza-dUMP, aza-dUDP and aza-dUTP were also separated from their aza-dC counterparts. The mass transitions of aza-dU and its nucleotides were based on those of dFdU and its nucleotides. To confirm that aza-dU was detectable with the described system we deaminated aza-dC with CDA and analyzed the product. Deaminated aza-dC products were indeed detected and separated from aza-dC, using the selected conditions.

Ex vivo incubations

We performed *ex vivo* incubations with aza-dC under different conditions (individuals, concentration and incubation time) and analyzed these samples with the qualitative method. In plasma and cell lysate we detected aza-dC only in the samples incubated with 10 and 100 µM. We could, however, detect aza-dC nucleotides in all cell lysates.

As for aza-dC, deaminated aza-dC was only detected in the samples incubated with high aza-dC concentrations. Aza-dU nucleotides were, on the other hand, not detected in plasma or cell lysate.

Patient samples

We scouted for evidence of deaminated aza-dC metabolites in the samples collected after the 9th infusion of the first treatment cycle. Aza-dU and its nucleotides could not be detected in these plasma or cell lysate samples. In contrast to the *ex vivo* experiments, aza-dC was not detected in these plasma and cell lysate samples, whereas its nucleotides were observed. The lack of detectable aza-dC in patient plasma is most likely caused by a combination of the low dose administered and rapid metabolism [21]. The absence of aza-dU and its nucleotides, can be explained by an actual lack of formation or their instability. We and others, have shown that aza-dC is a substrate for CDA [41-44] and that aza-dCMP is a substrate for dCMPD [45]. An actual lack of formation, therefore, seems unlikely. More likely, aza-dU and its nucleotides rapidly degrade to other metabolites, such as those proposed by Patel et al. [30].

Quantitative analysis of aza-dCMP, aza-dCDP and aza-dCTP

Because aza-dU and its nucleotides were not detected in any of the patient samples, we could restrict the quantitative analysis to aza-dCMP, aza-dCDP and aza-dCTP, with the focus being on the active metabolite aza-dCTP. Therefore, we analyzed cell lysates with a less specific, but more sensitive HPLC-MS method. Figure 3 shows a chromatogram from a patient sample. Using this method, however, we noticed a peak in the aza-dCTP mass transition of the blanks. This interference was caused by deoxycytidine triphosphate (dCTP) the natural variant of aza-dCTP. Although the masses of dCTP (467 Da) and aza-dCTP (468 Da) are slightly different, dCTP molecules containing a naturally occurring ^{13}C- or ^{15}N-isotope have the same parent and fragment mass as aza-dCTP (figure 1). Similarly, interferences caused by deoxycytidine were observed in the HPLC-MS/MS analysis of aza-dC by others [18]. Since the number of isotopes in dCTP, and thus its relative interference, are constant, the interference can be determined if the dCTP signal is known. We, therefore, additionally monitored the dCTP mass transition in each sample. Theoretically 5.5% of the dCTP molecules will give a signal in the aza-dCTP mass transition. This percentage is in close agreement with the 6% we determined by spiking blank cell lysate with different dCTP concentrations. With this percentage we calculated the interference caused by dCTP for each patient sample and found that 15.4% of the aza-dCTP signal could be attributed to dCTP in the sample containing the lowest aza-dCTP concentration. All other calculated interferences were lower than 7.20%.

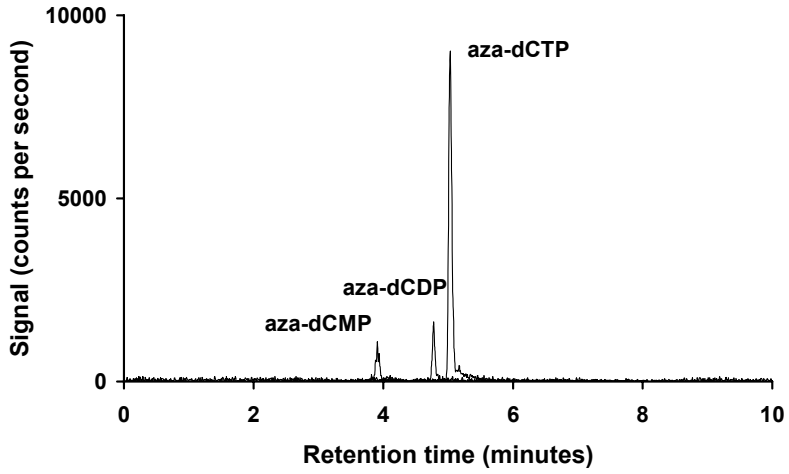

Figure 3. Chromatogram from a PBMC sample collected from patient 2 after the last infusion of the 5th treatment cycle.

Ex vivo incubations

Aza-dCTP was the main metabolite in all samples analyzed. Aza-dCMP and aza-dCDP accounted for 21.4-23.4% and 3.91-42.3% of the total aza-dC nucleotide concentration, respectively. The aza-dCTP concentrations determined in the *ex vivo* incubated samples are presented in figure 4A. The intracellular aza-dCTP levels increased with higher extracellular aza-dC concentrations. This increase was, however, not proportional. Most likely cellular aza-dC uptake or phosphorylation was saturated at higher concentrations, as also observed with other nucleoside analogs [28]. Finally, the data of the *ex vivo* incubations show a considerable inter-individual variability. This variability was even more pronounced between the patients, as discussed below.

Patient samples

In patient samples, aza-dCTP was the main metabolite, with aza-dCMP and aza-dCDP accounting for 2.08-28.8% and 2.33-21.2% of the total aza-dC nucleotide concentration, respectively.

Of the samples collected after the first cycle a very low aza-dCTP concentration (6.62 fmol/10^6 PBMCs) was detected in the sample from patient 1, whereas an aza-dCTP concentration of 308 fmol/10^6 PBMCs was found in patient 2 (figure 4B). Interestingly, this striking difference in active metabolite concentration agreed well with the clinical response later observed. Patient 1 did not show any objective response to the therapy, whereas patient 2 responded well and no longer required blood transfusions. Patient 3 also showed a good response to therapy when samples were collected, which was in line with the high intracellular aza-dCTP levels detected.

Resistance to nucleoside analogs can be caused by several mechanisms [46]. Aza-dC resistance has been associated with low dCK and nucleoside transporter activity, and high activity of CDA [7;41;47-49]. Conversely, increased sensitivity was observed in dCK overexpressing cells [50] and when the drug was administrated in combination with a CDA inhibitor [43]. All these mechanisms of resistance result in less intracellular aza-dCTP formation (figure 2) as observed in patient 1. A third mechanism of resistance is an increase in intracellular dCTP, the natural competitor of aza-dCTP [51]. The dCTP levels monitored in patient 1 were, however, not increased compared to those in other samples. Thus, increased dCTP levels were not the source of resistance in this patient. Currently, resistance to therapy can only be determined based on clinical response after several 6-week cycles. If a lack of aza-dCTP formation is indeed the main source of resistance, determination of aza-dCTP levels might offer a huge improvement in the assessment of response to therapy.

Aza-dC plasma concentrations reached in patients during similar dosing scheme are about 0.25 μM [21]. Based on the *ex vivo* experiments performed at 1, 10 and 100 μM relatively low aza-dCTP levels were thus expected in the patient samples. The aza-dCTP concentration in the

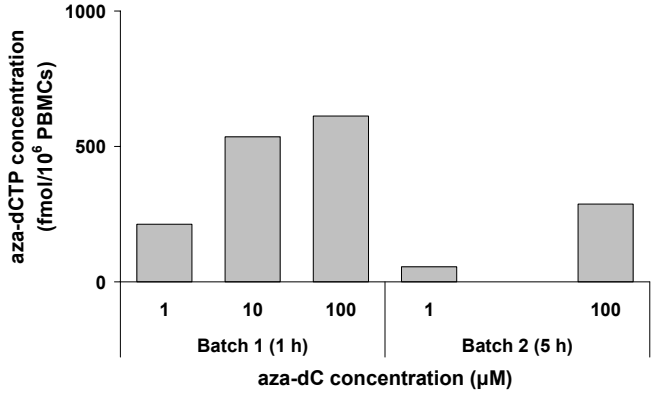

A

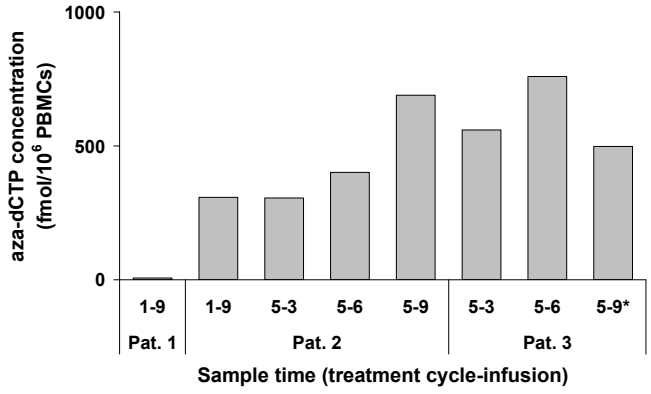

B

Figure 4. Intracellular aza-dCTP levels found in PBMCs after *ex vivo* incubations of whole blood from healthy volunteers with aza-dC (A) and in three patients receiving prolonged low-dose aza-dC treatment (B). * Sample was collected 25 minutes before the end of the infusion.

sample from patient 2 was, however, remarkably high compared to those found in the *ex vivo* experiments (figure 4). Since the sample was taken at the end of the 9th infusion, this indicated that aza-dCTP accumulated during the subsequent infusions of a treatment cycle. To assess the accumulation, we collected additional samples from patient 2 and 3 at the end of infusion 3, 6 and 9. The data presented in figure 4B show that aza-dCTP indeed accumulated in PBMCs during a treatment cycle. The accumulation rate indicates a half-life that exceeds the 4-hour dosing interval. The last sample from patient 3, which contains a relatively low aza-dCTP concentration, was collected 25 minutes before the end of the infusion. Assuming a long half-life, it is, however, very unlikely that the aberrant sample time was the cause of the low aza-dCTP levels detected. Pharmacokinetic studies performed in larger groups of patients should

confirm whether this unexpected result can be considered an outlier, or whether there is a pharmacokinetic explanation.
Cashen et al. found identical plasma aza-dC curves on day 1, 2 and 3 of a treatment cycle, showing that aza-dC does not accumulate in plasma using a similar dose scheme [21]. Our results show that, in contrast to aza-dC, the active metabolite aza-dCTP does accumulate during a treatment cycle.

Optimal dosing scheme

Knowledge of the intracellular pharmacology of aza-dC is critical in designing the optimal dosing scheme. The optimal dosing scheme should be aimed at reaching effective intracellular aza-dCTP levels for a period sufficiently long for all cells to go through the S-phase, in which aza-dCTP is incorporated into DNA. The concentration at which maximum hypomethylation occurs is, however, unknown and requires further investigation. The accumulation during therapy suggests that the current dosing scheme might not be optimal. More constant intracellular aza-dCTP levels could be reached by administration of a high loading dose followed by low maintenance doses. Using such a scheme, a sufficiently long half-life of aza-dCTP would allow once-daily, or even less frequent dosing making the current patient hospitalization unnecessary.

Conclusion

We successfully quantified aza-dC nucleotides in PBMCs of two patients receiving prolonged low-dose aza-dC. The absence of detectable aza-dCTP levels in a non-responding patient and the presence of significant aza-dCTP levels in 2 responding patient suggest that a lack of intracellular aza-dCTP formation is a source of resistance to therapy. Aza-dCTP accumulated during the 9-infusion cycle suggesting that a less intensive dosing scheme is feasible. Finally, deaminated aza-dC metabolites have not been detected in patient samples, which is probably due to their instability. Future research should corroborate our findings and determine the relationship between intracellular aza-dCTP levels, hypomethylation and clinical response.

References

[1] J. G. Herman, S. B. Baylin, N. Engl. J. Med. 349 (2003) 2042.
[2] P. A. Jones, S. B. Baylin, Nat. Rev. Genet. 3 (2002) 415.
[3] J. P. Issa, Clin. Cancer Res. 13 (2007) 1634.
[4] R. L. Momparler, Semin. Hematol. 42 (2005) S9.
[5] E. Jabbour, J. P. Issa, G. Garcia-Manero, H. Kantarjian, Cancer 112 (2008) 2341.
[6] Y. Oki, E. Aoki, J. P. Issa, Crit Rev. Oncol. Hematol. 61 (2007) 140.
[7] T. Qin, J. Jelinek, J. Si, J. Shu, J. P. Issa, Blood 113 (2009) 659.
[8] T. Qin, E. M. Youssef, J. Jelinek, R. Chen, A. S. Yang, G. Garcia-Manero, J. P. Issa, Clin. Cancer Res. 13 (2007) 4225.
[9] H. M. Kantarjian, J. P. Issa, Semin. Hematol. 42 (2005) S17-S22.
[10] A. Aparicio, C. A. Eads, L. A. Leong, P. W. Laird, E. M. Newman, T. W. Synold, S. D. Baker, M. Zhao, J. S. Weber, Cancer Chemother. Pharmacol. 51 (2003) 231.
[11] J. DeSimone, M. Koshy, L. Dorn, D. Lavelle, L. Bressler, R. Molokie, N. Talischy, Blood 99 (2002) 3905.
[12] G. E. Rivard, R. L. Momparler, J. Demers, P. Benoit, R. Raymond, K. Lin, L. F. Momparler, Leuk. Res. 5 (1981) 453.
[13] H. Kantarjian, J. P. Issa, C. S. Rosenfeld, J. M. Bennett, M. Albitar, J. DiPersio, V. Klimek, J. Slack, C. de Castro, F. Ravandi, R. Helmer, III, L. Shen, S. D. Nimer, R. Leavitt, A. Raza, H. Saba, Cancer 106 (2006) 1794.
[14] H. Kantarjian, Y. Oki, G. Garcia-Manero, X. Huang, S. O'Brien, J. Cortes, S. Faderl, C. Bueso-Ramos, F. Ravandi, Z. Estrov, A. Ferrajoli, W. Wierda, J. Shan, J. Davis, F. Giles, H. I. Saba, J. P. Issa, Blood 109 (2007) 52.
[15] J. P. Issa, G. Garcia-Manero, F. J. Giles, R. Mannari, D. Thomas, S. Faderl, E. Bayar, J. Lyons, C. S. Rosenfeld, J. Cortes, H. M. Kantarjian, Blood 103 (2004) 1635.
[16] B. Ruter, P. W. Wijermans, M. Lubbert, Cancer 106 (2006) 1744.
[17] R. L. Momparler, G. E. Rivard, M. Gyger, Pharmacol. Ther. 30 (1985) 277.
[18] Z. Liu, G. Marcucci, J. C. Byrd, M. Grever, J. Xiao, K. K. Chan, Rapid Commun. Mass Spectrom. 20 (2006) 1117.
[19] C. J. van Groeningen, A. Leyva, A. M. O'Brien, H. E. Gall, H. M. Pinedo, Cancer Res. 46 (1986) 4831.
[20] R. L. Momparler, D. Y. Bouffard, L. F. Momparler, J. Dionne, K. Belanger, J. Ayoub, Anticancer Drugs 8 (1997) 358.
[21] A. F. Cashen, A. K. Shah, L. Todt, N. Fisher, J. DiPersio, Cancer Chemother. Pharmacol. 61 (2008) 759.
[22] B. Hackanson, C. Robbel, P. Wijermans, M. Lubbert, Ann. Hematol. 84 Suppl 1 (2005) 32.
[23] A. S. Yang, K. D. Doshi, S. W. Choi, J. B. Mason, R. K. Mannari, V. Gharybian, R. Luna, A. Rashid, L. Shen, M. R. Estecio, H. M. Kantarjian, G. Garcia-Manero, J. P. Issa, Cancer Res. 66 (2006) 5495.
[24] Y. Oki, J. Jelinek, L. Shen, H. M. Kantarjian, J. P. Issa, Blood 111 (2008) 2382.
[25] R. L. Momparler, S. Cote, N. Eliopoulos, Leukemia 11 (1997) 175.
[26] M. Lemaire, G. G. Chabot, N. J. Raynal, L. F. Momparler, A. Hurtubise, M. L. Bernstein, R. L. Momparler, BMC. Cancer 8 (2008) 128.
[27] L. H. Wang, J. Begley, C. R. St, III, J. Harris, C. Wakeford, F. S. Rousseau, AIDS Res. Hum. Retroviruses 20 (2004) 1173.
[28] R. Grunewald, H. Kantarjian, M. J. Keating, J. L. Abbruzzese, P. Tarassoff, W. Plunkett, Cancer Research 50 (1990) 6823.
[29] K. T. Lin, R. L. Momparler, G. E. Rivard, J. Pharm. Sci. 70 (1981) 1228.
[30] K. Patel, S. M. Guichard, D. I. Jodrell, J. Chromatogr. B Analyt. Technol. Biomed. Life Sci. 863 (2008) 19.
[31] S. Grant, F. Rauscher, III, J. Margolin, E. Cadman, Cancer Res. 42 (1982) 519.
[32] V. Gandhi, Y. Z. Xu, E. Estey, Clin. Cancer Res. 4 (1998) 1719.

[33] S. A. Veltkamp, D. Pluim, O. van Tellingen, J. H. Beijnen, J. H. Schellens, Drug Metab Dispos. 36 (2008) 1606.
[34] S. A. Veltkamp, R. S. Jansen, S. Callies, D. Pluim, C. M. Visseren-Grul, H. Rosing, S. Kloeker-Rhoades, V. A. Andre, J. H. Beijnen, C. A. Slapak, J. H. Schellens, Clin. Cancer Res. 14 (2008) 3477.
[35] S. A. Veltkamp, D. Pluim, M. A. van Eijndhoven, M. J. Bolijn, F. H. Ong, R. Govindarajan, J. D. Unadkat, J. H. Beijnen, J. H. Schellens, Mol. Cancer Ther. 7 (2008) 2415.
[36] R. L. Momparler, M. Rossi, J. Bouchard, S. Bartolucci, L. F. Momparler, C. A. Raia, R. Nucci, C. Vaccaro, S. Sepe, Adv. Exp. Med. Biol. 195 Pt B (1986) 157.
[37] A. Cihak, Eur. J. Cancer 14 (1978) 117.
[38] S. A. Veltkamp, M. J. Hillebrand, H. Rosing, R. S. Jansen, E. R. Wickremsinhe, E. J. Perkins, J. H. Schellens, J. H. Beijnen, J. Mass Spectrom. 41 (2006) 1633.
[39] R. S. Jansen, H. Rosing, J. H. Schellens, J. H. Beijnen, J. Chromatogr. A 1216 (2009) 3168.
[40] R. S. Jansen, H. Rosing, C. J. de Wolf, J. H. Beijnen, Rapid Commun. Mass Spectrom. 21 (2007) 4049.
[41] N. Eliopoulos, D. Cournoyer, R. L. Momparler, Cancer Chemother. Pharmacol. 42 (1998) 373.
[42] J. Laliberte, V. E. Marquez, R. L. Momparler, Cancer Chemother. Pharmacol. 30 (1992) 7.
[43] M. Lemaire, L. F. Momparler, N. J. Raynal, M. L. Bernstein, R. L. Momparler, Cancer Chemother. Pharmacol. 63 (2009) 411.
[44] G. G. Chabot, J. Bouchard, R. L. Momparler, Biochem. Pharmacol. 32 (1983) 1327.
[45] R. L. Momparler, M. Rossi, J. Bouchard, C. Vaccaro, L. F. Momparler, S. Bartolucci, Mol. Pharmacol. 25 (1984) 436.
[46] L. Jordheim, C. M. Galmarini, C. Dumontet, Curr. Drug Targets. 4 (2003) 443.
[47] A. P. Stegmann, M. W. Honders, A. Hagemeijer, B. Hoebee, R. Willemze, J. E. Landegent, Ann. Hematol. 71 (1995) 41.
[48] R. L. Momparler, L. F. Momparler, Cancer Chemother. Pharmacol. 25 (1989) 51.
[49] R. L. Momparler, Pharmacol. Ther. 30 (1985) 287.
[50] C. M. Beausejour, J. Gagnon, M. Primeau, R. L. Momparler, Biochem. Biophys. Res. Commun. 293 (2002) 1478.
[51] R. L. Momparler, M. Y. Chu, G. A. Fischer, Biochim. Biophys. Acta 161 (1968) 481.

Chapter 4

Conclusion and perspectives

Conclusion and perspectives

The aim of this thesis project was to develop sensitive LC-MS/MS assays to quantitate nucleoside and nucleotide analogs in cells, and to apply these assays to preclinical and clinical studies in order to increase the knowledge of nucleoside analog pharmacology. Here, we evaluate these aims and discuss the major conclusions of the thesis in a broader perspective. Moreover, thoughts are given on possible future research.

Analytical aspects

With the presented synthesis method, nucleosides can be phosphorylated to their nucleotides in laboratories that are not specialized in organic synthesis. The ability to swiftly synthesize nucleotides makes laboratories flexible, allowing research on any nucleotide analog to start within a short period of time.

Over the past decade many approaches have been developed for the challenging analysis of nucleotide analogs with LC-MS/MS. The weak anion-exchange liquid chromatography method applied to multiple analytes in this thesis is a relatively simple and very sensitive method for the simultaneous quantitation of nucleoside mono-, di- and triphosphates. The developed porous graphitic carbon method demonstrates superior selectivity but required specific handling. Both methods showed good assay performances as demonstrated by their successful validations.

Because nucleotide analogs all share the same chemical basis structure, the various methods are often considered to be “general” methods for the analysis of nucleotides. Exactly because of these structural similarities, however, a myriad of potentially interfering endogenous nucleotides and nucleotide analogs is present in biological samples. In the work for this thesis, for example, we encountered the interference of the gemcitabine analytes in the mass transitions of their deaminated counterparts and the interference of deoxycytidine triphosphate in the mass transition of decitabine triphosphate. These problems were solved by using a selective chromatographic separation and by indirectly quantifying the interfering signal, respectively. Other interferences will, however, keep appearing in future analyses, requiring ongoing development of new analytical approaches.

Since the first publication on nucleotide analog analysis with LC-MS/MS in 1997, the number of published methods on the subject has quickly grown. This underlines that LC-MS/MS is currently the method of choice for quantitative bioanalysis of nucleotide analogs. In the past years, indirect methods still accounted for a considerable part of the total LC-MS/MS methods. However, the availability of powerful direct analyses, such as

those described in this thesis, will most likely cause a shift towards direct methods in the future.

Attention should be given to the steps preceding the actual LC-MS/MS analysis.
First of all, bioanalysis is almost exclusively performed in white blood cells. It is, however, questionable whether this matrix corresponds well to the actual target matrix. Possibly, better correlations with the clinical effect are found when analyses are performed in, for example, solid tumor cells, $CD4^+$-cells and leukemic cells, or even in subcellular compartments such as mitochondria. Alternatively, the analytical methods could be applied to determine the nucleotide analogs that are incorporated in nucleic acids as monophosphates. This would allow to determine the cumulative effect of a therapy.

Besides the choice of matrix the quantitation of the number of cells isolated is also pivotal in obtaining a correct final result (expressed as concentration per cell). Protein or DNA-based cell counting methods such as presented in this thesis can be performed in a central lab after sample storage. A DNA-based method is preferred over a protein determination because it is not affected by inevitable red blood cell contamination of samples. This approach, however, still requires a separate method for cell counting and analyte quantitation. Ideally, a compound present in each cell, in a constant concentration should be measured together with the nucleotide analogs.

Pharmacological aspects

Therapy resistance

The drug efflux pump breast cancer resistance protein (BCRP) is a very effective transporter of nucleoside analogs and their monophosphates. In addition, the detection of gemcitabine monophosphate concentrations in extracellular pleural fluid from patients indicates drug efflux pump activity. Drug efflux pumps can, thus, play an important role in resistance to nucleoside analog therapy. Resistance to therapy can be detected by determining intracellular nucleoside analog triphosphate levels, as demonstrated by the detection of considerable decitabine triphosphate levels in two patient responding to therapy, opposed to detection of low levels in a second patient that did not respond to therapy.

Toxicity

Deaminated gemcitabine triphosphate accumulates during prolonged oral gemcitabine dosing and can most likely cause severe toxicities. Other deoxycytidine analogs are also converted to their deaminated nucleotides

and show pharmacological activity. Finally, a very slow accumulation of tenofovir diphosphate was observed in peripheral blood mononuclear cells from a tenofovir-treated patient. Possibly this is related to the toxicities that are sometimes observed after years of tenofovir treatment.

Therapeutic drug monitoring

Because triphosphate analog levels are highly variable between patients and because under- or overdosing can have severe consequences, therapeutic drug monitoring (TDM) of nucleotide analogs should be considered.
The only analogs for which TDM of the active nucleotides is currently performed are 6-mercaptopurine and 6-thioguanine. TDM of active intracellular nucleotide analogs could reveal cancer therapy resistance already after the first dose. Alternatively, resistance could be detected on forehand by *ex vivo* incubations of patient blood. In the case of prolonged therapies, slow increases or decreases of nucleotide analogs, which would ultimately lead to adverse events, can be detected and prevented by therapy adjustments. Finally, TDM can aid in the development of optimal dosing schemes, as presented for decitabine in this thesis.

Measurements of intracellular nucleotide analogs in large populations and in specific cases are warranted to further elucidate the pharmacology of nucleoside analogs.

In conclusion, we have successfully developed and validated several sensitive and selective analytical methods for the quantitation of nucleoside and nucleotide analogs. Application of the methods to (pre)clinical studies revealed mechanisms and presence of resistance and toxicity.

Summary
Samenvatting

Summary

Cancer and HIV/AIDS are among the top 10 causes of death worldwide. Nucleoside analogs are an important class of drugs in anticancer therapy and form the backbone of antiretroviral therapy used against HIV. The compounds are, however, only active after intracellular conversion to their mono-, di- and triphosphate nucleotide form. Qualitative and quantitative analysis of these nucleotide forms is, therefore, pivotal in understanding their intracellular pharmacology.

In this thesis the development of sensitive liquid chromatography coupled to tandem mass spectrometry (LC-MS/MS) assays to quantitate nucleoside and nucleotide analogs in cells is described. Moreover, these assays were applied to preclinical and clinical studies, in order to increase the knowledge of nucleoside analog pharmacology.

Synthesis of nucleotide analogs

In *chapter 1* the synthesis of small amounts of nucleotide analogs from nucleoside analogs is described. These nucleotide analogs were required as reference and internal standards in quantitative analytical assays. Good yields were be obtained after drying of the starting material and using reagents in a large excess. By using tributylammonium phosphate in the final reaction step, a mixture of nucleoside mono-, di- and triphosphates could be obtained from a single reaction.

Bioanalysis of intracellular nucleoside and nucleotide analogs

In *chapter 2* the bioanalysis of nucleoside and nucleotide analogs in cells is described. First, an overview of the myriad of analytical methods for the quantitative determination of nucleotide analogs in cells is given (*chapter 2.1*). This literature review focuses on the methods using liquid chromatography coupled to mass spectrometry (LC-MS), which has become the method of choice, despite initial difficulties. Furthermore, challenges associated with these analyses are identified and discussed.

The development and validation of an assay for cladribine nucleotides is described in *chapter 2.2*. Using weak anion-exchange chromatography coupled to tandem mass spectrometry the mono-, di- and triphosphate of this antileukemic agent could be quantified in cultured cells (Madin-Darby canine kidney II cells) and growth medium. A pH gradient was used to separate and elute the nucleotides from the column. The use of a fused

silica instead of a stainless steel spray capillary improved the assay performance.
In *chapter 2.3,* a similar assay was developed and validated for the 6 nucleotide forms of emtricitabine and tenofovir. These antiretroviral agents were determined in white blood cells and the applicability of the assay was shown for samples from a patient on treatment with the drugs. Interestingly some nucleotide analogs appeared to accumulate over a period of months.

The development of a novel chromatographic system for the separation of nucleosides and nucleotides using porous graphitic carbon is outlined in *chapter 2.4*. Despite the apolar graphite surface, the ionic nucleotides could be retained on the carbon surface without the addition of ion-pairing agents. Elution was performed using the anion bicarbonate. The method showed an unsurpassed selectivity allowing the simultaneous quantification of deoxycytidine and deoxyuridine analog nucleosides and nucleotides. Unconventionally, the separation capabilities of the column were maintained by oxidizing the column before use and by injecting acid between each analysis.

In *chapter 2.5* the applicability of the method for biological matrices is shown. Using the chromatography described in *chapter 2.4* we were able to separate the nucleoside and nucleotide forms of the anticancer agent gemcitabine and of its deaminated metabolite (2',2'-difluorodeoxyuridine; dFdU). The method was validated for the simultaneous quantification of these 8 analytes in white blood cells. Addition of the internal standards to lysed cells prior to centrifugation was essential to obtain accurate results. Using the method, these analytes were detected in a patient for the first time.

The final chapter of this section (*chapter 2.6*) compares two common methods for the quantification of the number of white blood cells in a sample. Quantification of the number of cells in a sample is pivotal in calculating the amount of analyte per cell. The DNA-based quantitation method was found to be superior over the protein-based method because it was unaffected by red blood cell contamination. This DNA-base method was finally validated.

Pharmacology of nucleoside analogs

The analytical methods described in *chapter 2* were then applied to (pre)clinical studies (*chapter 3*). In *chapter 3.1* the role of the drug-efflux pump breast cancer related protein (BCRP) in resistance against anti-cancer nucleoside analogs was investigated. It was found that cells that overexpressed this drug-efflux pump were less sensitive to nucleoside

analogs. Using the assay described in *chapter 2.2* we concluded that BCRP extruded both cladribine and its monophospate from cells. In line with these results, only low levels of active cladribine triphosphate were found in resistant cells.

Chapter 3.2 describes a clinical study in which low doses of gemcitabine were administered orally to patients for the first time. The exposure to gemcitabine and its triphosphate was very low due extensive first-pass metabolism. A lethal hepatic toxicity observed was possibly related to accumulation of the triphosphate of deaminated gemcitabine, a previously unrecognized metabolite.

We hypothesized that metabolites similar to this previously unrecognized metabolite might be formed from other deoxycytidine analogs as well. *Chapter 3.3* provides a literature overview of the formation and pharmacological activity of deoxyuridine analog nucleotides during deoxycytidine analog therapy. It is concluded that many deoxycytidine analogs are converted to deoxyuridine nucleotides in cells. This conversion occurs at the monophosphate level, and only inside cells. Moreover, it is shown that these nucleotides can have pharmacological activity. Finally, the role of these possibly active secondary metabolites in treatment with deoxycytidine analogs is discussed.

In *chapter 3.4* the nucleotides of decitabine are analyzed. We scouted for the presence of deaminated decitabine nucleotides in white blood cells, but found none. We did, however, detect decitabine nucleotides. Of the 3 patients from which white blood cells were collected, 2 showed considerable decitabine triphosphate levels, whereas 1 only showed low decitabine triphosphate levels. Remarkably, these results corresponded to the clinical effect. The 2 patients with high levels responded well to therapy, whereas the third died due to disease progression. Currently, response to therapy can only be determined after several 6-week cycles. Moreover, decitabine triphospate accumulated when decitabine was administered every 4 hours during 3 days. Possibly a less intensive dosing scheme without hospitalization could be as effective as the current dosing scheme. Further research is warranted to corroborate these results and to devise the optimal dosing scheme.

In conclusion, despite apparent incompatibilities, LC-MS is currently the method of choice for the analysis of intracellular nucleotide analogs. In this thesis several LC-MS methods are developed and validated. Application of these methods to preclinical and clinical research can reveal active triphosphate levels that are too low or too high. Low triphosphate levels can be caused by drug-efflux pumps and ineffective activation of the

nucleosides. Low triphosphate levels can result in undertreatment, which is especially undesired in the treatment of cancer and HIV/AIDS. High triphosphate levels, on the other hand, can cause severe toxicities. Monitoring of nucleoside analog triphosphates should, therefore, be performed for some analogs. Finally, the pharmacokinetics and pharmacology of many nucleoside and nucleotide analogs are still largely unknown. More research should be performed to further unravel the pharmacology of nucleoside analogs.

Samenvatting

Kanker en HIV/AIDS staan beiden in de top tien van wereldwijde doodsoorzaken. Nucleoside analogen vormen een belangrijke groep geneesmiddelen in de behandeling van kanker en zijn ook de ruggengraat van de antiretrovirale therapie tegen HIV. Nucleoside analogen zijn echter pas actief nadat ze in cellen zijn omgezet in hun mono-, di- en trifosfaat nucleotide vorm. Kwalitatieve en kwantitatieve analyse van deze nucleotide vormen is daarom van groot belang om de intracellulaire farmacologie van nucleoside analogen te begrijpen.

In dit proefschrift is de ontwikkeling en validatie van gevoelige vloeistofchromatografie - massa spectrometrie (LC-MS/MS) methodes beschreven. Met deze methodes kunnen nucleoside en nucleotide analogen in cellen worden gekwantificeerd. Vervolgens zijn deze methodes toegepast op preklinische en klinische studies om zo de kennis over de farmacologie van nucleoside analogen te vergroten.

Synthese van nucleotide analogen

In *hoofdstuk 1* is de synthese van kleine hoeveelheden nucleotide analogen uit nucleoside analogen beschreven. Deze nucleotide analogen waren niet commercieel verkrijgbaar, maar wel nodig als referentie of interne standaard in kwantitatieve analyse methodes. Goede reactieopbrengsten werden verkregen na drogen van het uitgangsmateriaal en door een grote overmaat aan reagentia te gebruiken. Door tributylammonium fosfaat te gebruiken in de laatste reactiestap werd een mengsel van nucleoside mono-, di- en trifosfaat verkregen uit een enkele reactie.

Bioanalyse van intracellulaire nucleoside en nucleotide analogen

In *hoofdstuk 2* wordt de bioanalyse van nucleoside en nucleotide analogen in cellen beschreven. Eerst wordt een overzicht gegeven van de vele analyse methodes voor de kwantitatieve bepaling van nucleotide analogen in cellen (*hoofdstuk 2.1*). Deze literatuur studie is vooral gericht op de methodes die gebruik maken van vloeistof chromatografie gekoppeld aan massa spectrometrie (LC-MS). Ondanks de aanvankelijke problemen is LC-MS de meest gebruikte methode voor de bioanalyse van nucleotide analogen geworden. In het hoofdstuk worden ook de valkuilen van deze analyses besproken.

De ontwikkeling en validatie van een methode voor de nucleotides van cladribine is beschreven in *hoofdstuk 2.2*. De mono-, di- en trifosfaat van dit middel tegen leukemie konden worden gekwantificeerd in gekweekte cellen (Madin-Darby canine kidney II cellen) en kweek medium door gebruik te maken van zwakke anion-uitwisseling chromatografie gekoppeld met massa spectrometrie. Om de nucleotides te scheiden en van de kolom te elueren is gebruik gemaakt van een pH gradiënt. Door gebruik te maken van een fused silica in plaats van roestvrij stalen capillair werd de methode voldoende reproduceerbaar.

In *hoofdstuk 2.3* wordt een vergelijkbare methode beschreven voor de 6 nucleotide vormen van emtricitabine en tenofovir. Deze antiretrovirale middelen zijn bepaald in witte bloedcellen. De methode is uiteindelijk toegepast op monsters van een patiënt die met een emtricitabine-tenofovir combinatie behandeld werd. Opvallend was dat een aantal nucleotide analogen leek te accumuleren gedurende een periode van maanden.

De ontwikkeling van een nieuw chromatografisch system voor de scheiding van nucleosides en nucleotides met een grafiet kolom is beschreven in *hoofdstuk 2.4*. Ondanks het apolaire grafiet oppervlak vertoonden de zeer polaire nucleotides retentie op de grafietkolom, zonder gebruik te maken van een ion-paar vormer. Met behulp van bicarbonaat konden de nucleotides van de kolom worden geëlueerd. De methode heeft een zeer hoge selectiviteit waardoor de nucleosides en nucleotides van deoxycytidine en deoxyuridine analogen tegelijk konden worden gekwantificeerd. Het scheidingsvermogen werd op ongebruikelijke wijze behouden door de kolom voor gebruik te oxideren en door zuur te injecteren tussen iedere analyse.

Vervolgens wordt in *hoofdstuk 2.5* getoond dat de methode ook toepasbaar is op biologische matrices. Met het chromatografische systeem uit *hoofdstuk 2.4* konden de nucleoside en nucleotide vormen van het anti-kanker middel gemcitabine en van de gedeamineerd metaboliet 2',2'-difluorodeoxyuridine (dFdU) worden gescheiden. De methode is gevalideerd voor de gelijktijdige kwanificering van deze 8 analieten in witte bloedcellen. Voor juiste resultaten bleek het essentieel de interne standaarden aan cellysaat toe te voegen voor centrifugeren. Met deze methode zijn de analieten voor het eerst gemeten in een patiënt.

In het laatste hoofdstuk (*hoofdstuk 2.6*) van het bioanalyse gedeelte worden twee methodes voor de kwantificering van het aantal witte bloedcellen in een monster vergeleken. Kwantificering van het aantal witte bloedcellen in een monster is noodzakelijk om de hoeveelheid analiet per

cel te bepalen. De op DNA gebaseerde methode bleek beter dan de op eiwit gebaseerde methode omdat deze niet beïnvloed werd door vervuiling met rode bloedcellen. De DNA-methode is daarom gevalideerd.

Farmacologie van nucleoside analogen

De analyse methodes die in *hoofdstuk 2* zijn beschreven zijn vervolgens toegepast op (pre)klinische studies (*hoofdstuk 3*). In *hoofdstuk 3.1* is de rol van de geneesmiddelpomp breast cancer related protein (BCRP) in resistentie tegen anti-kanker nucleosides onderzocht. Cellen waarin deze pomp tot overexpressie was gebracht waren minder gevoelig voor nucleoside analogen. Met behulp van de analyse methode uit *hoofdstuk 2.2* konden we concluderen dat BCRP zowel cladribine als cladribine monofosfaat uit cellen pompt. In overeenstemming met deze resultaten bleken resistente cellen nauwelijks het actieve cladribine trifosfaat te bevatten.

In *hoofdstuk 3.2* wordt een klinische studie beschreven waarin patiënten voor het eerst een lage dosis oraal gemcitabine toegediend kregen. De blootstelling aan gemcitabine en gemcitabine trifosfaat was erg laag door sterk first-pass metabolisme. Een dodelijke levertoxiciteit die optrad was mogelijk gerelateerd aan accumulatie van het trifosfaat van gedeamineerd gemcitabine (dFdU). Dit was een nog niet eerder herkende metaboliet van gemcitabine.

Soortgelijke metabolieten zouden ook bij andere deoxycytidine analogen kunnen ontstaan. Daarom is in *hoofdstuk 3.3* een literatuurstudie beschreven waarin de vorming en farmacologische activiteit van deoxyuridine analogen tijdens deoxycytidine therapie wordt onderzocht. De conclusie is dat vele deoxycytidine analogen in cellen worden omgezet in deoxyuridine nucleotides. Deze omzetting vindt vooral plaats op het monofosfaat niveau, en alleen binnen cellen. Bovendien wordt in het hoofdstuk de activiteit van deze nucleotides beschreven. Tenslotte wordt de rol van deze mogelijke actieve metabolieten in de behandeling met deoxycytidine analogen bediscussieerd.

In hoofdstuk 3.4 worden de nucleotides van decitabine geanalyseerd. We hebben naar de aanwezigheid van gedeamindeerde decitabine nucleotides gezocht, maar konden deze niet aantonen. Wel zijn de nucleotides van decitabine zelf aangetoond. Van de 3 patiënten waarbij witte bloedcellen zijn afgenomen hadden er 2 aanzienlijke decitabine trifosfaat concentraties, terwijl er 1 slechts lage decitabine trifosfaat spiegels had. Deze resultaten kwamen zeer goed overeen met het klinische effect. De 2 patiënten met hoge spiegels reageerden goed op de therapie, terwijl de derde patiënt is overleden aan progressie van de ziekte.

Op dit moment kan respons op decitabine therapie pas worden bepaald na een aantal 6-weekse behandelings cycli. Bovendien accumuleerde decitabine trifosfaat als decitabine iedere 4 uur gedurende 3 dagen werd toegediend. Mogelijk is een minder intensieve behandeling, waarbij ziekenhuis opname niet noodzakelijk is, even effectief. De resultaten uit deze pilot studie moeten in vervolgonderzoek worden bevestigd.

Concluderend, LC-MS is op dit moment de beste methode voor de analyse intracellulaire nucleotide analogen. In dit proefschrift is de ontwikkeling van verschillende LC-MS methodes beschreven. Door deze methodes toe te passen op (pre)klinisch onderzoek kunnen te lage en te hoge spiegels van het actieve trifosfaat worden herkend. Lage trifosfaat spiegels worden onder andere veroorzaakt door geneesmiddel pompen en beperkte fosforylering van de nucleosides. Lage trifosfaat spiegels kunnen leiden tot onderbehandeling, wat ongewenst is bij de behandeling van kanker er HIV/AIDS. Te hoge trifosfaat spiegels kunnen echter voor ernstige bijwerkingen zorgen. De nucleoside trifosfaat spiegels van een aantal analogen zouden daarom bij patiënten moeten worden gecontroleerd. Over de farmacokinetiek en farmacologie van vele nucleoside analogen bestaan nog vragen. Deze vragen zullen in verder onderzoek beantwoord moeten worden.

Samenvatting voor niet-ingewijden

Nucleoside en nucleotide analogen vormen een groep geneesmiddelen die veel wordt gebruikt tegen HIV en kanker, maar ook tegen ontstekingsziektes zoals de ziekte van Crohn.

Om zich te kunnen delen en vermenigvuldigen moeten kankercellen en virussen hun DNA kopiëren. Hiervoor gebruiken ze de vier nucleosides deoxyadenosine (dA), deoxyguanosine (dG), deoxycytosine (dC) en deoxythymidine (dT). Dit zijn de natuurlijke bouwstenen van DNA. Nucleoside analogen zijn stoffen die sterk lijken op deze natuurlijke bouwstenen (vergelijk bijvoorbeeld deoxycytidine met de analogen daarvan op p 24 en de andere analogen op p 25-27). Door de sterke gelijkenis worden ook de nucleoside analogen door kankercellen en virussen als bouwstenen gebruikt om hun DNA te kopiëren. De kleine maar essentiële verschillen met de natuurlijke varianten zorgen er echter voor dat het DNA minder snel gekopieerd wordt en dat er DNA met foute bouwstenen ontstaat. Ze zijn daarom ook wel eens “rubber donuts” genoemd: ze zien er uit als echt, maar je kunt je tanden er op breken en je erin verslikken. Door remming van de DNA replicatie wordt uiteindelijk de tumorgroei en virusvermenigvuldiging onderdrukt.

Nucleoside analogen zijn na toediening niet direct actief. De analogen moeten eerst uit het bloed in de cel worden opgenomen, waarna er door verschillende enzymen achtereenvolgens drie fosfaat groepen aan gekoppeld worden. Zodra er een fosfaatgroep aan een nucleoside zit heet het een nucleotide. Het trifosfaat dat uiteindelijk ontstaat is de actieve vorm die in DNA kan worden ingebouwd. De vorming van een trifosfaat is weergegeven in het figuur op p 255 met zidovudine (AZT), het eerste effectieve geneesmiddel tegen HIV, als voorbeeld. Bij een te lage trifosfaat concentratie worden de kankercellen en virussen niet geremd, terwijl een te hoge concentratie tot ernstige bijwerkingen kan leiden. Het is dus van belang de juiste concentratie in cellen te bereiken. De mate van omzetting naar de actieve trifosfaat vorm verschilt echter van persoon tot persoon en kan moeilijk voorspelt worden.

In dit proefschrift is eerst beschreven hoe nucleoside mono-, di- en trifosfaten in witte bloedcellen kunnen worden gemeten. Vervolgens zijn deze methodes toegepast op gekweekte cellen en patiënten om beter te begrijpen waarom ze bij de ene patiënt wel werken en bij de andere niet.

Niet alle analogen die we in cellen wilden bepalen waren commercieel verkrijgbaar. In het eerste gedeelte van het proefschrift is daarom een

methode beschreven waarmee de stoffen zelf gemaakt konden worden (*hoofdstuk 1.1*).
In het tweede gedeelte worden verschillende analyse methodes beschreven. In *hoofdstuk 2.1* is eerst een overzicht gegeven van alle methodes die er op dit moment zijn ontwikkeld om nucleotide analogen in cellen te bepalen. Het hoofdstuk richt zich op methodes die gebruik maken van massa spectrometers. Dit zijn zeer gevoelige en selectieve detectoren. In *hoofdstuk 2.2* wordt een methode beschreven voor de bepaling van de nucleotides van cladribine in een gekweekte cellen. Cladribine is een nucleoside analoog dat gebruikt wordt tegen leukemie. Een soortgelijke methode is beschreven in *hoofdstuk 2.3*. Met deze methode konden de nucleotides van emtricitabine en tenofovir, beide veel gebruikt tegen HIV, in witte bloedcellen worden gemeten. In *hoofdstuk 2.4* is een nieuw soort methode ontwikkeld voor de gelijktijdige bepaling van nucleoside en nucleotide analogen. Deze methode is in *hoofdstuk 2.5* verder ontwikkeld voor de bepaling van gemcitabine en de omzettingsproducten daarvan. Gemcitabine wordt gebruikt bij de behandeling van verschillende soorten tumoren.
De witte bloedcellen waarin wordt gemeten worden voor de analyse uit bloed van de patiënt geïsoleerd. De hoeveelheid geïsoleerde witte

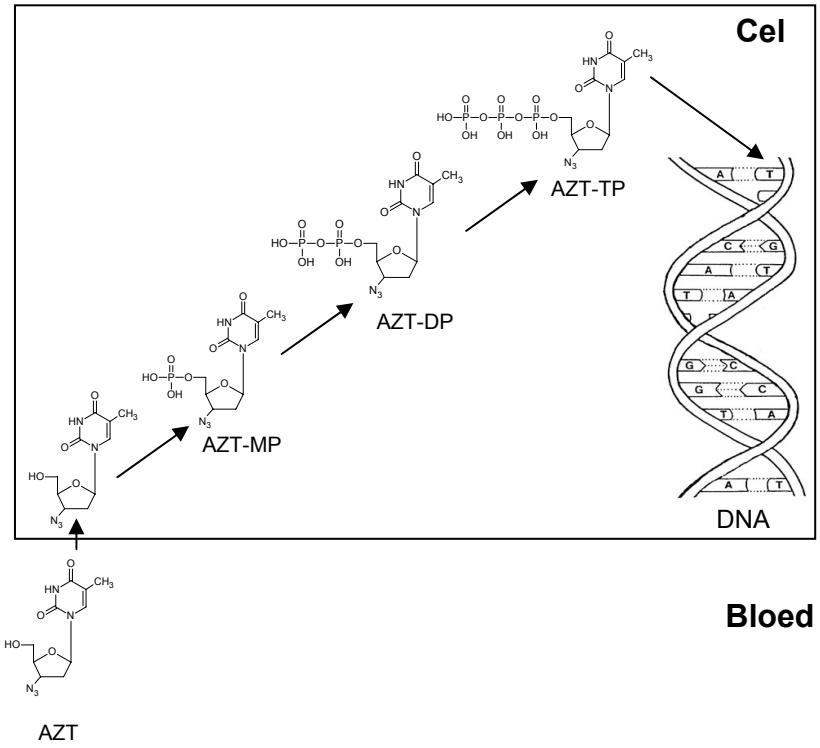

bloedcellen verschilt echter van monster tot monster. Daarom is in *hoofdstuk 2.6* een methode beschreven om de hoeveelheid geïsoleerde witte bloedcellen te bepalen. Dit is gedaan op basis van de hoeveelheid DNA in een monster.

In het derde gedeelte zijn de ontwikkelde analyse methodes gebruikt om de (on)werkzaamheid van nucleoside analogen beter te begrijpen.
Verminderde effectiviteit van nucleoside analogen komt meestal doordat er minder actief nucleoside trifosfaat in de cellen zit. Dit kan verschillende oorzaken hebben. Geneesmiddelpompen pompen geneesmiddelen de cel uit en kunnen daardoor de effectiviteit verminderen. In *hoofdstuk 3.1* is het effect van de geneesmiddelpomp breast cancer resistance protein (BCRP) op de effectiviteit van verschillende analogen getest. In cellen met meer BCRP bleek veel minder cladribine trifosfaat te zitten. De BCRP pomp bleek zowel cladribine als cladribine monofosfaat uit de cel te pompen en zo de cellen ongevoelig te maken. In *hoofdstuk 3.2* is het nucleoside gemcitabine voor de eerste keer oraal aan patiënten toegediend. Door omzetting in de lever was de blootstelling aan gemcitabine en gemcitabine trifosfaat laag. Wel werden aanzienlijke concentraties van een tweede, tot dan toe onbekende, trifosfaat gemeten. Dit tweede trifosfaat heeft mogelijk een zeer ernstige bijwerking veroorzaakt. Aangezien gemcitabine sterk op andere nucleoside analogen lijkt kunnen vergelijkbare tweede trifosfaten ook bij andere analogen ontstaan. *In hoofdstuk 3.3* is een literatuurstudie beschreven waarin de vorming en het effect van deze omzettingsproducten is bekeken. De omzettingsproducten bleken ook bij andere analogen voor te komen en hadden ook daar een effect op cellen.
Tenslotte is in *hoofdstuk 3.4* gekeken naar het nucleoside analoog decitabine. Dit analoog wordt gebruikt tegen myelodysplastisch syndroom, een soort leukemie. In de witte bloedcellen van drie patiënten is de hoeveelheid decitabine trifosfaat bepaald. Twee van de drie patiënten hadden hoge trifosfaat spiegels, terwijl de derde patiënt nauwelijks decitabine trifosfaat in de witte bloedcellen had. Dit verschil kwam goed overeen met het klinische beeld: de eerste twee patiënten reageerden goed op de therapie terwijl de derde aan de ziekte is overleden. Mogelijk kan hiermee in de toekomst al aan het begin van een kuur worden bepaald of de kuur aan zal slaan of niet. Bovendien wijzen de resultaten erop dat éénmaaldaagse toediening in plaats van toediening om de vier uur ook effectief kan zijn. Patiënten hoeven dan niet meer in het ziekenhuis te worden opgenomen.

Het in dit proefschrift geschreven onderzoek laat zien hoe belangrijk het is om de actieve trifosfaten in cellen te meten. Door de metingen konden zowel ernstige bijwerkingen als een gebrek aan werkzaamheid worden verklaart.

Dankwoord
Curriculum Vitae
List of Publications

Dankwoord

Wat is het snel gegaan. Het ene moment zit je in de trein van Groningen naar Amsterdam op weg naar een sollicitatie, het andere moment schrijf je het dankwoord van je proefschrift. Toch is er in de tussentijd een hoop gebeurt, en dat heb ik niet alleen gedaan.

Allereerst wil ik alle patiënten bedanken die zonder eigen belang aan de studies hebben meegewerkt. Zonder jullie was veel van dit onderzoek niet mogelijk geweest.

Verder wil ik mijn promotoren, Jos Beijnen en Jan Schellens, en mijn co-promotor Hilde Rosing bedanken.
Jos, hoe krijg je het voor elkaar? In de raad van bestuur van een ziekenhuis zitten, het hoofd van een apotheek zijn, zoveel promovendi begeleiden en dat allemaal ook nog goed doen. Ik snap er niets van, maar heb er groot respect voor. Bedankt voor de vrijheid, het vertrouwen en de goede begeleiding.
Jan, bedankt voor de interessante gemcitabine discussies en je kritische blik. Bedankt ook voor de hulp bij mijn plannen om in tumorcellen zelf te meten.
Hilde, te pas en te onpas heb je tijd gemaakt om mijn problemen op een praktische manier op te lossen en om naar mijn verhalen te luisteren. Na zulke overleggen kwam ik een lijst experimenten rijker, maar vele kopzorgen armer je kamer weer uit. Dank ook voor het kwaliteitsgevoel, dat ik op het laatst bijna begon te overdrijven. Ik heb veel van je geleerd.

Ook wil ik de leden van de beoordelingscommissie, Prof dr. ir. A.C. Beijnen, Prof dr. A.J.R. Heck, Prof dr. G.J. de Jong, Prof dr. G.J. Peters, dr. W.J.M. Underberg en dr. P.W. Wijermans bedanken voor hun werk.

Veel mensen hebben bijgedragen aan het onderzoek dat in dit proefschrift staat beschreven.
Cocky, ik vond het super om samen met je de HPLC in het radionucliden lab te doorgronden en de bergen aan data van de transportproeven te verklaren. Ik hoop nog vele kilometers met je te hard te lopen en vele drankjes met je te drinken. Ook Piet Borst en Marcel de Haas wil ik bedanken voor de samenwerking in het cladribine onderzoek.
Sander, het gemcitabine werk met jou heeft een grote invloed op mijn onderzoek gehad. En het is geen slechte invloed geweest. Bedankt daarvoor. Helaas was je eerder klaar dan ik en heb ik het de laatste tijd zonder de discussies en gezelligheid op het werk moeten doen. Gelukkig kan dat ook buiten het werk onder het genot van een scroppino met

"processo". Binnen het gemcitabine onderzoek wil ik ook Enaksha Wickremsinhe van Eli Lilly bedanken voor het leveren van de referentiestoffen. Ten slotte ben ik dank verschuldigd aan Sjaak Burgers voor de hulp bij de gemcitabine metingen in pleuravocht en longbiopten.
Rob, op een maandje na zijn we tegelijk begonnen met onze promotie. Jij op HIV en ik op de analyse van fosfaatjes. Al snel hadden we iets gevonden waarin we konden samenwerken: de analyse van HIV-fosfaatjes. Tijdens onze 4 jaar hebben we samen vele hoogtepunten, maar ook crises meegemaakt. We hebben ze allemaal doorstaan en nu zijn we klaar. Het was mooi! Wiete, veel succes maar vooral plezier met de HIV-fosfaatjes.
Joke, bedankt voor alle hulp bij het isoleren van PBMC's, de Bradfords en de DNA metingen. En natuurlijk voor de gezelligheid. Ook Dick Pluim bedankt voor de behulpzaamheid bij de Bradford en andere experimenten.
Pierre Wijermans wil ik bedanken voor de prettige samenwerking in het decitabine onderzoek. Ik denk dat ons werk de basis heeft gelegd voor vruchtbaar vervolgonderzoek.

Andere collega's zijn niet bij specifieke projecten betrokken geweest maar ben ik wel zeer dankbaar.
Michel, jij hebt mij ingewijd in de geheimen van gemcitabine trifosfaat en MSen. Al snel wilde ik met die MSen dingen doen die niet gebruikelijk waren. Je hebt me goed in de gaten gehouden, waar nodig ingegrepen, en zo de MSen werkend gehouden. Zonder jou zou dat wel eens heel anders kunnen zijn gelopen. Bedankt ook voor alle troubleshooting en goede ideeën. Bas, bedankt voor alle technische hulp die ik in het begin hard nodig had. Matthijs, het was goed om te horen dat je weer bij het slotervaartziekenhuis kwam werken. Ik waardeer je scherpe vragen en kritische houding. Roel, hoewel ik niet zo van kwaliteitsdocumentatie hou heb ik er toch flink wat van geproduceerd. Ik heb zelfs meegedacht over formulieren, AWV's en OTJTR's. En ik heb ervan geleerd. Bedankt. Ook voor je koppel-inspanningen. Abadi en Luc, ik hoop nog vele Rambo, Terminator en Wii avondjes met jullie te beleven. Lianda en Ciska, bedankt voor de gezellige gesprekken. Ook de mensen van het QC-lab: Kees, Anissa, Jan en Dieuwke en oud-collega's Carolien, Rianne en Mariët, bedankt!

En dan zijn er natuurlijk nog de OIO's. Allereerst mijn oude en nieuwe kamergenoten. Het begon in de onderwereld met Suu, Wandena en Liia. Jullie hebben me ingewijd in alle OIO-geheimen. Suu, jammer dat je al zo vroeg klaar was. Ik mis je heldere analyses over vrouwen en andere belangrijke zaken. Liia, het was top om zolang bij je op de kamer te zitten. Hoewel je het nog een beetje hebt weten te rekken, was ook jij helaas vertrokken voordat ik klaar was. Onze gesprekken over proefjes, dates en

hypercarb kolommen zal ik niet vergeten. Bedankt. Later kwamen ook Carola, Bas, Thomas en Anne-Charlotte in de “analyse” kamer. Carola, dank voor de discussies en de hulp bij de laatste hordes. Bas, bedankt voor de gezelligheid en het iets langer in leven houden van mijn plant. Thomas, je rust en humor zijn fantastisch. Bovendien ben je een francofiel, classicofiel en bekwaam psychoanalyticus. Wat kan iemand zich nog meer van een kamergenoot wensen? Anne-Charlotte, bedankt voor je interesse en het welkom dat ik iedere vroege morgen weer krijg. Ik vind het leuk nog een tijd met je te kunnen samenwerken.
Ook de andere OIO’s hebben mij een mooie tijd bezorgd.
Lieve Ly, bedankt voor de pains au chocolat, snoepjes en ijsjes, de wijntjes, fietsliften en pannenkoeken. Bedankt ook voor alle uitjes naar concerten, de hulp bij de leesmappen en je bloed. En zo kan ik nog wel even doorgaan. Bedankt voor alles. Joost, bedankt voor je humor, gezeur, enthousiasme, bizarre onderzoek en mooie verhalen. Johannes, ik hoop dat we nog vele voetbal overwinningen mogen meemaken. Markus, David, Stijn: de mannen die mij overspoeld hebben met gemcitabine trifosfaat samples. Het was leuk om met jullie samen te werken. Zonder de andere keetbewoners waren de keet en de OIO-weekenden niet hetzelfde geweest. Nienke, Jelte, Susanne, Jolanda, Rik, Tine, Annemieke, Mariska, Denise en Jurjen, bedankt. Ook de mensen van het NKI: Nienke, Maarten, Suzanne, Lotte, bedankt. En natuurlijk Sander en Roos: jullie zijn een mooi stel.
En dan is er ook nog de oude garde: Natalie, Marie-Christine, Corine, Sabien, Anthe, Judith en Tessa. Bedankt voor de mooie tijd.
Elke, ik wordt altijd enthousiast als ik met jou over onderzoek praat. Bedankt voor alle wijze raad en je luisterende oor. Alwin, bedankt voor de farmacokinetische adviezen en mooie verhalen.
En tenslotte nog de toekomst. Ellen, heel veel plezier met het verdere nucleotide onderzoek. Er liggen nog vele ontdekkingen op je te wachten.

Tenslotte nog mijn vrienden en familie.
Reinoud en Peter, ik heb de filmpjes de laatste tijd moeten overslaan, maar heb nu weer alle tijd voor middeleeuwse actie met hooiwagens en zwaarden. Robert Jan, de cover van het proefschrift ziet er gelikt uit. Bedankt daarvoor en voor de adviezen over het binnenwerk.
En dan mijn paranimfen. Lucas en Ron, een mooier stel paranimfen kan ik me niet voorstellen. Ron, het is alweer 11 jaar geleden dat we farmacie zijn gaan studeren. Elf jaar vol met studiereisjes, duikreisjes, surfreisjes en gewone reisjes. Ik hoop dat er nog vele volgen. Lucas, je weet niet half hoe mooi ik het vind dat je mijn paranimf wil zijn. Ik heb er het volste vertrouwen in dat je, mocht ik het begeven, alle vragen met overtuiging zal beantwoorden. Het is een eer jullie achter me te hebben staan tijdens de verdediging.

Lieve Bouwien en Dick, bedankt voor jullie interesse. Ik ben blij met de nieuwste aanwinst van de familie.
Lieve pap en mam, het is niet voor niets dat ik dit proefschrift aan jullie heb opgedragen. Als jonge onderzoeker en bommenmaker vertrouwden jullie mij al, en dat vertrouwen is in alle jaren niet minder geworden. Altijd kon ik rekenen op jullie steun en interesse. Jullie hebben een heel gelukkige zoon voortgebracht.

Lieve Moes, jij hebt misschien nog wel het meeste onder dit proefschrift moeten leiden. De avonden met jou waren altijd iets om naar uit te kijken tijdens al het werk. Bedankt voor al het geduld, begrip en je liefde. Ik ben heel blij met je.

Robert

Amsterdam, 2009

Curriculum Vitae

Robert Jansen is op 16 mei 1980 geboren in Voorburg. In 1998 behaalde hij zijn VWO diploma aan de Pantarijn scholengemeenschap in Wageningen en in datzelfde jaar begon hij met de studie farmacie aan de Rijksuniversiteit Groningen. De doctoraalopleiding werd afgesloten met een wetenschappelijke stage bij de farmacologie en toxicologie afdeling van het Centre Hospitalier Universitaire in Limoges, Frankrijk. Onder leiding van Prof. dr. D.R.A. Uges en Prof. Dr. P. Marquet is onderzoek verricht naar een algemene toxicologische screeningsmethode met behulp van LC-MS/MS. In 2005 werd het apothekersdiploma behaald. Aansluitend is gestart met het promotieonderzoek dat is beschreven in dit proefschrift. Het onderzoek is uitgevoerd in het Slotervaartziekenhuis in Amsterdam, onder begeleiding van Prof. dr. J.H. Beijnen, Prof. dr. J.H.M. Schellens en Dr. H. Rosing.

List of publications

Jansen R, Lachatre G, Marquet P; "LC-MS/MS systematic toxicological analysis: comparison of MS/MS spectra obtained with different instruments and settings", *Clin Biochem*. 2005 Apr;38(4):362-72.

Bosch TM, Huitema AD, Doodeman VD, **Jansen R**, Witteveen E, Smit WM, Jansen RL, van Herpen CM, Soesan M, Beijnen JH, Schellens JH; "Pharmacogenetic screening of CYP3A and ABCB1 in relation to population pharmacokinetics of docetaxel" *Clin Cancer Res*. 2006 Oct 1;12(19):5786-93.

Lagas JS, Vlaming ML, van Tellingen O, Wagenaar E, **Jansen RS**, Rosing H, Beijnen JH, Schinkel AH; "Multidrug resistance protein 2 is an important determinant of paclitaxel pharmacokinetics", *Clin Cancer Res*. 2006 Oct 15;12(20 Pt 1):6125-32.

Veltkamp SA, Hillebrand MJ, Rosing H, **Jansen RS**, Wickremsinhe ER, Perkins EJ, Schellens JH, Beijnen JH; "Quantitative analysis of gemcitabine triphosphate in human peripheral blood mononuclear cells using weak anion-exchange liquid chromatography coupled with tandem mass spectrometry", *J Mass Spectrom*. 2006 Dec;41(12):1633-42.

Jansen RS, Rosing H, de Wolf CJ, Beijnen JH; "Development and validation of an assay for the quantitative determination of cladribine nucleotides in MDCKII cells and culture medium using weak anion-exchange liquid chromatography coupled with tandem mass spectrometry", *Rapid Commun Mass Spectrom*. 2007;21(24):4049-59.

Veltkamp SA, **Jansen RS**, Callies S, Pluim D, Visseren-Grul CM, Rosing H, Kloeker-Rhoades S, Andre VA, Beijnen JH, Slapak CA, Schellens JH; "Oral administration of gemcitabine in patients with refractory tumors: a clinical and pharmacologic study", *Clin Cancer Res*. 2008 Jun 1;14(11):3477-86.

de Wolf C, **Jansen R**, Yamaguchi H, de Haas M, van de Wetering K, Wijnholds J, Beijnen J, Borst P; "Contribution of the drug transporter ABCG2 (breast cancer resistance protein) to resistance against anticancer nucleosides", *Mol Cancer Ther*. 2008 Sep;7(9):3092-102

Jansen RS, Rosing H, Schellens JH, Beijnen JH; "Retention studies of 2'-2'-difluorodeoxycytidine and 2'-2'-difluorodeoxyuridine nucleosides and nucleotides on porous graphitic carbon: Development of a liquid chromatography-tandem mass spectrometry method", *J Chromatogr A*. 2009 Apr 10;1216(15):3168-74

ter Heine R, Huitema ADR, **Jansen RS**, Smits PHM, van Gorp ECM, Wagenaar JFP, Beijnen JH. Mulder, JW**; "**Prolonged exposure to tenofovir monotherapy 1 month after treatment discontinuation because of tenofovir-related renal failure", *Antiviral Therapy*. 2009; 14**:** 299-301

Oostendorp RL**,** Huitema AD, Rosing H, **Jansen RS**, ter Heine R, Keessen M, Beijnen JH, Schellens JH; "Co-administration of ritonavir strongly enhances the apparent oral bioavailability of docetaxel in patients with solid tumors", *Clin Cancer Res*. 2009 Jun 15;15(12): 4228-33

Koolen SLW, Huitema ADR, **Jansen RS**, van Voorthuizen T, Beijnen JH, Smit WM, Schellens JHM; "Pharmacokinetics of gemcitabine and metabolites in a patient with double sided nephrectomy: A case report and a review of the literature", *Oncologist. accepted for publication*

Jansen RS, Rosing H, Schellens JH, Beijnen JH; "Simultaneous quantification of 2'-2'-difluoro-deoxycytidine and 2'-2'-difluoro-deoxyuridine nucleosides and nucleotides in white blood cells using porous graphitic carbon chromatography coupled with tandem mass spectrometry", *Rapid Commun Mass Spectrom. Accepted for publication*

Jansen RS, Rosing H, Schellens JH, Beijnen JH; "Deoxyuridine analog nucleotides in deoxycytidine analog treatment: secondary active metabolites?", *submitted for publication*

Jansen RS, Rosing H, Schellens JH, Beijnen JH; "Facile small scale synthesis of nucleoside 5'-phosphate mixtures", *submitted for publication*

Jansen RS, Rosing H, Schellens JH, Beijnen JH; "Mass spectrometry in the quantitative analysis of intracellular nucleotide analogs", *submitted for publication*

Jansen RS, Rosing H, Kromdijk W, ter Heine R, Schellens JH, Beijnen JH; "Simultaneous quantification of emtricitabine and tenofovir nucleotides in peripheral blood mononuclear cells using weak anion-exchange liquid chromatography coupled with tandem mass spectrometry", *submitted for publication*

Jansen RS, Rosing H, Schellens JH, Beijnen JH; "Protein versus DNA as a marker for peripheral blood mononuclear cell counting", *Submitted for publication*

Jansen RS, Rosing H, Wijermans PW, Schellens JH, Beijnen JH; "Decitabine triphosphate levels in patients receiving prolonged low-dose decitabine administration: a pilot study", *Submitted for publication*